REFER TO COLOUR CD

Indian and Northern Affairs Canada / Affaires indiennes et du Nord Canada

Exploration and Geological Services Division, Yukon Region

SEDIMENTOLOGY OF PLACER GRAVELS NEAR MT. NANSEN CENTRAL YUKON TERRITORY

W.P. LeBarge

1995

Canada

12-4
1:500

EXPLORATION AND GEOLOGICAL SERVICES DIVISION
YUKON REGION

BULLETIN 4

SEDIMENTOLOGY OF PLACER GRAVELS NEAR MT. NANSEN, CENTRAL YUKON TERRITORY

W.P. LeBarge

1995

Minister of Supply and Services Canada 1995
Available in Canada through
authorized bookstore agents and other bookstores

or by mail from:
Canadian Government Publishing Centre
Supply and Services Canada
Ottawa, Canada K1A OS9

and primarily from:
Exploration and Geological Services Division
Indian and Northern Affairs Canada
#345-300 Main St.
Whitehorse, Yukon
Canada Y1A 2B5

QS-Y093-000-EF-A1
ISBN 0-662-22923-1
Cat. No. R71-53/4-1995E

Published under the authority of the Hon. Ron Irwin, M.P., Minister of Indian and Northern Affairs Canada, Whitehorse, Yukon, 1995.

Cover: Crystalline gold particle from a placer deposit on Back Creek, a right limit tributary of Victoria Creek. Field of view is approximately 1 cm.

Recommended Citation:

LeBarge, W.P., 1995. Sedimentology of Placer Gravels near Mt. Nansen, Central Yukon Territory, Bulletin 4, Exploration and Geological Services Division , Indian and Northern Affairs Canada, Yukon Region, 155 p.

PREFACE

This bulletin is essentially an edited version of a Master's thesis which was completed by the author, William LeBarge, at the University of Calgary during a two-year leave of absence from Exploration and Geological Services Division. Fieldwork for this study occurred in 1992, and laboratory analyses were completed at the University of Calgary the following winter. This study is a significant contribution towards the understanding of the sedimentology of placer gravels within the pre-Reid glacial limits, and it is hoped that ensuing workers will be able to use this study as a framework in further efforts to describe surficial deposits of the Mt. Nansen area. As with many such studies, this one could not have been completed without the cooperation and support of the local placer miners, and it is hoped that they will be able to make use of this study to better understand the geological history, geomorphology and placer sedimentology of their mining area.

T.J. Bremner
Chief Geologist
Exploration and Geological Services Division
Indian and Northern Affairs Canada
Yukon Region

ACKNOWLEDGEMENTS

I would like to thank my thesis supervisor Dr. Fran Hein for her guidance and support with this project, as well as Dr. Len Hills, who provided encouragement and direction in the early stages of this study. This project would also not have been possible without the support and encouragement of Steve Morison (Director, Mineral Resources Directorate, Northern Affairs Program, Yukon Region) who permitted me to take a leave of absence from the Geology Division to concentrate on this project. I am also grateful for the financial assistance provided by the Northern Careers Program, Public Service Commission, Yukon Region, and the support of the people in that office, especially Maureen Osland.

Much appreciation goes to J.P. Rankin, who provided enthusiastic field assistance during a cold and rainy field season.

Joint fieldwork and geological discussions with Dr. Lionel E. Jackson, Jr., Geological Survey of Canada, Terrain Sciences Division, Vancouver were of much value. Dr. Alejandra Duk-Rodkin, Terrain Sciences Division, Geological Survey of Canada, Calgary, was of immense help in airphoto interpretation and useful discussions regarding the paleogeography of the Mt. Nansen area.

Paulina Mindermann was of great assistance in digital drafting of the sections and X-Ray diffraction plots, and in aiding in the final compilation of the manuscript of both the thesis and this bulletin.

I would also like to thank geotechnician Deb Gladiotis (University of Calgary) for her assistance in interpreting X-Ray diffraction plots, and in using the Scanning Electron Microscope.

Finally, this study would not have been possible without the cooperation and kindness of the placer miners, especially Ted Tullis, Bill Trerice, Eugene Curley, John Bush and the people of BYG Resources.

W.P. LeBarge
Placer Geologist
Exploration and Geological Services Division
Indian and Northern Affairs Canada
Yukon Region

TABLE OF CONTENTS

LIST OF FIGURES

LIST OF TABLES

Sedimentology of Placer Gravels near Mt. Nansen, Central Yukon Territory

Abstract

Unconsolidated sediments in the Mount Nansen area can be subdivided into eight clastic facies: 1) clay-rich diamicton; 2) massive/stratified silt/clay; 3) massive/disorganized pebbly sand/sand; 4) stratified pebbly sand/sand; 5) disorganized muddy gravel; 6) massive/stratified sandy gravel; 7) disorganized gravel; and 8) massive to crudely stratified gravel. Diamicton is interpreted as glacial till; other facies are fluvial/glaciofluvial in origin.

Sediments have a number of geomorphic settings, including : 1) Holocene colluvium, alluvial fans and stream deposits; 2) Reid periglacial alluvial fans; and 3) pre-Reid glacial and glaciofluvial deposits.

Previous workers suggested that significant placer gold concentrations occur only in alluvium that lies either upon bedrock or glacial till. New data from this study suggests that significant amounts of placer gold also occur in the diamicton, primarily at the diamicton/bedrock contact. Gold concentration in the diamicton is likely due to glacial erosion and incorporation of a supergene-enriched bedrock mantle and pre-existing auriferous alluvium.

Résumé

Les sédiments non consolidés de la région de Mount Nansen se laissent subdiviser en huit faciès clastiques: 1) un diamicton riche en argile; 2) un silt/une argile massifs/stratifiés; 3) un sable caillouteux massif/sans structure; 4) un sable caillouteux stratifié; 5) un gravier boueux sans structure; 6) un gravier sableux massif/stratifié; 7) un gravier sans structure; et 8) un gravier massif à grossièrement stratifié. On a interprété le diamicton comme étant un till; les autres faciès sont d' origine fluviatile/fluvioglaciaire.

Les sédiments se présentent dans plusieurs contextes géomorphologiques, et sont notammen: 1) des colluvions, des cônes de déjection et des sédiments fluviatiles d'âge Holocène; 2) des cônes de déjection périglaciaires de l'époque de l'avancée de Reid; et 3) des dépôts glaciaires et fluvioglaciaires antérieurs à l' avancée de Reid.

Les chercheurs précédents on suggéré qu'il n'existait des concentrations significatives d'or placérien que dans les alluvions reposant soit sur le substratum rocheux soit sur le till. Les nouvelles données apportées par cette étude suggèrent que des quantités significatives d'or placérien existent aussi dans le diamicton, principalement au contact entre ce diamicton et le substratum rocheux. Les concentrations d'or dans le diamicton sont probablement le résultat de l'érosion glaciaire et de l'incorporation d'un manteau rocheux enrichi par des processus supergènes, et d'alluvions aurifères préexistantes.

INTRODUCTION

The exploitation of alluvial concentrations of gold continues to be a major industry in the Yukon, as it has been since the Klondike Gold Rush of 1898. Production of placer gold has averaged 125,000 crude ounces per year for the last five years, although a modern day production record began in 1988 and peaked in 1989 with 169,345 crude ounces of gold produced, a value not seen since 1917. Gold production in 1994 increased slightly with 107,392 crude ounces mined to the end of October, which represents a 5% increase over the same period in 1993 (van Kalsbeek, 1994). The placer mining industry annually employs 700 to 800 people in an average of 200 operations, most of which are small (3-4 employees) family-owned and operated mines (LeBarge, 1990).

Most historic mining areas in the Yukon, such as the Klondike and Sixtymile districts, lie beyond the limit of Pleistocene Cordilleran glaciations. Although most of the past and current production of gold has been derived from these unglaciated areas, placer reserves in these areas are slowly being depleted, as evidenced by the general decline in production since 1989. Placer mining does occur in several glaciated areas of the Yukon, although the search for economic placer deposits is complicated by the presence of glacial drift and the erosion of pre-existing placers. Exploration for new placer deposits in new placer areas is essential, and it is likely that production of placer gold from glaciated areas will increase in relative importance as new placer reserves are discovered in these under-explored areas.

Background

The study area is situated in central Yukon, (Figure 1) in NTS 115 I 3, approximately 60 kilometres west of the village of Carmacks (Figure 2, Table 2). It is accessible from Whitehorse by the all-weather Klondike highway to Carmacks, and by a summer-only road that originates at Carmacks. The entire trip from Whitehorse takes approximately 3 hours by road. An airstrip capable of supporting a DC-3 exists at Carmacks, and an unmaintained bush airstrip lies near Victoria Creek at the Carmacks - Mt. Nansen road crossing. Helicopters can be hired in Whitehorse or Carmacks.

Gold was first discovered in placer deposits in the Mt. Nansen area in 1899. Mr. Henry S. Back, on a prospecting trip from Selkirk with Mr. H. Kline, found "good panning" on Nansen Creek at the mouth of Discovery Creek in July 1899. He returned to the area in 1907 with his son Frank H. Back. The first claim staked in the area was Discovery claim on Nansen Creek, which was staked on June 13, 1910, by Frank H. Back and Tom Bee (Cairnes 1915a). Serious mining began to take place in the area shortly thereafter and nearly all creeks in the area were at one time staked end to end, although many were allowed to lapse.

Gold continues to be mined from Nansen and Victoria creeks and their respective tributaries. Although Klaza River and its tributaries appear to have been largely ignored, in 1985 an unnamed left-limit (left-bank, facing downstream) tributary of Klaza River was staked and mining has taken place since 1986.

Table 1 - Placer Gold Production Record - Mt. Nansen Area

Creek	Tributary of	1910-1914	1978-1988	1989-1993	1910-1993
Back Creek	Victoria Creek	--	555	456	1011
Discovery Creek	Nansen Creek	40	--	158	198
East Fork Nansen	Nansen Creek	225	--	--	225
Klaza tributaries	Klaza River	--	594	831	1425
Nansen Creek	Nisling River	180	1218	1203	2601
Victoria Creek	Nisling River	--	294	436	730

Total Recorded Production - 6190 crude ounces

Recorded gold production from this area totals only 6190 crude ounces (Table 1), although much more gold has probably been recovered. For instance, although two placer mines operated on Back Creek in 1992 (employing at least six people for 3 months), production of gold was recorded as only 9 crude ounces (Placer Mining Section, 1993). Much of this is probably due to present legislation which requires that only gold which is to be exported out of the country to be recorded in the form of a royalty charged by the Mining Recorder. In addition, although placer gold was mined in the years 1914 to 1978, specific production records are not available.

Nansen and Victoria creeks lie outside of the limits of the Late Wisconsin McConnell and Early Wisconsin Reid glaciations. They were, however, subjected to at least two much earlier, 'pre-Reid' glacial episodes (Bostock, 1966, Hughes, 1987).

The economic placers in Nansen Creek have been reported to occur upon a "boulder clay" horizon, which may represent a till left by one of these early glaciations (Bostock, 1936a; 1966).

Gravels are often frozen, range in thickness from 1 to 8 metres (averaging 5 to 6 metres), with a moderate amount (0.5 to 3 metres) of organic material. Many of the Mt. Nansen gold placers lie above the treeline.

Previous Work

J.B. Tyrrell and R.G. McConnell commenced the first of the annual Yukon geological surveys in 1898. Tyrrell was assigned the area west of Lewes (now Yukon) River and south of Fort Selkirk. In July of 1898, Mr. Tyrrell completed a compass and pace survey from Hutshi Lakes along the Nordenskiold River to its confluence with Lewes (Yukon) River. In August, Tyrrell traveled south on the Nordenskiold River to a western tributary (probably Rowlinson Creek), following it to the headwaters of a southern branch. He then crossed over a range of granite mountains to the Nisling River, which he followed west to the Hutshi-Fort Selkirk trail, and then turned south towards Aishihik. Mr. Tyrrell's references to the geology of the area (Tyrrell and McConnell, 1898) include noting the more or less severely glaciated character of the area, with many valley bottoms filled with unstratified boulder-clay or till and the presence of terraces of stratified clay, sand or gravel. He also mentions that fine gold is found in some of the tills and gravel terraces where these deposits have been derived from argillite or mica-schist. Most of his references are probably directed towards the Kluane and Aishihik areas and McConnell glacial features of Late Wisconsin age. Specific references to the features of Nisling and Nordenskiold rivers are absent.

Cairnes (1910) briefly described the Quaternary deposits of the area in GSC Memoir 5. Generally noted was the change of topography and deposits from the heavily-glaciated southern Yukon to northwestern margins of glaciation in central Yukon. He noted that near the margins of the glaciation processes of deposition dominate and the result is drift-covered valleys rather than deeply scoured valleys. He also noted that deposits at the glacial limits generally consist of sands and gravels while the finer silts and clays dominate the southern areas. He mentioned the presence of the White River ash, which he estimated to cover an area of at least 25,000 square miles, from Lake Bennett in northern British Columbia to Five Fingers, where it was observed to be 11 inches thick.

Cairnes (1910, 1915a, 1915b) was the first to comprehensively document placer mining activity and describe the surficial deposits in the area of Nansen and Victoria creeks. Limited geological mapping in 1914 resulted in the production of a geological map (Map 151A) of the 7.5 by 10 mile area which Cairnes designated the Nansen District. A memoir that was to accompany the map was apparently never produced. His observations were, however, documented in the Geological Survey, Department of Mines Summary Report for 1914.

At the time (1914), most of the gold that had been mined from the district came from Nansen Creek and two of its tributaries, Discovery Creek and the East Fork of Nansen Creek (locally designated the East Fork), along with its tributary, the South Fork of the East Fork of Nansen Creek (locally known as the South Fork).

Cairnes (1915a) described Nansen Creek as being floored with a thick deposit of boulder-clay, overlain by a 20 to 25 foot thick covering of sand, gravel and muck. The gold was described as being obtained from the gravels near the surface and also near the gravel/boulder-clay interface, the boulder-clay acting as a "clay bedrock". Discovery claim on Nansen Creek was reported to have produced $1200 to $1500 worth of gold that year, which at $16 US (approx.) per raw ounce is approximately 80 ounces.

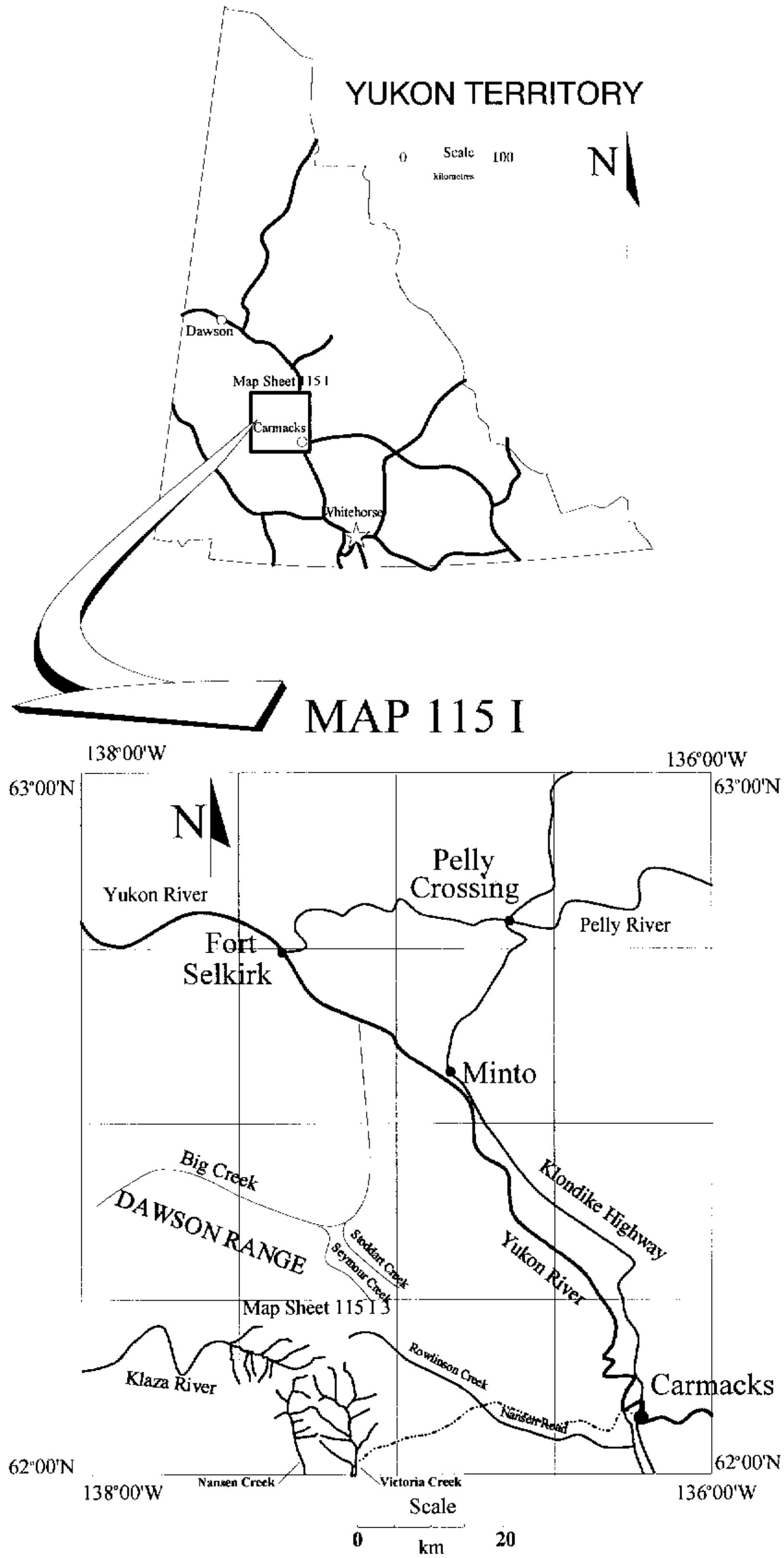

Figure 1 - Location Map - Carmacks Map Sheet- NTS 115I

Another claim on Nansen Creek that year recovered 45 ounces in a two month period, with the total 1914 production estimated at up to 180 raw ounces. Gold was also reported to occur in mineable quantities near the surface in irregular mounds and in "wave-like piles of gravel" between Courtland Creek (a left-limit tributary of Nansen Creek) and the East Fork of Nansen Creek. A Keystone drill was brought in by Mr. Betterton and Mr. Morgan in the winter of 1913-14, and 10 holes were sunk near Discovery Claim on Nansen Creek. These apparently reached into the boulder-clay but it is not known if they reached bedrock. The remnants of this drill currently reside on the left limit of Nansen Creek between Dolly and Weber creeks.

Discovery Creek, and its right limit tributary Eliza Creek, was also producing good values of placer gold. A claim at the mouth of Eliza Creek was reported to have produced $200 to $300 (or 15 to 20 raw ounces) worth of gold in 1912-13. Also in 1912, a Mr. George McDad is reported to have sunk a 20 foot shaft 1.5 miles from the mouth of Discovery Creek, and recovered about 20 ounces of gold. The largest nugget recovered on Discovery Creek was reported to be one ounce.

The East Fork of Nansen Creek to the mouth of South Fork was held in 1914 by three men, Mr. Conrad Printz and Mr. E.L.C. Delapola, who owned the lower 4 claims, and Mr. Albert Cristensen, who owned the upper three claims. The mouth of East Fork to the end of the first four claims (about 2000 feet) contained 6 feet of gravel overlying boulder-clay. Gold grades were reported to be $1.50 per cubic yard, or approximately 0.10 ounces per cubic yard. Continuing up the valley, the boulder-clay is apparently not present in the valley and the gold values occur on or near bedrock, in a 4 to 16 foot thick gravel layer that lies beneath 4 to 6 feet of surface muck. Where cracks and crevices exist the gold extends into bedrock a depth of up to 3 feet. Production from the East Fork was estimated at the time to total 150 raw ounces of gold.

Two miners, a Mr. Miller and a Mr. Shaw, worked the South Fork near its mouth in the winter of 1913-14. They reportedly hoisted gravel through a shaft a distance of 20 feet to bedrock, and recovered $1200 worth of gold from 4500, 8 pan buckets, which would be a grade of about 0.29 ounces per cubic yard. A lustrous black telluride mineral was apparently associated with and often attached to the gold.

Weber Creek at the time was being worked by Mr. Courtney Mack. The section is described as 3 to 6 feet of muck overlying boulder-clay which extended down to bedrock.

A right-limit tributary of Victoria Creek, Back Creek, was reported to be mined by Mr. John Rymar in three shafts which sunk to bedrock 26 to 30 feet below the surface.

Cairnes (1915a) estimated the total gold production from 1910 when mining began to 1914 was $5000 to $7000, or 310 to 440 raw ounces.

H.S. Bostock commenced geological mapping in the Carmacks area during the 1931 field season. Bostock (1934) mentioned that five miners were working on Nansen Creek and its tributaries while two men were working on Back Creek, and that gold had been recovered from these creeks in the previous twenty years. He noted that the gold-bearing placers of Nansen and Victoria creeks drain bedrock of rhyolite and granite porphyries, although most of the Yukon placers occur in areas of Yukon Group mica schist. Bostock also noted that the placers in the vicinity of Nansen and Victoria creeks occur outside of the limits of the last (McConnell) ice sheet, but that boulder-clay of probable glacial origin had been found in some of the placer workings. Bostock encountered some of this boulder-clay in 1933 and noted that it contained completely rotted pebbles and was buried under "more recent deposits formed by normal erosive agents", probably colluvium and poorly sorted alluvium. Of the presence of placer gold, he noted that when the boulder-clay was present the paystreak rested on it, and where the boulder-clay was absent the paystreak rested on bedrock. Apparently no paystreak was observed on bedrock beneath the boulder-clay. He also observed that glacial deposits of the Selkirk area had been partially destroyed and modified, and these were thought to be older than the most recent glacial deposits (McConnell).

The Nansen District glaciation appeared to be older yet as the evidence of glaciation has been all but destroyed with the exception of the boulder-clay. He surmised that placers in the Nansen Creek area probably formed after the disappearance of the early ice sheet, whose extent is indicated by the high elevation of the boulder-clay occurrences and certain drainage features.

H.S. Bostock's geological fieldwork from 1931 to 1935 resulted in the production of GSC Memoir 189, Carmacks District, Yukon, which described in detail the hardrock and placer deposits of the area. He described the boulder-clay in the vicinity of Nansen Creek as the oldest glacial deposits in the district.

TABLE 2 - LEGEND

Mt. Nansen area - Creeks and Roads

3000 feet ASL	5500 feet ASL
3500 feet ASL	6000 feet ASL
4000 feet ASL	Secondary Roads
4500 feet ASL	Creeks and Rivers
5000 feet ASL	EFN 3-2 Section Location

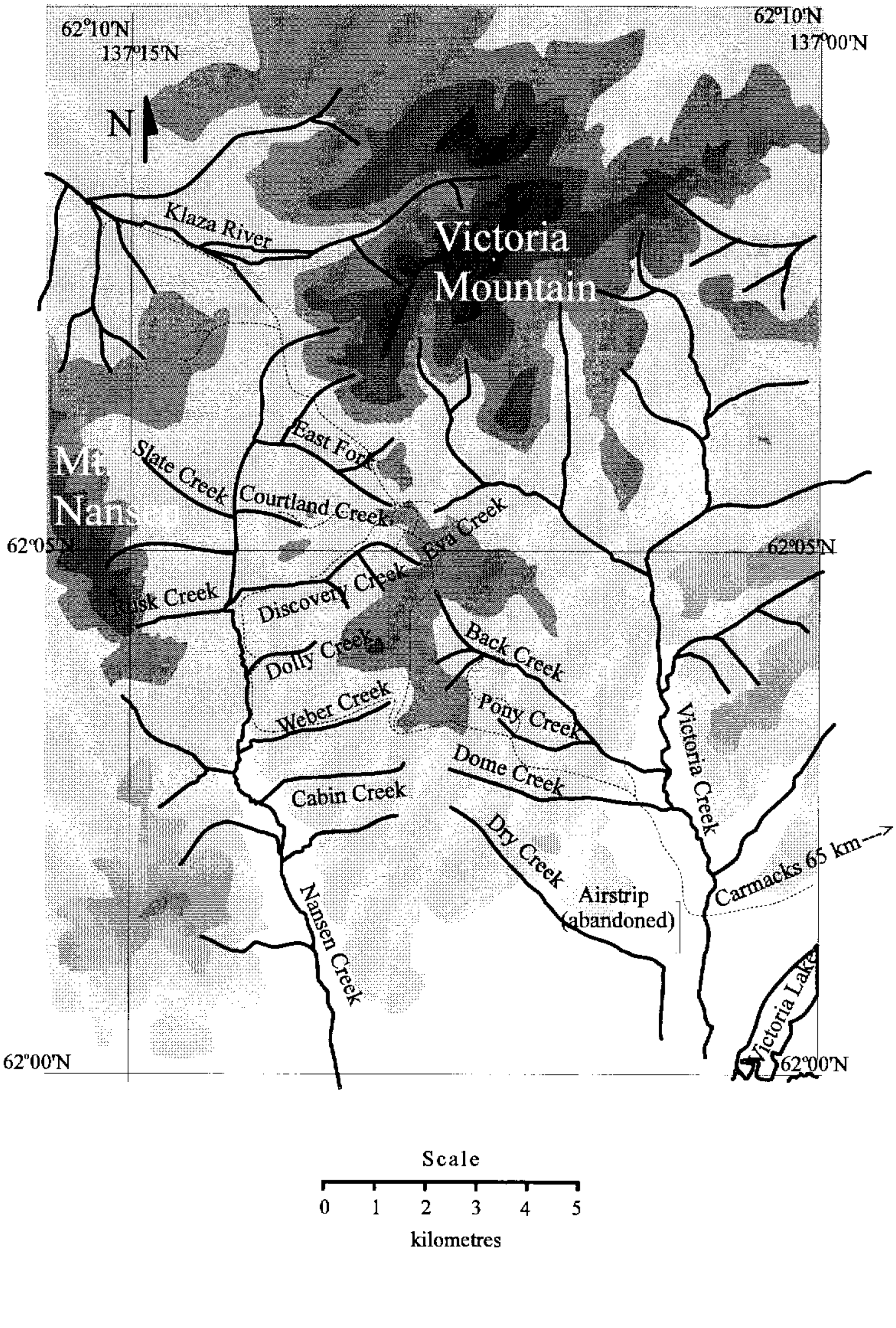

Figure 2 - Mt. Nansen Field Area - Creeks and Roads

A section on Back Creek was described by Bostock as muck, underlain by rusty stream gravel and sand, underlain by brown clay with fragments of rock and in places, rusty stream gravel and sand, underlain by blue clay holding fragments of rotted schist and granite and striated clasts of andesite, 4 to 12 inches long. He asserted that the blue clay is the remnant of an old glacial boulder-clay, and that the overlying deposits are due to normal erosion. He also noted that except for the presence to certain sand terraces and this blue boulder-clay, the area exhibits features of an unglaciated terrain. Miners at the time noted that this blue clay is present at the base of many placer cuts, and that no pay was found under it on bedrock. He noted that most of the placers were noted to occur at the heads of creeks where the quantity of water was small and bedrock was not exposed. One feature that Bostock noted is the presence of large quantities of sand, especially in the vicinity of Nisling River valley and in the upper reaches of Victoria Creek. This sand forms terraces which slope both downstream and towards the middle of the valley in which they lie. He noted that it was moderately fine, and was composed of mostly quartz and feldspar. He could discern no signs of stratification. He speculated that this sand was deposited in an ice margin lake on top of moraine-enclosing stagnant ice. Bostock also noted that the sands, gravels and boulder-clays associated with the last glaciation showed remarkably little weathering. A layer of white ash was also noted near the surface. He also referred to another, similar layer of ash 6 inches to 4 feet below the first, the two layers being separated by fine soil or sand. This lower ash was exposed on a few cut banks in the Pelly and Yukon River. Bostock reported that the character of the gold recovered varied from fine, rough and wiry gold in the upper reaches of tributaries, with fair proportions of coarse and rounded gold in the lower reaches of tributaries, to largely fine gold in the main valley of Nansen Creek. The associated heavy minerals included galena, barite, pyrite and sphalerite. It was noted that the economic placers occurred in areas of acid Tertiary intrusives and that they formed after the last glaciation in the area.

Bostock (1935,1936b,1937,1938) noted that placer mining continued in the Nansen Creek district from 1934 to 1937, with some lode prospecting in 1935 and "exceptionally good cleanups" (placer gold recoveries) reported on Nansen and Victoria creeks in 1936.

No further work in the area was documented until H.S. Bostock described the placer deposits of the area in GSC paper 65-36. Bostock described a till seen in 1947 at the 4000 foot elevation in the upper reaches of Discovery Creek. Above the 4600 foot level he described a section of over 20 feet of rotten gravel on deeply-weathered bedrock, overlain by angular gravel and soil. Bostock suggested that the gravel belonged to the same glaciation that left the till below. An early date was suggested for this advance, because of the lack of noticeable glacial topographic features, the presence of gold-bearing placer gravels on top of the till, and the extensive modification due to solifluction over the till and gravel. It was with this evidence that this event was named the Nansen advance. He also suggested that due to the high elevation of the deposits the advance probably existed beyond the locality in which they were found.

On the basis of airphoto interpretation and fieldwork, Bostock (1966) surmised that along the Klaza River between the present headwaters of Lonely Creek and the mouth of Magpie Creek are several topographic and drainage features which show that a drainage reversal had taken place. The divide between Lonely Creek and Klaza River lies in a large open valley. Klaza River from the divide to Magpie Creek has a terrace that slopes against the present stream direction, towards Lonely Creek. Two large tributaries enter Klaza River at an obtuse angle, turning more than 90 degrees to enter the main stream. Klaza River, at least as far as Magpie Creek, therefore formerly flowed southeast down Lonely Creek valley, the drainage reversal being caused by ice blocking of Lonely Creek valley. Lonely Creek and a parallel creek to the southwest have hummocks of drift and scattered ponds in their wide valleys. Because of the freshness of the hummocky topography along Lonely Creek and Klaza River above Magpie Creek and the relatively older character of Klaza River below Magpie Creek, Bostock suggests that the drainage reversal happened earliest during the Nansen advance and the drift was left by a later, Klaza advance. He also noted that the general levels of the drainage reversal features and where he described the Nansen till roughly corresponded. Thus, he differentiated between the Nansen (oldest) and Klaza (youngest) glacial advances.

Hughes et al. (1968) described the Mt. Nansen area in GSC paper 68-34. A glacial map of Yukon

Territory south of 65 degrees latitude was produced. The limit previously mapped by Bostock (1966) as Nansen is listed as pre-Reid, and the limit previously named Klaza is listed as uncorrelated phenomena. This represents a generalization from Bostock's earlier interpretation.

Hughes et al. (1972) described soil development on drift of pre-Reid to McConnell age as part of a field excursion guidebook to Central Yukon for the 24th International Geological Congress.

Quaternary geology, soil development, and permafrost features of Yukon were summarized in the Guidebook to Quaternary Research in Yukon, part of the XII INQUA Congress, by S.R. Morison and C.A.S. Smith (eds.) in 1987.

Klassen et al. (1987) produced GSC Map 9-1985, surficial geology of the East half of 115I, based on fieldwork by Klassen and Morison in 1978-1979. This was the first comprehensive stratigraphic description of the unconsolidated deposits of the Carmacks area.

The bedrock geology of 115 I3 (north half) and 115 I6 (south half) was mapped at 1:50,000 scale by Carlson (1987).

A surficial geology map and accompanying memoir of NTS 115I in four 1:125 000 scale maps is currently being produced by Dr. Lionel Jackson, Terrain Sciences Division, Geological Survey of Canada, Vancouver, B.C.

Rationale and Objectives of Study

It is evident from the preceding summary of previous geological fieldwork that an accurate and comprehensive study of the unconsolidated deposits in the Mt. Nansen area has yet to be undertaken. Previous workers have not sufficiently described the sedimentology of the unconsolidated deposits, or how the deposits are related to the distribution of placer gold. Several questions need to be addressed, including:

1: What is the sedimentology of the unconsolidated deposits of the Nansen and Victoria creeks?
2: How are the unconsolidated deposits distributed?
3: Which facies contain placer gold?
4: Are the previous assumptions made about the Quaternary history of the area (Bostock, (1966); Hughes et al., (1968)), valid, or should they be re-examined on the basis of new geomorphic and sedimentologic data?

The objectives of this study are thus as follows:
1) to describe the sedimentology of the glacial and fluvial deposits;
2) produce a surficial geological map;
3) construct a paleogeographic model;
4) describe the Quaternary history of the area, and;
5) characterize the distribution of gold concentrated in placer deposits.

Field and Laboratory Methodology

Thirty-one gravel sections were described and sampled in the valleys and tributaries of Nansen and Victoria creeks (Table 3, Figure 3). Sections were located on a variety of glacial and fluvial landform types, and were chosen to represent a cross-valley profile in each drainage. Due to the historic placer mining in the area and the subsequent amount of disturbed material, only sections with an overlying layer of White River Ash or a significant thickness of organic material (greater than 0.5 m) were chosen for description. One hundred ninety matrix samples averaging 250 grams each were collected and fifty-three 0.02 m^3 bulk samples were taken from selected units in each section.

Bulk samples were sluiced in the field using a 1.8 m portable longtom sluicebox (Figure 6). The collection mechanism consisted of outdoor carpeting mats overlain by an expanded metal grid. Heavy minerals were hydraulically concentrated in grooves laying perpendicular to water flow. Concentrates were hand-panned and heavy minerals including gold were collected in small vials. Gold content and any unusual minerals were noted in the field.

Following the methods of Folk (1974), matrix samples were air-dried in the lab, disaggregated and dry-sieved through #10, #18, #35, #60, #120, and #230 Tyler mesh screens. Fractions were then weighed and saved in separate bags. The clay-size fractions from eighteen samples were separated and processed by X-Ray diffraction. Several samples from coarser fractions were grain-mounted and examined with a petrographic microscope.

Heavy mineral concentrates were dried and separated magnetically by hand, and gold was hand-separated by panning. Heavy minerals were then examined beneath a petrographic microscope.

Scanning electron microscope analysis was performed on gold samples from Nansen Creek, the East Fork of Nansen Creek, Back Creek and Klaza River. Spectrographic analyses were performed and photomicrographs were taken of selected grains.

Table 3 - Location of Measured Sections

Section name	Creek	Latitude	Longitude	Elevation (feet ASL)
VIC 1-1	Victoria Creek	62°01'30"N	137°03'02"W	3210
VIC 1-2	Victoria Creek	62°01'30"N	137°03'02"W	3220
VIC 1-3	Victoria Creek	62°01'30"N	137°03'02"W	3225
NAN 1-1	Nansen Creek	62°03'42"N	137°13'00"W	3560
DOL 1-1	Dolly Creek	62°03'50"N	137°12'55"W	3600
LBAC 1-1	Back Creek	62°03'00"N	137°05'27"W	3450
LBAC 2-2	Back Creek	62°03'00"N	137°05'27"W	3450
MBAC 1-1	Back Creek	62°04'00"N	137°08'00"W	4000
UBAC 1-1	Back Creek	62°04'11"N	137°08'40"W	4315
WEB 1-1	Weber Creek	62°03'31"N	137°10'28"W	3950
WEB 2-1	Weber Creek	62°03'27"N	137°10'45"W	3960
EFN 1-1	East Fork	62°05'48"N	137°11'26"W	4040
EFN 2-1	East Fork	62°05'48"N	137°11'26"W	4025
EFN 2-2	East Fork	62°05'48"N	137°11'26"W	4030
EFN 3-1	East Fork	62°05'48"N	137°11'26"W	4005
EFN 3-2	East Fork	62°05'48"N	137°11'26"W	4005
EFN 4-1	East Fork	62°05'42"N	137°11'26"W	4200
DIS 1-1	Discovery Creek	62°04'50"N	137°09'33"W	4370
DIS 1-2	Discovery Creek	62°04'50"N	137°09'33"W	4350
DIS 1-3	Discovery Creek	62°04'50"N	137°09'33"W	4340
DIS 2-1	Discovery Creek	62°05'00"N	137°10'00"W	4170
DIS 2-9	Discovery Creek	62°05'00"N	137°10'00"W	4270
DIS 2-11	Discovery Creek	62°05'00"N	137°10'00"W	4270
DIS 2-12	Discovery Creek	62°05'00"N	137°10'00"W	4270
LDIS 1-1	Discovery Creek	62°04'45"N	137°11'08"W	4000
EVA 1-1	Eva Creek	62°05'32"N	137°08'40"W	4105
EVA 2-1	Eva Creek	62°05'31"N	137°08'51"W	4015
K 1-1	Klaza River	62°07'36"N	137°16'08"W	4000
K 1-2	Klaza River	62°07'36"N	137°16'08"W	4000
K 1-3	Klaza River	62°07'36"N	137°16'08"W	4000
K 2-1	Klaza River	62°07'39"N	137°16'08"W	3980

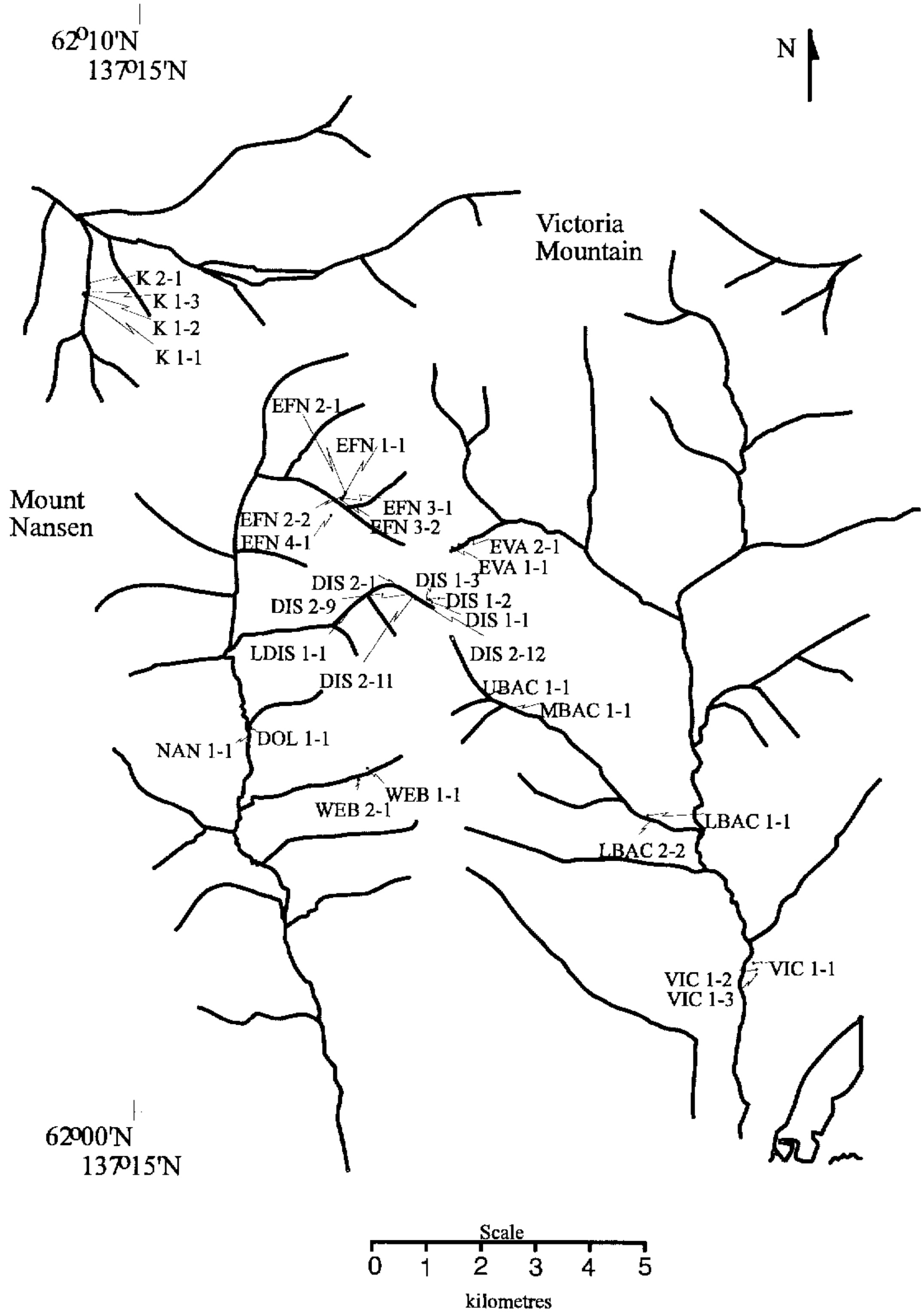

Figure 3 - Mt. Nansen Area - Section Locations

BEDROCK GEOLOGY

Tectonic Framework

Regional stratigraphic analyses of supracrustal rocks show that the North American Cordillera (including Yukon) is comprised of an ancient North American margin onto which suspect or exotic terranes accreted sometime in the Mesozoic (Tempelman-Kluit, 1979a; Monger and Price, 1979; Monger et al., 1982; Coney et al., 1980; Coney, 1989; Hansen, 1989). Although more than 50 terranes have been recognized, those with similar tectonostratigraphic features have been grouped into broad geologic and physiographic belts (Gabrielse et al., 1991). These include (east to west) the Rocky Mountain Belt, the Omineca Crystalline Belt, the Intermontane Belt, the Coast Plutonic Complex and the Insular Belt.

In Yukon, the Rocky Mountain Belt is formed by Mackenzie Platform and Selwyn Basin northeast of the Tintina Trench. The Omineca Crystalline Belt includes the Yukon-Tanana Terrane, Slide Mountain Terrane, and the Cassiar Platform. The Intermontane Belt in Yukon consists of Quesnellia, Cache Creek and Stikinia Terranes which form the Whitehorse Trough. The Coast Plutonic Belt consists of the Windy-McKinley and Nisling Terranes, while the Insular Belt includes the Alexander and Wrangellia Terranes (Wheeler and McFeely, 1991; Gabriesle et al., 1991; Coney et al., 1980; Templeman-Kluit, 1979b).

Yukon is dissected by two major dextral strike-slip fault systems which slice the Territory into three parts. The Tintina Fault lies in central Yukon and is the locus of at least 450 km of dextral strike-slip movement (Tempelman-Kluit, 1979b). Stratigraphic, structural and paleomagnetic evidence suggest a dextral displacement of at least 250 km on the Denali fault in southwest Yukon (Templeman-Kluit, 1981).

Yukon terranes can be grouped into either autochthonous (ancient North American margin) or allochthonous (suspect or transported) terranes. Autochthonous terranes can be further subdivided into displaced continental margin, pericratonic and accreted terranes. Mackenzie Platform and Selwyn Basin form the ancient North American Margin in Yukon, and displaced continental margin includes Arctic Alaska, Cassiar, Nisling and Porcupine Terranes. Yukon-Tanana Terrane is considered pericratonic as it as been interpreted as a distal, mostly clastic part of North American continent which has been sliced off and later, highly deformed and metamorphosed (Wheeler and McFeely, 1991). Slide Mountain , Quesnellia, Cache Creek, Stikinia, and Windy-McKinley form the Intermontane Superterrane. Alexander and Wrangellia form the Insular Superterrane and Chugach Terrane and undivided metamorphics form the Outer Terranes (Wheeler and McFeely, 1991; Coney et al., 1980; Hansen, 1989). The dominant terranes in the Carmacks map sheet (NTS 115I) are Yukon-Tanana, Stikinia and Nisling, which are shown in Figure 4.

Regional Geology

Basement metamorphic rocks of the Yukon Tanana Terrane in the Dawson Range are intruded by hornblende-biotite granodiorite of the Upper Triassic to Jurassic (Gabrielse et al., 1991). Klotassin Batholith and porphyritic syenite and quartz monzonite of the Jurassic Big Creek Plutonic Suite. These are in turn intruded by granodiorite and granite of the Early Cretaceous Dawson Range batholith and intermediate to felsic porphyry dykes, fine-grained biotite granite, andesite to latite massive flows and lapilli tuff, and quartz-feldspar porphyry of the Late Cretaceous (Grond et al., 1984) Mount Nansen Volcanic Suite. The Mount Nansen Volcanics may be cogenetic with parts of the Dawson Range Batholith. The latest intrusion is the Late Cretaceous Carmacks Volcanic Suite, which is relatively flat-lying and consists of basalt flows, andesite flows and associated pyroclastics, and felsic pyroclastics and associated glassy domes or plugs (Carlson, 1987) .

Metallogeny

Mineral deposits present in the area include porphyries, veins, skarns and placer. Porphyry occurrences consist of low grade Cu-Mo mineralization with local, high-level gold enrichment. Breccias and quartz-feldspar porphyry dykes with anomalous precious metal values occur within and peripheral to the porphyry intrusions.

Gold and silver-bearing quartz veins also occur proximal to the porphyry intrusions and are related to NW and NE-trending fracture systems. Intrusions in calcareous metasediments of Yukon-Tanana Terrane often contain gold-bearing iron-rich skarns. Placer deposits of Recent valley alluvium and Pleistocene terraces occur in several areas proximal to felsic intrusions and precious metal-bearing mineral deposits (Carlson, 1987).

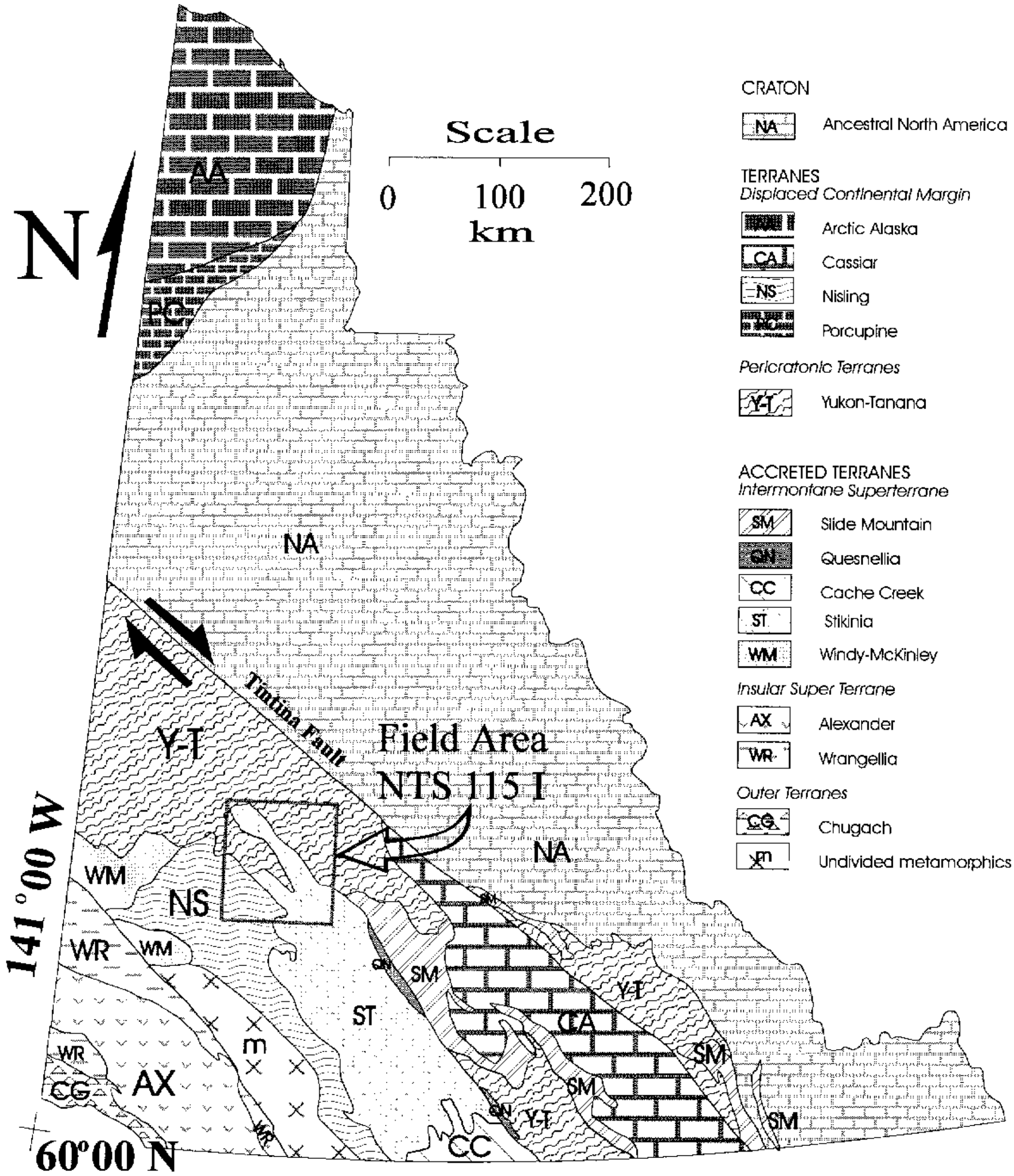

Figure 4 - Yukon Tectonic Assemblages (after Wheeler and McFeely, 1991)

Local Geology

In the southern part of the study area the bedrock consists of Paleozoic and older schist and gneiss of the basement metamorphic complex, while the northern part is dominated by early Cretaceous Casino granodiorite. A mixture of late Cretaceous Mount Nansen andesite volcanics and felsic porphyry dykes occur centrally. A north-trending fault crosses the area along Nansen Creek valley, and two northeast-trending faults cross the area at Weber Creek and north of Courtland Creek. A northwest-trending fault crosses the area roughly from Back Creek, through the upper reaches of Discovery Creek, and then intersects the northeast-trending fault at Courtland Creek. Figure 5 shows the major geological bedrock units present. Table 5 is the legend to the bedrock geology map.

Local Mineral Deposits

Mineral deposits in the study area include the Brown-McDade vein (Au,Ag), Weber and Huestis veins (Au,Ag), the Cyprus porphyry (Cu,Mo), the Esansee or Tawa veins (Au,Ag,Pb,Zn), the Goulter (Au,Ag), Divide (Au) Lonely (Cu,Au), Rusk (Cu,Mo,Ag,Au) and Dows (Au) mineral deposits.

These are shown on Figure 5, and a brief summary of the major characteristics follows:

MINFILE #: 115I 065 (Mount Nansen)
COMMODITIES: Au,Ag
DEPOSIT TYPE: Vein

GEOLOGY

The Weber and Huestis veins are strong shear zones, striking northwest and dipping steeply west, that cut highly altered Paleozoic? schist and gneiss intruded by dykes and stocks of Lower Cretaceous porphyry. Mineralization is associated with lenses of quartz within the shears, which contain pyrite, arsenopyrite and minor amounts of galena, chalcopyrite, sphalerite and various silver minerals.

The Weber and Huestis veins are paralleled by other veins, the most significant of which is the Flex Vein system, however mineralization in the Flex zone is highly erratic. The veins are truncated by a major cross fault at their north end.

Table 4 shows gold and silver ore reserves for the Weber and Huestis veins.

MINFILE #: 115I 064 (Brown-McDade)
COMMODITIES: Au,Ag
DEPOSIT TYPE: Vein

GEOLOGY

A 30 metre wide vein-fault which trends northwest and dips steeply west cuts Lower Cretaceous granodiorite and feldspar porphyry of the Mount Nansen Group. The shear zone contains lenses of grey quartz with pyrite and arsenopyrite and minor chalcopyrite, galena, tetrahedrite, sphalerite and stibnite. Haloes of lower grade mineralization and argillic alteration surround the high grade veins.

Proved open pit reserves consist of 124,600 tonnes grading 10.4 g/t Au and 98 g/t Ag and probable underground reserves are 193,706 tonnes grading 14.5 g/t Au and 100 g/t Ag.

MINFILE #: 115I 066 (Cyprus)
COMMODITIES: Cu, Mo
DEPOSIT TYPE: Porphyry

GEOLOGY

Pyrite, chalcopyrite and molybdenite occur as disseminations and in quartz veinlets and are mainly concentrated within the phyllic phase of a concentric alteration zone peripheral to breccia bodies. The breccias are associated with a complex of subvolcanic plugs and dykes of rhyodacite porphyry, and quartz-feldspar porphyry and andesitic rocks of the Mt. Nansen Group.

Table 4 - Mt. Nansen Ore Reserves

Zone	Category	Tonnes	Au (g/t)	Ag (g/t)
Huestis	proved and probable underground	85 727	14.0	283
Weber	proved and probable underground	58 524	10.9	600
Flex	possible open pit and underground	114 851	7.5	200
Orloff-King	possible open pit	84 584	2.1	52

This complex has intruded a Triassic batholith and several metasedimentary roof pendants. The porphyry complex forms a northwesterly trending zone about 3.2 km long and 1.6 km wide. Two subcircular breccia pipes with a quartz-tourmaline matrix have a maximum diameter of 150 m on surface. Similar breccias found at depth have a matrix of quartz only.

The quartz-tourmaline zone is surrounded by successive phyllic, argillic and propylitic alteration zones. Minor amounts of galena and sphalerite also occur in veinlets within the porphyry complex. Leaching extends to depths of up to 60 m and has resulted in a weak supergene zone 0 to 90 m thick, in which chalcocite coats pyrite and, to a lesser extent, chalcopyrite. Grades vary considerably with the best values in the range of 0.5 to 0.6% Cu and 0.06% MoS_2, associated with fractured zones where supergene chalcocite is well developed. The average hypogene grade is about 0.1 to 0.15% Cu and 0.01% MoS_2. Average copper grades appear to be twice as high in the supergene zone.

Arsenopyrite and pyrite-bearing quartz veins occur in sericitized and argillically-altered northwest-trending shear zones in the granodiorite.

MINFILE #: 115I 067 (Esansee)
COMMODITIES: Ag,Au,Pb
DEPOSIT TYPE: Vein

GEOLOGY

Stringers of oxidized and leached galena, arsenopyrite, sphalerite and pyrite occur in a northwest-trending, 1.6 metre wide vein-fault. This fault dips steeply southwest and cuts a granitic intrusion. Selected specimens of galena-rich mineralization average 2068 g/t Ag, 44.7% Pb, 36.4 g/t Au and 1.3% Zn.

MINFILE #: 115I 084 (Lonely)
COMMODITIES: Cu
DEPOSIT TYPE: Porphyry

GEOLOGY

A small stock of weakly altered, brecciated and pyritized mid-Cretaceous feldspar porphyry contains disseminated arsenopyrite and chalcopyrite. Unaltered feldspar lies to the east and north and unaltered granodiorite lies to the south and west. Quartz stringers in the porphyry occur along a clay-altered, silicified major north-trending structure.

Quartz specimens assayed up to 1.6 g/t Au and 15 g/t Ag.

MINFILE #: 115I 119 (Dows)
COMMODITIES: Au
DEPOSIT TYPE: Vein

GEOLOGY

Gold occurs in chalcedonic quartz-sulphide veins and wide zones of silicification along the margins of manganese-stained and clay-altered quartz-feldspar porphyry dykes. The veins and dykes cut limestone, schist and quartzite of probable Paleozoic age which dip at a moderate angle to the northwest. Several silicified zones occur with arsenopyrite.

MINFILE #: 115I 093 (Goulter)
COMMODITIES: Au,Ag
DEPOSIT TYPE: Vein

GEOLOGY

Two north-trending fault zones are marked by wide anastomosing networks of gold-bearing quartz veins and altered porphyry dykes which extend for more than a kilometre. The zones roughly parallel two north-flowing tributaries of Discovery Creek and are named the Willow Creek zone (east) and the Eliza Creek zone (west). The veins are closely associated with porphyry dykes, are highly altered and oxidized, and contain cerussite or galena, argentite and electrum, along with pyrite, arsenopyrite, sphalerite and chalcopyrite.

In the Willow Creek zone, the host rock is granodiorite, and two sets of veins are recognized. The first phase veins strike NNW and consist of brecciated quartz, calcite, pyrite and arsenopyrite. These veins are surrounded by wide alteration zones and the hanging wall is often faulted. Gold and silver values are generally low, but sporadic values up to 27.4 g/t Au and 102.8 g/t Ag have been recorded. The second phase veins range from 0.5 to 12 metres in width, and form two sets striking NNE and NNW. These veins consist of a cerussite or galena-rich core surrounded by lower grade white vuggy quartz, and a narrow kaolinite alteration halo. Assays as high as 62% Pb and 3428 g/t Ag have been recorded. Supergene oxidation forms veins of white mud. Gold values are erratic and are generally much lower than the silver and lead values. Copper, antimony, zinc and arsenic values are also widely variable.

In the Eliza Creek zone, the host rock is diorite and schist. Multiple parallel veins follow both NNW

Table 5
LEGEND - BEDROCK GEOLOGY

Quaternary

17	Unconsolidated sediments

Late Cretaceous to Paleocene

15	Late intrusions (15c - medium to coarse-grained potassic gabbro)
13	Lower andesite member - Carmacks suite(13at - andesite tuff and agglomerate)

Cretaceous to Paleocene

9	Porphyry dykes (9a - plagioclase hornblende porphyry, 9c- quartz-feldspar porphyry, 9e - gabbro to syenite, plagioclase +/- hornblende porphyry)
8	Bow Creek Granite (8c - pink aphanitic dykes)
7	Mount Nansen Volcanics (7a - andesite to latite flows, 7ax,at - tuff, 7bt - welded vitric tuff, 7c - flow-banded quartz-feldspar porphyry)

Early Cretaceous

5	Dawson Range Batholith (5a - Casino granodiorite)

Early Jurassic

4	Mount Freegold meta-plutonic suite (4a - orthoclase-hornblende porphyritic syenite, 4b - plagioclase-hornbleende monzonite)
3	Klotassin meta-plutonic suite

Paleozoic and older

2	Schist and gneiss units (2c - biotite-quartz-feldspar schist, 2d - amphibolite)
1	Metasedimentary unit (1b - quartz-feldspar mica schist)

Other Features

	Faults
	Contacts
•65	Mineral Deposit - Minfile number
	Roads

for detailed lithological descriptions refer to Carlson (1987)

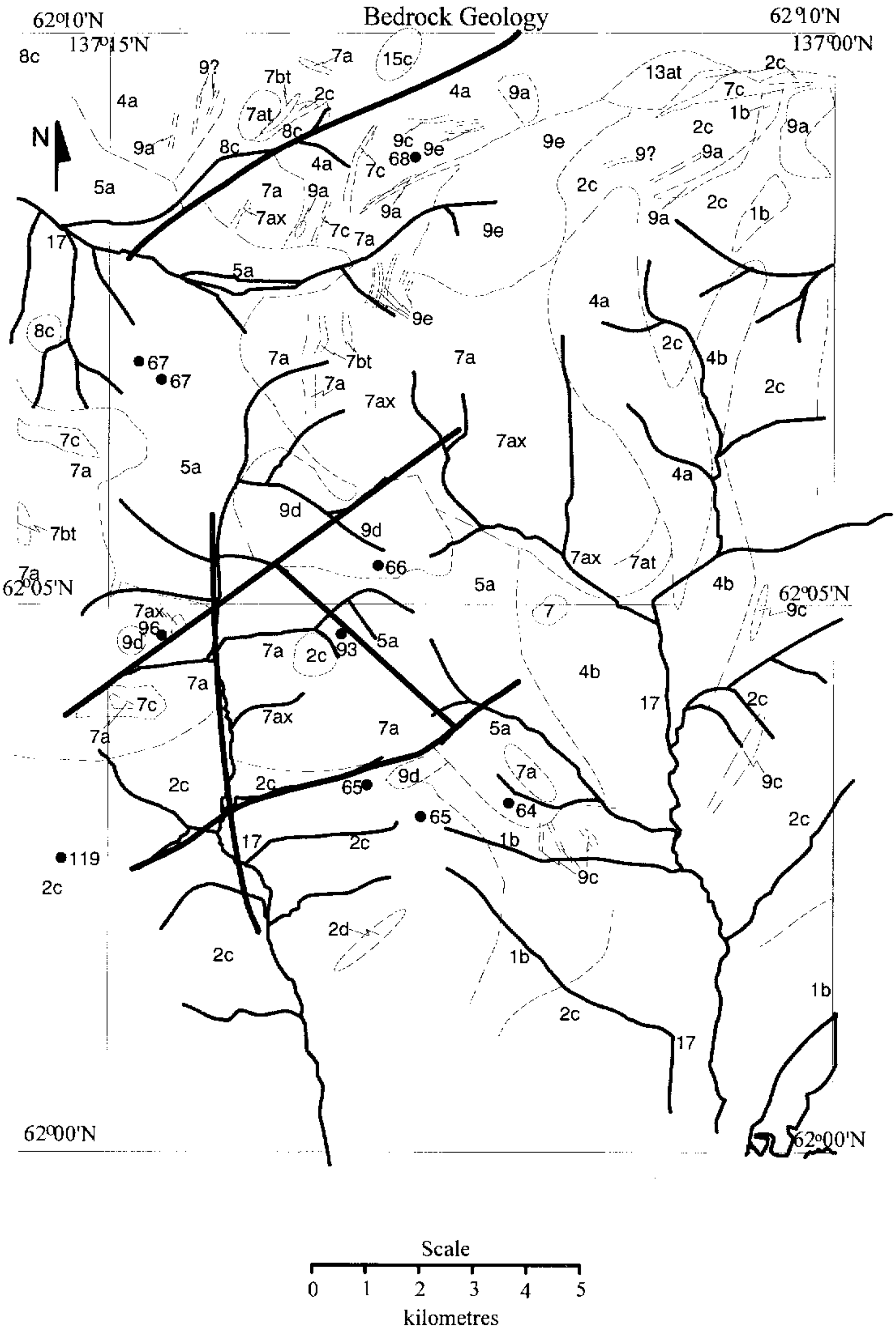

Figure 5 - Bedrock Geology (after Carlson, 1987)

and NNE trends, forming an interconnecting network. Individual veins are up to 12 m wide, sometimes closely associated with subparallel porphyry dykes.

MINFILE #: 115I 068 (Divide)
COMMODITIES: Au,Ag
DEPOSIT TYPE: Vein

GEOLOGY

Quartz veins containing minor sulphides and sporadic high gold values are associated with feldspar porphyry dykes of mid-Cretaceous age which cut Jurassic porphyritic syenite. The main vein structure has been traced for a length of 425 m and grades range from about 15 to 35 g/t Au. Specimens from trenches have assayed up to 98.5 g/t Au and 192 g/t Ag.

MINFILE #: 115I 096 (Rusk)
COMMODITIES: Cu,Mo,Ag,Au
DEPOSIT TYPE: Vein, disseminations

GEOLOGY

Rhyolite of the Cretaceous Mt. Nansen Group is cut by a 1 metre wide vein containing pyrite, arsenopyrite, galena, sphalerite and quartz. Approximately 500 metres west of the vein, finely disseminated molybdenite and chalcopyrite occur with minor pyrite and pyrrhotite in Mt. Nansen Group andesite. Molybdenite also occurs with sugary quartz and minor galena and sphalerite in widely spaced fracture fillings.

Figure 6 - Bulk samples of each facies were sluiced in the field and heavy minerals including gold were collected and examined. The 1.8 m longtom sluice was custom built for Northern Affairs.

PHYSIOGRAPHIC SETTING

Introduction

Nansen and Victoria creeks are situated on the Yukon Plateaus (Figure 7) within the glaciated southeastern tip of the Klondike Plateau. (Bostock, 1948; Mathews, 1986). The limits of several advances of the Cordilleran ice sheet are evident in the form of successive southeasterly retreating glacial deposits and ice marginal features (Figure 8). Near the limits of the ice advances, the tops of many tablelands stood above the ice sheet, especially in the most recent glacial event (Hughes et al., 1972). The most significant topographic feature is the Dawson Range, with its highest elevation reaching 6634 feet (2022 m) at Apex Mountain.

North of the field area the Yukon Plateau is unglaciated, and consists of deep, narrow valleys separated by long, smooth ridges of uniform elevation. Ridges are mainly continuous or connected by high saddles (Bostock, 1957).

The Yukon Plateau exhibits a relief of 2000 feet or more, but the skyline is markedly even interrupted only occasionally by prominent peaks or mountain ranges (Bostock, 1936a). The upland surface of the Yukon Plateau has been least modified on the southwest side of the Dawson Range, where the elevation ranges from 4000 to 5000 feet and streams such as the Klaza River cut in their valleys 1000 to 1500 feet below (Bostock, 1936a).

Discussion

Several modifications in drainage have been noted in the area, and are indicated by the presence of certain geomorphic features. Many valleys contain disproportionately small streams, and several broad valleys in the area contain no streams at all. Open-system pingos, which often form in small valleys with relatively narrow valley floors, are abundant within unglaciated and ancient glaciated parts of the Yukon Plateau, and rare within the limits of recent glaciations (Hughes, 1969).

The drainage of the district is generally trellis-type, with two directions, northwest and northeast being predominant. An unusual, converging, curvilinear drainage arrangement is present in the vicinity of Nansen Creek (Figure 9). Unusually large, sandy fans occupy the major tributary valleys of Nansen and Victoria creeks (Figure 10), forming several levels of terraces that have been dissected in varying degrees.

Unusual drainage features also relate to Lonely Creek and Klaza River. Bostock (1936a) noted that the divide between Lonely Creek and Klaza River is in a nearly flat, large open valley with steep tributary valleys. Lonely Creek flows south and Klaza River flows northwest from the divide. Klaza River from the divide to Magpie Creek is wide and flat, and has a terrace that slopes against the present stream direction, towards Lonely Creek. Other oddities in drainage in this reach of Klaza River have been observed including two large tributaries which enter Klaza River at an obtuse angle, turning more than 90 degrees to enter the main stream. These features suggest that Klaza river, at least as far as Magpie Creek, formerly flowed southeast down Lonely Creek valley.

A similar feature can be observed on the unnamed stream which lies in a northwest-trending valley immediately to the southwest of Lonely Creek. Airphoto interpretation shows that the headwaters of this stream previously extended farther up the valley to the northwest. These previously-existing headwaters now flow southwest and form the easternmost tributary of Schist Creek. These drainage diversions are consistent with the interpretation of Bostock (1936a), who suggested that an ice sheet advanced up Lonely Creek valley, from the southeast to the northwest. The valley that encompasses the unnamed stream immediately to the southwest of Lonely Creek valley must have also contained a tongue of this ice sheet.

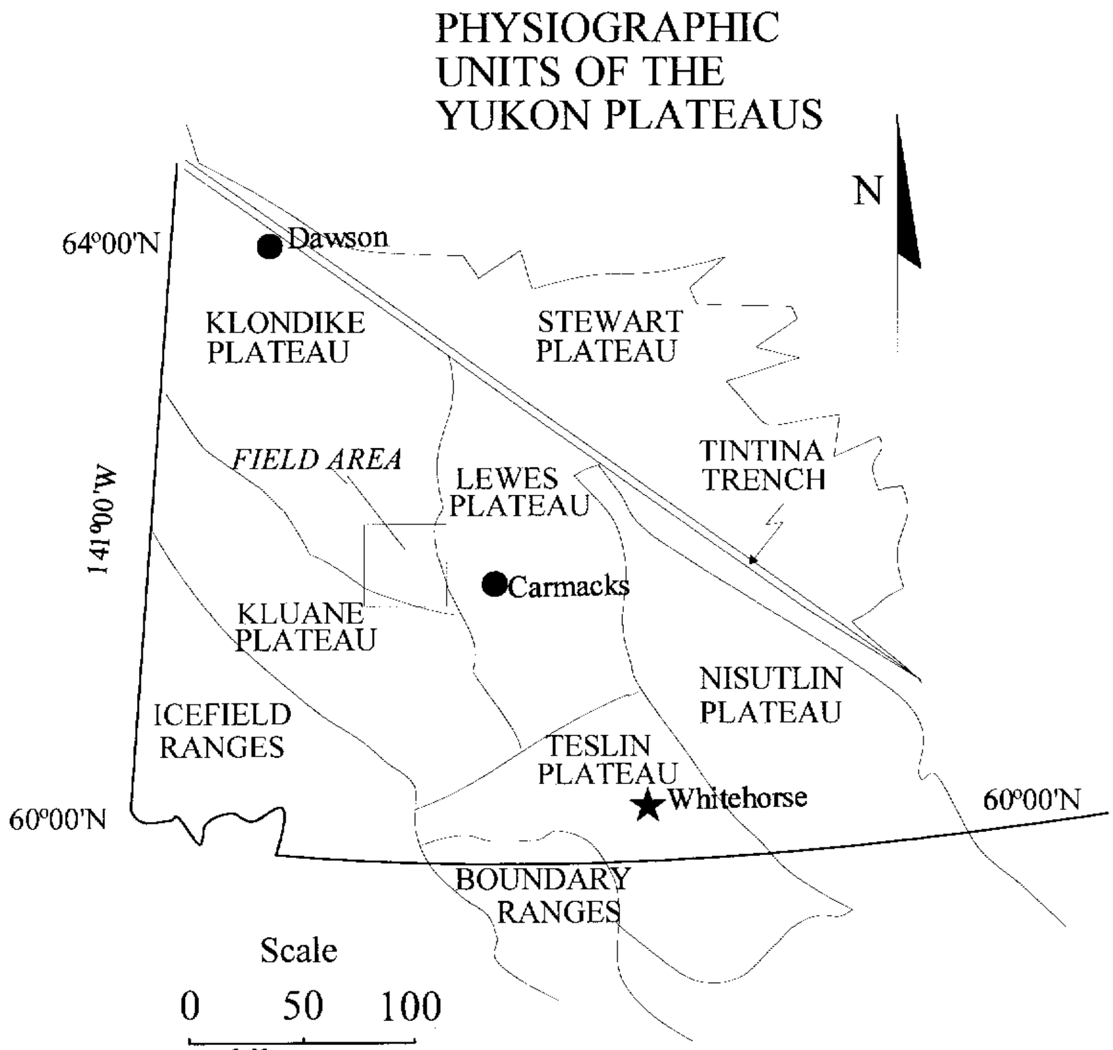

Figure 7 - Physiographic Units of the Yukon Plateaus (modified from Mathews, 1986)

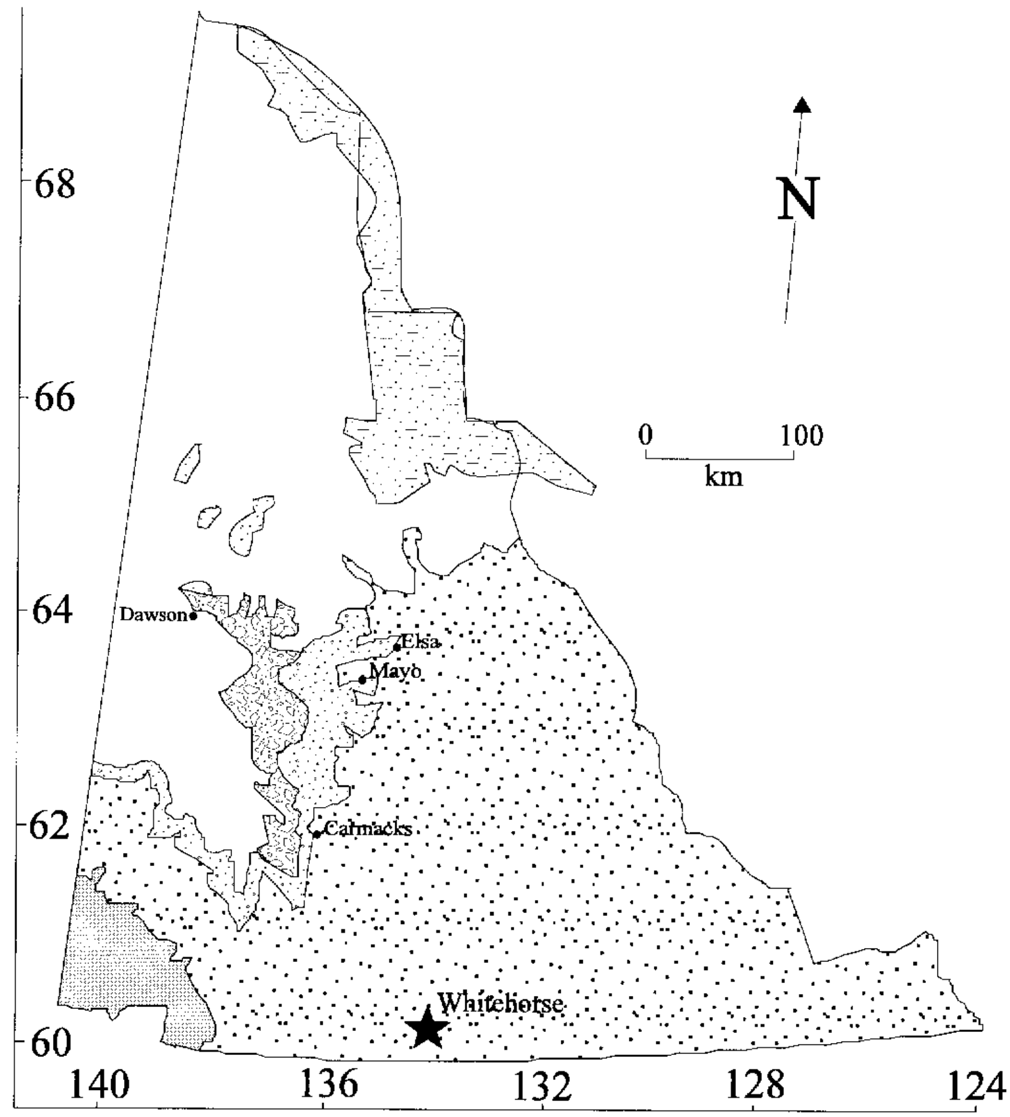

Unglaciated Terrain

Undifferentiated nonglacial deposits

Glaciated Terrain

McConnell glacial deposits

Hungry Creek or Buckland glacial deposits

Reid glacial deposits

Icefield glaciers

pre-Reid glacial deposits

Figure 8 - Limits - Cordilleran Ice Sheet (after Hughes, 1987)

Glacial History and Geochronology

Several glacial events have been described in the central Yukon, including the Nansen (oldest), Klaza, Reid and McConnell advances (Bostock, 1966; Hughes et al., 1968). Glacial features of the Nansen and Klaza advances are very subdued and have not been differentiated outside of the area mapped by Bostock (Bostock, 1966; Hughes, 1987; Hughes et al., 1989). Reid and McConnell glaciations did not reach the Mt. Nansen area, although the area was certainly subjected to the climatic influences of these ice sheets.

At Fort Selkirk, located at the confluence of the Pelly and Yukon Rivers, a cemented till is overlain by a succession of gravel and sand, silt containing 20 cm of Fort Selkirk Tephra, and Selkirk Group basalt (Hughes, 1987; Tempelman-Kluit, 1979a). The Fort Selkirk tephra has been dated by fission-track methods as between 0.84 and 0.94 Ma old (Naeser et al., 1982), while the basalt has been dated by K/Ar methods to be 1.08 Ma old (Hughes, 1987). Bostock (1966) considered the till to correlate with the Nansen or an older advance, while glacial striations on the surface of the basalt were considered to belong to the Klaza advance. The fission-track and K/Ar dates therefore represent a maximum age for the Nansen advance, and a minimum age for the Klaza advance. There are no dates directly relevant to the end of the Klaza or the beginning of the Reid advance (Hughes, 1987), however Cordilleran ice began retreating from the Reid limit more than 42.9 Ka. ago, based on radiocarbon-dated wood found in Sheep Creek tephra (which overlies Reid drift) in the Ash Bend site, Stewart River (Lowden and Blake, 1968; Hughes, 1987). Preliminary dates for Sheep Creek tephra are in the range of 150 Ka. (Duk-Rodkin, pers. comm., 1994), so the Reid ice likely began to retreat prior to that time.

The onset of McConnell glaciation has been recently dated as less than 29.6 Ka (Hughes, 1987), and dates for the retreat of McConnell ice are in the range of 10.3 +/- .15 Ka (Hughes, 1987).

Surficial Deposits

The character of the unconsolidated deposits in the Carmacks (NTS 115I) map-sheet varies considerably. The southeast corner of the sheet was recently glaciated, while the northwestern part of the map-sheet is unglaciated. The central part of the map-sheet is distinguished by subdued, very old, glaciated terrain. The following is a generalized stratigraphic column, adapted from Klassen et al., (1987):

O - organic deposits of peat and muck.
C - colluvium
E - aeolian sand
A - alluvial complexes including fans, terraces, deltas and alluvial valley bottom deposits.
G- glaciofluvial complexes including ice-contact glaciofluvial deposits, meltwater channels, glaciofluvial deltas and glaciolacustrine deposits
M - lodgement and ablation till of varying thicknesses
R - bedrock and bedrock rubble

At least two volcanic events are represented by tephras in the area, the most prominent being the White River Ash. The White River Ash consists of two slightly overlapping lobes, a northern lobe which has been dated between 1500 and 1890 years B.P., and a larger, eastern lobe dated at 1250 years B.P. (Lerbekmo and Campbell, 1969; Lerbekmo et al., 1975). The source of this tephra is Mt. Bona, Alaska, near the Yukon-Alaska border, approximately 250 km west of the field area. A second, lower ash has been described by Bostock (1936a) in cut banks of the Pelly and Yukon rivers, several inches to several feet below the uppermost, separated by a layer of fine sand or silt. In addition, several miners report volcanic ash within their mining sections (LeBarge and Hein, 1990; Placer Mining Section, 1991).

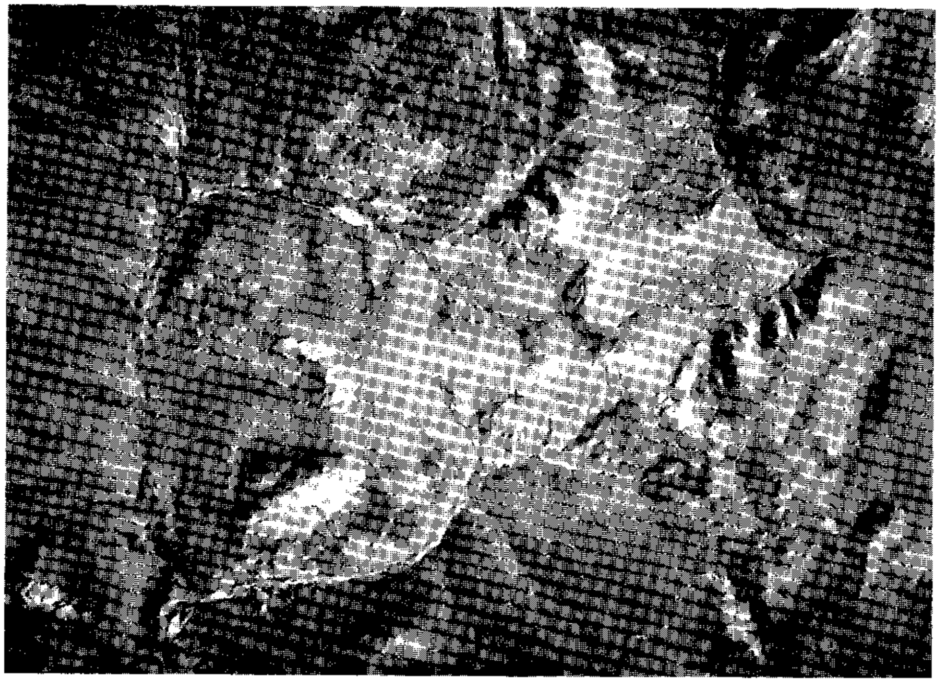

Figure 9 - The East Fork and northern tributaries of Nansen Creek exhibit subdued topography and distinctive curvilinear drainage patterns. NAPL photo A11069-92.

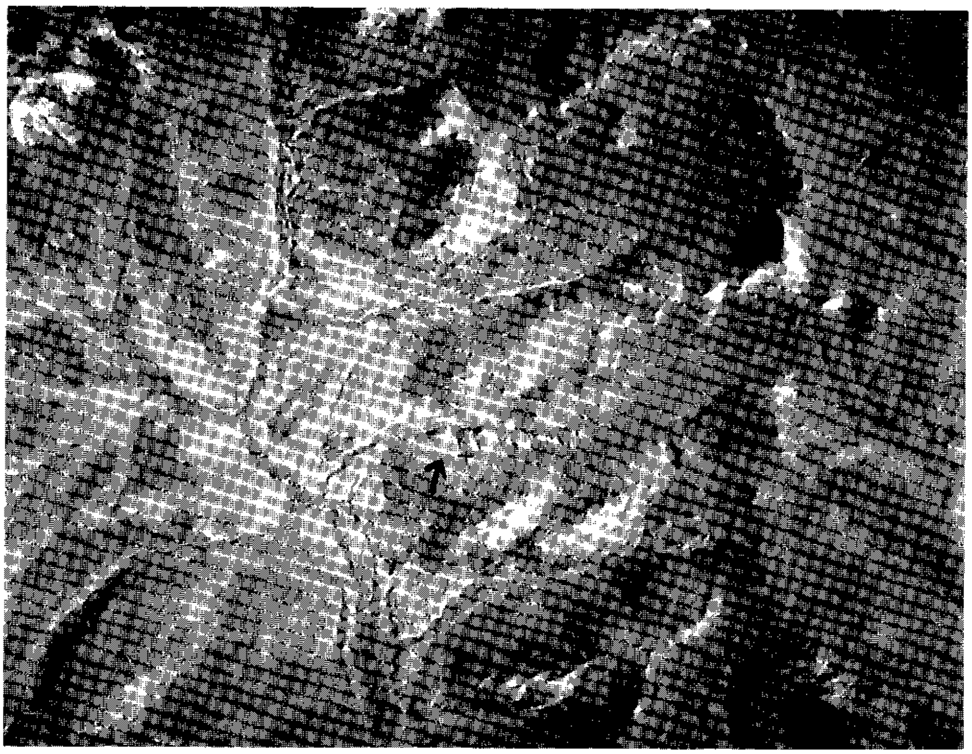

Figure 10 - Large, sandy alluvial fans project from Nansen Creek tributaries Weber and Cabin creeks. Arrow indicates a large dissected terrace on Cabin Creek. NAPL photo A11069-53.

REFER TO COLOUR CD

FACIES SCHEME

Introduction

The term "facies" has generally been used by various authors as the classification of a body of rock or sediment based on a unique set of characteristics that set it apart from other bodies of rock or sediment. Modern usage originated with de Raaf et al. (1965) who used "lithological, structural and organic aspects detectable in the field" to subdivide a group of formations into facies. Walker (1984) noted that this subdivision is essentially a classification procedure which depends on the objectives of the study as well as the time available and the abundance of physical and biological structures in the rocks. Middleton (1978) noted that although facies will ultimately be given an environmental interpretation, the facies definition must be quite objective and based on the total field aspect of the rocks themselves.

The facies scheme utilized in the study area was designed with the above in mind. It was revised throughout the field season and adjusted as new lithologies were encountered. The objectives of the study were constantly kept in mind so that the facies scheme would be neither too simplistic nor too complex to achieve the goals of the study in the amount of time available. Although several facies occurred in widely varying genetic settings, care was taken not to add environmental interpretation into the facies descriptions.

The main characteristics of each bed which were described in the field were: lithology (percent of gravel, sand, silt and clay), maximum grain size (based on ten largest clasts), clast angularity, sedimentary structures, clast support, sorting, contacts, and accessories. Gravel and sand units were described according to the modified Wentworth scale (Wentworth, 1922) and classified according to the AGI (American Geological Institute) classification scheme (Detrich et al., 1982). Table 6 summarizes the main aspects of each facies described.

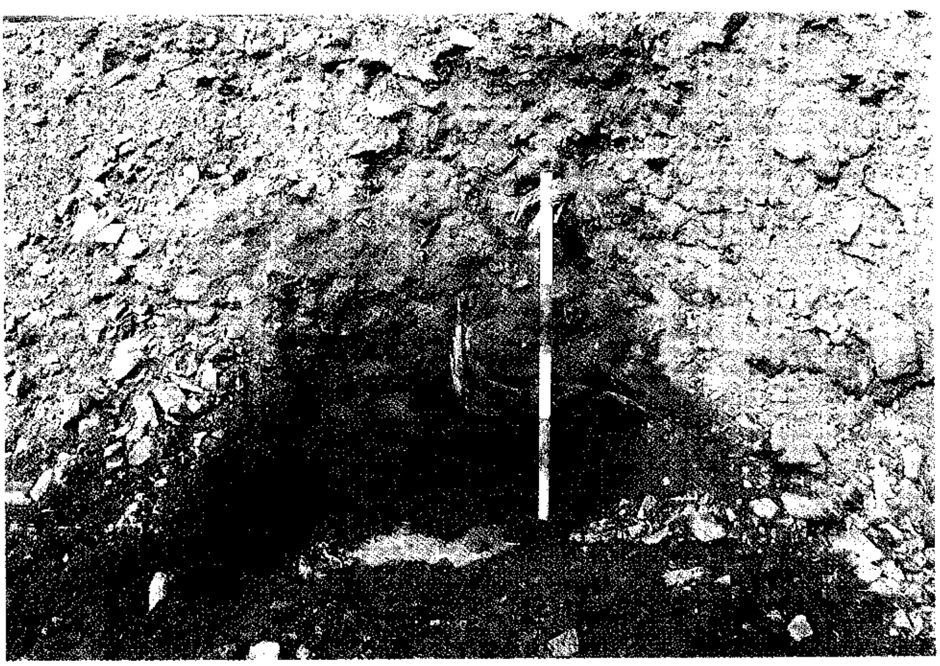

Figure 11 - Measured section K 1-3 shows one of several buried organic horizons (Facies 1) in the Klaza River locality. Note the stump in growth position, which has been radiocarbon dated at 4600a +/- 60 B.P.

REFER TO
COLOUR CD

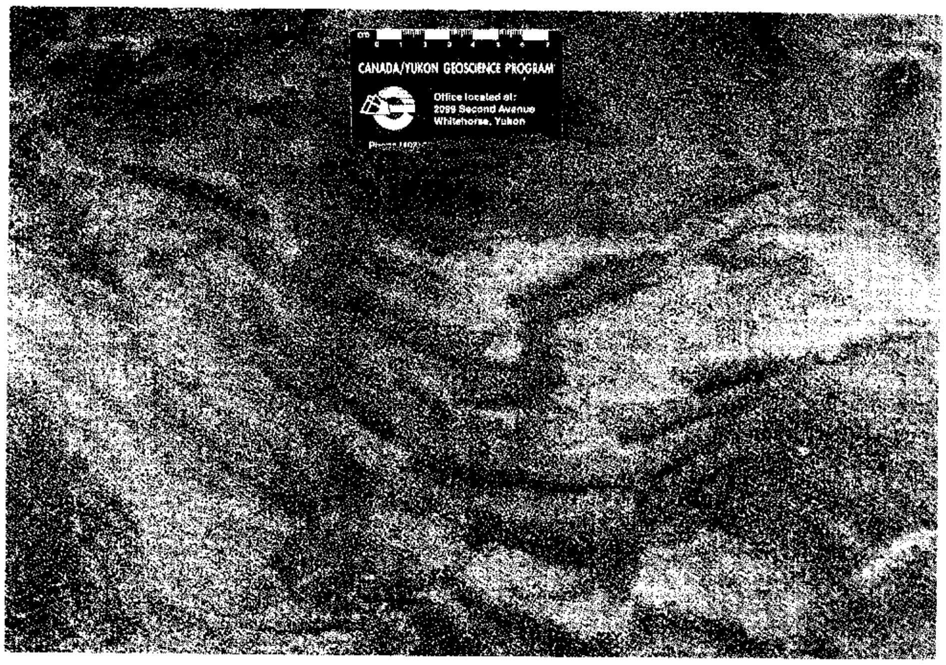

Figure 12 - Facies 2, a convoluted, faulted tephra, lies beneath several feet of mud and fine sand at Eva Creek, measured section EVA 2-1. This unit is also exposed similarly in upper Discovery Creek. White River Ash caps the sequence near the present topographical surface.

General Facies Descriptions

Facies 1 - Organic

This facies (shown in Figure 11) includes recent and older organic material. Organic grade varies from present day and Holocene plant material to fibric peat material found lower in most sections. A total of 41 beds were encountered, comprising 15.24% of the total beds measured. The following sections contained Facies 1: LBAC 1-1, LBAC 2-2, UBAC 1-1, EFN 1-1, EFN 2-2, EFN 3-1, EFN 3-2, EFN 4-1, WEB 1-1, WEB 2-1, K 1-1, K 1-2, K 1-3, K 2-1, EVA 1-1, EVA 2-1, DIS 1-1, DIS 1-2, DIS 1-3, DIS 2-1, DIS 2-9, DIS 2-11, DIS 2-12, LDIS 1-1, VIC 1-1, VIC 1-2, VIC 1-3, NAN 1-1, DOL 1-1.

Facies 2 - Tephra

Two tephras are present. The most recent, found near the present day surface, is the White River Ash (Lerbekmo and Campbell, 1969; Lerbekmo et al., 1975). Its grain size is generally medium sand and it is overlain in most areas by only a few centimetres of organic material. The second tephra (Figure 12) is found associated with silts and fine sands within one metre of the present day surface. It is occasionally found in the same sections as the White River Ash. This ash has yet to be dated. A total of 18 beds were encountered, comprising 6.69% of total beds measured. The following sections contained Facies 2: LBAC 1-1, LBAC 2-2, EFN 1-1, EFN 2-2, WEB 2-1, K 2-1, 1-1, EVA 1-1, EVA 2-1, DIS 1-1, DIS 1-2, DIS 2-1, DIS 2-11, VIC 1-1, VIC 1-2, VIC 1-3.

REFER TO
COLOUR CD

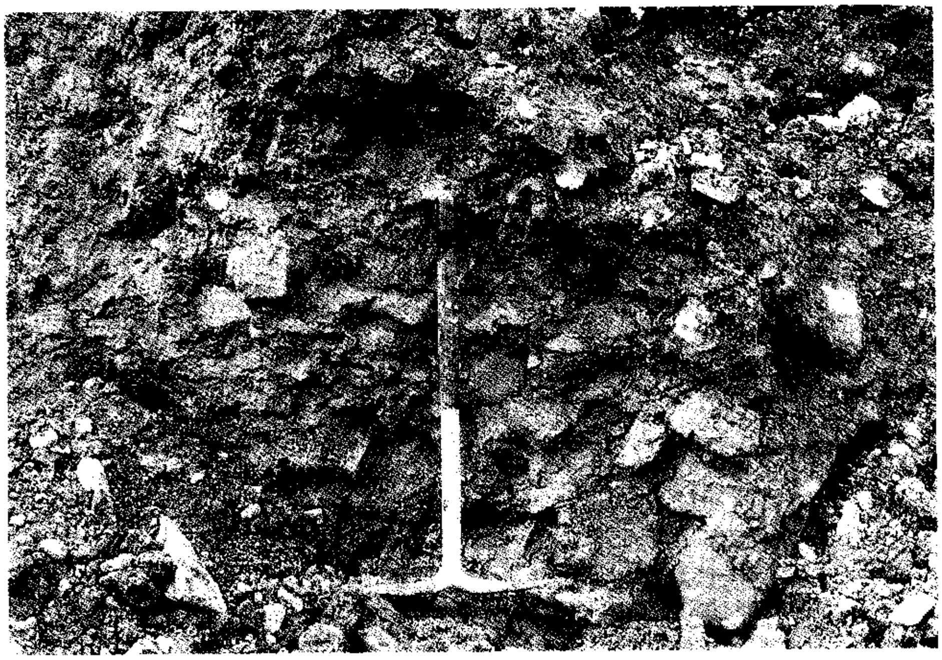

Figure 13 - Facies 3, disorganized cobble-boulder diamicton, occurs in the Klaza River locality, section K 2-1, unit A. Some placer gold has been mined from this unit. The pick is 65 cm long.

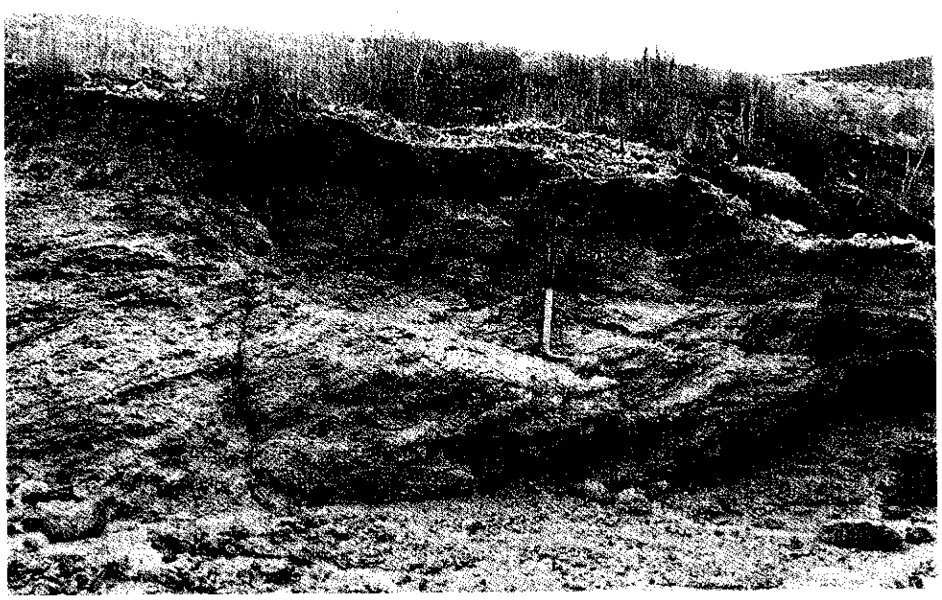

Figure 14 - An unusual stratified pebbly diamicton is overlain by colluvium on the East Fork of Nansen Creek. The unit is clay-rich, contains weathered granodiorite clasts and has strata that dip uphill.

REFER TO COLOUR CD

Figure 15 - Cobbly diamicton of Facies 3 occurs on Nansen Creek, measured section NAN 1-1. This clay-rich unit contains numerous weathered clasts and significant placer gold concentrations.

Facies 3 - Diamicton

This unit varies from clast- to matrix-supported, is disorganized and contains pebble to boulder size clasts in a matrix of clay, silt, and sand. Some units are mud-dominated and some are sand-dominated. It is very poorly sorted, and clasts are angular to subrounded. In many sections this facies is gold-bearing and is mined as the pay unit (Figures 13 and 15). A total of 19 beds were encountered, comprising 7.06% of total beds measured. The following sections contained Facies 3: EFN 3-1, EFN 3-2, WEB 1-1, K 2-1, NAN 1-1, UBAC 1-1.

Facies 4 - Massive and stratified silt and clay

This unit is composed of disorganized and massive to stratified silt and clay, with varying amounts of other minor components including sand and tephra (Figure 16). Pebbles and cobbles comprise less than 25%. A total of 14 beds were encountered, comprising 5.20% of total beds measured. The following sections contained Facies 4: K 1-1, K 1-2, K 1-3, K 2-1, EVA 1-1, EVA 2-1, DIS 1-1, DIS 1-2, DIS 2-1, DIS 2-11, LDIS 1-1.

REFER TO COLOUR CD

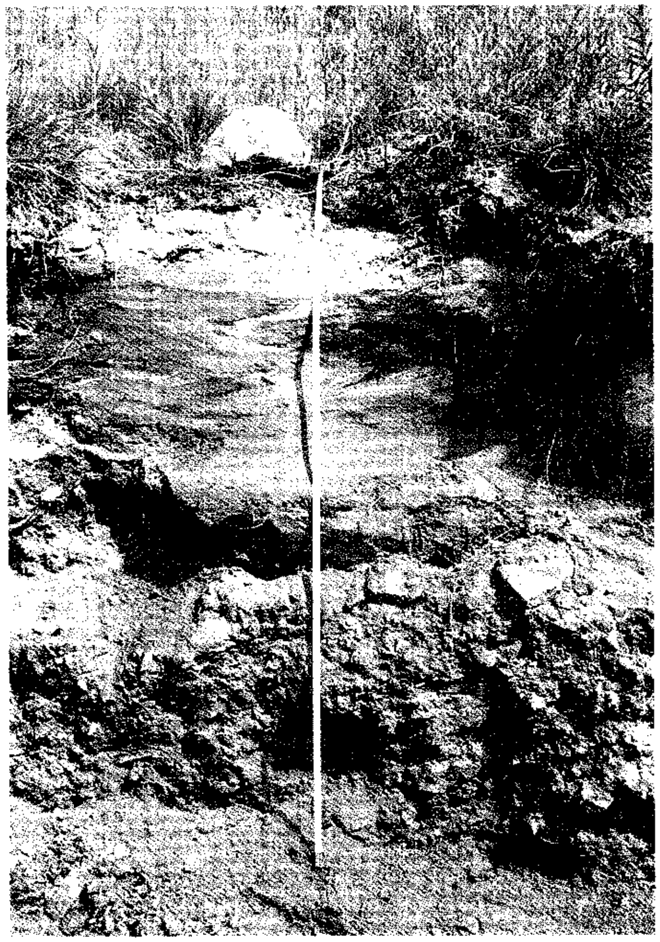

Figure 16 - Stratified silt and clay of Facies 4 overlies disorganized pebble-cobble gravel of Facies 9 at Eva Creek section EVA 1-1, and is in turn overlain by White River Ash. Traces of an older tephra are mixed with the silt and clay.

Facies 5 - Massive and disorganized pebbly sand and sand

This facies is composed of massive to disorganized, poorly- to well-sorted fine to coarse sand (Figure 19). Other fine sediments occur in minor amounts such as mud and tephra. Pebbles and cobbles occur in amounts of less than 25%. A total of 13 beds were encountered, comprising 4.83% of total beds measured. The following sections contained Facies 5: MBAC 1-1, EFN 2-2, WEB 1-1, WEB 2-1, EVA 2-1.

Facies 6 - Stratified pebbly sand and sand

This facies is composed of moderately to well-sorted fine to coarse granular sand with less than 25% pebbles and cobbles. Sedimentary structures include wavy and parallel stratification, planar tabular cross-beds (Figure 17), trough cross-beds, current ripples and convoluted bedding. A total of 34 beds were encountered, comprising 12.64% of total beds measured. The following sections contained Facies 6: LBAC 1-1, LBAC 2-2, MBAC 1-1, EFN 1-1, EFN 2-2, WEB 1-1, WEB 2-1, EVA 2-1, DIS 1-1, DIS 1-2, DIS 1-3, DIS 2-1, DIS 2-9, LDIS 1-1, VIC 1-1, VIC 1-2, VIC 1-3, K 1-2, NAN 1-1, DOL 1-1.

REFER TO COLOUR CD

Figure 17 - Planar tabular cross-stratified pebbly sand (Facies 6) is truncated by pebble cobble gravel of Facies 10 on measured section DIS 1-3, upper Discovery Creek.

Figure 18 - Disorganized muddy pebble-cobble gravel of Facies 7 conformably overlies sandy pebble gravel of Facies 8 at measured section EVA 2-1, Eva Creek.

REFER TO
COLOUR CD

Figure 19 - Massive pebbly sand of Facies 5 and massive sandy pebble-cobble gravel of Facies 8 are intercalated on an alluvial fan in the mid-reaches of Discovery Creek, section LDIS 1-1.

Figure 20 - Disorganized gravel of Facies 9 overlies stratified gravel of Facies 10 at measured section EFN 2-1, on the East Fork of Nansen Creek. This section is highly weathered and is interpreted as pre-Reid glaciofluvial outwash.

REFER TO COLOUR CD

Figure 21 - A pre-Reid glaciofluvial channel (measured section DIS 2-9) cuts bedrock at an elevation of 4270 feet on upper Discovery Creek.

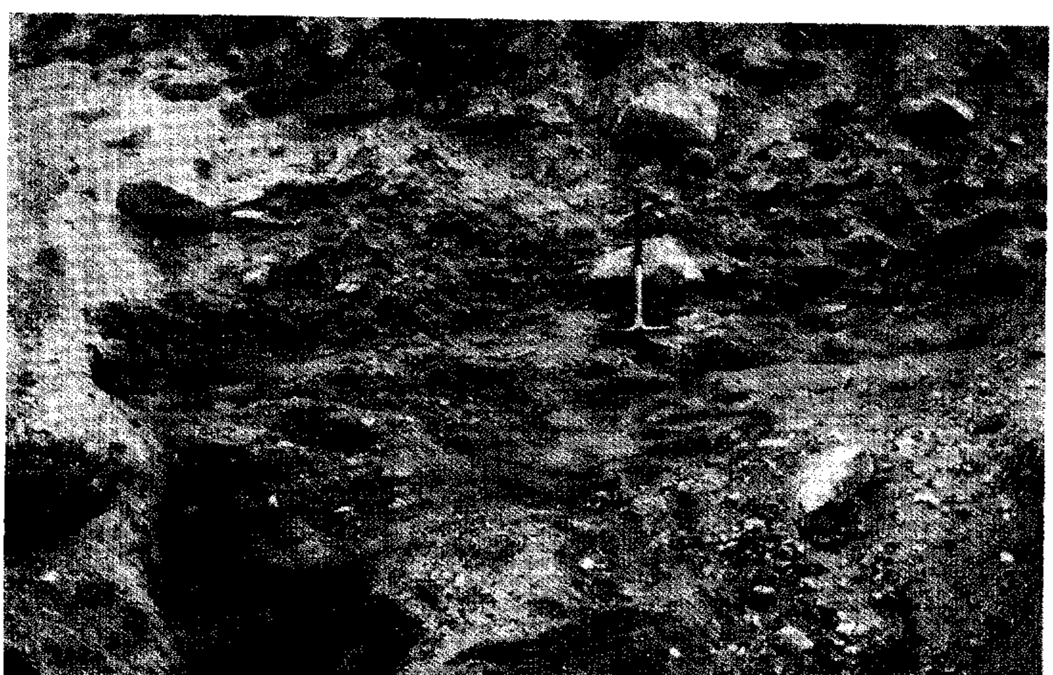

Figure 22 - A close-up of measured section DIS 2-9 shows massive to crudely stratified boulder-cobble gravel of Facies 10. Measured fabric in this highly weathered section shows a paleoflow direction which is transverse to the present valley.

REFER TO COLOUR CD

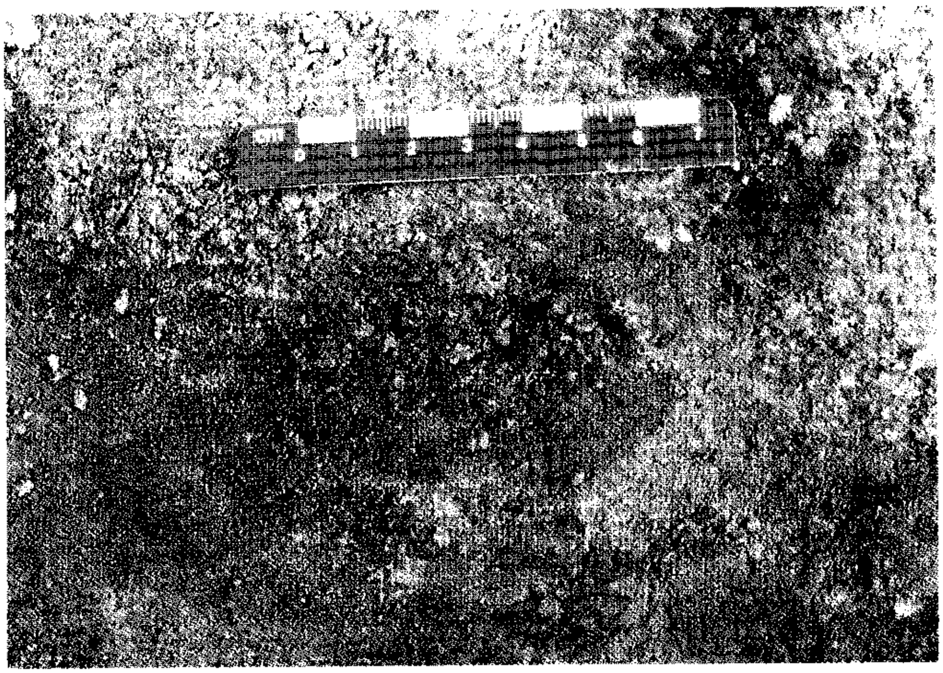

Figure 23 - Weathered arsenopyrite and pyrite occur in clay-altered pods in the bedrock near measured section DIS 2-9. Sulphides can be excavated as medium sand-sized grains.

Facies 7 - Disorganized muddy gravel

This facies is composed of gravels containing between 25% and 50% clasts and more clay and silt than sand. Strata are disorganized or crudely stratified and the units are mainly matrix-supported (Figure 18). Clasts vary from pebbles to cobbles and sorting is poor to moderate. A total of 7 beds were encountered, comprising 2.60% of total beds measured. The following sections contained Facies 7: K 2-1, EVA 1-1, EVA 2-1, EFN 2-1, EFN 2-2.

Facies 8 - Massive and stratified sandy gravel

This facies is composed of gravels containing between 25% and 50% clasts and more sand than clay and silt. Strata are massive, disorganized, or stratified and units are matrix- to clast-supported (Figures 18 and 19). Clasts vary from pebbles to boulders and sorting is poor to moderate. A total of 35 beds were encountered, comprising 13.01% of total beds measured. The following sections contained Facies 8: LBAC 2-2, MBAC 1-1, EFN 1-1, EFN 2-1, EFN 2-2, EFN 3-1, EFN 3-2, WEB 1-1, WEB 2-1, K 1-2, K 1-3, K 2-1, EVA 2-1, DIS 1-1, DIS 1-2, DIS 1-3, DIS 2-11, LDIS 1-1, DOL 1-1.

Facies 9 - Disorganized gravel

This facies is composed of gravels containing over 50% clasts. Units are disorganized and clast-to matrix-supported, and clast size includes pebbles, cobbles and boulders (Figure 20). Sorting is generally moderate. A total of 17 beds were encountered, comprising of 6.32% of total beds measured. The following sections contained Facies 9: EFN 1-1, EFN 2-1, EFN 2-2, K 2-1, EVA 1-1, DIS 1-1, DIS 1-3, VIC 1-3, NAN 1-1, DOL 1-1.

Facies 10 - Massive to crudely stratified gravel

This facies is composed of gravels containing over 50% clasts. Units are massive to crudely stratified and clast-supported, and clast size ranges from pebbles to boulders (Figures 20 to 23). Units are moderately to well-sorted. A total of 71 beds were encountered, comprising 26.39% of total beds measured. The following sections contained Facies 10: LBAC 1-1, 2-2, MBAC 1-1, UBAC 1-1, EFN 1-1, EFN 2-1, EFN 4-1, K 1-1, K 2-1, DIS 1-1, DIS 1-2, DIS 1-3, DIS 2-1, DIS 2-9, DIS 2-11, DIS 2-12, LDIS 1-1, VIC 1-1, VIC 1-2, VIC 1-3, NAN 1-1, WEB 1-1.

Table 6
Summary of Facies Characteristics

Facies	Name	Lithology	Sedimentary Structures	Sorting	Clast Support	Accessories
1	Organic horizons	Recent and older organic material	Undulatory nature	Not applicable	Not applicable	Silt and clay in varying amounts
2	Tephra	Volcanic ash	Convolutions, faulting	Well-sorted	Not applicable	Fine sand, silt and organics
3	Diamicton	Clay, silt, sand and gravel	Disorganized	Very poorly sorted	Clast- to matrix-supported	Gold in significant concentrations
4	Massive and stratified silt and clay	Silt and clay, gravel < 25%	Massive to stratified	Moderately to well-sorted	Not applicable	Fine sand, tephra
5	Massive and disorganized pebbly sand and sand	Fine to coarse sand, gravel < 25%	Massive to disorganized	Poorly to well-sorted	Not applicable	Silt and clay, tephra
6	Stratified pebbly sand and sand	Fine to coarse sand, gravel < 25%	Stratification, convolutions	Moderately to well-sorted	Not applicable	Mn and Fe staining
7	Disorganized muddy gravel	Pebble-cobble gravel 25% to 50%, silt + clay > sand	Disorganized to crudely stratified	Poorly to moderately-sorted	Matrix-supported	Organic material in varying amounts
8	Massive and stratified sandy gravel	Pebble-boulder gravel 25% to 50%, sand > silt + clay	Disorganized to massive to stratified	Poorly to moderately-sorted	Clast- to matrix-supported	Organic material in varying amounts
9	Disorganized gravel	Pebble-boulder gravel >50%	Disorganized	Moderately-sorted	Clast-supported	Gold in varying concentrations
10	Massive to crudely stratified gravel	Pebble-boulder gravel >50%	Massive to crudely stratified	Moderately- to well-sorted	Clast-supported	Gold in varying concentrations

DEPOSITIONAL PROCESSES

Grain Size Characteristics

Field estimates of grain size were completed for all clastic facies. Proportions of sand, silt, and clay were visually estimated, and for gravel units, relative percentages of clasts versus matrix were noted and classified according to the modified Wentworth scale (Wentworth, 1922). The ten largest clasts were also measured and examined for lithology. Matrix samples from all facies were sieved and weighed in the laboratory, and results were plotted for each facies on grain size distribution plots. Grain size statistical data for all facies was generated using the method of moments (Folk, 1974).

Grain Size Distribution

Average matrix grain size distribution for each facies plotted either cumulatively (Figure 24) or individually (Figure 25) show that Facies 1 (organic), 2 (tephra), 4 (massive and stratified silt and clay), and 6 (stratified sand) are dominated by grain sizes of less than .125 mm (very fine sand or finer), while Facies 3 (diamicton) and 7 (disorganized muddy gravel) shows a depletion of the fine to medium sand size.

Cumulative and individual plots of field estimates of overall composition (Figures 26 and 27) show more distinct relationships between each facies. Facies 4 (massive and stratified silt and clay) and Facies 7 (disorganized muddy gravel) show significant amounts of mud, whereas Facies 5 (massive and disorganized sand), 6 (stratified sand) and 8 (massive and stratified sandy gravel) show the significant amounts of fine to medium sand. Facies 8, 9 and 10 show the dominance of gravel while Facies 3 (diamicton) is nearly bimodal with strong peaks in both the mud and gravel fractions.

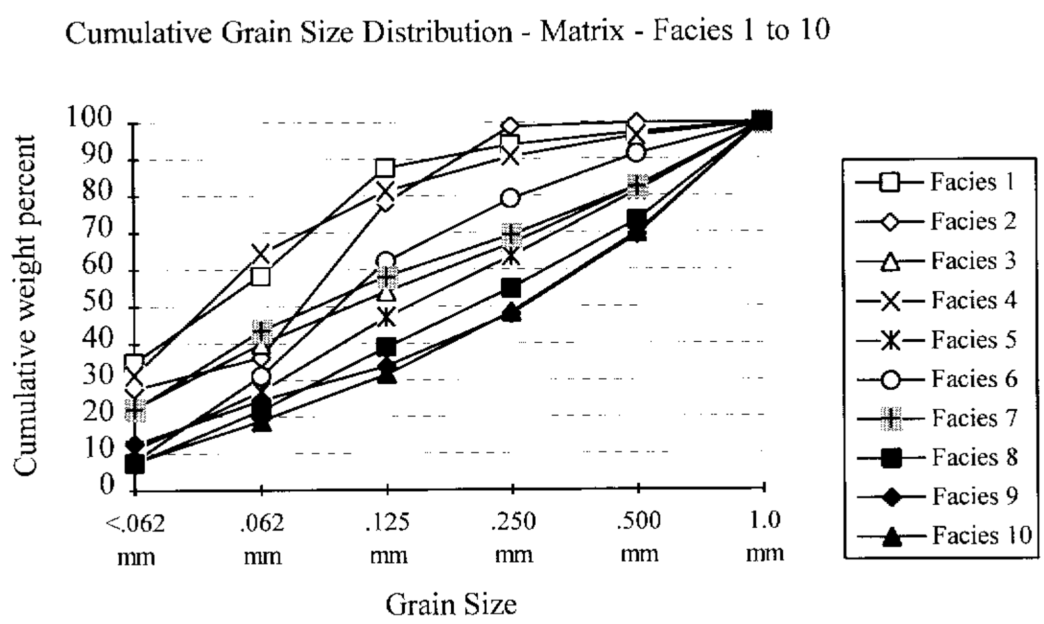

Figure 24

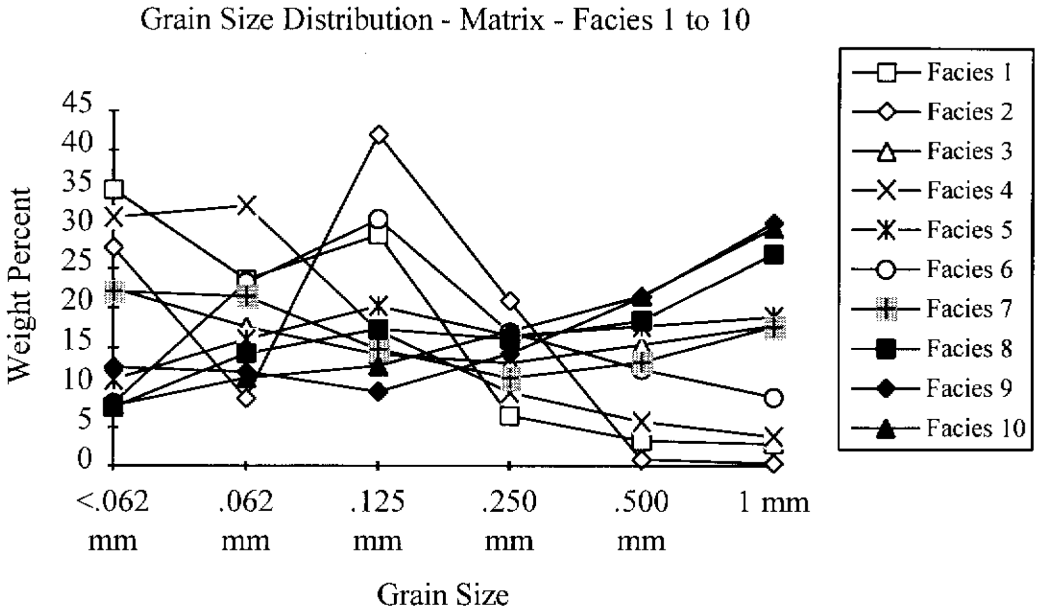

Figure 25

Table 7
Bed thickness and maximum particle size data
MPS - average of ten largest clasts

Facies	Bed thickness - cm average (range)	MPS avg. (cm)	MPS std deviation	MPS min. (cm)	MPS max. (cm)	Number of analyses
3	74.32 (20.0 - 290.0)	22.38	18.44	6.50	153.0	11
4	17.08 (11.3 - 25.0)	11.07	3.39	4.50	19.5	3
5	42.00 (10.0 - 70.0)	7.79	5.34	2.00	27.2	5
6	61.86 (25.0 - 125.0)	6.61	2.68	3.10	18.5	7
7	27.50 (10.0 - 40.0)	12.85	6.81	2.00	32.0	6
8	42.08 (10.0 - 117.5)	11.65	6.19	2.00	36.9	34
9	65.85 (20.0 - 200.0)	15.08	8.21	4.50	49.2	13
10	63.04 (5.0 - 390.0)	13.06	8.36	1.50	59.5	69

Maximum Particle Size (MPS) From Ten Largest Clasts

Maximum particle size data was generally a reflection of sorting. Table 7 shows the average, maximum, minimum, standard deviation and range of values for clast size of each facies based on the ten largest clasts measured in the field. As expected, the diamicton has the largest average, maximum, minimum, range and standard deviation of clast size. The smallest range of values (reflected in the MPS standard deviation) was found in pebbly stratified sand, Facies 6.

Maximum Particle Size (MPS) vs Bed Thickness (Bth)

The relationship between maximum particle size (MPS) and bed thickness (Bth) has been used to distinguish between gravels and conglomerates of various genetic origins (Nemec and Steel, 1984).

Subareal cohesive debris flows can often be distinguished from cohesionless debris flows, and alluvial fans may be discerned from fan deltas. With this in mind, maximum particle size vs bed thickness was plotted for Facies 3 and 7 to 10. These are shown in Figures 28 to 32. In Facies 3 and 7, there was no evidence of a clear relationship between maximum particle size and bed thickness. This is in part due to the small sample size of each facies. For Facies 8 to 10, the relationship was clearer with the best population cluster occurring in Facies 10. This is probably due to the better sorting of this facies. Table 7 shows that the largest average bed thickness was encountered in Facies 3 - diamicton, and the smallest average bed thickness was Facies 4 - silt and clay. The largest range of bed thicknesses was in Facies 10 - massive to crudely stratified gravel, followed by Facies 3 - diamicton and Facies 9 - disorganized gravel. Facies 4 - silt and clay had the smallest range of bed thicknesses.

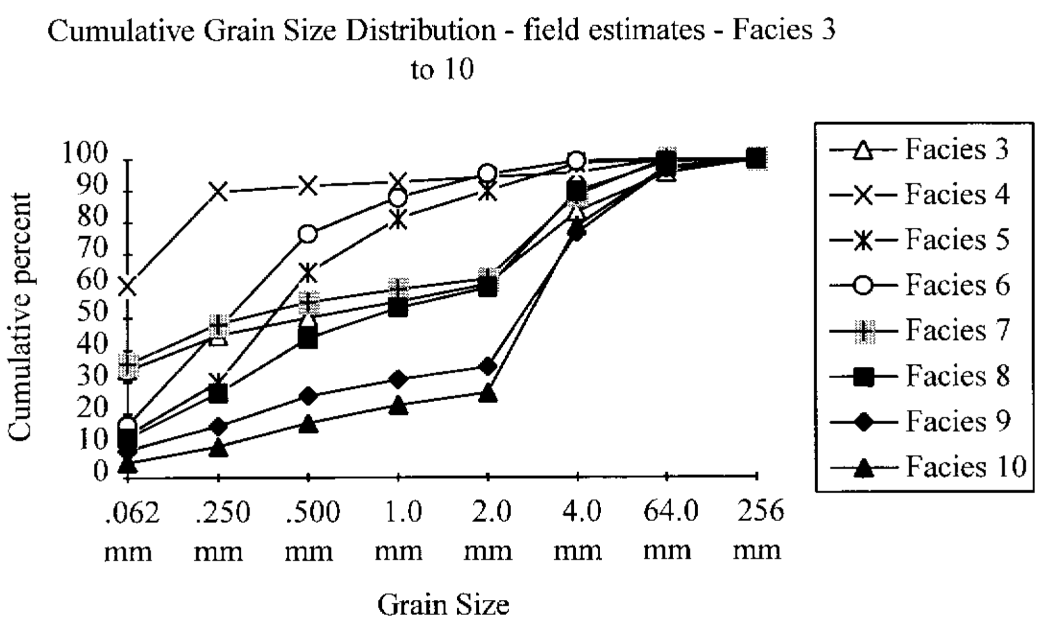

Figure 26

Grain Size Distribution - field estimates - Facies 3 to 10

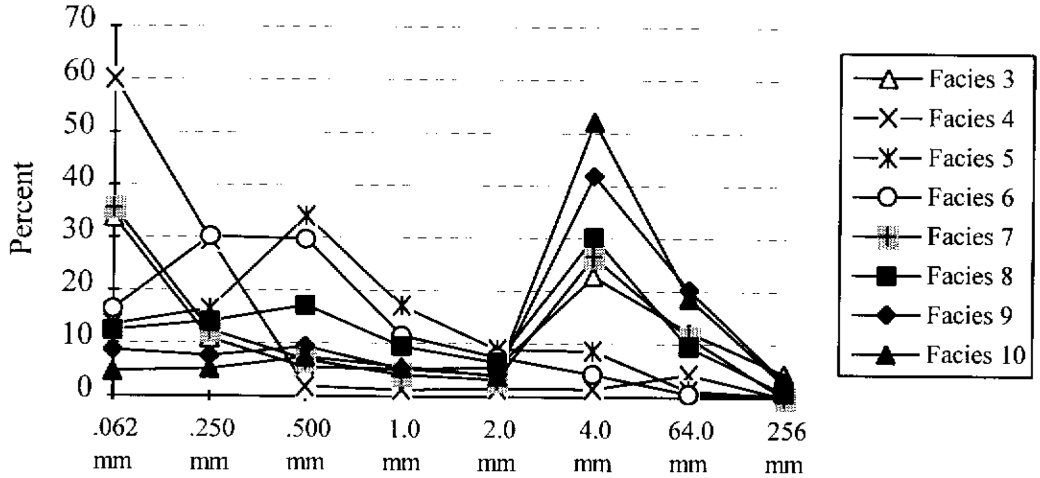

Figure 27

MPS vs. Bth - Facies 3 - Diamicton

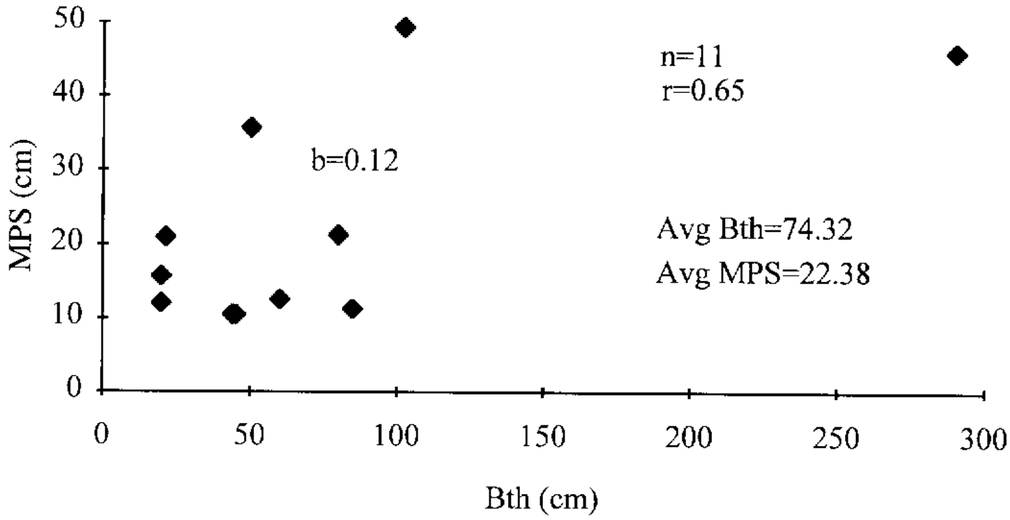

Figure 28

MPS vs. Bth - Facies 7 - Disorganized muddy gravel

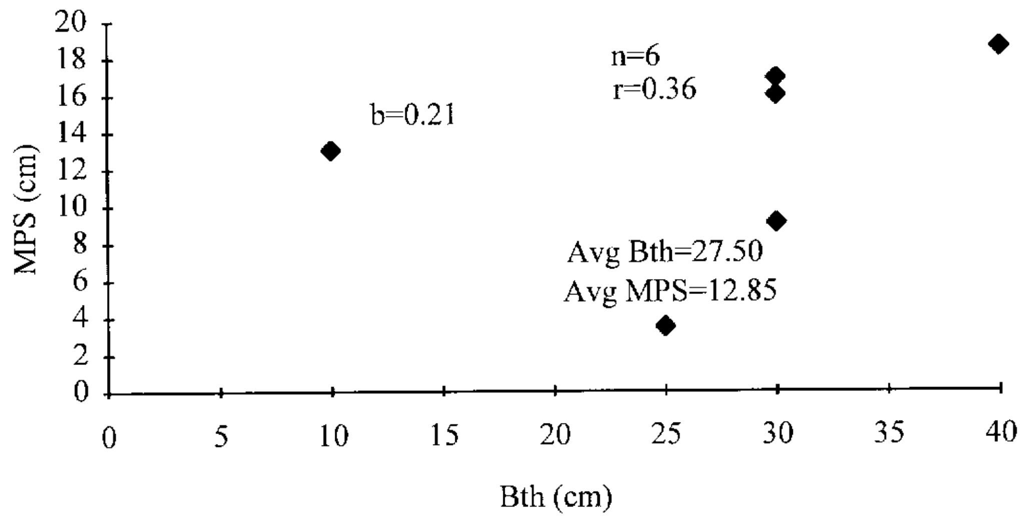

Figure 29

MPS vs. Bth - Facies 8 -Massive and stratified sandy gravel

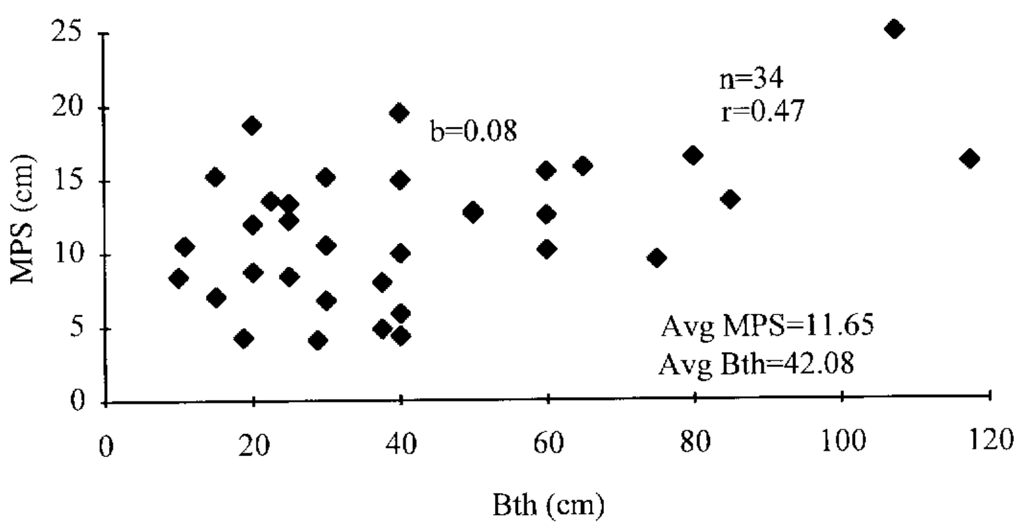

Figure 30

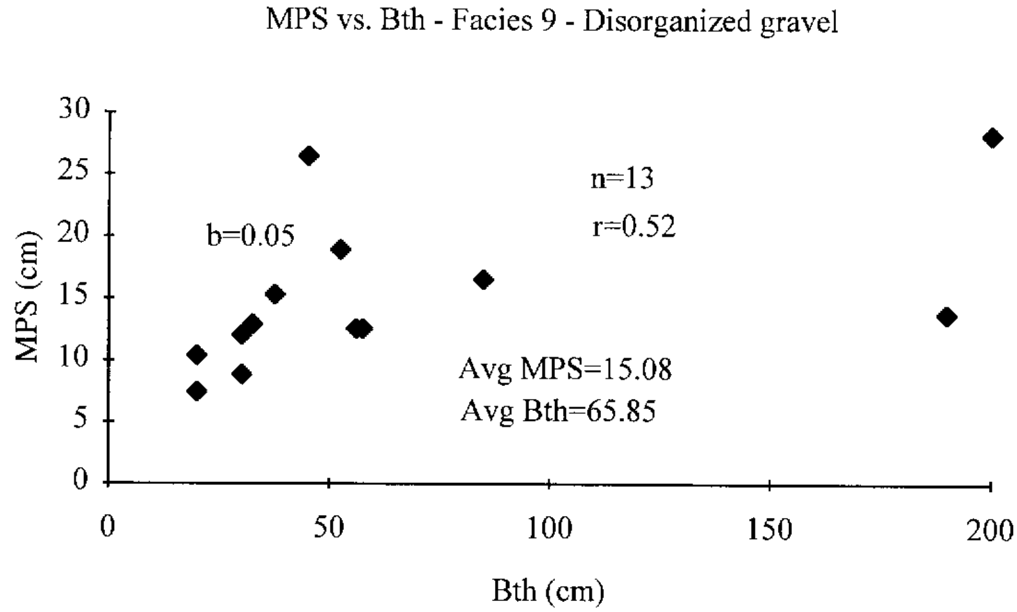

Figure 31

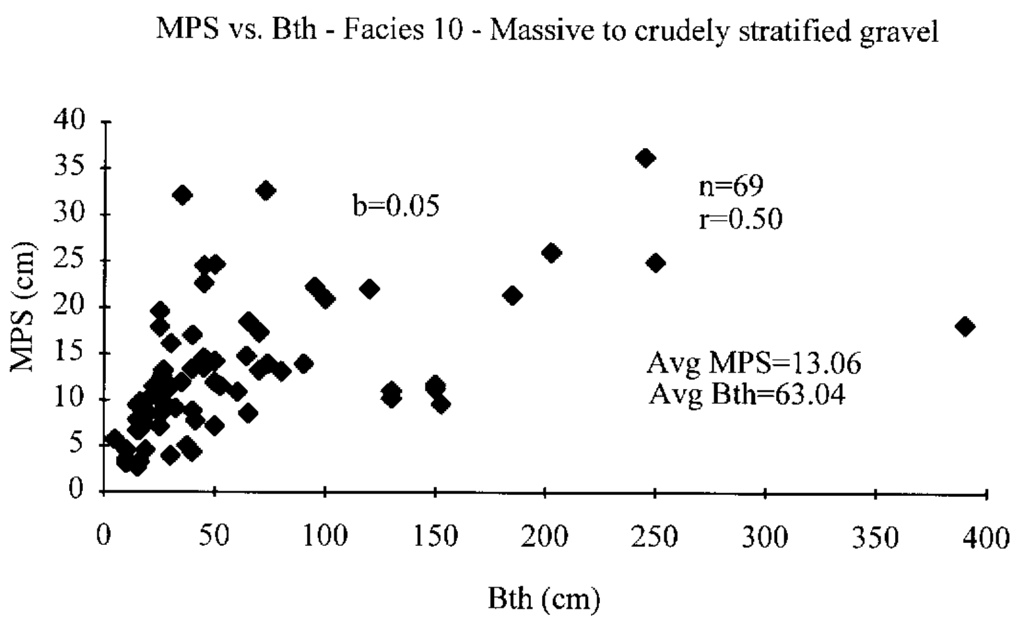

Figure 32

STATISTICAL TREATMENT OF GRAIN-SIZE DATA

Introduction

The following formulas were used for calculating grain-size parameters by the moment method:

Mean (first moment)

$$\bar{x}_\phi = \frac{\sum fm}{n}$$

Standard deviation (second moment)

$$\sigma_\phi = \sqrt{\sum f\left(m - \overline{x_\phi}\right)^2 / 100}$$

Skewness (third moment)

$$Sk_\phi = \frac{\sum f\left(m - \overline{x_\phi}\right)^3}{100\sigma_\phi^3}$$

Kurtosis (fourth moment)

$$K_\phi = \frac{\sum f\left(m - \overline{x_\phi}\right)^4}{100\sigma_\phi^4}$$

where:

f = percent (frequency) of each grain size grade
m= midpoint of each grain size grade in phi values
n= total number in sample; 100 when f is in percent.

Table 8 illustrates the use of this method in calculating statistical grain-size data for the matrix of Facies 3, diamicton. This method was used for calculating grain-size statistical distributions for the laboratory analyses and field descriptions for all facies.

The following are the calculated values corresponding to the variables in Table 8.

$$\sum f = 100.00$$

$$\sum fm = 215.55$$

$$\sum f\left(m - \bar{x}\right)^2 = 328.73$$

$$\sum f\left(m - \bar{x}\right)^3 = -73.31$$

$$\sum f\left(m - \bar{x}\right)^4 = 1731.33$$

Mean $\bar{x}_\phi = \frac{\sum fm}{n} = 2.16$

Standard deviation

$$\sigma_\phi = \sqrt{\sum f\left(m - \overline{x_\phi}\right)^2 / 100} = 1.81$$

Skewness $Sk_\phi = \frac{\sum f\left(m - \overline{x_\phi}\right)^3}{100\sigma_\phi^3} = -0.12$

Kurtosis $K_\phi = \frac{\sum f\left(m - \overline{x_\phi}\right)^4}{100\sigma_\phi^4} = 1.60$

Table 8
Statistical Data for Matrix Component of Facies 3

$\phi(class)$	-1 to 0	0 to +1	+1 to +2	+2 to +3	+3 to +4	>4
$m(midpt)$	-0.50	0.50	1.50	2.50	3.50	4.50
$f(weight\%)$	17.71	15.30	12.99	14.09	17.55	22.36
fm	-8.86	7.65	19.49	35.22	61.41	100.6
$m-\bar{x}$	-2.66	-1.66	-0.66	0.34	1.34	2.34
$(m-\bar{x})^2$	7.05	2.74	0.43	0.12	1.81	5.50
$f(m-\bar{x})^2$	124.9	41.92	5.58	1.67	31.72	122.9
$(m-\bar{x})^3$	-18.72	-4.54	-0.28	0.04	2.43	12.89
$f(m-\bar{x})^3$	-331.7	-69.40	-3.66	0.58	42.65	288.2
$(m-\bar{x})^4$	49.72	7.51	0.18	0.01	3.27	30.22
$f(m-\bar{x})^4$	880.8	114.9	2.40	0.20	57.34	675.7

Table 9 - Matrix Grain Size Distribution - from Lab Analyses
Facies 1 to 10

Facies	Avg. mean (phi)	Avg. std dev. (phi)	Skewness (phi)	Kurtosis (phi)	Avg. Wt. % Mud	Avg. Wt. % Sand	Number of analyses
1	3.22	1.25	-0.92	3.60	34.91	65.09	3
2	2.90	1.14	0.21	1.97	27.57	72.43	4
3	2.16	1.81	-0.12	1.60	22.36	77.64	16
4	3.14	1.35	-1.00	3.30	31.38	68.62	7
5	1.80	1.63	0.08	1.82	10.96	89.04	12
6	2.22	1.38	-0.37	2.37	8.01	91.99	32
7	2.25	1.80	-0.26	1.65	22.03	77.97	5
8	1.46	1.63	0.30	1.85	7.47	92.53	24
9	1.38	1.77	0.52	1.88	12.53	87.47	17
10	1.26	1.62	0.55	2.10	7.67	92.33	66

Discussion

Table 9 shows the statistical data for the laboratory analyses (matrix component) of Facies 1 to 10. Table 10 shows the statistical data for the field descriptions (total grain size distribution) for Facies 3 to 10.

Matrix grain size distribution

Average Mean

The average mean matrix grain-size distribution generally reflects a gradation from clay-rich to clay-poor facies, with the highest average phi values in Facies 3 and 4 and the lowest average phi values in Facies 10.

Average Standard Deviation

The average standard deviation for the matrix grain size distribution is highest for Facies 3, diamicton, which reflects the very poor sorting of the fine portion of this facies.

The next highest average standard deviation in grain size distribution for the matrix is seen in Facies 7, muddy gravel. Gravels and massive sand generally have intermediate average standard deviations (in descending order - Facies 9,5,8,10), which reflects the better sorting of the fine fraction. Lower average standard deviations occur in Facies 6, stratified sand, muddy and organic Facies 4 and 1. Facies 2, tephra, has the best sorting and the lowest average standard deviation.

Folk (1974) assigned verbal terms of sorting to values of standard deviation. Using that classification, the matrix of each facies would be considered poorly sorted.

Skewness

Using the verbal scale of Folk (1974), coarsely skewed Facies include 6,7,4, and 1; while Facies 3 and 5 are nearly symmetrically distributed. Finely skewed Facies include 2,8,9, and 10.

Field estimates of grain size distribution

Average Mean

The average mean grain-size distribution from field estimates generally reflects a gradation from muddy to sandy to gravelly facies with the highest average mean phi values in Facies 4 and 6, intermediate average mean phi values in Facies 5,7 and 3, and the highest average mean phi values in Facies 8, 9, and 10.

Average Standard Deviation

The average standard deviation for the overall grain size distribution from field estimates is highest for Facies 4, which reflects the tendency for this facies to have randomly interspersed clasts (probably derived from colluvium), resulting in poor sorting. Facies 3, 7 and 8 also have high average standard deviations as a result of poor sorting. Lower average standard deviations occur in Facies 9, 6, 5 and 10 which reflects the better sorting of these sandy and gravelly facies.

Skewness

Using the verbal scale of Folk (1974), Facies 8 and 3 are strongly coarse skewed, Facies 9,7 and 10 are coarsely skewed, Facies 5 is nearly symmetrically distributed and Facies 4 and 6 are finely skewed.

Table 10 - Grain Size Distribution - from Field Estimates
Facies 3 to 10

Facies	Avg. mean (phi)	Avg. std dev. (phi)	Skewness (phi)	Kurtosis (phi)	Avg. % Mud	Avg. % Sand	Avg. % Gravel	Number of analyses
3	0.04	4.70	-0.39	1.74	33.72	26.80	39.47	19
4	3.57	4.86	0.23	1.75	60.07	34.21	5.71	14
5	1.32	2.88	0.09	3.23	13.46	76.54	10.00	13
6	2.01	3.06	0.56	2.35	16.50	78.74	4.76	33
7	0.54	4.57	-0.19	1.53	35.64	26.50	37.86	7
8	-0.48	3.54	-0.43	2.12	12.41	47.01	40.57	35
9	-2.36	3.32	-0.28	1.96	8.58	26.16	65.26	19
10	-2.86	2.87	-0.14	2.34	4.69	21.86	73.46	68

CLAST LITHOLOGY AND PROVENANCE

Introduction

Clast lithology data were gathered simultaneously with maximum particle size measurements, as clast types were noted during determination of the ten largest clasts (D_{10} data) of each gravel bed. All units in each section were grouped except NAN 1-1A', which was calculated separately.

With reference to bedrock types in the field area, and considering present drainage patterns, lithologies were considered to be either proximal, medial, or distal. Proximal lithologies are locally derived, medial lithologies are derived from within the basin and distal lithologies are derived from outside the basin. Proximal lithologies were usually granodiorite, granite, quartz-feldspar porphyry, vein quartz and andesite. Medial lithologies were usually andesite, granodiorite, granite, schist and gneiss, while any sedimentary rock was considered distal.

Notable exceptions are the lower reaches of Victoria Creek where schist and gneiss are proximal, and the East Fork of Nansen Creek where schist and gneiss are medial.

Discussion

Table 11 summarizes the clast provenance for each of the various drainages. Most sections have clasts of proximal or medial provenance, however there is a relatively high abundance of sedimentary rocks in sections on Back Creek and Nansen Creek. This is mainly a reflection of the dominance of Facies 3, diamicton, in these sections. Facies 3 generally had a higher proportion of distal and medial clasts than all of the other facies. Unit NAN 1-1A' has an unusually high amount (27%) of sedimentary rocks, strongly suggesting a glacial genetic origin. Also worth noting is the surprisingly low amount of proximal clasts in Victoria Creek. This could be due to the rapid rate of weathering of the schist bedrock , resulting in poor preservation potential.

Table 11 - Summary of Clast Provenance

Drainage	Percent proximal	Percent medial	Percent distal
Back Creek	93	5	2
Discovery Creek	99	0	1
Dolly Creek	70	30	0
East Fork Nansen	49	51	0
Eva Creek	96	4	0
Klaza River	46	54	0
Nansen Creek (all units excluding NAN 1-1A'	94	0	6
Unit NAN 1-1A'("older till")	73	0	27
Victoria Creek	7	91	2
Weber Creek	89	11	0

Conclusions

Matrix grain size distribution within Facies 1 (organic), 2 (tephra), 4 (massive and stratified silt and clay), and 6 (stratified sand) are dominated by grain sizes of less than .125 mm (very fine sand or smaller), whereas Facies 3 (diamicton) and 7 (disorganized muddy gravel) are depleted in the fine to medium sand size. Facies 8, 9 and 10 have significant amounts of fine to medium sand in the matrix.

Field estimates of overall composition show that Facies 4 (massive and stratified silt and clay) and Facies 7 (disorganized muddy gravel) show significant amounts of mud, whereas Facies 5 (massive and disorganized sand), 6 (stratified sand) and 8 (massive and stratified sandy gravel) show the significant amounts of fine to medium sand. Facies 8, 9 and 10 are dominated by gravel while Facies 3 (diamicton) is nearly bimodal with both mud and gravel fractions.

Maximum particle size data is generally a reflection of sorting. Facies 3 - diamicton, has the largest average, maximum, minimum, range and standard deviation of clast size, while pebbly stratified sand, Facies 6, has the smallest range of values.

For maximum particle size versus bed thickness, there is no clear relationship for Facies 3 to 7. For Facies 8 to 10, a clearer relationship is evident with the best population cluster occurring in Facies 10. These differences are attributable to the patchy distribution of pebbles in Facies 4 to 7, and the better sorting of Facies 10. The largest average bed thickness is encountered in Facies 3 - diamicton, and the smallest is seen in Facies 4 - silt and clay. The largest range of bed thicknesses is in Facies 10 - massive to crudely stratified gravel, followed by Facies 3 - diamicton and Facies 9 - disorganized gravel. Facies 4 - silt and clay, has the smallest range of bed thicknesses.

Statistical treatment of matrix grain size distributions shows that the average mean phi values decrease from clay-rich to clay-poor facies. Average standard deviations are highest for the poorly-sorted diamicton and disorganized muddy gravel and lowest for stratified sand and mud. Mud and muddy gravel facies tend to have matrix distributions that are coarsely skewed, while sand, sandy gravel and gravel facies tend to have matrix distributions that are finely skewed.

Statistical treatment of overall grain size distributions from field estimates shows a decrease in average mean phi values from muddy to sandy to gravelly facies. Average standard deviation is highest for Facies 4, followed by Facies 3, 7 and 8, reflecting poor sorting. Better-sorted Facies 9, 6, 5 and 10 have lower average standard deviations.

The overall grain size distributions of Facies 8, 3, 9, 7 and 10 are coarsely skewed, while Facies 4 and 6 are finely skewed. Facies 5 is nearly symmetrically distributed.

Clast lithologies for the most part are a reflection of local bedrock types, however significant amounts of distal (sedimentary) clasts are encountered in Back Creek and Nansen Creek. This is mainly a reflection of the dominance of Facies 3, diamicton, which generally had a higher proportion of sedimentary clasts than all other facies. Unit NAN 1-1A', which is poorly exposed in Nansen Creek, has the largest proportion of distal (sedimentary) lithologies, which may be a function of a glacial genetic origin.

CLAY MINERALOGY AND SECONDARY FEATURES

Clay Mineralogy

The sedimentary history of an area is determined not only by the various depositional environments present, but by later modifying factors such as physical and chemical weathering. The most important secondary processes in central Yukon are related to the development of soils, cryogenic (ice-related) processes, and periglacial features.

Often the climatic history of an area can be determined by examining the type and extent of soils (past and present) and the secondary features present.

Formation of soils and clay minerals

Soils are the product of weathering of parent materials, which may be a variety of materials including bedrock, unconsolidated sediments, and even pre-existing soils. In areas of temperate and tropical climate, soils generally form by processes of chemical weathering and are often well-formed. In cooler climates, soils are mainly produced by the physical breakdown of parent materials and are generally poorly formed. In extremely cold (such as periglacial) climates soils may not form at all. Cryogenic structures are also important features formed under these climatic conditions.

One of the diagnostic features of soils are the type and amount of clay and clay-size (<2 μm) minerals present. The most common clay mineral groups are illites, kaolinites, and smectites (Deer et al., 1992). Various other clay minerals are less common such as vermiculites and several mixed-layer clays (illite/smectite, illite/kaolinite, and smectite/kaolinite) and chlorite.

Kaolinite formation

Kaolinite forms from the weathering and low-temperature hydrothermal alteration of feldspars, muscovite and other Al-rich silicates usually derived from acid rocks such as granites, rhyolites, and quartz diorites (Deer et al., 1992). The derivation from feldspar is as follows:

$$2KAlSi_3O_8 + 3H_2O \rightarrow Al_2Si_2O_5(OH)_4 + 4SiO_2 + 2K(OH)$$

In this instance the silica and KOH are leached away.

Illite formation

Illite forms from a variety of parent minerals including muscovite, kaolinite and feldspar. Under alkaline conditions the alteration of feldspar results in the preservation of K and illite rather than kaolinite will form:

$$3KAlSi_3O_8 + 2H_2O \rightarrow KAl_2(AlSi_3O_{10})(OH)_2 + 6SiO_2 + 2K(OH)$$

Smectite formation

Smectites are a group of clay minerals which show expandability, taking up water or organic molecules between their structural layers. Principal smectites are dioctahedral montmorillonite, beidellite and nontronite, and trioctahedral saponite, hectorite and sauconite.

Dioctahedral smectite is generalized by the formula:

$$(0.5\ Ca,Na)_{0.7}(Al,Mg,Fe)_4[(Si,Al)_8O_{20}](OH)_4.nH_20$$

Trioctahedral smectite is generalized by the formula:

$$(0.5\ Ca,Na)_{0.7}(Mg,Fe,Al)_6[(Si,Al)_8O_{20}](OH)_4.nH_20$$

Smectite forms from the alteration of basic rocks or volcanic material under alkaline conditions. In particular, the variations beidellite and nontronite are widely found in soils (often mixed with illite) derived from the weathering of basic rocks (Deer et al., 1992).

Smectite is also found as a hydrothermal alteration product around metalliferous veins or deposits (Deer et al., 1992).

X-Ray Diffraction Analyses

Introduction

X-Ray diffraction analyses are based on the principle that X-rays passing through a layered silicate mineral will be diffracted, as stated by Bragg's Law (Moore and Reynolds, 1989):

$$2d\sin\theta = n\lambda$$

where d = spacing between layers in angstroms (A^o);
θ = angle of incidence of x-rays;
and λ = X-Ray wavelength
n = number of wavelengths

Eighteen matrix samples were prepared for X-Ray diffraction analysis. Each sample was analyzed in four different ways, for a total of 72 separate analyses. These consisted of X-Ray diffraction analysis of the bulk (<.062 mm) fraction, the clay (<2 μm) fraction, the glycolated (ethylene glycol) clay fraction, and the heated (1 hr at 580°C) clay fraction, according to the methods of Moore and Reynolds (1989).

The presence of illite was indicated by a peak at a d-spacing of approximately $10A^o$, which did not change after heating or glycolation. Kaolinite was confirmed by the presence of a peak at a d-spacing of $7A^o$, which collapsed after heating and expanded slightly after glycolation. Smectite and illite/smectite mixed layers were confirmed by broad peaks at d-spacings between $12A^o$ and $15A^o$. Both smectite and illite/smectite shift to the right after heating and to the left after glycolation. Chlorite was confirmed by peaks at d-spacings of $7A^o$ and $14A^o$, which essentially remain stable after heating and glycolation. The presence of oxides was shown by a high background in the bulk sample analysis (Moore and Reynolds, 1989).

Discussion

X-Ray diffraction plots of 2θ versus CPS (counts per second) for each clay sample are contained in Appendix B. Table 12 shows a summary of results from these analyses, with approximate percentages of each clay mineral present, as well as the Munsell colors of each sample.

The presence of illite/smectite mixed-layer clays is one of the diagnostic features of soils developed on pre-Reid glacial drift (outwash and till) surfaces (Foscolos et al., 1977, Smith et al., 1986; Tarnocai, 1987).

Smectite or illite/smectite mixed layers were encountered in significant amounts throughout most of Facies 3, the diamicton; from samples EFN 2-1G, EFN 2-2E2, and DIS 2-9E of Facies 9 and 10; and from bedrock sample DIS 2-12B1. Samples EFN 2-1G and EFN 2-2E2 were derived from the top of a deeply-weathered, colluvially-buried gravel section exposed by placer mining on East Fork, and DIS 2-9E was sampled at the top of a deeply-weathered boulder gravel filled channel high on Discovery Creek. Sample DIS 2-12B1 was derived from nearby deeply-weathered bedrock. Within Facies 3, samples NAN 1-1A' and WEB 1-1A returned the highest values of smectite or illite/smectite.

Oxides and chlorite were less abundant in the samples, with strong oxides noted only in samples EFN 3-1A, EFN 3-1D, and EFN 2-2A. Chlorite was noted in significant amounts in samples NAN 1-1D and EFN 4-1A.

The dry Munsell color of the matrix of each of the samples that were analyzed varied from 5Y 5/6 (olive) to 5YR 5/6 (yellowish red) to 10 YR 5/4 (yellowish brown) and 10 YR 6/6 (brownish yellow). Interesting to note is the 10YR 8/2 (very pale brown) of sample DIS 2-12B1, derived from deeply-weathered bedrock, which also had the highest calculated amount of smectite or illite/smectite mixed layer clays.

Table 12 - Summary of Results from X-Ray Diffraction Analyses

Unit	Facies	Illite	Kaolinite	Smectite or Illite/Smectite	Chlorite	Oxides	Munsell color
NAN 1-1A'	3	20	44	36	present	present	5Y 5/6
NAN 1-1A	3	31	40	29	none	trace	10YR 6/6
EFN 3-1A	3	32	42	26	none	strong	10YR 6/6
EFN 3-1B	3	38	41	21	none	none	10YR 6/2
EFN 3-1D	3	30	43	10	17	strong	10YR 5/4
UBAC 1-1B	3	33	40	27	trace	trace	10YR 5/4
K 2-1A	3	25	37	21	17	trace	10YR 6/6
WEB 1-1A	3	26	38	36	trace	trace	10YR 5/4
DIS 1-2C	8	60	40	---	none	trace	10YR 5/4
NAN 1-1D	9	38	35	---	27	none	10YR 5/4
EFN 2-1G	9	29	32	39	none	present	10YR 6/6
EFN 2-2A	9	trace	trace	---	none	strong	5YR 5/6
EFN 2-2E2	9	37	35	28	none	present	5YR 5/6
DIS 2-9A	10	52	48	---	none	present	10YR 6/6
DIS 2-9E	10	33	31	36	trace	present	10YR 6/6
DIS 2-12B1	bdrx	30	18	52	none	none	10YR 8/2
EFN 4-1A	10	37	15	---	48	present	10YR 5/4
VIC 1-1A	10	---	---	---	trace	present	10YR 5/4

Secondary Features

Introduction

Important secondary features of the sediments in the study area are mainly of a periglacial origin. These include sand wedges, cryoturbated horizons, and ventifacts.

Sand wedges occur as a result of ice wedge casts which are produced by strong cooling at temperatures below -6 degrees Celsius (Selby, 1985), generally in conditions cooler than present. Sediments such as aeolian sand and minor amounts of silt and clay eventually replace the ice in the ice-wedge. Cryoturbation is the displacement of sediment horizons due to differential freezing of groundwater in areas where permafrost is prevalent.

Ventifacts are pebbles and boulders which have been abraded by extreme conditions of wind over a long period of time. They have a large range of surface shapes with plane or curved faces and two or more facets present. Often they are flat on one side and polished on the other. Less resistant minerals are often eroded out leaving a pitted surface on the clast (Selby, 1985).

Discussion

Table 13 shows a summary of the types of periglacial and secondary features encountered in the study area. While ventifacts were observed in seven sections and cryoturbation was observed in five sections, sand wedges and clay skins were observed in only two (separate) sections. Since sand wedges and clay skins are more common in older deposits and have a greater potential for reworking, these features are less abundant.

Table 13
Summary of periglacial and secondary features

Section	Ventifacts	Cryoturbation	Sand wedges	Clay skins
EFN 2-2	yes	not seen	not seen	yes
EFN 4-1	yes	not seen	not seen	not seen
WEB 1-1	yes	not seen	not seen	not seen
WEB 2-1	yes	not seen	yes	not seen
EVA 1-1	not seen	yes	not seen	not seen
EVA 2-1	not seen	yes	not seen	not seen
NAN 1-1	yes	not seen	not seen	yes
LBAC 1-1	yes	not seen	yes	not seen
DOL 1-1	possibly	possibly	not seen	not seen
K 1-1	not seen	yes	not seen	not seen
DIS 1-1	not seen	yes	not seen	not seen
DIS 2-9	yes	not seen	not seen	not seen
VIC 1-1	not seen	yes	not seen	not seen

Conclusions

In very cold glacial or periglacial conditions, clay minerals are formed from the physical breakdown of the parent materials (Chamley, 1989). This would presumably be the case in the Mt. Nansen area during the pre-Reid, Reid and McConnell glaciations. During the interglacial periods, however, warmer and more humid climatic conditions were prevalent (Foscolos et al., 1977; Jackson, 1993). Chemical weathering under these conditions would have a larger effect and clay minerals would be produced mainly from the alteration of feldspars and micas (Chamley, 1989).

Bedrock in the Mt. Nansen area consists mainly of intermediate volcanics, acid intrusives, and metamorphic basement rocks. Since most of the unconsolidated materials are of local origin, the clay minerals present in these materials are derived mainly from andesite, granodiorite, rhyolite and schist. Granodiorite would supply the muscovite and potassium feldspar necessary for illite and kaolinite, while the andesite would supply the plagioclase feldspar and ferromagnesium minerals necessary for smectite. Hydrothermal aureoles around metalliferous vein deposits (such as the Goulter occurrence) may also supply smectite to the system.

Several researchers, including Foscolos et al., (1977); Smith et al., (1986); and Tarnocai, (1987) have determined that distinct soil morphologies are associated with glacial drift surfaces of pre-Reid, Reid and McConnell age. These and related pedological studies have been used to interpret the Quaternary history of central Yukon. Distinguishing properties include solum depth, B horizon (Munsell) color, clay skin development, coarse fragment weathering, paleoargillic horizons, clay mineralogy and periglacial features. Others, including Kodama et al., (1976) have studied the clay mineralogy of soils in the unglaciated terrain of north and central Yukon.

One of the diagnostic features of soils developed on pre-Reid glacial drift is the presence of illite/smectite mixed-layer clays (Foscolos et al., 1977). Significant amounts of smectite or illite/smectite mixed layers were encountered in several samples from Facies 3, the diamicton; from samples EFN 2-1G, EFN 2-2E2, and DIS 2-9E of Facies 9 and 10; and from bedrock sample DIS 2-12B1.

The Munsell color of the matrix of each of the samples that were analyzed were either 10YR, 5YR or 5Y. Of all the samples, only EFN 2-2E2 was yellowish red (5YR 5/6), however nearby deeply-weathered bedrock (sample DIS 2-12B1) was only 10YR 8/2 (very pale brown). Since clay skins were also observed on ventifact clasts from unit EFN 2-2E2, this unit is likely the Wounded Moose Paleosol (as defined by Smith et al., 1986).

Clay mineralogy and Munsell color data therefore indicates that sections EFN 2-1, EFN 2-2, and DIS 2-9 and diamicton units of Facies 3 are consistent with surfaces of pre-Reid age.

Cryoturbation due to active permafrost is common in this area of central Yukon. As all of the cryoturbated sediments were observed to be high in each section (near to the present surface), this is attributed to recent and active permafrost activity.

Ventifacts were encountered in measured sections on East Fork, Weber, Nansen and Lower Back Creek, and sand wedges were encountered on Weber and Lower Back Creek. It can be assumed that at some point these sediments were subjected to extreme glacial or periglacial climatic conditions, either the pre-Reid, Reid or McConnell glaciations. As these features were rarely encountered however, relative abundances (as described by Tarnocai, 1987) cannot be used to infer an age of these deposits.

FACIES INTERPRETATIONS

Introduction

The genetic origins of each facies were interpreted based on lithologic descriptions, grain size characteristics and sedimentary structures. Table 15 summarizes the facies interpretations.

Facies 1 - Organic

The organic grade of this material varied from recent plant detritus to fibric peat material which was occasionally found lower in some sections. Four radiocarbon analyses were performed (Table 14), none of which returned a date which was older than 7740a B.P. All of the organic beds encountered were therefore of Holocene age.

Facies 2 - Tephras

The White River Ash consists of two slightly overlapping lobes, a northern lobe occurring between 1500 and 1890 years B.P. and a larger, eastern lobe occurring at 1250 years B.P. (Lerbekmo and Campbell, 1969; Lerbekmo et al., 1975). The source of this tephra is Mt. Bona, Alaska, near the Yukon-Alaska border, approximately 250 km west of the field area. In the area of the study, the uppermost tephra is found in nearly every measured section, very near to the present day surface. This corresponds well with the mapped distribution of the eastern lobe of the White River Ash.

The lower tephra is found within one metre of the present day surface, occasionally in the same sections as the White River Ash. Several samples of this tephra have been submitted for to the Geological Survey of Canada for dating.

In measured sections along Eva Creek, the lower tephra is cryoturbated and underlain by an organic horizon which has been dated at 1580 +/- 60a B.P. (Beta - 60293).

Since the White River Ash is found capping this section one metre above, and the tephras are separated by stratified sand and silt, the lower tephra must correspond to either the earlier lobe of the White River Ash (previously unmapped at this locality) or an undocumented volcanic event.

Facies 3 - Diamicton

This unit is interpreted as till and resedimented till. Facies characteristics such as very poor-sorting, disorganized structure, bullet and flat-iron clast morphology (Figure 33) and lateral continuity are typical of glacial tills (Ashley et al. 1985; Eyles and Miall, 1984). The diamicton lies directly upon bedrock on Klaza River, East Fork and Weber Creek. In most of those drainages it is laterally continuous on the valley floors. With the exception of unit NAN 1-1A', clasts from the diamicton are nearly all locally derived, so deposition of this unit may have been from a local (alpine) ice advance centered in the Dawson Range, which was contemporaneous to (and probably merged with) Cordilleran pre-Reid ice moving in from the south. Although few of the clasts are striated (Figure 34) this is probably related to the fact that the local rocks (andesite and granodiorite) do not striate as well as other lithologies such as sandstone and limestone.

The diamicton of NAN 1-1A', "the older till", contains numerous striated clasts of sandstone, limestone, schist and quartzite with much less andesite and granodiorite than any other unit, and is seen only intermittently in deep sections in Nansen Creek, where it lies beneath and sometimes adjacent to diamicton of unit NAN 1-1A. This unit is interpreted as a till, likely related to the earlier of the two pre-Reid glaciations which is only preserved in patchy hummocks deep in the valley floor of Nansen Creek.

Table 14
Carbon 14 dates of organic material

Laboratory number	Sample number	C^{14} age (years B.P.)	Range (+/-)	Material	Comments
Beta - 60293	EVA 2-1H	1,580	60	peat	undulatory
Beta - 60296	VIC 1-1F	2,090	60	peat	convoluted
Beta - 60294	K 1-3C	4,600	60	wood	'in situ' stump
Beta - 60295	K 2-1K	7,740	80	peat	continuous

REFER TO COLOUR CD

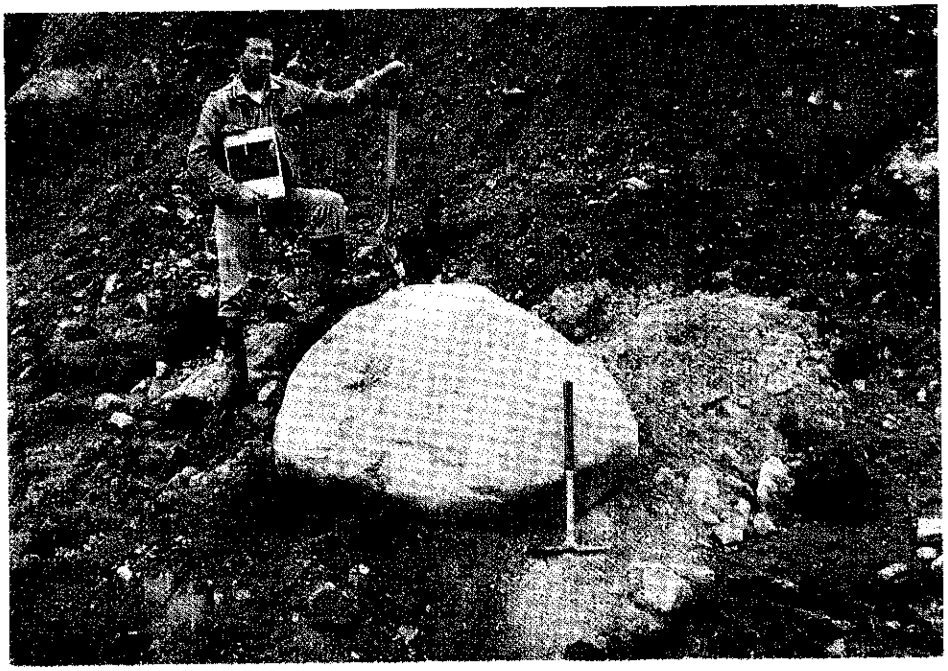

Figure 33 - A large bullet-shaped boulder was exposed by placer mining operations at an elevation of 4300 feet ASL on Back Creek. This streamlined boulder was derived from a diamicton which lay directly on bedrock. The diamicton in this location is interpreted as a glacial till.

Figure 34 - Glacially-striated boulders also occur on the East Fork of Nansen Creek.

Facies 4 - Massive and stratified silt and clay

Massive silt and clay and horizontally laminated silt and clay are interpreted as being deposited during fallout of suspended sediment in a lacustrine or pond environment. Horizontal laminations are due to temporal variation in the grain-size and supply of suspended sediment (Harms et al., 1982). Gravel-size clasts are contributed as a minor component by colluvial processes.

Ripple and cross-stratified silt and clay are interpreted as being deposited by tractive (bed-load) processes in low shear-stress environments, as fluvial overbank material peripheral to fluvial channels or on bar tops (Harms et al., 1982). Stratification is mainly due to grain-size differences and bedform migration due to temporal and spatial variations in tractive sediment load (Harms et al., 1982).

Facies 5 - Massive and disorganized pebbly sand and sand

This facies is interpreted as being deposited from fallout deposition during a rapid transition from high flood flow to lower fluvial flow conditions, where the rapid decrease in flow does not allow tractive bed structures to form (Blatt et al., 1980; Harms et al., 1982). Facies characteristics such as the massive structure, occasional pebbles and variable sorting support this interpretation.

Facies 6 - Stratified pebbly sand and sand

This facies is interpreted as being sedimented on planar or curvilinear surfaces, such as the surface of mid-channel or point-bars. Parallel stratification is mainly due to grain-size differences attributed to changing flow-regime and tractive sediment load, while current ripples and cross-bedding are due to the migration of bedforms of various sizes (Harms et al., 1982). Trough cross-beds may be the result of sand waves (large current ripples), while planar tabular cross-beds may represent the slip-face of a downstream-migrating channel bar. Pebbles when present are transported as bedload material. Convolutions are the result of dewatering due to subsequent sediment loading.

Facies 7 - Disorganized muddy gravel

This facies is interpreted as proximal debris flows and mudflows. Facies characteristics such as a high proportion of mud versus sand, matrix-support and disorganized structure are typical of debris flows in proximal alluvial fan environments (Harms et al., 1982; Miall, 1977, 1978; Rust, 1978). Other characteristics such as discontinuous nature of the beds, the presence of organic material and the subangular to angular clasts are consistent with this interpretation.

Facies 8 - Massive and stratified sandy gravel

Horizontally-stratified sandy gravels are interpreted as being deposited by sheetfloods (Brodzikowski and Van Loon, 1991) in a periglacial environment. Gravel and sand are transported by high energy conditions (such as hyperconcentrated flood flows) and deposited simultaneously under rapidly waning flood conditions. Rapidly variable discharges are typical of glacial and periglacial environments and result in thin, discontinuous beds of gravelly sediment deposited in the mid-reaches of alluvial fans (Bull, 1972; Miall, 1977; Wells, 1984).

Massive sandy gravels are the result of waning flow deposition of sand which infiltrates the matrix of previously deposited gravels (Frostick et al., 1984).

Facies 9 - Disorganized gravel

Facies characteristics such as high clast to matrix ratios, scoured bases and disorganized fabric infer that this facies was deposited by high fluvial flood flows in erosive channel scours. Removal of the finer sediment by erosion frequently leads to the accumulation of the coarsest fraction as a lag, which armors the surface and prevents further scour (Blatt et al., 1980).

Facies 10 - Massive to crudely stratified gravel

This facies is interpreted as having been deposited as channel lags and low-relief gravel bars in a high-sediment load, braided stream or alluvial fan environment (Bull, 1972; Miall, 1977). Massive gravel beds are deposited in channel thalwegs under waning flood conditions, while crude parallel stratification is the result of diffuse gravel sheets or longitudinal gravel bars which migrate only during peak floods, and form under fluctuating discharge conditions (Rust, 1972; Hein and Walker, 1977). The rare trough cross-bedding is either the result of scour and fill of channel bottoms (Miall, 1977) or the migration of gravel dunes in the channel bed (Blatt et al., 1980; Harms et al., 1982) under deeper water conditions than those that produce crude horizontal stratification.

Table 15
Summary of Facies Interpretations

Facies	Lithology	Level of shear stress	Significant reworking	Depositional environment	Method of deposition
1	Organic horizons	Very low	no	Adjacent to fluvial stream	Organic growth
2	Tephra	Very low	yes	Volcanic eruption	Aeolian
3	Diamicton	Low	yes	Glacial ice	Meltout of till, resedimentation of till
4	Massive and stratified silt and clay	Very low to low	dewatering	Ponds, abandoned channels	Stagnant to very low flow
5	Massive and disorganized pebbly sand and sand	High	no	Fluvial channels and channel margins	Rapidly waning high fluvial flood flow
6	Stratified pebbly sand and sand	High	no	Point-bar and channel bar tops	Normal fluvial flow
7	Disorganized muddy gravel	Medium to high	no	Proximal alluvial fans	Sediment-laden debris and mud flows
8	Massive and stratified sandy gravel	Medium to high	yes, matrix infilling	Braid bars, alluvial fans	Hyper-concentrated flood flows to waning flood flows
9	Disorganized gravel	High	no	Fluvial channels, proximal alluvial fans	High fluvial flood flow
10	Massive to crudely stratified gravel	High	no	Braided fluvial channels, proximal -medial alluvial fans	High fluvial flood flow to normal fluvial low

PALEOENVIRONMENTAL RECONSTRUCTION

Facies Associations and Vertical Transitions

Introduction

Several parameters, including facies associations, field relationships, airphoto interpretation, weathering characteristics and secondary features were used to infer the paleoenvironmental origins of each measured section. Table 16 summarizes the paleoenvironmental interpretations and facies associations for each section in the study area.

Vertical facies transitions for each section are grouped by genetic category and summarized in Table 17.

Discussion

Colluvium and deeply-weathered bedrock

Colluvium and deeply-weathered bedrock were the primary materials in sections DIS 2-11 and DIS 2-12, although deeply-weathered bedrock was found underlying sections UBAC 1-1, DIS 1-1, DIS 1-2, DIS 1-3, DIS 2-1, DIS 2-11, DIS 2-12 and EVA 2-1. Bedrock has been degraded and clay-altered not only by processes of long-term, deep-weathering, but by hydrothermal alteration of bedrock near mineralized quartz veins and quartz-feldspar porphyry dykes. This is especially evident in section DIS 1-2, which is underlain by a hydrothermally-altered quartz-clay vein.

In many sections on Discovery Creek, deeply-weathered bedrock has been transported short distances downslope by colluvial processes, resulting in a gradual transition from deeply-weathered bedrock to a homolithic gravel. Although clasts are generally equigranular, sorting is highly variable and depends on the amount of clay material which remains with the original material during transport. As a result, facies present can be mud, sand, or poorly-sorted to well-sorted gravel. No particular vertical facies transitions could be discerned in the colluvium.

Alluvial fans

Sections MBAC 1-1, DIS 2-1, K 1-1, K 1-2 and K 1-3 are interpreted as alluvial fans of Holocene age. With the exception of DIS 2-1, all of these fans lie at or near the 4000 foot elevation. The most common Facies are 4 (mud), 5 (massive sand) and 8 (massive and stratified sandy gravel). Less common Facies are 7 (disorganized muddy gravel), 6 (stratified sand), 9 (disorganized gravel) and 10 (massive to crudely stratified gravel). A Holocene age is inferred by field relationships and the amount of organic material present, usually as a component of Facies 4. Alluvial fans show both coarsening upward and fining upward vertical facies transitions. Massive sand (Facies 5) often alternates with massive to crudely stratified gravel (Facies 10).

Fluvial stream deposits

Sections VIC 1-1, DIS 1-1, DIS 1-2, DIS 1-3, LBAC 1-1, EVA 1-1 and EVA 2-1 are interpreted as fluvial stream deposits. All DIS and EVA sections are gulch streams, while LBAC 1-1 is a sandy braided stream and VIC 1-1 forms a fluvial terrace. Common Facies are 10 (massive to crudely stratified gravel), 4 (massive and stratified mud), 6 (stratified sand) and 8 (massive and stratified sandy gravels). Less common Facies are 7 (disorganized muddy gravels) and 9 (disorganized gravel). Field relationships and the presence of moderate amounts of organic material infer a Holocene age for these deposits, except LBAC 1-1 which may be McConnell because of the presence of an ice-cast sand wedge. Facies generally fine upward in fluvial stream deposits, and there is a tendency for massive to crudely stratified gravel (Facies 10) to alternate with stratified sand (Facies 6). Gulch stream channels show a tendency of Facies 8 (massive and stratified sandy gravel) to alternate with Facies 10.

Periglacial alluvial fans

Sections WEB 1-1, WEB 2-1, LDIS 1-1 and LBAC 2-2 are interpreted as periglacial alluvial fans. Common Facies are 6 (stratified sand) and 8 (massive and stratified sandy gravel). Less common Facies are 3 (diamicton - which unconformably underlies section WEB 1-1) and 10 (massive to crudely-stratified gravel). The presence of sand wedges and the absence of organics infer a Reid age for these deposits. Terraces of these fans occur at several levels, at least two of which can be recognized on Weber Creek (Figures 35 to 37). There is a strong tendency for Facies 6 (stratified sand) and Facies 8 (stratified sandy gravel) to occur together in vertical facies transitions. These couplets are often bounded by Facies 10 (massive to crudely stratified gravel).

Periglacial valley fills

Sections DOL 1-1, VIC 1-2, VIC 1-3 and NAN 1-1 are interpreted as periglacial valley fills. Common Facies are 6 (stratified sand), 9 (disorganized gravel) and 10 (massive to crudely stratified gravel). Less common Facies are 3 (diamicton - which unconformably underlies NAN 1-1) 5 (massive sand) and 8 (massive and stratified sandy gravel). At least three levels can be recognized as terraces on both Victoria and Nansen creeks. McConnell-age meltwaters have truncated these deposits at the confluences between Nisling River and Victoria and Nansen creeks. As with periglacial alluvial fans, Facies 6 and 8 often occur together, however there is a tendency for fining upward of facies, with Facies 10 more dominant lower in the sections.

Glacial deposits

Sections NAN 1-1, EFN 3-1, EFN 3-2, UBAC 1-1 and K 2-1 are interpreted as mainly glacial deposits. The most dominant Facies is 3 (diamicton), which represents glacial till and resedimented glacial till. Glaciofluvial outwash of Facies 10 lies above the glacial till of Facies 3 in section UBAC 1-1. A similar deposit of outwash resting upon till was noted during cursory examinations at Discovery Creek, and have also been noted by other workers (Bostock, 1966; Jackson, 1993). Unconformably overlying the till and outwash are colluvium (EFN 3-1 and EFN 3-2), alluvial fans (K 2-1) and periglacial valley fills (NAN 1-1). Disorganized muddy gravel (Facies 7), massive and stratified sandy gravel (Facies 8), and stratified sand (Facies 6) are dominant in these overlying sequences. The age of the deposits ranges from pre-Reid for the till and outwash to Holocene for the colluvium. Vertical facies transitions of glacial deposits are characterized by several repetitions of Facies 3 (diamicton), followed by the various facies which characterize the unconformably overlying colluvium, alluvial fans and periglacial deposits.

Glaciofluvial terraces

Sections EFN 1-1, EFN 2-1, EFN 2-2 and EFN 4-4 are interpreted as glaciofluvial terraces. Dominant Facies are 9 (disorganized gravel) and 10 (massive to crudely-stratified gravel). All sections except EFN 4-1 are overlain by colluvial sequences consisting mainly of Facies 7 (disorganized muddy gravel) and 8 (massive and stratified sandy gravel). Glaciofluvial terraces show a small tendency to coarsen upwards, with the few sandy facies present (Facies 6 - stratified sand and Facies 8 - massive and stratified sandy gravel) occurring lower in the sections. This is followed vertically by various unconformably overlying facies of colluvium and alluvial fans.

Glaciofluvial channels

Section DIS 2-9 is interpreted as an ice-marginal glaciofluvial channel. This section consists mainly of massive to crudely stratified gravel (Facies 10) which deeply cuts bedrock high on Discovery Creek. Paleoflow directions of this channel lie at nearly right angles to the current valley, roughly following Nansen Creek valley. This must have formed as an ice-marginal channel during the last pre-Reid glaciation. As with the glaciofluvial terraces, the tendency is for coarsening upwards, with the only finer facies (Facies 6 - stratified sand) occurring lower in the section.

Table 16
Facies associations and paleoenvironmental interpretations for measured sections

Section name	Facies present	Genetic interpretation	Inferred age	Elevation (feet ASL)
DIS 2-11	1,2,4,5,8,10	Colluvium/weathered bdrx	Holocene	4270
DIS 2-12	1,10	Colluvium/weathered bdrx	Holocene	4270
MBAC 1-1	5,6,8,10	Alluvial fan	Holocene	4000
DIS 2-1	1,2,4,5,6,10	Alluvial fan	Holocene	4170
K 1-1	1,2,4,5,10	Alluvial fan	Holocene	4000
K 1-2	1,4,5,6,8	Alluvial fan	Holocene	4000
K 1-3	1,4,5,8	Alluvial fan	Holocene	4000
VIC 1-1	1,2,6,10	Fluvial stream (terrace)	Holocene	3210
DIS 1-1	1,2,4,6,8,9,10	Fluvial stream (gulch)	Holocene	4370
DIS 1-2	1,2,4,6,8,10	Fluvial stream (gulch)	Holocene	4350
DIS 1-3	1,6,8,9,10	Fluvial stream (gulch)	Holocene	4340
LBAC 1-1	1,2,6,10	Fluvial stream (braided)	McConnell /Holocene	3450
EVA 1-1	1,2,4,7,9	Fluvial stream (gulch)	Holocene	4105
EVA 2-1	1,2,4,6,7,8	Fluvial stream (gulch)	Holocene	4015
WEB 1-1	1,3,5,6,8,10	Glacial/periglacial alluvial fan	Reid	3950
WEB 2-1	1,2,6,8	Periglacial alluvial fan	Reid	3960
LDIS 1-1	1,4,6,8,10	Periglacial alluvial fan	Reid	4000
LBAC 2-2	1,2,6,8,10	Periglacial alluvial fan	Reid	3450
DOL 1-1	1,6,8,9	Periglacial valley fill	Reid	3600
VIC 1-2	1,2,5,6,10	Periglacial valley fill	Reid	3220
VIC 1-3	1,2,6,9,10	Periglacial valley fill	Reid	3225
NAN 1-1	1,3,6,9,10	Glacial/periglacial valley fill	pre-Reid/ Reid	3560
EFN 3-1	1,3,6,8	Glacial/colluvium	pre-Reid/ Holocene	4005
EFN 3-2	1,3,8	Glacial/colluvium	pre-Reid/ Holocene	4005
UBAC 1-1	1,3,10	Glacial->glaciofluvial/colluvium	pre-Reid/ Holocene	4315
K 2-1	1,2,3,4,7,8,9,10	Glacial/alluvial fan	pre-Reid/ Holocene	3980
EFN 1-1	1,2,6,8,9,10	Glaciofluvial terrace/colluvium	pre-Reid/ Holocene	4040
EFN 2-1	7,8,9,10	Glaciofluvial terrace/colluvium	pre-Reid/ Holocene	4025
EFN 2-2	1,2,5,6,7,8,9	Glaciofluvial terrace/colluvium	pre-Reid/ Holocene	4030
EFN 4-1	1,10	Glaciofluvial terrace	pre-Reid	4200
DIS 2-9	1,6,10	Glaciofluvial channel	pre-Reid	4270

Table 17
Vertical Facies Transitions

Section name	Vertical Facies transitions	Environmental interpretation
DIS 2-11	8->10->4->5->1->5->1	Colluvium
DIS 2-12	10->10->1	Colluvium
MBAC 1-1	10->10->10->10->10->10->5->10 ->5->8->6	Alluvial fan
DIS 2-1	10->5->10->6->5->4->6->1->5->2->1	Alluvial fan
K 1-1	10->4->1->4->5->10->4->2->1	Alluvial fan
K 1-2	1->4->8->6->1->5->8	Alluvial fan
K 1-3	1->4->1->5->8	Alluvial fan
VIC 1-1	10->6->10->6->10->1->6->1->2->1	Fluvial stream (terrace)
DIS 1-1	10->10->8->9->6->2->4->2->1	Fluvial stream (gulch)
DIS 1-2	10->8->6->10->8->10->4->2->1	Fluvial stream (gulch)
DIS 1-3	9->10->10->10->10->6->10->8->10- >1	Fluvial stream (gulch)
LBAC 1-1	10->6->10->6->10->1->2->1	Fluvial stream (braided)
EVA 1-1	9->9->7->4->2->1	Fluvial stream (gulch)
EVA 2-1	8->8->7->8->4->4->1->2->1->6->1	Fluvial stream (gulch)
WEB 1-1	3->5->6->10->6->10->6->8->8->1	Glacial/periglacial alluvial fan
WEB 2-1	6->8->6->2->1	Periglacial alluvial fan
LDIS 1-1	10->10->6->8->10->10->8->4->1	Periglacial alluvial fan
LBAC 2-2	10->8->6->8->10->6->8->1->2	Periglacial alluvial fan
DOL 1-1	8->6->8->9->8->6->1->6	Periglacial valley fill
VIC 1-2	10->10->6->10->10->6->10->5->2->1	Periglacial valley fill
VIC 1-3	10->9->10->10->6->10->10->6->10 ->6->2->1	Periglacial valley fill
NAN 1-1	3->10->10->9->10->6->10->6->1	Glacial/periglacial valley fill
EFN 3-1	3->3->3->6->3->3->8->1	Glacial/colluvium
EFN 3-2	3->3->3->8->8->1	Glacial/colluvium
UBAC 1-1	3->10->3->3->3->3->10->10->1	Glacial- >glaciofluvial/colluvium
K 2-1	3->3->3->3->10->9->9->7->10->7 ->1->4->2->1->8->10->7	Glacial/alluvial fan
EFN 1-1	8->6->10->9->9->8->2->1	Glaciofluvial terrace/colluvium
EFN 2-1	10->10->8->10->10->8->9->7	Glaciofluvial terrace/colluvium
EFN 2-2	9->7->6->9->9->9->8->8->8->5->8 ->1->2->1	Glaciofluvial terrace/colluvium
EFN 4-1	10->1	Glaciofluvial terrace
DIS 2-9	10->6->10->10->10->10->1	Glaciofluvial channel

REFER TO
COLOUR CD

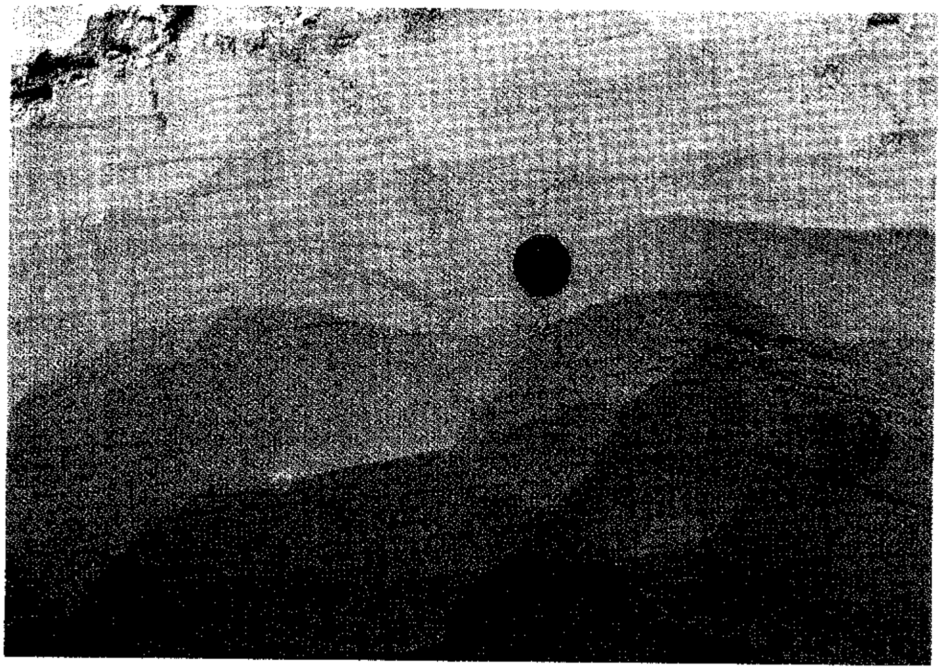

Figure 35 - Stratification consists of wavy parallel and ripple laminations in measured section WEB 2-1, located on a remnant alluvial terrace. An ice cast sand wedge can be discerned near the lens cap.

Figure 36 - A remnant alluvial terrace on the upper reach of Weber Creek has been dissected by the present stream, near the locality for measured section WEB 1-1.

REFER TO COLOUR CD

Figure 37 - Interbedded cross-stratified sand and gravel occur in a remnant alluvial terrace on Weber Creek. Gravel clasts are angular, ventifacts are common and fine to medium sand is well-sorted. Measured section WEB 2-1.

Schematic Profiles and Lateral Relationships

Introduction

Figures 38 to 47 show schematic profiles and general lateral relationships between measured sections for each drainage. Sections were correlated based on field relationships and facies trends. Table 18 is the legend for the schematic profiles and all of the measured sections.

Discussion

Discovery Creek

Discovery Creek is characterized by three types of sedimentation, glaciofluvial channels (DIS 2-9), gulch gravels (DIS 1-1, DIS 1-2 and DIS 1-3), and periglacial alluvial fans (LDIS 1-1). At elevations of 4200 feet ASL and above, the glaciofluvial channel cuts bedrock in a paleoflow direction perpendicular

Table 18
Legend for schematic profiles and measured sections

LITHOLOGY

BEDROCK	ASHY FINE SAND
ORGANIC	FINE SAND
TEPHRA	MEDIUM TO COARSE SAND
CLAY	MODERATELY TO WELL-SORTED GRAVEL
SILT	POORLY-SORTED GRAVEL
SILT AND CLAY	DIAMICTON

ACCESSORIES

GOLD OCCURRENCE (n=number of colors present)	IRON STAINING
MANGANESE STAINING	ORGANIC MATERIAL

Table 18 (continued)
Legend for schematic profiles and measured sections

SEDIMENTARY STRUCTURES

HORIZONTAL STRATIFICATION	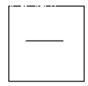	WAVY LAMINATIONS	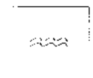
MASSIVE BEDDING	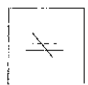	WAVY TO PARALLEL LAMINATIONS	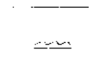
CROSS-STRATIFICATION	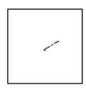	CONVOLUTED LAMINATIONS	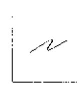
PLANAR CROSS-STRATIFICATION	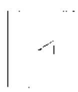	FAULTING	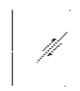
TROUGH CROSS-STRATIFICATION		INTRABEDS	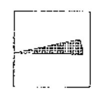
RIPPLE BEDDING			

CONTACTS

SHARP	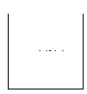	LOADED	
GRADATIONAL	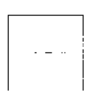	UNDULATING	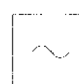
EROSIONAL	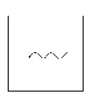	NOT VISIBLE	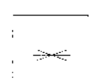

to the present valley, and is in turn cut by gulch gravels and the present stream. At approximately 4000 feet ASL and below, periglacial fan sedimentation (LDIS 1-1) is present on two levels, one higher on the south wall of the valley and one lower on the north wall of the valley. These are cut by the present stream channel.

East Fork Nansen Creek

The northern valley wall of the East Fork at approximately 4000 feet ASL is characterized by glacial till (EFN 3-1 and EFN 3-2), overlain by glaciofluvial outwash (EFN 2-1 and EFN 2-2), overlain by colluvium. Much of the glaciofluvial outwash has been eroded and in many places the glacial till is overlain directly by colluvium (EFN 3-1 and EFN 3-2). Recent stream gravels cut these sequences near the valley centre. At 4200 feet ASL on the southern valley wall, deeply-weathered kame terraces of glaciofluvial gravel (section EFN 4-1) are sporadically preserved and dissected by colluvial processes.

Eva Creek

Eva Creek (sections EVA 1-1 and EVA 2-1) is characterized by gulch gravels which overlie deeply-weathered bedrock and are overlain by overbank silts. Layers of tephra occur on two levels within the overbank silts, which also show evidence of cryoturbation. Organic material below the lower tephra (section EVA 2-1) has been radiocarbon dated at 1580a B.P. (Beta - 60293). All units generally thicken downvalley.

Upper/Middle Back Creek

Upper to middle Back Creek is characterized by a glacial till overlain by thin layer of glaciofluvial gravel (UBAC 1-1), which is cut by subsequent alluvial fan sedimentation (MBAC 1-1). The entire sequence is in turn overlain by colluvium, and cut by the present stream channel.

Lower Back Creek

Lower Back Creek consists of a periglacial alluvial fan (LBAC 2-2) which is cut by a sandy braided stream (LBAC 1-1). This in turn is cut by the present stream.

Weber Creek

Weber Creek consists of two levels of periglacial alluvial fan terraces, WEB 1-1 and WEB 2-2. Section WEB 1-1 is situated in the northern side of Weber Creek valley, is underlain by a pre-Reid till, and overlain by several feet of colluvium. WEB 2-2 is a higher, apparently separate periglacial terrace which sits on the southern side of Weber Creek valley. The exact relationship between these two terraces is unclear.

Nansen/Dolly Creek

The transition from Dolly Creek to Nansen Creek is characterized by a proximal to distal periglacial fan sequence. This sequence lies unconformably on pre-Reid till at Nansen Creek section NAN 1-1, and active aeolian sand overlies section DOL 1-1 at Dolly Creek.

Victoria Creek

Victoria Creek is characterized by a periglacial valley fill (sections VIC 1-2 and VIC 1-3), which is truncated by (lower) fluvial terraces (VIC 1-1) and the present stream channel. A large permafrost ice-wedge separates VIC 1-1 from VIC 1-2 and VIC 1-3, and considerable disruption of silt and organic units results. A paleosol of possible Reid age is evident across the periglacial valley fill exposure (sections VIC 1-2 and VIC 1-3), and an organic layer in VIC 1-1 below the disrupted layer has been radiocarbon dated at 2090a B.P.

Klaza River (unnamed tributary)

The sediments on the unnamed tributary of Klaza River at 4000 feet ASL and below consist of an alluvial fan sequence (K 1-1, K 1-2 and K 1-3) which unconformably overlies glacial till (section K 2-1). All sedimentary units thicken down-valley and towards valley centre. Above 4000 feet ASL alluvial fan sediments rest directly on weathered bedrock. Organic material from a metre above the glacial till (Facies 3 - diamicton) has been radiocarbon dated at 7740a B.P. (Beta - 60295). Higher in the alluvial fan sequence, organic material has been dated at 4600a B.P. (Beta - 60294).

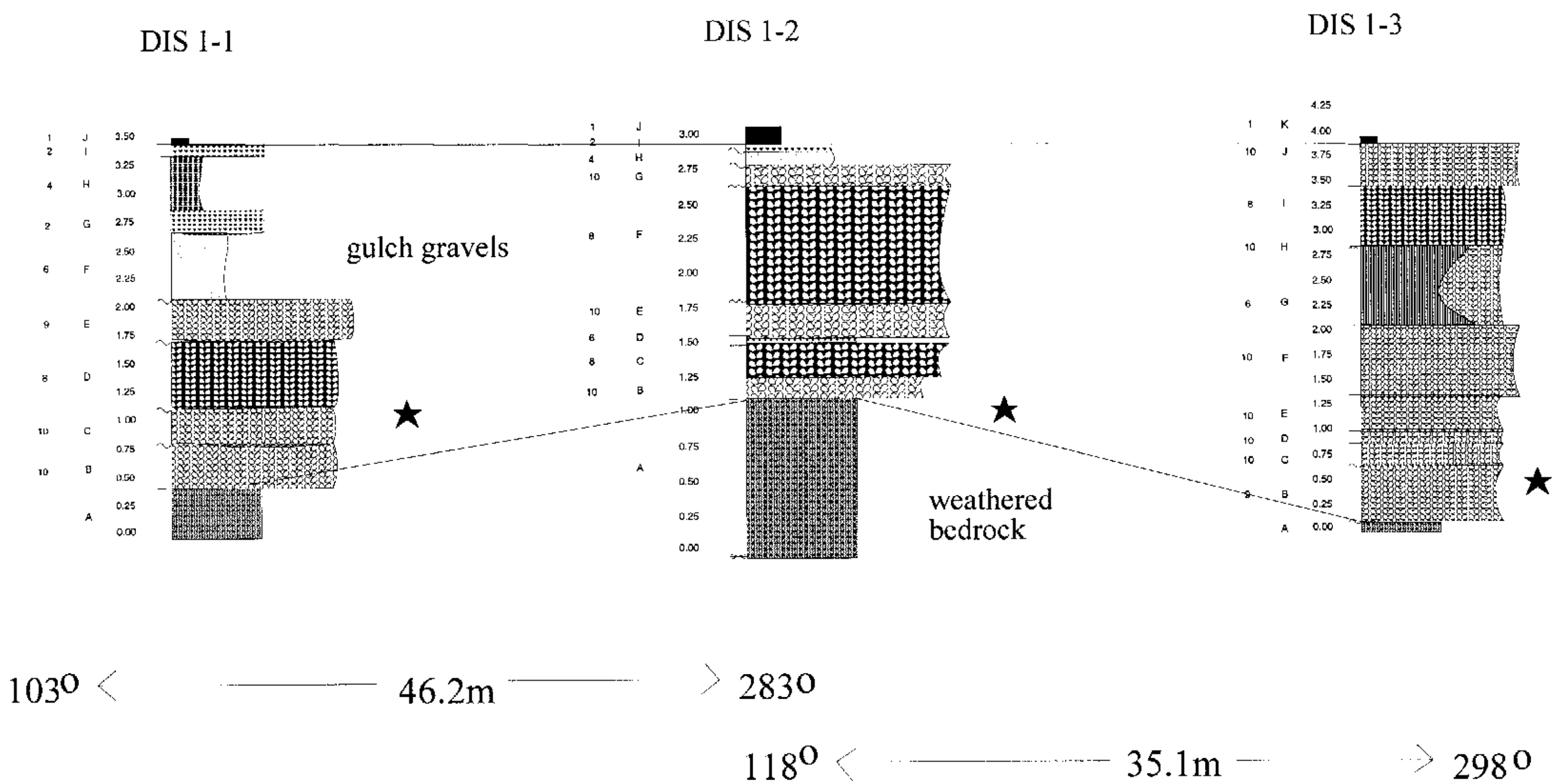

Figure 38 - Schematic Profile for Discovery Creek Sections DIS 1-1 to DIS 1-3

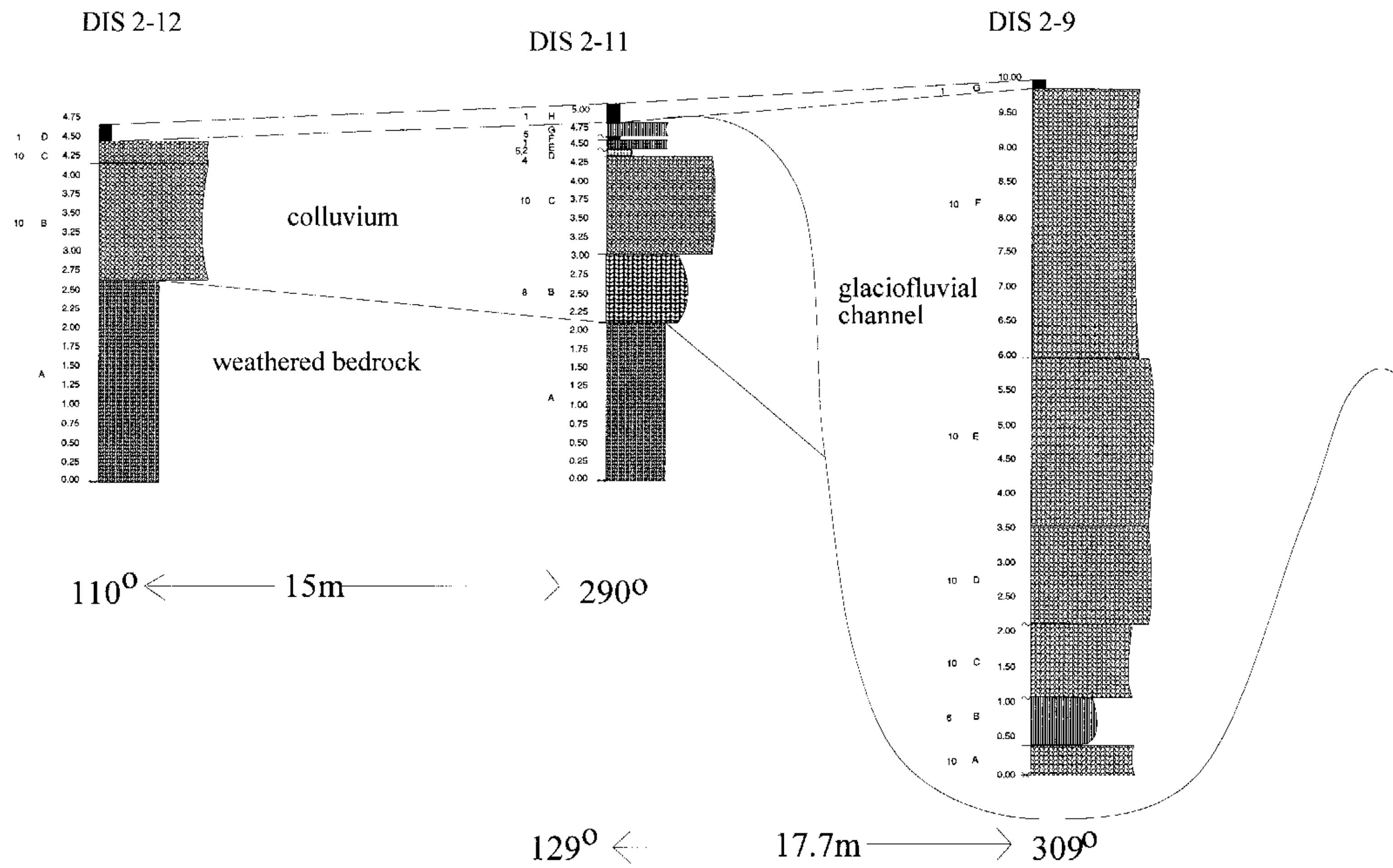

Figure 39 - Schematic Profile for Discovery Creek Sections DIS 2-9 to DIS 2-12

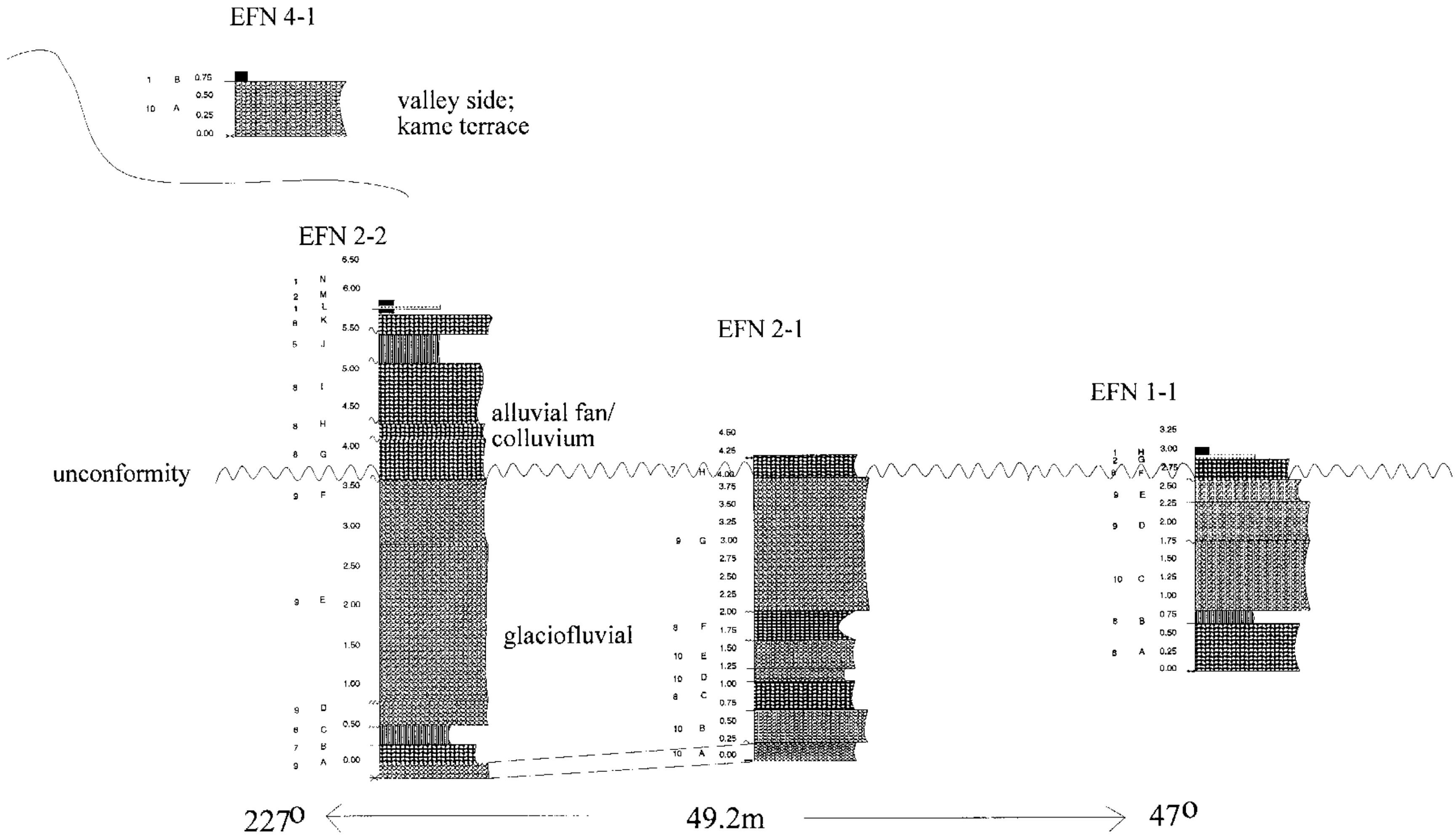

Figure 40 - Schematic Profile for East Fork Nansen Sections EFN 1-1, 2-1, 2-2 and 4-1

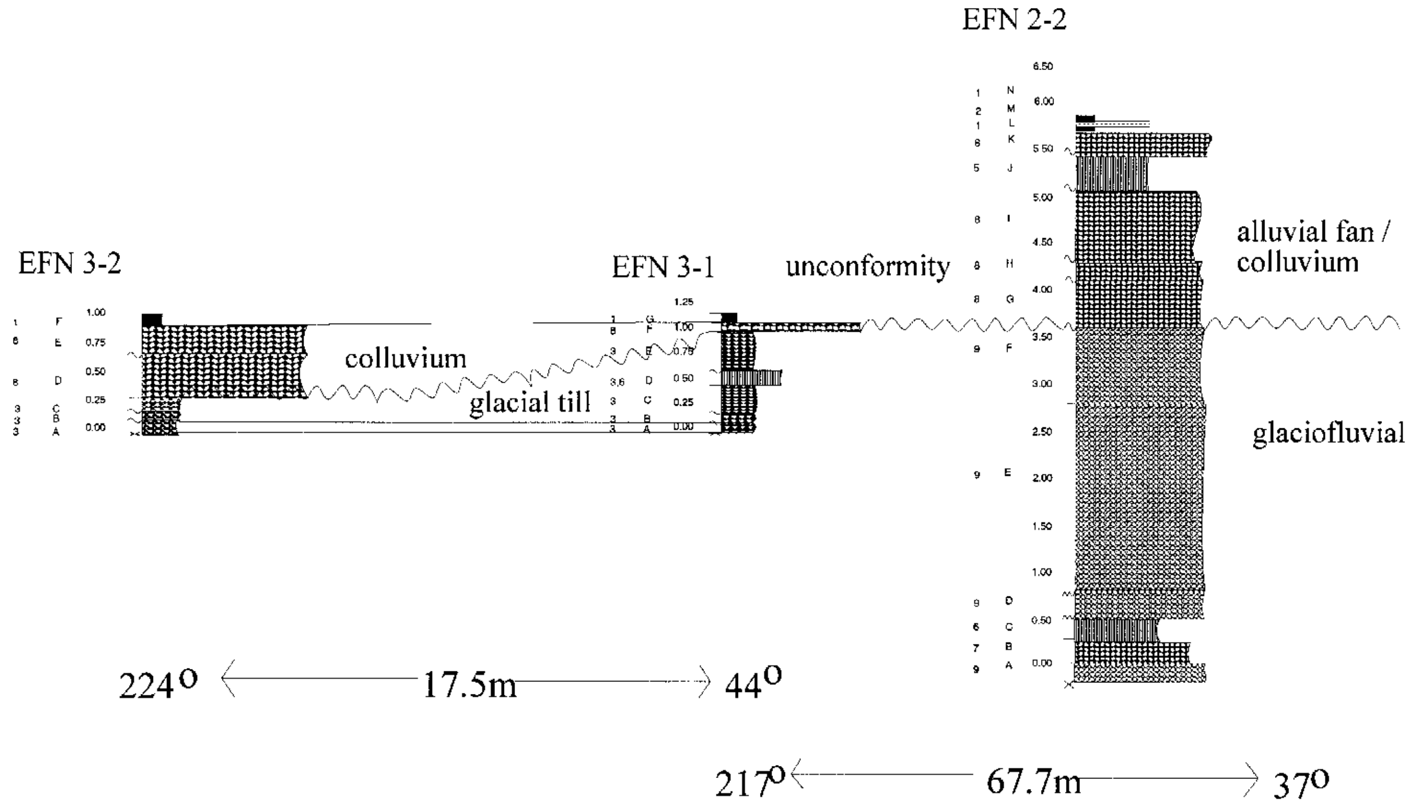

Figure 41 - Schematic Profile for East Fork Nansen Sections EFN 2-2, 3-1 and 3-2

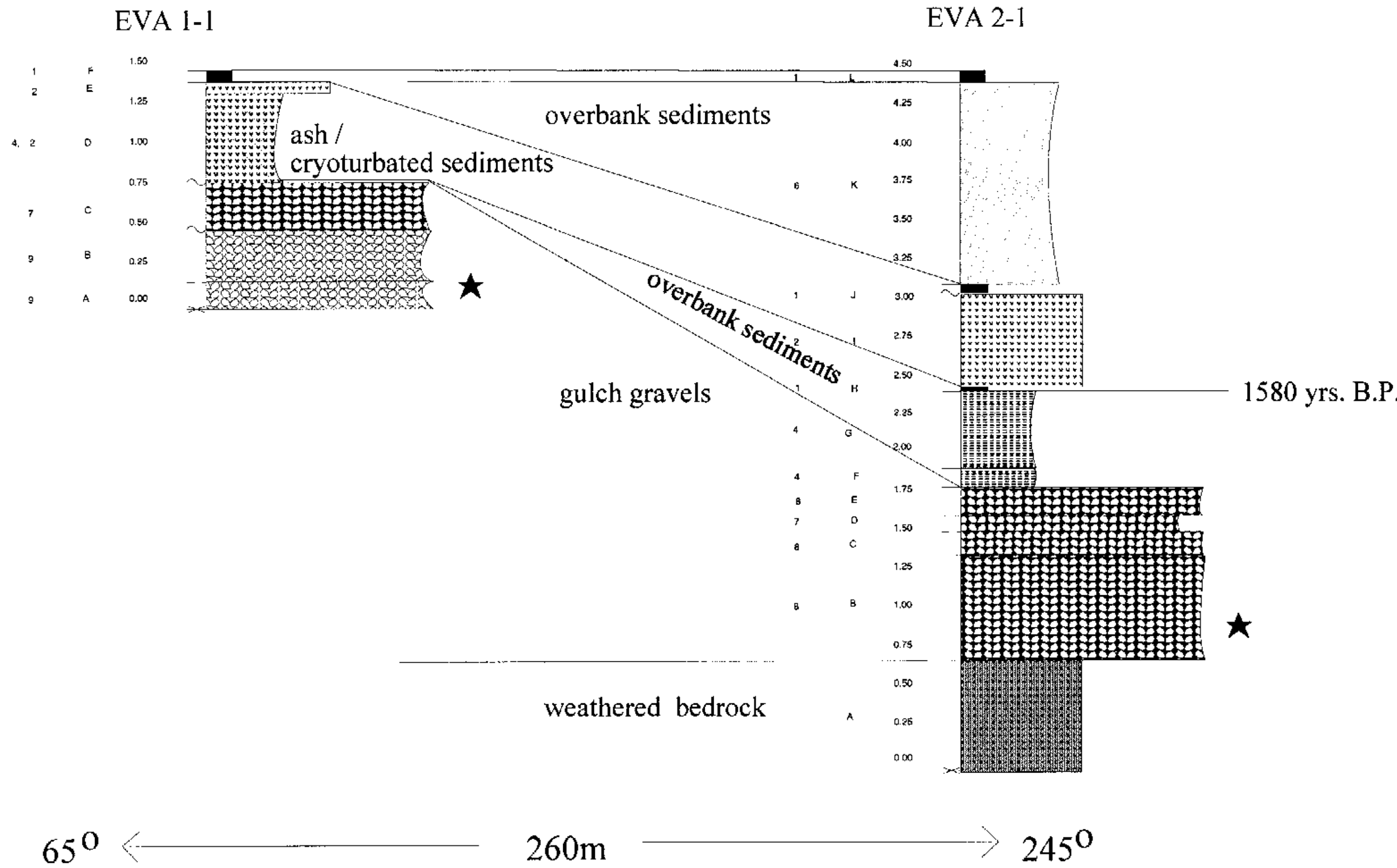

Figure 42 - Schematic Profile for Eva Creek Sections 1-1 and 2-1

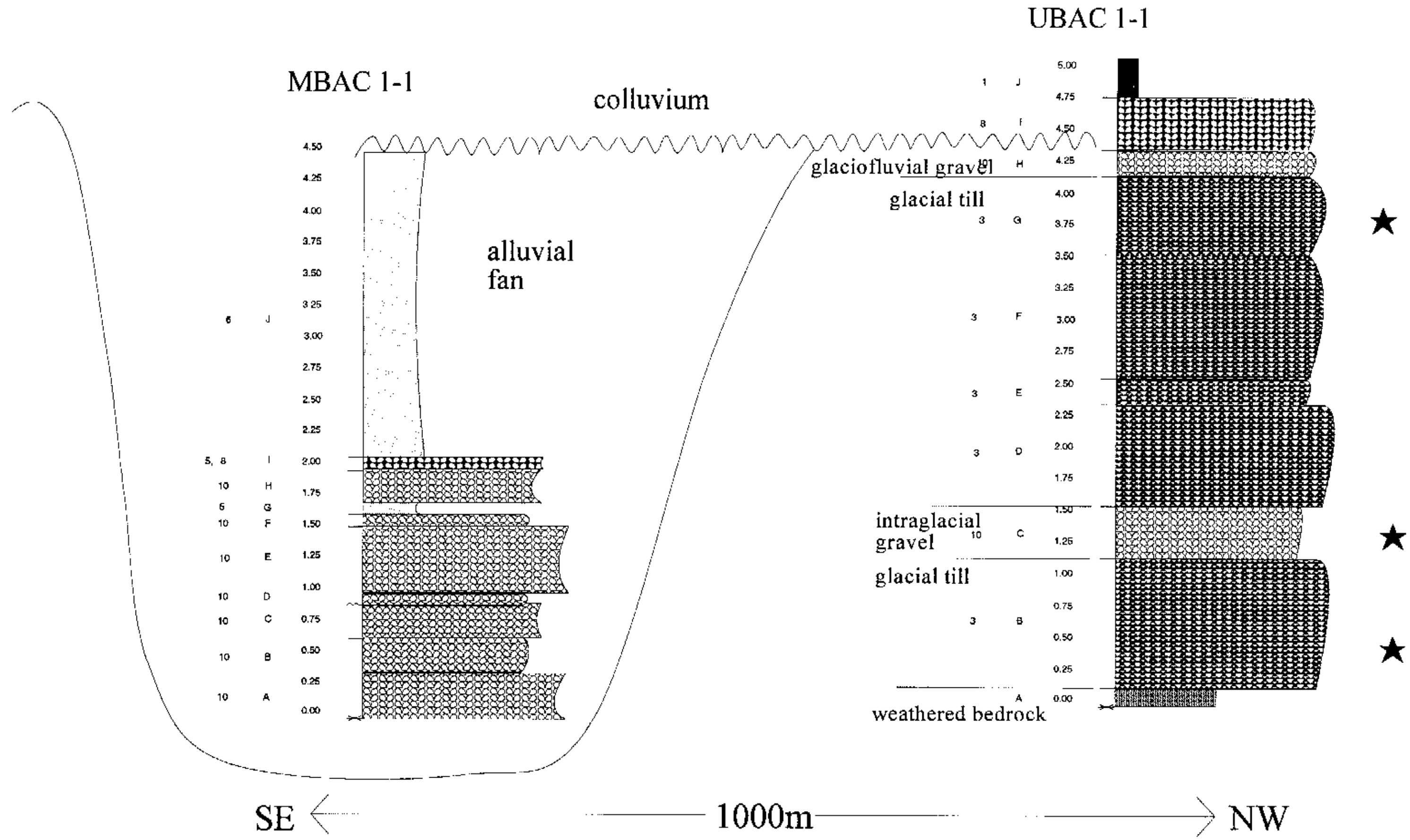

Figure 43 - Schematic Profile for Back Creek Sections MBAC 1-1 and UBAC 1-1

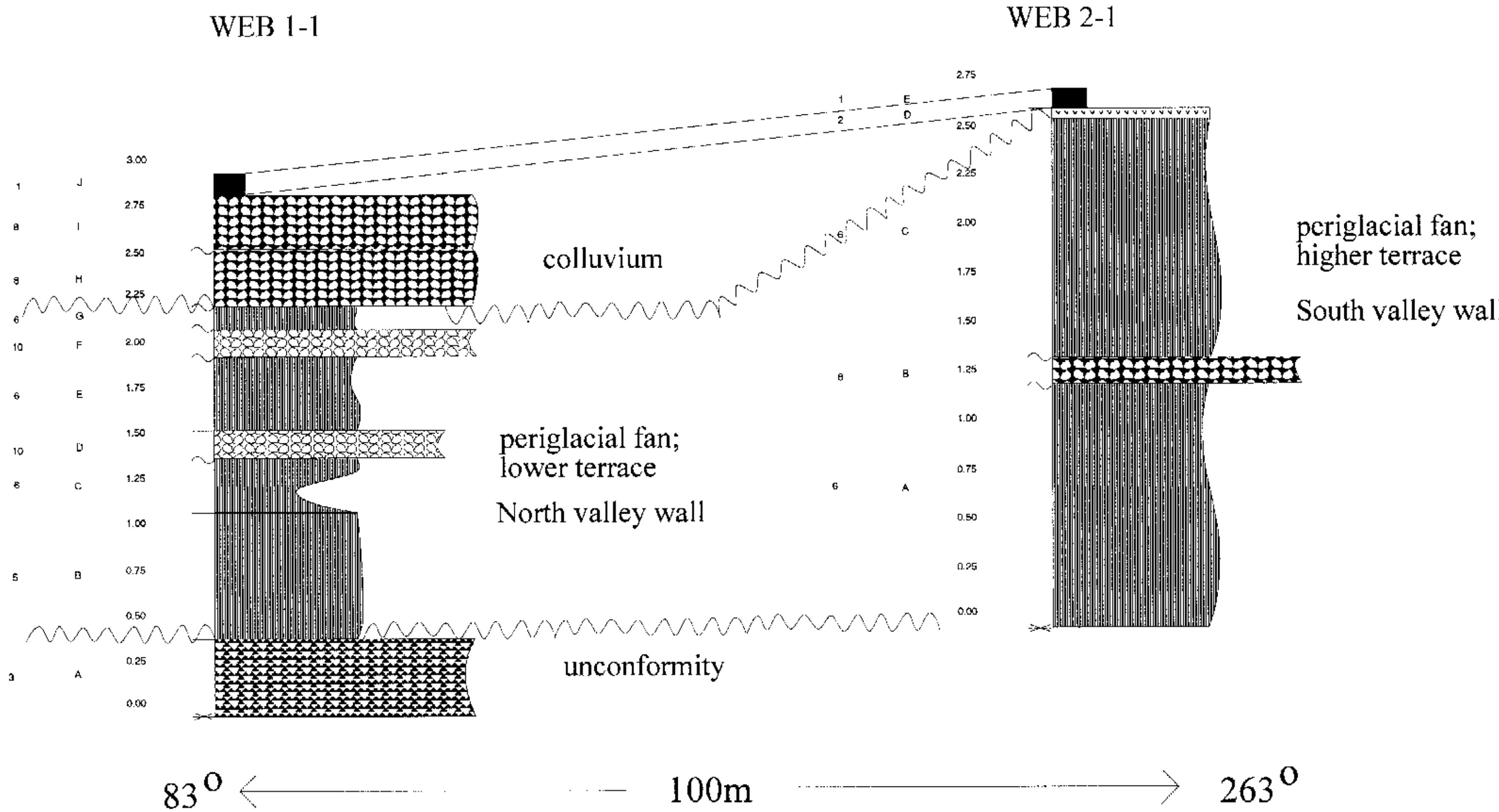

Figure 44 - Schematic Profile for Weber Creek Sections WEB 1-1 and 2-1

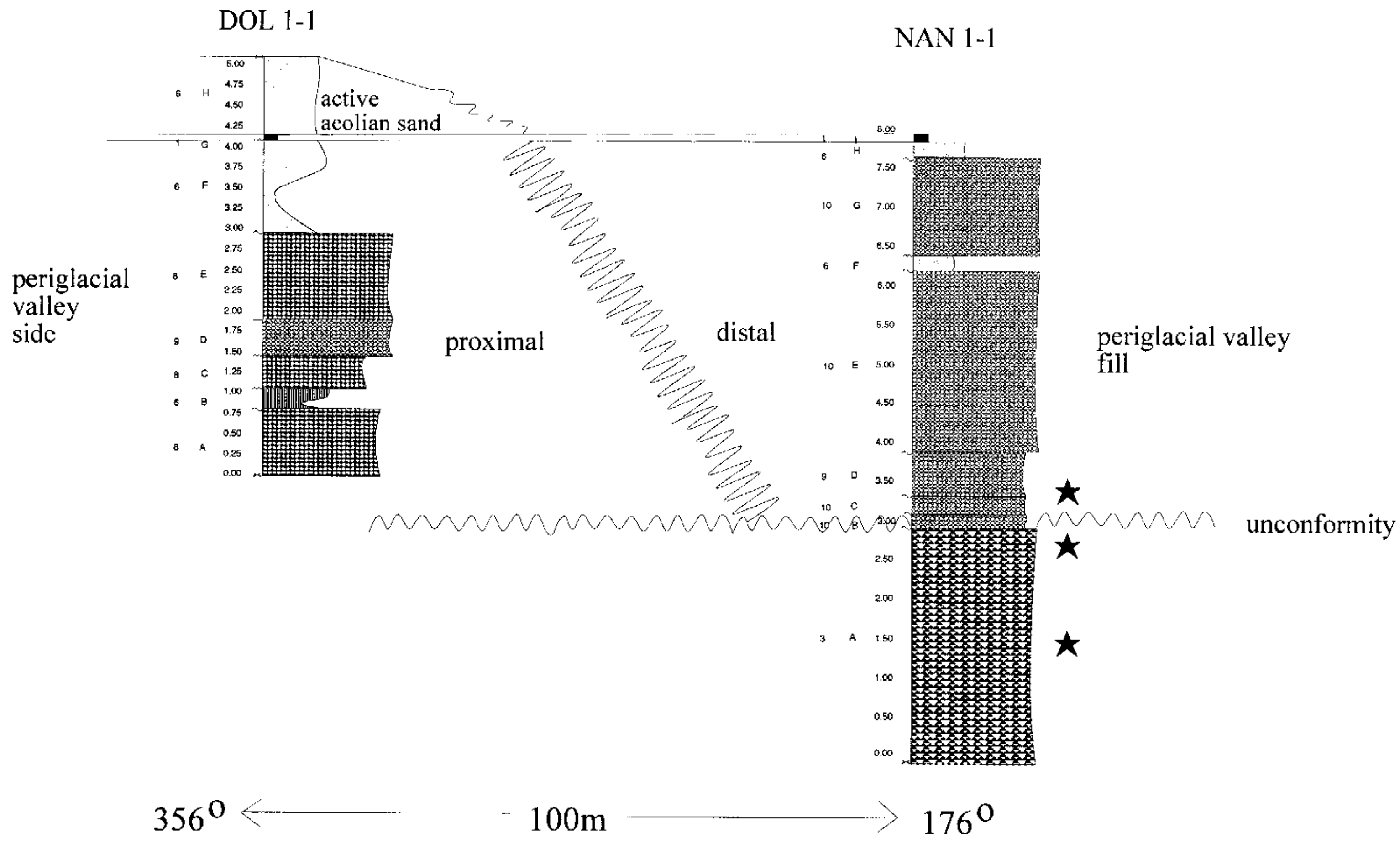

Figure 45 - Schematic Profile for Nansen and Dolly Creek Sections NAN 1-1 and DOL 1-1

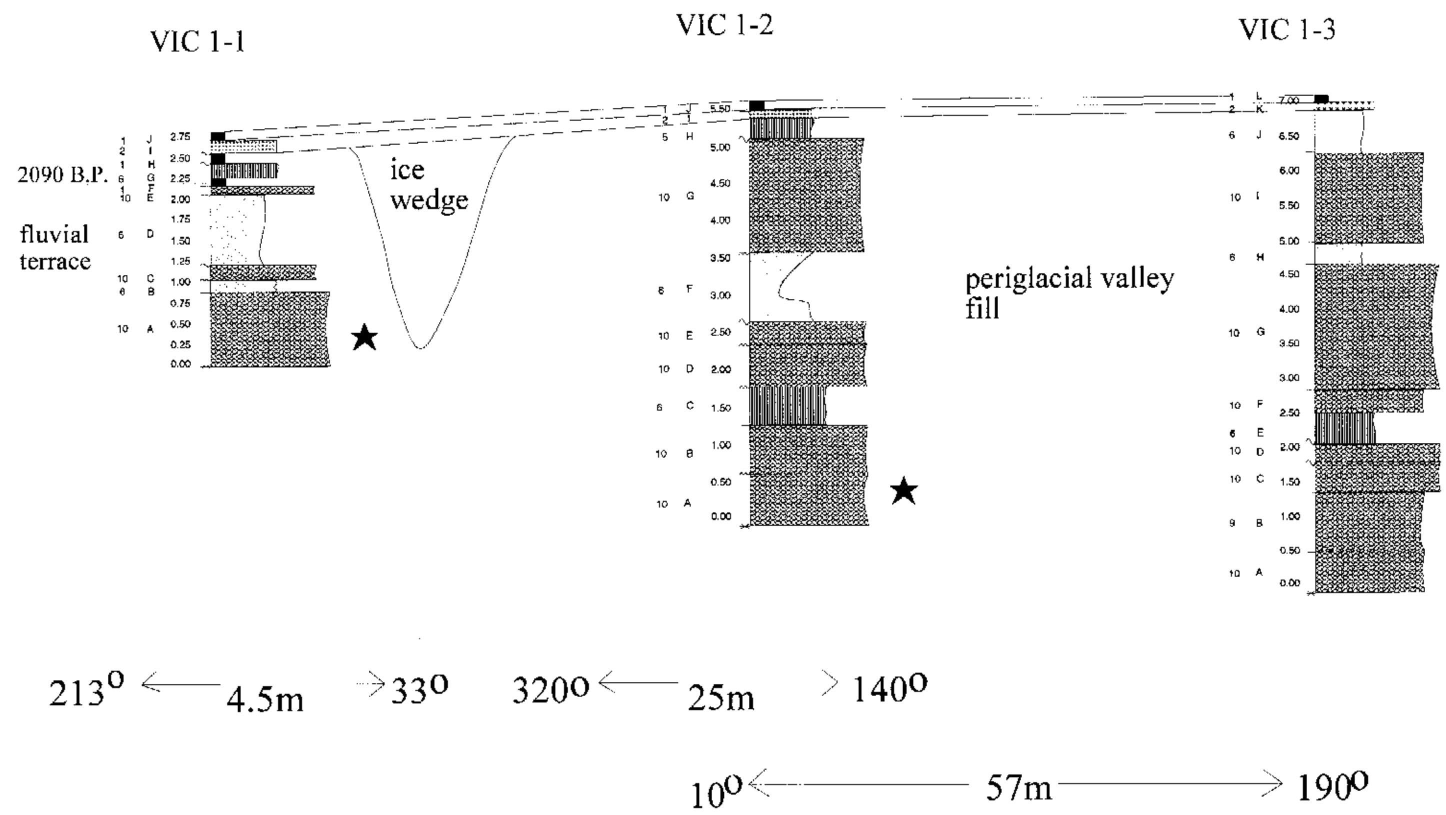

Figure 46 - Schematic Profile for Victoria Creek Sections VIC 1-1, 1-2 and 1-3

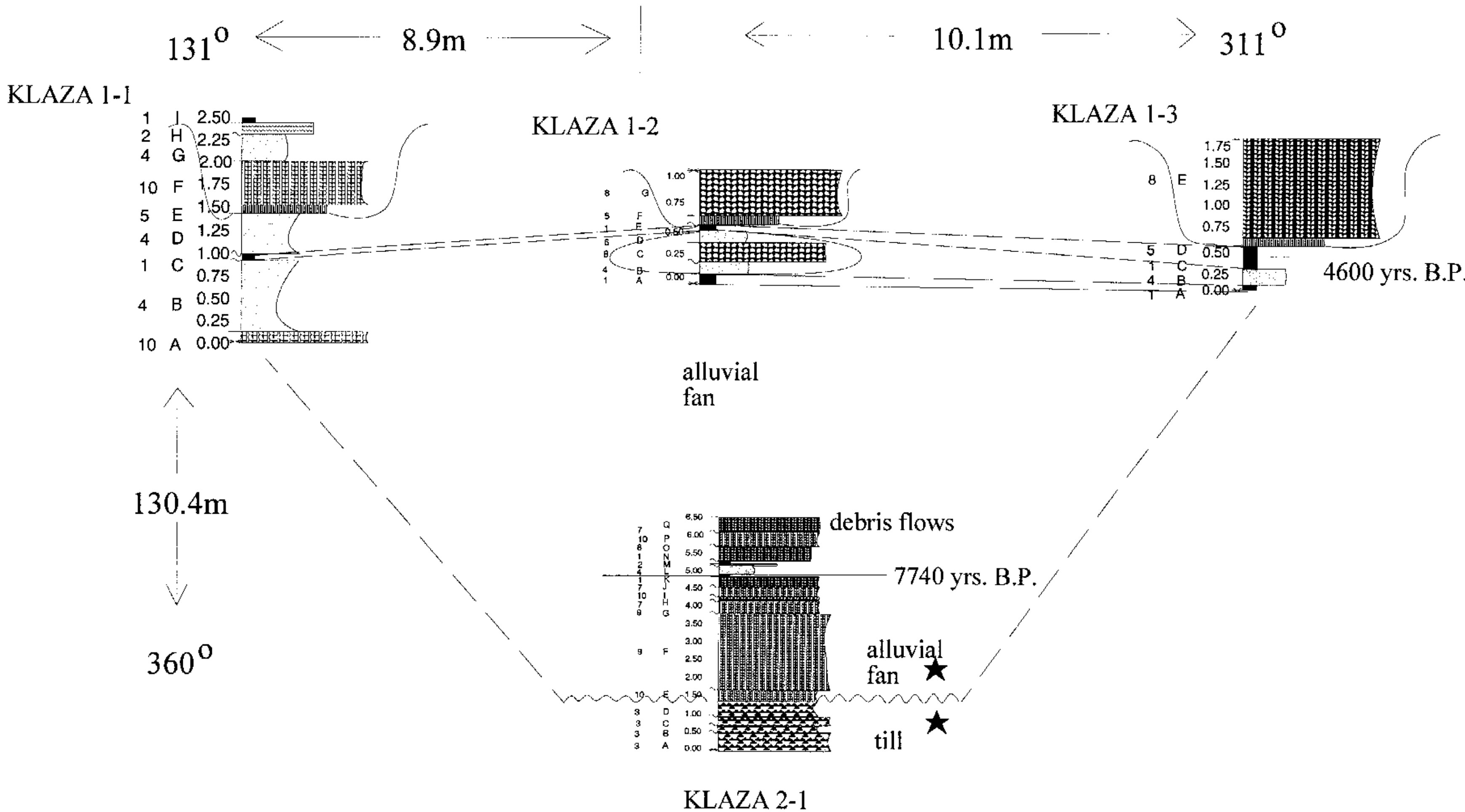

Figure 47 - Schematic Profile for Klaza River Sections K 1-1, 1-2, 1-3 and 2-1

Surficial Geology and Paleogeography

Introduction

Using airphoto interpretation and fieldwork, the surficial geology of the Nansen and Victoria creek areas was mapped at 1:50 000 scale. Figure 48 is a 1:100 000 scale map showing the main surficial features of the study area, while Figure 49 is a view of the surficial features of the northern tributaries of Nansen Creek. Table 19 is the legend for the surficial maps.

Discussion

Bedrock

Bedrock is exposed on most ridges at elevations of 4500 feet and above. In addition, scattered tors occur at lower elevations, mainly near an elevation of 4000 feet.

Recent deposits

Recent bar and channel deposits of stream gravels, low fluvial terraces and alluvial fans occur proximal to present stream courses in all drainages.

Colluvial veneer

Colluvium is ubiquitous in the field area, occupying the slopes between bedrock exposures and valley-side and valley-floor alluvial deposits. Older deposits of glaciofluvial gravels and till are overlain by colluvium on the East Fork and on Discovery Creek.

Reid and older deposits

Several levels of alluvial terraces occur along Nansen and Victoria creeks and their major tributaries.

Table 19
Legend for Surficial Geology Maps

Recent

Recent alluvium - recent alluvial fans, recent fluvial bar and channel deposits,adjacent terraces

Colluvial veneer - includes scattered occurrences of resedimented till and reworked glaciofluvial sediments

Pre-Reid

Kame terraces - north facing valley side, East Fork

Bedrock

Includes tors, felsenmeer

Reid

Alluvial terraces - includes at least three terrace levels

Secondary features

Glaciofluvial channels

Roads

Figure 48 - Surficial Geology - Mt. Nansen Field Area

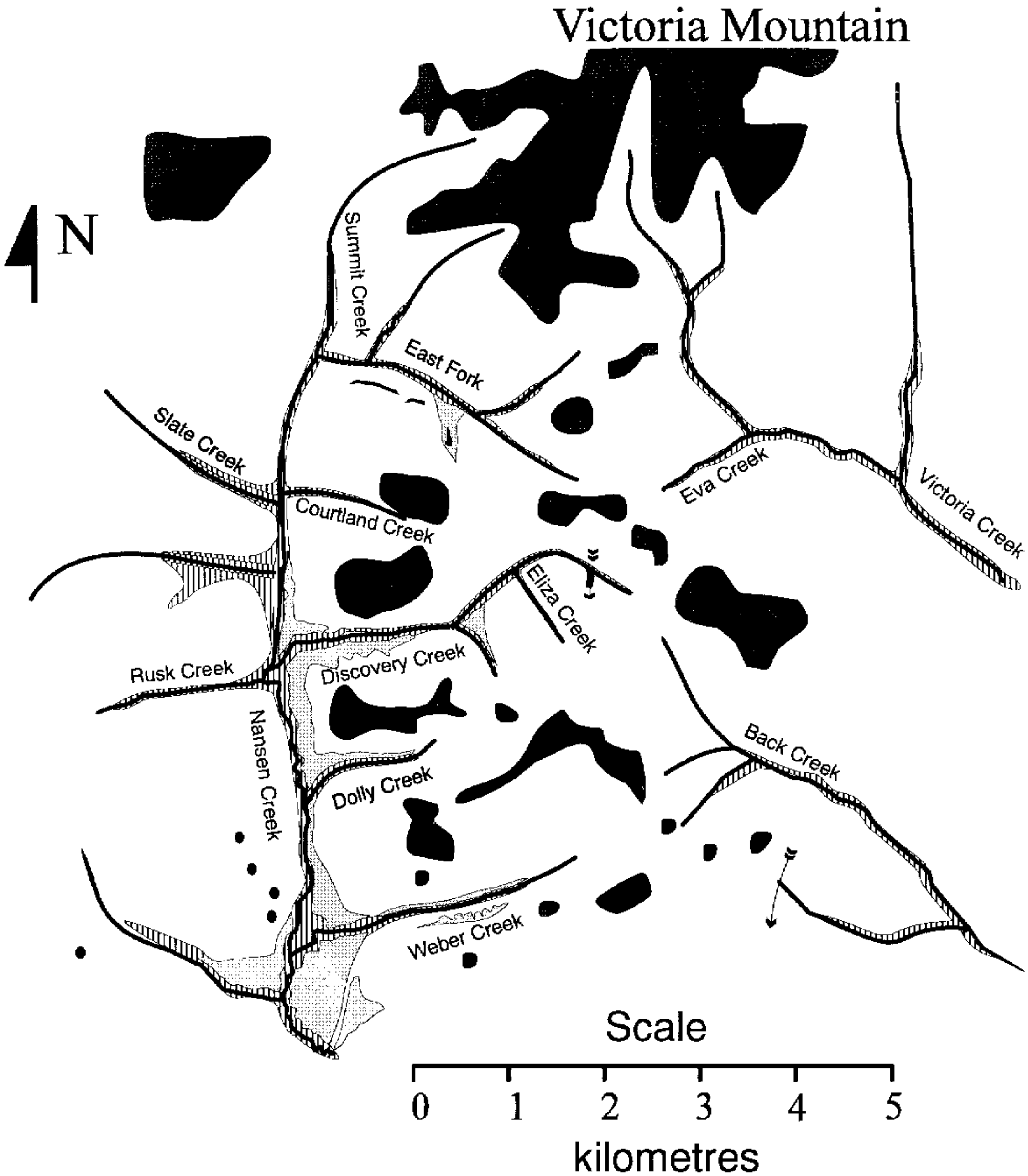

Figure 49 - Surficial Geology - Nansen Creek

Three major levels of terraces occupy the valley of Victoria Creek as far upstream as Back Creek, and along the valley of Nansen Creek as far north as Weber Creek. These generally range in elevation from 3100 to 3500 feet.

A second set of terraces occurs along major tributaries such as the northernmost and the next-to-northernmost left-limit tributaries of Victoria Creek, Victoria Creek tributary Dome Creek, and Nansen Creek tributaries Cabin, Weber, Dolly and Discovery creeks.

These terraces dominate the southern (north-facing) slopes of these tributary valleys, and have a fan-like morphology. They generally range in elevation from 3700 to 4000 feet.

Pre-Reid deposits

Kame terraces of pre-Reid glaciofluvial gravel occur along the southern (north-facing) valley wall of the East Fork of Nansen Creek, at an elevation of approximately 4200 feet. In addition, an ice-marginal channel of glaciofluvial gravel cuts bedrock at the 4270 foot elevation on Discovery Creek.

Scattered occurrences of pre-Reid till are mixed with colluvium on the south-facing slope of Discovery Creek , in occasional pockets on the north-facing slope of Discovery Creek (where it is sometimes overlain by thin glaciofluvial gravels), and on the upper reaches of Back Creek.

Facies Distribution

Facies 1

Facies 1, organic material, is present throughout the field area, mainly concentrated on valley slopes and valley bottoms. Except in areas of exposed bedrock or scattered active aeolian deposits, organic material occupies the present topographic surface. Thick deposits often occur with permafrost on the southern (north-facing) sides of valleys.

Facies 2

Facies 2, tephra, occurs on most valley slopes and in valley bottoms, where it is often thickened through reworking by fluvial and aeolian processes. Tephra occurs mainly within a few centimetres of the present topographic surface, mainly overlain by organic material.

Facies 3

Facies 3, diamicton, occurs scattered on valley slopes (where it is overlain by and mixed with colluvium) and deep within major valleys, where it is overlain by several metres of younger sediment.

Facies 4

Facies 4, massive and stratified silt and clay, occurs adjacent to present stream courses, on low fluvial terraces and in ponds and abandoned channels.

Facies 5

Facies 5, massive sand, occurs throughout the field area, however it is most often associated with proximal to medial alluvial fans which occur as terraces along major valleys and their tributaries.

Facies 6

Facies 6, stratified sand, occurs throughout the field area, but is most often associated with fluvial terraces and the distal portions of alluvial fans.

Facies 7

Facies 7, disorganized muddy gravel, occurs on valley slopes throughout the field area, where it is associated with the proximal regions of alluvial fans.

Facies 8

Facies 8, massive and stratified sandy gravel, occurs throughout the field area, however it is mainly associated with medial to distal portions of periglacial alluvial fans.

Facies 9

Facies 9, disorganized gravel, is associated with glaciofluvial terraces, medial periglacial alluvial fans and fluvial stream (gulch) gravels adjacent to present stream courses.

Facies 10

Facies 10, massive to crudely stratified gravel, occurs throughout the field area, in fluvial stream sediments, on fluvial terraces, as well as the medial to distal portions of alluvial fans, glaciofluvial terraces and channels, and periglacial alluvial fans and valley fills.

Valley Profile

Introduction

Figure 50 is a schematic valley profile of Nansen and Victoria Creeks. This profile was compiled from combined data including surficial geology, observed field relationships and facies data from measured sections. Vertical elevations are approximate, and no horizontal scale is implied.

Discussion

As the valley profile shows, a variety of facies associations and stratigraphic relationships occur in the valleys of Nansen and Victoria Creek and their major tributaries. A till interpreted to be deposited by the older of at least two pre-Reid glaciations is preserved only in patches and hummocks on the major valley floors. A younger pre-Reid till occurs intermittently along major valley walls and tributary valley walls where it is overlain by a variety of alluvial and colluvial deposits. Pre-Reid glaciofluvial gravels occupy terraces and cut bedrock on north-facing (southern) valley walls.

Two sets of alluvial terraces occur; 1) remnant tributary valley alluvial terraces, which occupy the (mainly southern) valley walls of major tributaries, and 2) remnant main valley alluvial terraces, which occupy the valleys of Victoria and Nansen creeks, where at least three levels can be discerned.

Along major tributary valleys, colluvium and recent alluvial fans overlie older glacial and glaciofluvial deposits. Recent gulch gravels have dissected and reworked older glacial, glaciofluvial and alluvial deposits.

Paleogeographic History

Introduction

Figures 51to 61 show the interpreted palegeographic history of the field area. These are based on field relationships, surficial geology and facies distribution data from measured sections.

Table 20 is the legend for the paleogeographic maps.

Discussion

Prior to the onset of periodic Pleistocene glaciations, a long period of humid tropical weathering occurred in the Tertiary. This left a thick mantle of highly-weathered and eroded bedrock (Figure 51).

The first of a minimum of two pre-Reid ice advances occurred at least 1 Ma B.P. (Hughes, 1987). This ice advance left only limited evidence, such as ice-marginal scours in bedrock along Mt. Nansen, and patchy occurrences of till along the valley floor of Nansen Creek. Only the highest points (above approximately 4500 feet ASL) of Mt. Nansen and Victoria Mountain were above the scouring effects of this ice sheet (Figure 52).

After deglaciation (Figure 53) and a lengthy ice-free period (Hughes, 1987) during which there was extensive weathering (Figure 54), a second pre-Reid glaciation occurred. As this Cordilleran ice sheet advanced, a local ice-centre probably originated in the Dawson Range (Jackson, 1993).

This likely began as cirque glaciers (Figure 55), progressed to valley glaciers (Figure 56) and eventually merged with the Cordilleran ice-sheet advancing from the south (Figure 57).

Following deglaciation, the climate returned at least once to warmer conditions than those of today, (Foscolos et al., 1977; Tarnocai, 1987) resulting in the extensive weathering of both bedrock and pre-Reid glacial and glaciofluvial deposits (Figure 58).

Figure 50 - Schematic Profile - Nansen and Victoria Creeks

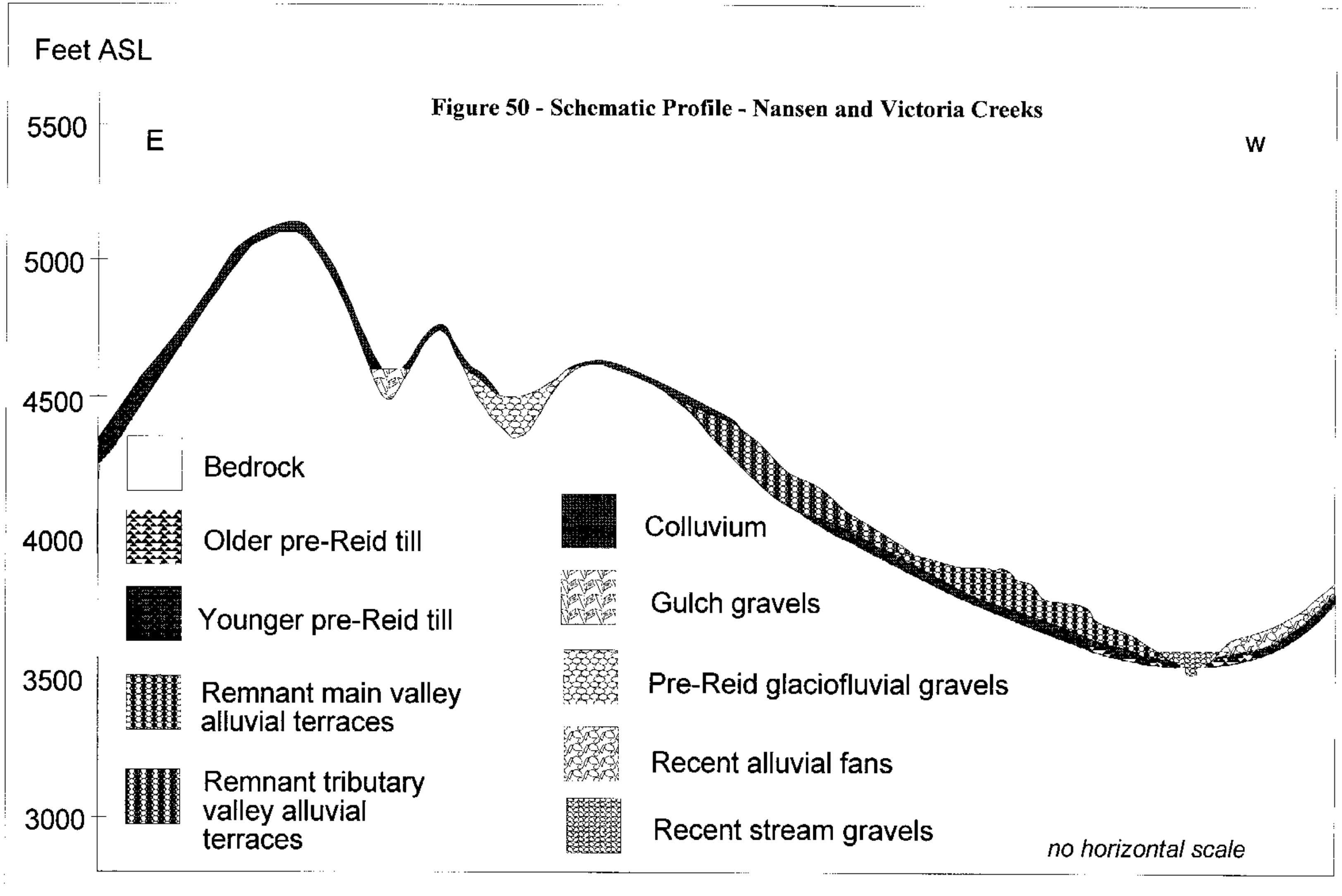

During the Reid glaciation, Cordilleran glacier ice did not advance up the valleys of Nansen and Victoria Creeks. However, the area was subjected to extremes of temperature as the ice sheet advanced down Nisling River valley. A rising base level resulted in extensive aggradation in the valleys of Nansen and Victoria creeks (Figure 59), reaching its maximum extent when Reid ice was only a few kilometres to the southeast in the Nisling River valley. Periglacial conditions prevailed and gravels deposited during this time commonly contained ventifacts and ice-cast gravel and sand wedges. During deglaciation, dropping base levels resulted in the degradation and dissection of pre-existing alluvial fans and subsequent aggradation on lower levels (Figure 60). This occurred at least three times, each lower fan being dissected by later degradation.

Gulch placer gravels at higher levels may have formed during this time.

During McConnell glaciation, ice did not advance close to Nansen and Victoria creeks, however base levels of Nisling River were probably raised enough to cause aggradation in Nansen and Victoria creeks. Some alluvial fan sedimentation probably occurred at this time. Wind-blown deposits of loess blanketed the area and filled hollows in tributary valleys.

Deglaciation and dropping base levels from the end of McConnell glaciation to the present has generally caused the present streams to degrade, leaving low relief terraces adjacent to present stream courses and further dissecting older alluvial terraces where they are proximal to present streams (Figure 61). Colluvial processes remained active on tributary valley slopes.

Table 20 - Legend for Paleogeographic Maps

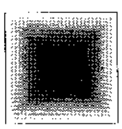	Deeply-weathered surface	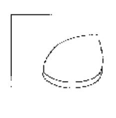	Ice sheet
	Rivers	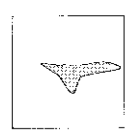	Alluvial fans
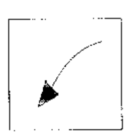	Direction of ice movement	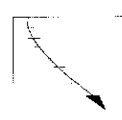	Ice-marginal glaciofluvial channel

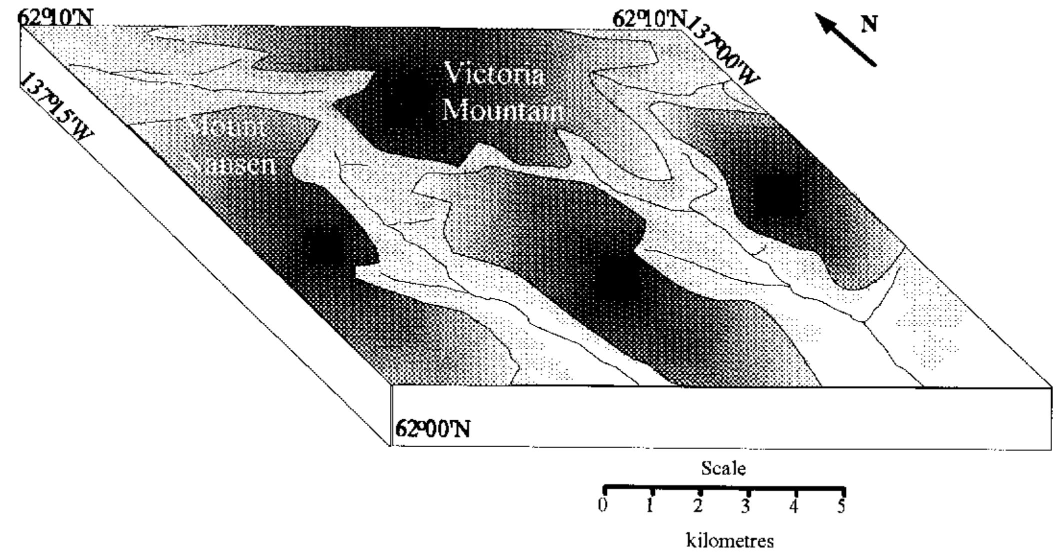

Figure 51 - Tertiary - Deeply-weathered bedrock mantle

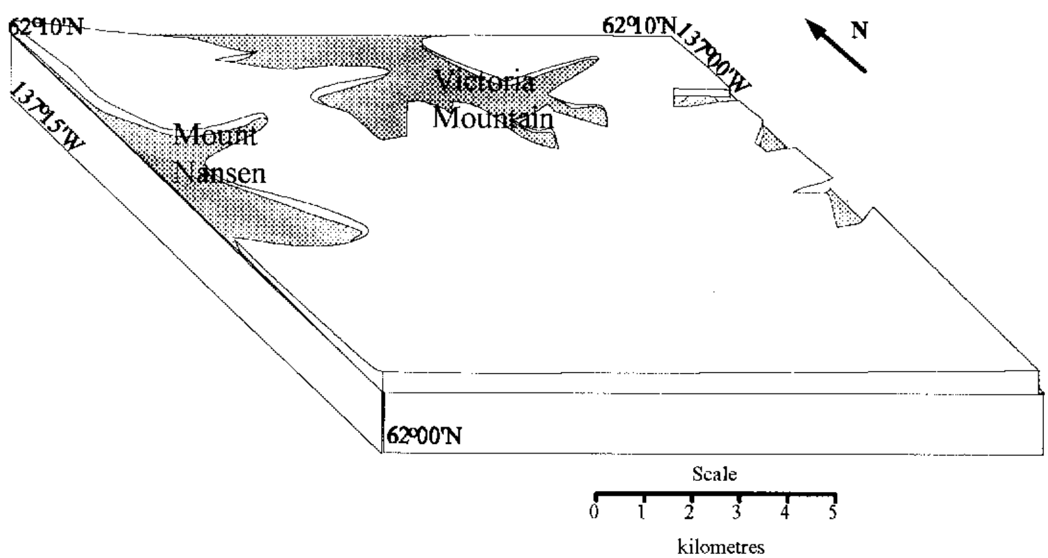

Figure 52 - Cordilleran Ice Sheet - early pre-Reid glaciation

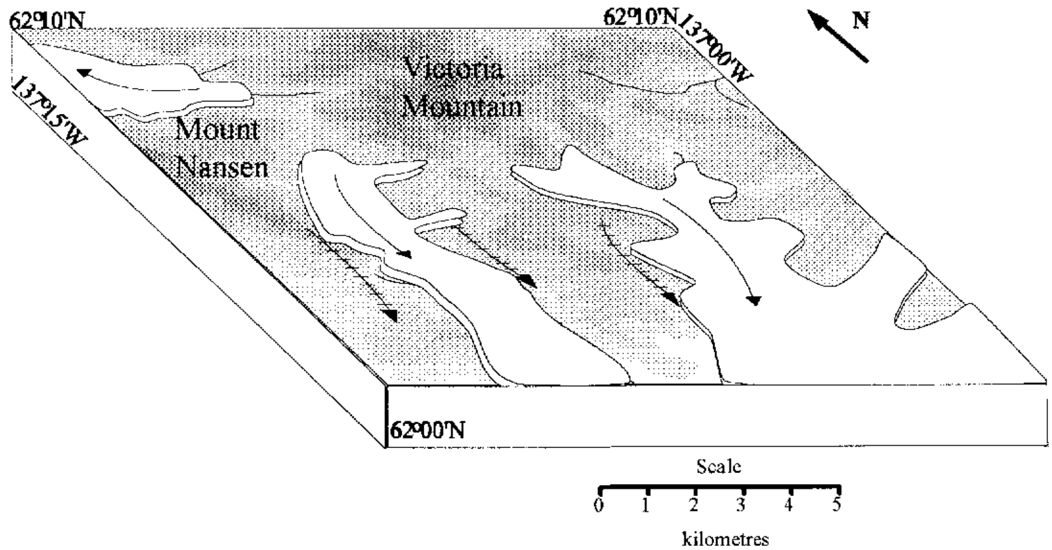

Figure 53 - Deglaciation - early pre-Reid glaciation

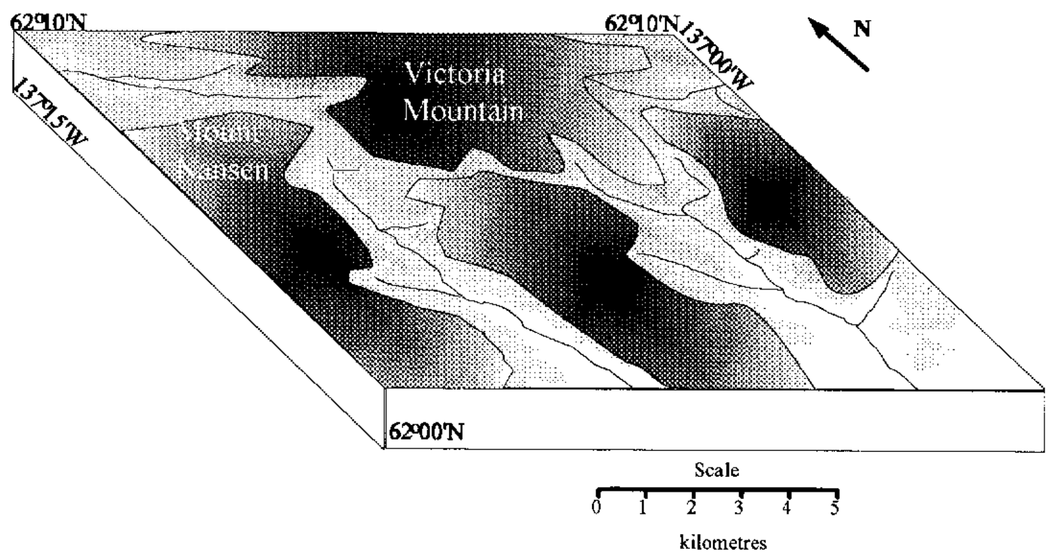

Figure 54 - Pre-Reid interglacial weathering - deeply-weathered bedrock mantle

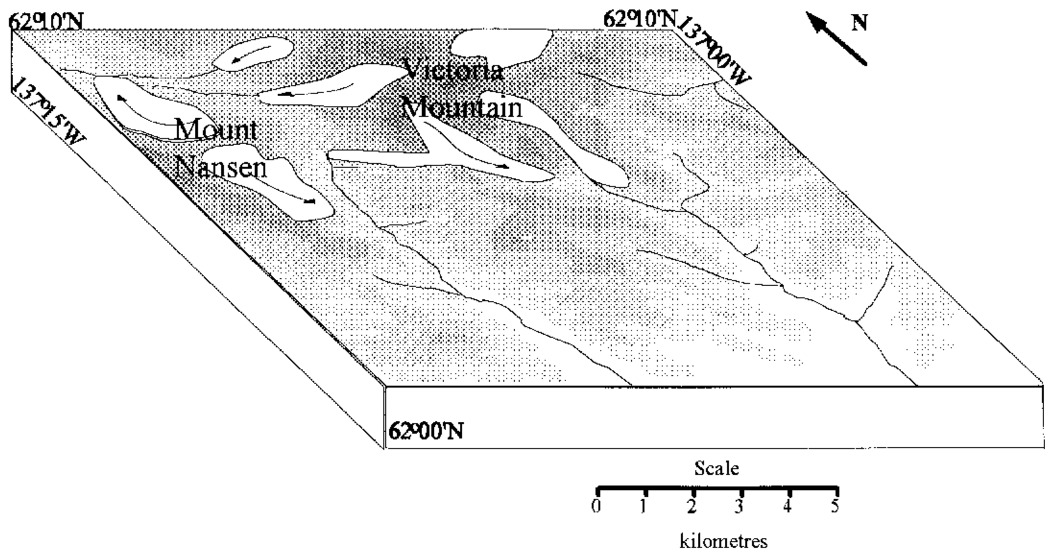

Figure 55 - Late pre-Reid glaciation - formation of cirque glaciers

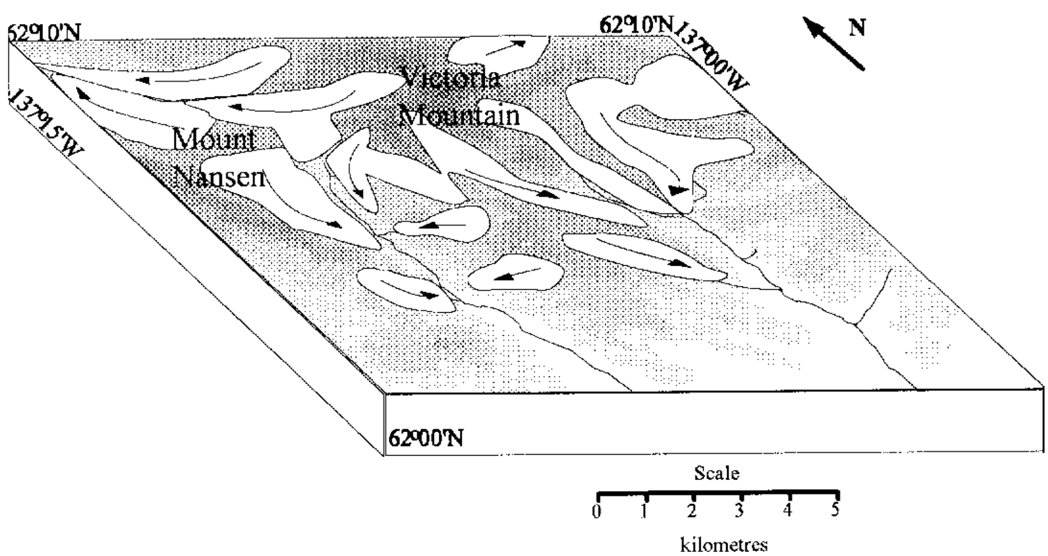

Figure 56 - Late pre-Reid glaciation - formation of valley glaciers

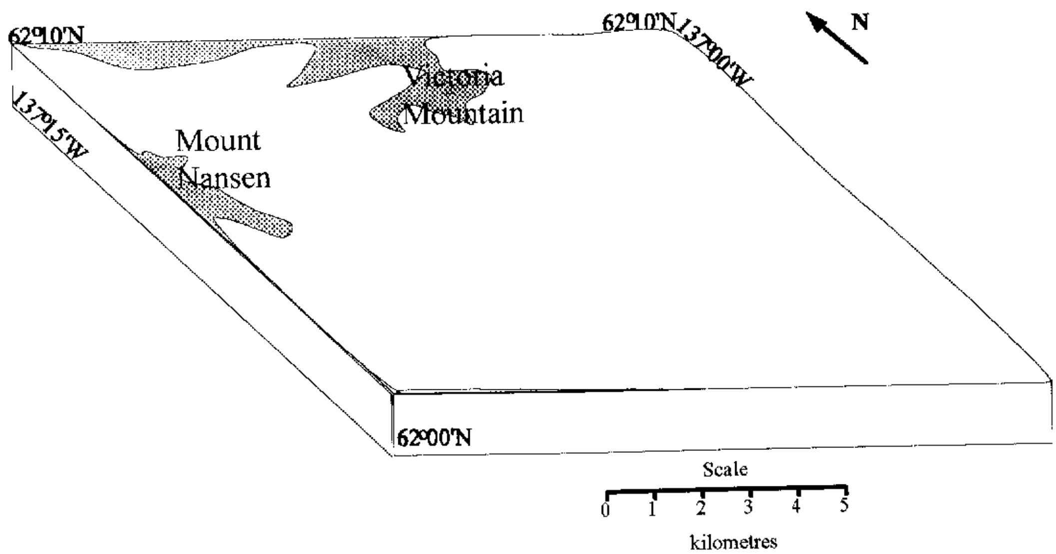

Figure 57 - Late pre-Reid glaciation - full glacial stage

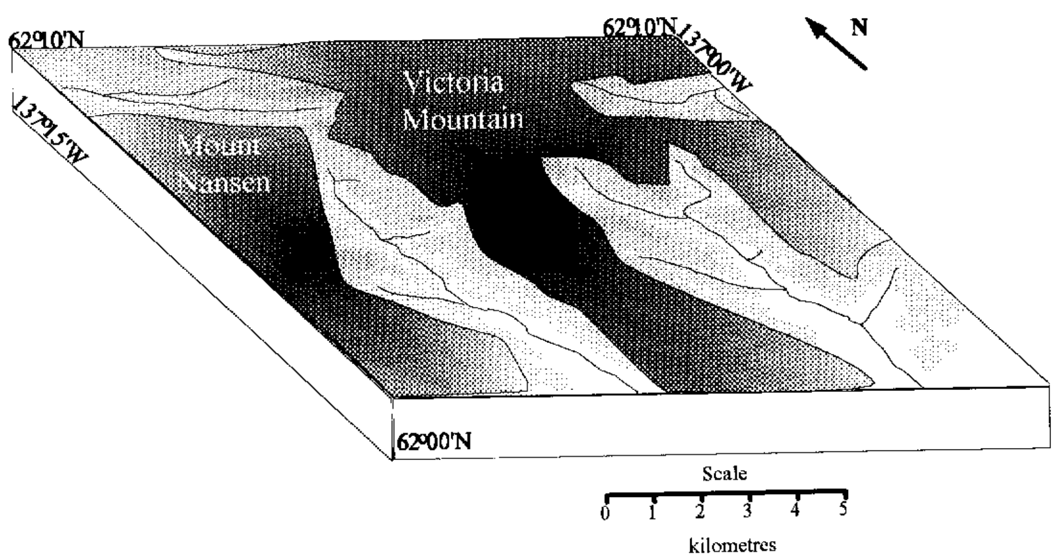

Figure 58 - Pre-Reid/Reid interglacial - weathering of bedrock and pre-Reid glacial deposits

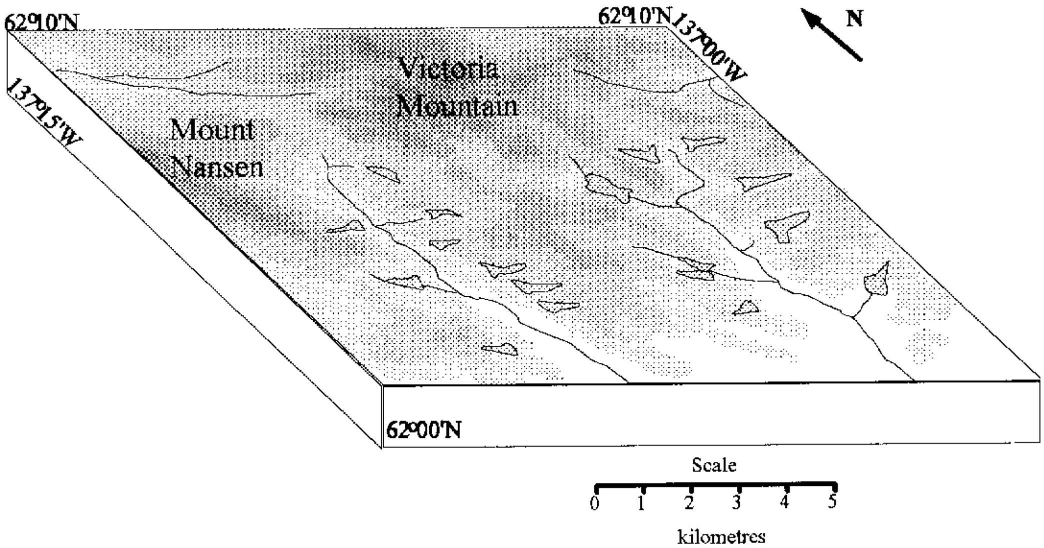

Figure 59 - Reid age alluvial fan sedimentation - initial stage

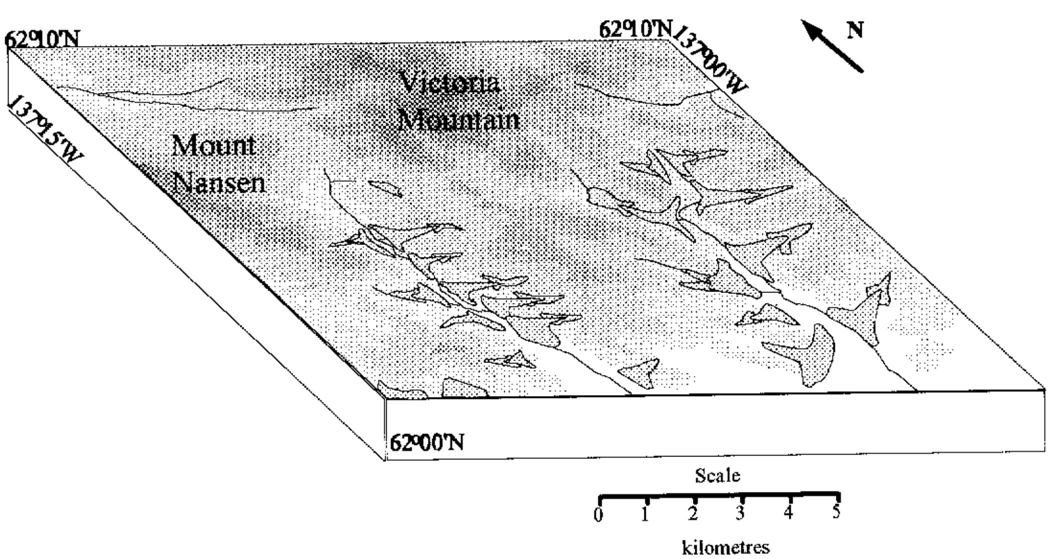

Figure 60 - Reid age alluvial fan sedimentation - dissection of pre-existing alluvial fans and sedimentation at lower levels

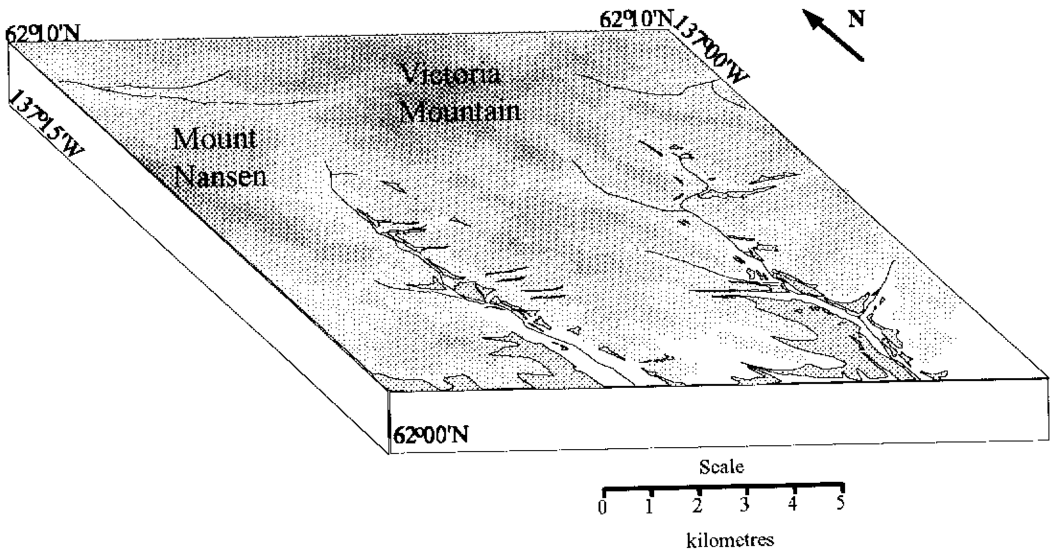

Figure 61 - Formation of remnant alluvial terraces by dissection of Reid deposits

PLACER GOLD MINERALIZATION

Bulk Sampling

Introduction

The amount and approximate size of gold grains, and metallic minerals present in each bulk sample is shown in Table 21. Heavy minerals are abbreviated as follows: Mt - magnetite, Py - pyrite, Hm - hematite, Ga - galena, Gn - garnet. Other terms: (+) = large amount of indicated mineral present and (-) = small amount of indicated mineral present.

The sizes of the gold grains were visually estimated. Figures 62 and 63 show the average amount of gold grains encountered by facies and by paleoenvironment, respectively.

Bulk sampling results

As a result of relatively few samples and small sample sizes, the gold content in the bulk samples is highly variable, however certain trends do emerge. Figure 62 shows that the highest average amount of gold encountered is in the diamicton, Facies 3. Moreover, as evident in Table 21, Facies 3 has consistently high amounts of gold. Significant amounts of gold are also present in Facies 10, massive to crudely stratified gravel, and Facies 9, disorganized gravel.

Figure 63 illustrates that the highest average amount of gold grains encountered is in the glacial paleoenvironment, which corresponds closely to the presence of Facies 3, diamicton. This is followed by periglacial valley fill, however this sample is biased by the high amount of gold grains found in NAN 1-1C,D which was sampled very close to the gravel - diamicton unconformity in measured section NAN 1-1. Fluvial, alluvial fan, colluvial, and gulch paleoenvironments average roughly half as many gold grains as the glacial paleoenvironment, and glaciofluvial paleoenvironments have the least amount of gold.

Table 21
Gold results - Bulk Sampling

Sample	Facies	Paleoenvironment	Gold grains > 2 mm	Gold grains 1.0 - 2.0 mm	Gold grains 0.5 - 1.0 mm	Gold grains < 0.5 mm	Total gold grains	Metallic minerals
DIS 1-2A	----	bedrock	0	0	5	0	5	mt
K 2-1A1	3	glacial	5	8	20	20	53	mt (+)
K 2-1A2	3	glacial	1	6	25	20	52	mt
K 2-1D	3	glacial	2	2	10	10	24	mt
UBAC 1-1B	3	glacial	1	0	3	0	4	mt
UBAC 1-1D	3	glacial	1	0	0	0	1	mt
UBAC 1-1G	3	glacial	0	0	6	0	6	mt
NAN 1-1A	3	glacial	0	5	35	20	60	mt (+)
DIS 2-1G	4	alluvial fan	0	0	4	0	4	mt
DIS 2-1C,D	5	alluvial fan	0	2	20	10	32	mt
DIS 1-2D	6	gulch	0	1	2	5	8	mt
DIS 1-3G	6	gulch	0	0	7	4	11	mt
DIS 2-1E	6	alluvial fan	0	0	2	2	4	mt
EVA 1-1C	7	gulch	0	0	5	0	5	mt
DIS 1-1D	8	gulch	0	0	5	15	20	mt
DIS 1-2C	8	gulch	0	0	1	10	11	mt
DIS 1-2F	8	gulch	0	0	2	6	8	mt
DIS 1-3I	8	gulch	0	1	7	0	8	mt
EFN 1-1A	8	glaciofluvial	0	0	2	0	2	mt
EFN 3-2D	8	glacial	0	0	1	3	4	mt (+)
EVA 2-1B1	8	gulch	0	0	6	0	6	mt
EVA 2-1B2	8	gulch	0	4	0	0	4	mt
K 1-3E	8	alluvial fan	0	0	3	5	8	mt
DIS 1-1E	9	gulch	0	0	4	8	12	mt
DIS 1-3B,C,D	9,10	gulch	0	16	5	0	21	mt,py
K 2-1F	9	alluvial fan	0	0	2	2	4	mt,py (+)
EFN 2-2E	9	glaciofluvial	1	0	4	0	5	mt
EVA 1-1A	9	gulch	0	1	0	0	1	mt

Table 21 (continued)
Gold Results - Bulk Sampling

Sample	Facies	Paleoenvironment	Gold grains > 2 mm	Gold grains 1.0 - 2.0 mm	Gold grains 0.5 - 1.0 mm	Gold grains < 0.5 mm	Total gold grains	Metallic minerals
DIS 1-1B	10	gulch	0	1	6	6	13	mt
DIS 1-1C	10	gulch	0	2	6	3	11	mt
DIS 1-2B	10	gulch	0	6	8	8	22	mt
DIS 1-3E	10	gulch	0	0	4	9	13	mt
DIS 1-3F	10	gulch	0	3	7	5	15	mt (+)
DIS 1-3H	10	gulch	0	3	12	3	18	mt
DIS 1-3J	10	gulch	0	0	13	0	13	mt
DIS 2-9A	10	glaciofluvial	0	3	5	5	13	mt
DIS 2-9E	10	glaciofluvial	1	2	8	0	11	mt
DIS 2-9F	10	glaciofluvial	0	1	3	4	8	mt
DIS 2-11C	10	colluvium	0	0	4	10	14	mt,gn,ga
LDIS 1-1B	10	periglacial alluvial fan	0	0	3	3	6	mt
LDIS 1-1A	10	periglacial alluvial fan	0	1	5	0	6	mt
UBAC 1-1H	10	glacial	0	0	4	4	8	mt
UBAC 1-1C	10	glaciofluvial	0	0	4	0	4	mt
LBAC 1-1A	10	fluvial	1	0	9	0	10	mt
LBAC 2-2A	10	periglacial alluvial fan	0	0	0	1	1	mt (+)
LBAC 2-2E	10	periglacial alluvial fan	0	0	2	10	12	mt (+)
EFN 4-1A	10	glaciofluvial	0	0	1	0	1	mt
EFN 2-1A	10	glaciofluvial	0	1	0	0	1	mt
NAN 1-1C,D	10,9	periglacial valley fill	0	0	40	10	50	mt (+)
NAN 1-1E	10	periglacial valley fill	0	0	7	0	7	mt,hm
VIC 1-2A	10	periglacial valley fill	0	0	4	0	4	mt (+)
VIC 1-1A	10	fluvial	0	0	11	0	11	mt

Average number of gold grains by facies

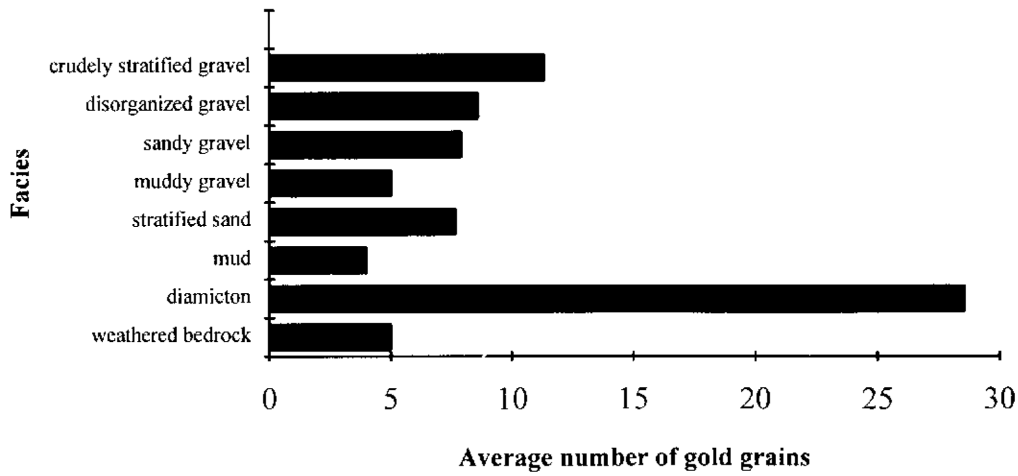

Figure 62

Average number of gold grains by paleoenvironment

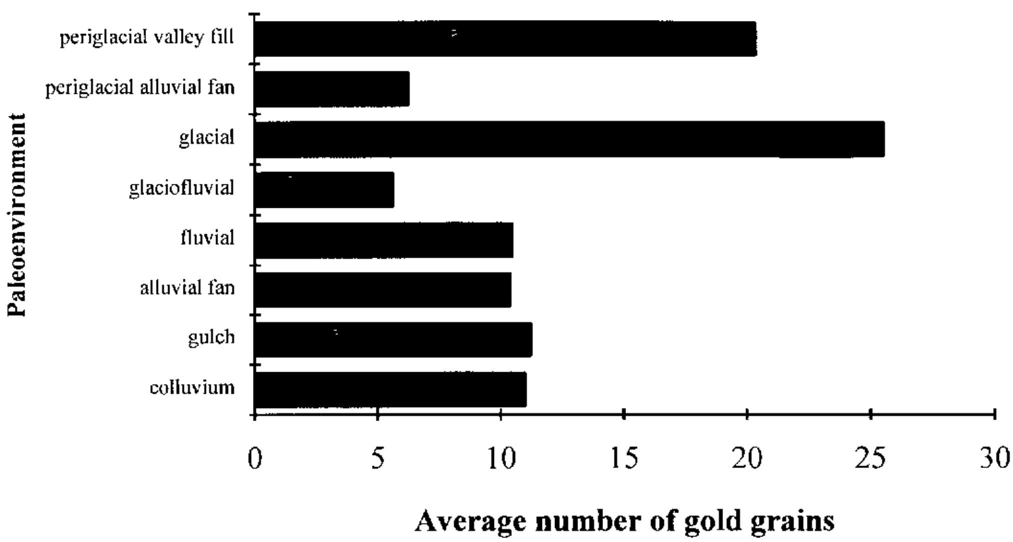

Figure 63

Gold Morphology and SEM Analyses

Introduction

Various gold samples from placer mining operations on Nansen Creek, East Fork, Klaza River, and Back Creek were examined and photographed using a Nikon camera attached to a Zeiss binocular microscope (Figures 64 to 67). In addition, gold grains obtained from bulk samples NAN 1-1A, UBAC 1-1B, DIS 1-3B,C,D, and K 2-1A1 were examined with a Cambridge Model 250 Scanning Electron Microscope (Figures 68 to 71). Table 22 summarizes the results of mesoscopic examination of gold grains. Table 23 summarizes the results of microscopic analysis of gold using the scanning electron microscope.

Table 22
Summary of observed mesoscopic morphological features of gold

Creek	Wires	Angular	Dendritic	Rounded	Folded	Striated
Klaza River	yes	yes	yes	yes	no	yes
Back Creek	yes	yes	yes	yes	no	no
East Fork	yes	no	yes	yes	no	no
Nansen Creek	no	no	yes	yes	yes	no

Discussion

Gold morphology varied widely on a macroscopic scale, with dendritic, crystalline, wiry, angular and rounded gold encountered in nearly all drainages. Nansen Creek gold had the only folded grains observed mesoscopically, while striations were observed only on samples from Klaza River. Angular grains of gold, particularly when found attached to quartz, are likely derived from local vein sources (Boyle, 1979), while well-rounded gold grains have undergone at least a few kilometres of fluvial transport (Boyle, 1979; Herail, 1988). Wiry, crystalline and dendritic gold have been described as diagnostic of residual placers formed through supergene enrichment of bedrock gold sources (Morison, 1989; Wilson, 1984).

On a microscopic scale, gold from the diamicton was found to have embedded quartz and striations, features which indicate some measure of ice transport (Herail, 1988; Herail et al., 1989). These characteristics appear to post-date other morphological features similar to those acquired during long distance fluvial transport, such as unusual smoothness, recumbent folding and rounded edges. This implies a period of fluvial transport prior to emplacement in the till, and it is quite likely the glacial event eroded and incorporated a pre-existing placer deposit.

REFER TO
COLOUR CD

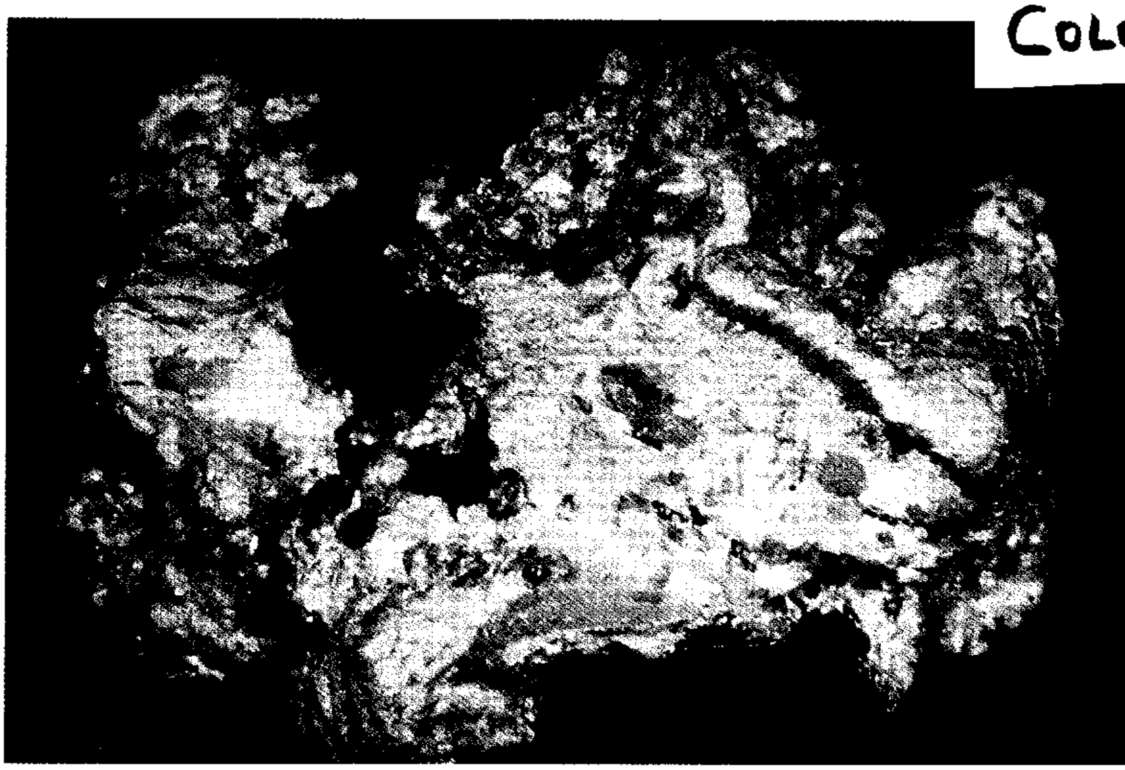

Figure 64 - Angular gold grain from alluvial fan gravels on Klaza River. Field of view approximately 1 cm.

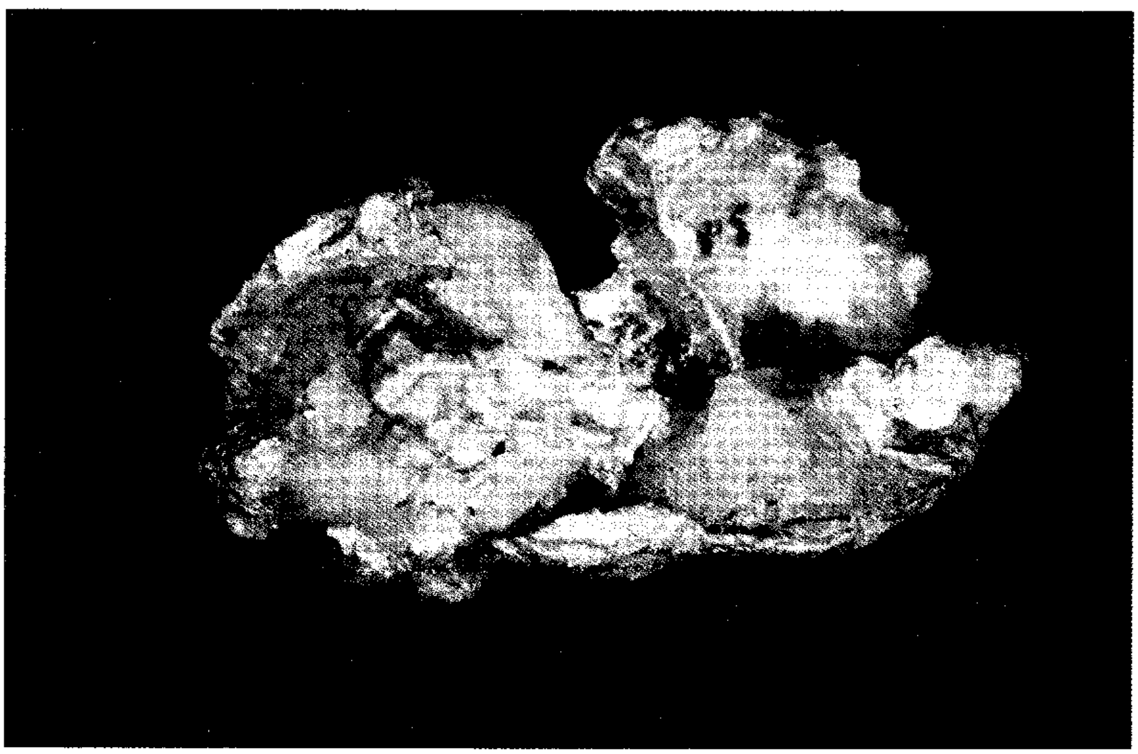

Figure 65 - Gold specimen from Back Creek with attached quartz. Field of view 1 cm.

REFER TO COLOUR CD

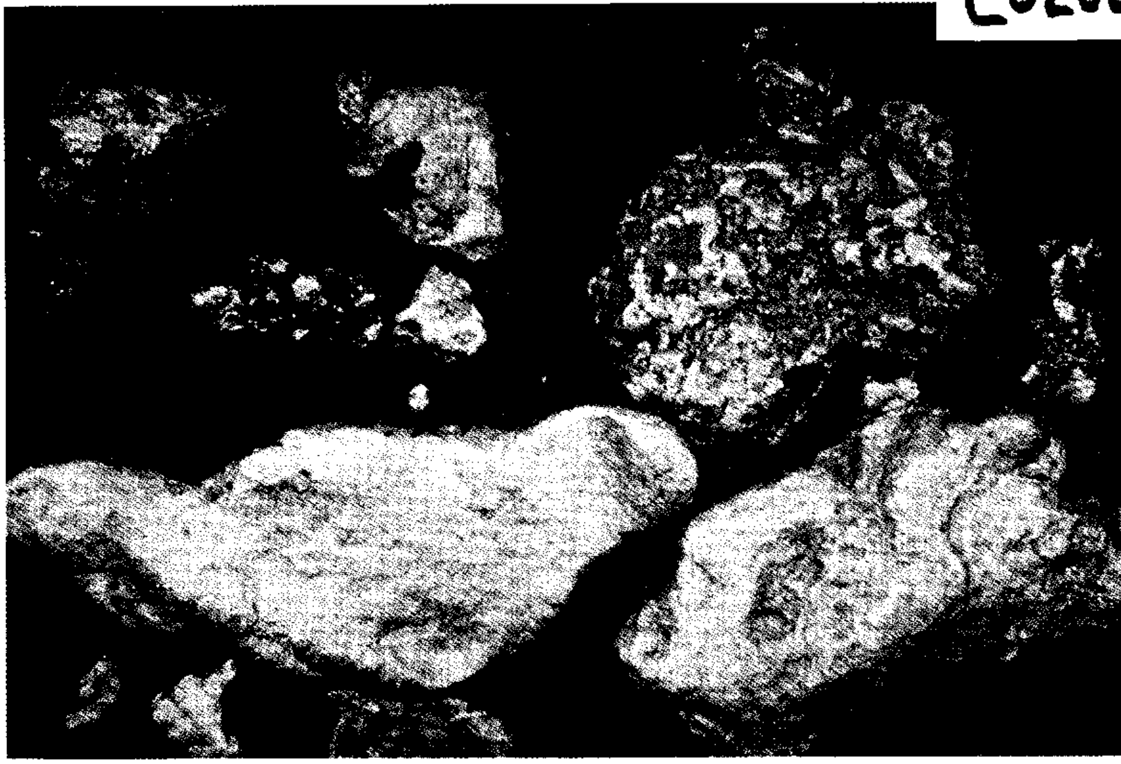

Figure 66 - An assortment of shapes are found in gold from the main valley of Nansen Creek. The silver grain in the upper left hand corner is bismuthinite. Field of view 3 cm.

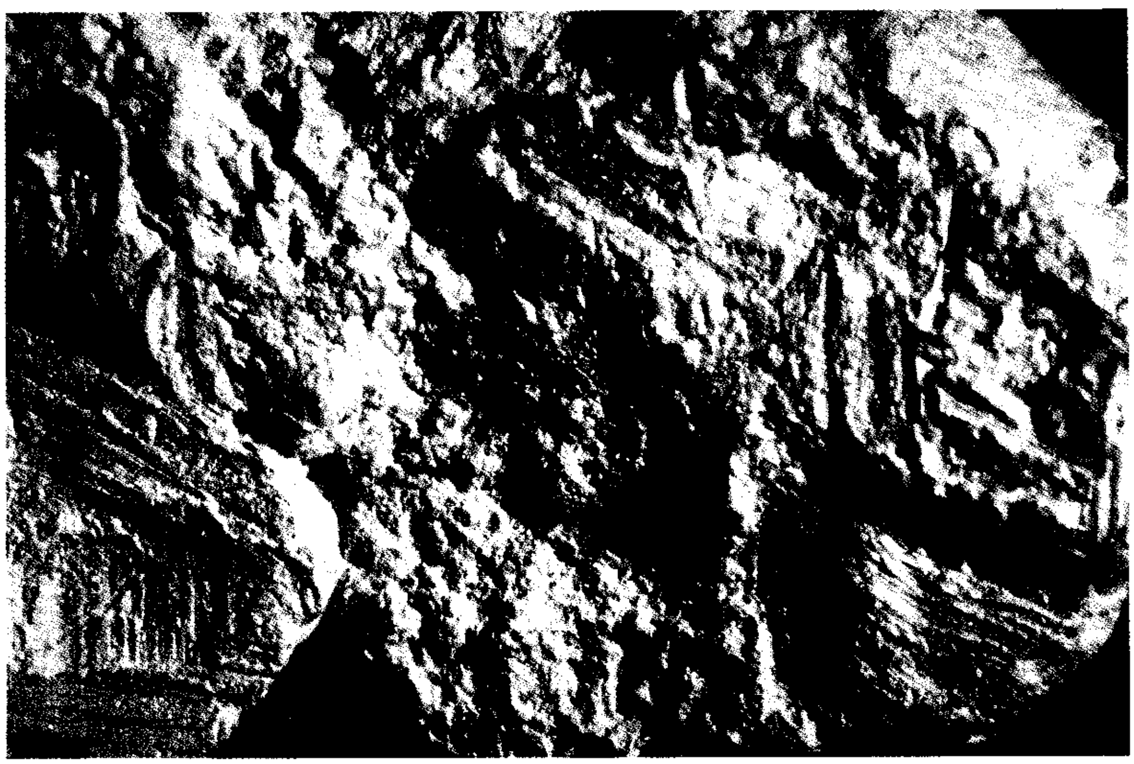

Figure 67 - Striations on a flat gold specimen from Klaza River. Field of view 5 mm.

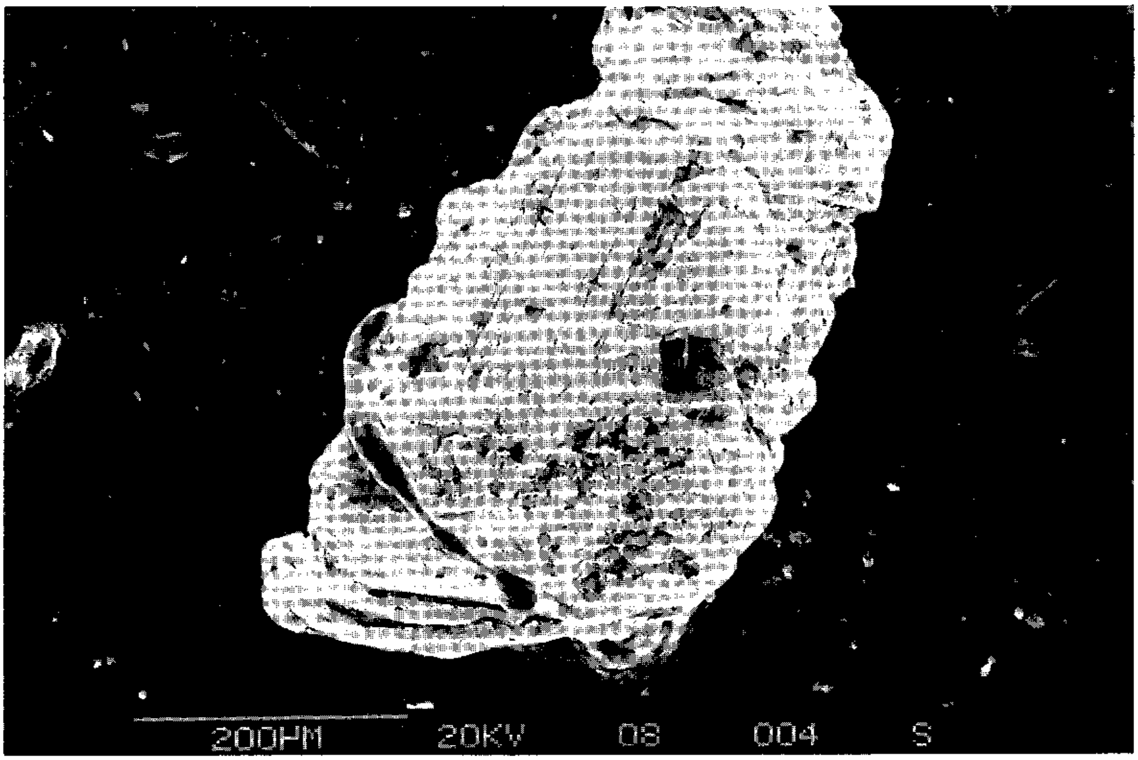

Figure 68 - Scanning electron photomicrograph of a gold grain derived from a diamicton on upper Back Creek. Grain has been folded, rounded and embedded with quartz. Remnant crystal outlines can be discerned.

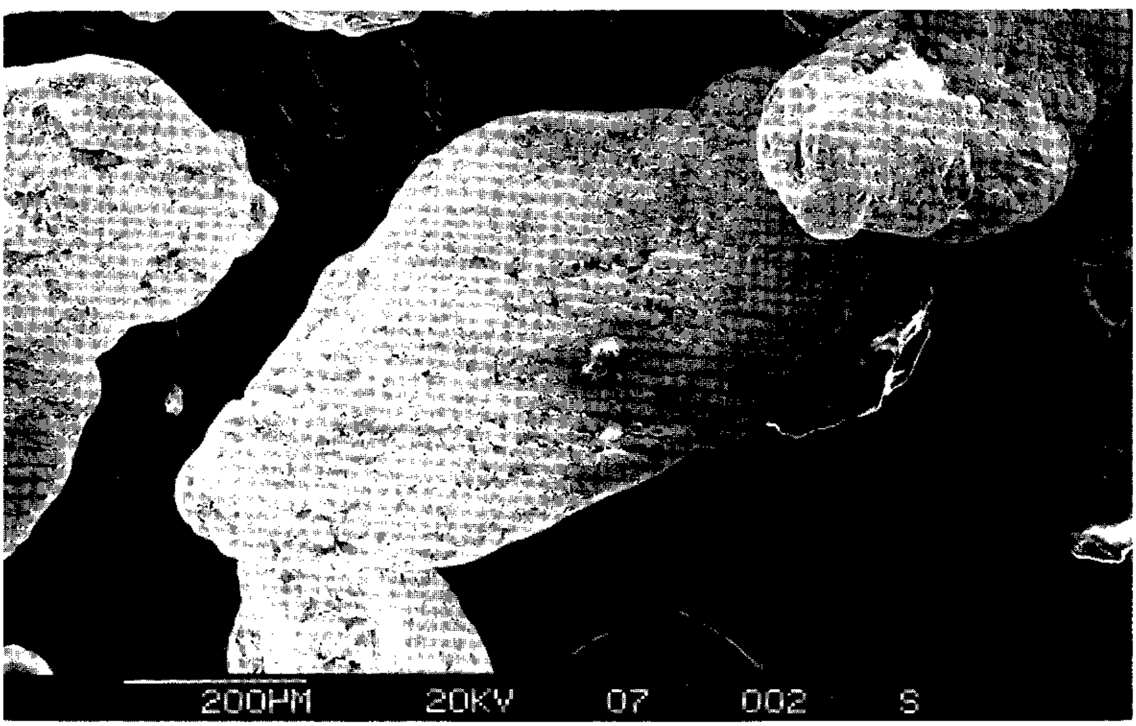

Figure 69 - Scanning electron photomicrograph shows rounded and pitted gold derived from a diamicton on Nansen Creek. Embedded quartz is visible in the centre of the largest grain.

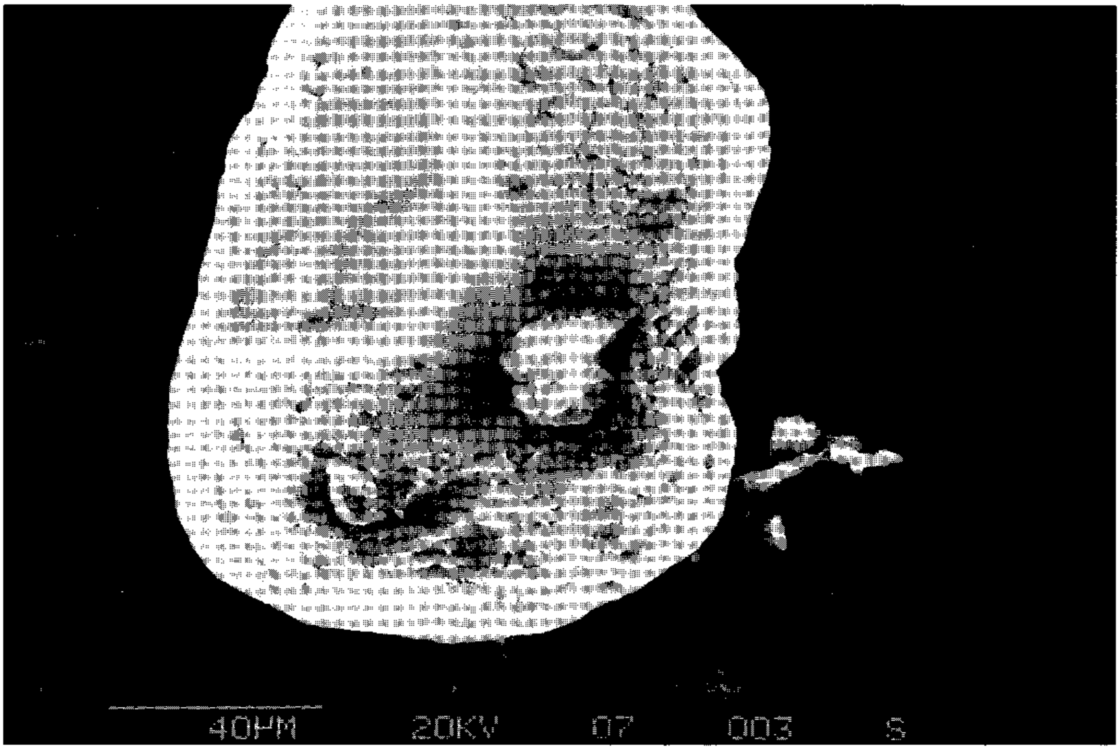

Figure 70 - Scanning electron photomicrograph of a rounded gold grain which has been embedded with quartz. Specimen is from a diamicton on Nansen Creek.

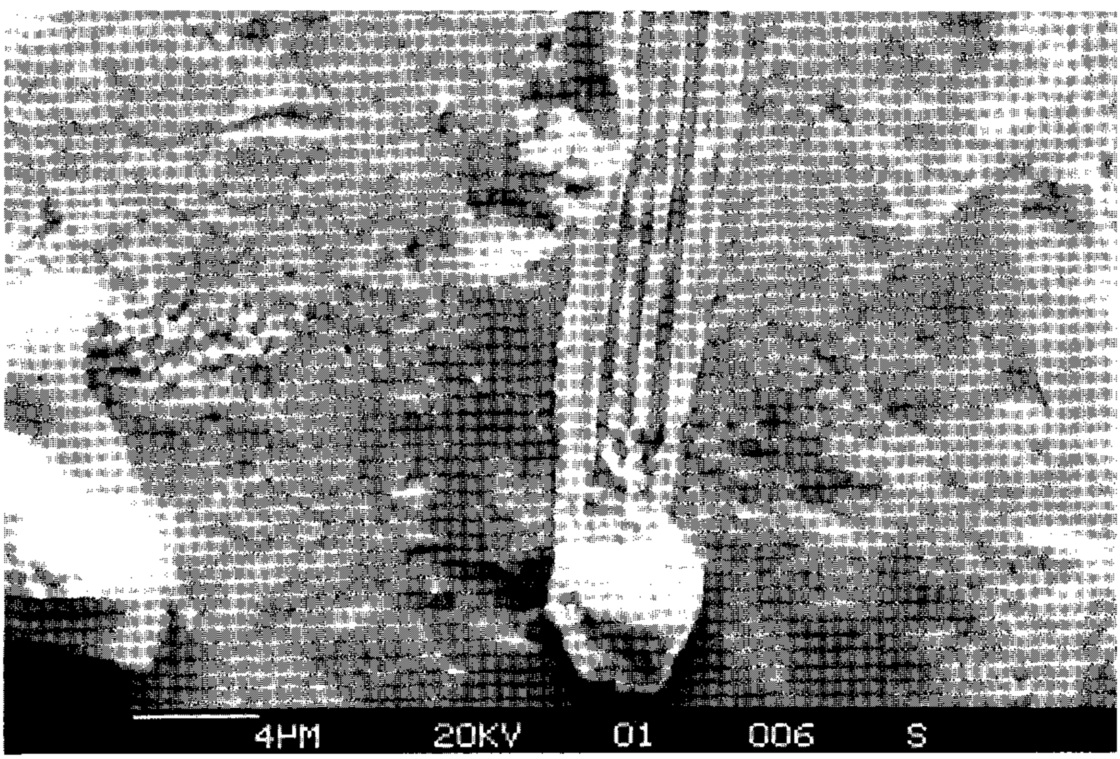

Figure 71 - Scanning electron photomicrograph of a quartz grain which has embedded and striated the surface of a gold grain. Specimen is from Klaza River.

Table 23
Summary of Gold Morphology from SEM Analyses

Unit	Creek	Grain types	Diagnostic features and accessory minerals
NAN 1-1A	Nansen Creek	mostly rounded grains	embedded quartz, striations
UBAC 1-1B	Back Creek	mixture of subangular and rounded grains	embedded quartz, some recumbent folding, electrum, galena, pyrite
DIS 1-3B,C,D	Discovery Creek	mixture of angular to subrounded grains	embedded quartz, bismuth, electrum, pyrite
K 2-1A1	Klaza River	mostly rounded grains	embedded quartz, striations

Controlling Mechanisms for Placer Gold Mineralization

Bedrock Sources

Significant bedrock sources of gold are often lacking near many placer deposits (Boyle, 1979; Morison, 1985). In contrast, several substantial bedrock sources of gold are documented, have been mined and are currently being explored in the Mt. Nansen area (Yukon Minfile, 1993). Most of the placer deposits that have been mined in this area are proximal to one or more of these bedrock sources. Some local placers (e.g. Discovery Creek - measured section DIS 1-2) often lie directly upon mineralized bedrock. It can be assumed that regardless of the hydrological and sedimentological concentrating mechanisms of placer formation, local point sources of gold are the main controlling factor in placer formation in the Mt. Nansen area.

Paleoenvironmental Controls

The Mt. Nansen area was subjected to several lengthy periods of warm, temperate to tropical weathering prior to the pre-Reid glaciations, between the pre-Reid glaciations and at least once since then (Foscolos et al., 1977; Jackson, 1993). This resulted in weathering of bedrock to depths of over one hundred metres and subsequent supergene enrichment of gold through chemical transport and precipitation. Dendritic, crystalline and wire gold have been suggested to be the result of supergene migration and precipitation of gold (Morison, 1989; Wilson, 1984). These types of gold are abundant in all drainages in the Mt. Nansen area.

Sedimentological and Hydrological Controls

Mechanisms for concentration of placer gold varied with each facies, all of which contained placer gold. The most abundant gold is encountered in Facies 3, diamicton. Significant concentrations of placer gold generally only occur in this environment where a glacier has cut through a primary mineralized zone (Herail et al., 1989). Some re-concentration may also occur within subglacial meltwater channels (Eyles and Kocsis, 1989).

Gold and other heavy minerals are also concentrated at bedrock or other impenetrable surfaces through reworking and downcutting during repeated flood events (Cheney and Patton, 1967).

A variety of hydrological processes are responsible for heavy mineral accumulation in other facies, including selective sorting of mineral grains through entrainment, suspension, shear, and transport (Slingerland, 1984). Segregation and deposition of heavy minerals is also accomplished by flow separation which occurs at abrupt changes in the stream bed geometry (Best and Brayshaw, 1985).

Conclusions

Although glacial material is not generally regarded as gold-bearing (Boyle, 1979; Morison, 1989), significant concentrations of gold can occur where glaciers cut primary mineralized zones (Herail et al., 1989). On Klaza River, Nansen Creek and Back Creek, a glacially-derived diamicton appears to be the main gold-bearing unit, at least in a zone close to bedrock.

Gold is also concentrated at the gravel/diamicton and gravel/bedrock interface, primarily in Facies 9 (disorganized gravel) and Facies 10 (massive to crudely-stratified gravel). The primary mechanism of concentration in these facies is likely to be selective entrainment of lighter mineral grains during major flood events, which results in an accumulation of heavy minerals (Slingerland, 1984). Protracted reworking of gravels would result in increasing concentrations of heavy minerals at bedrock or other impermeable surfaces (Cheney and Patton, 1967).

Gold concentration in the diamicton may be the result of glacial erosion and incorporation of a mantle of eroded bedrock material which was subjected to a long period of extensive weathering prior to glaciation (Eyles and Kocsis, 1989). The morphology of the gold in the diamicton indicates that an alluvial placer deposit was incorporated into a lodgement till and possibly reconcentrated to some degree by subglacial meltwaters. Wiry and dendritic gold in this lodgement till material infers that gold from supergene enriched residual placers was also incorporated into the lodgement till.

Previous workers (Cairnes, 1915a; Bostock, 1936a; 1966) suggested that significant placer gold concentrations occur only in alluvium that lies either upon bedrock or on glacial till and no gold is present either in or below the till on bedrock. New data from this study suggests that significant amounts of placer gold also occur within the diamicton, primarily at the diamicton/bedrock contact.

SUMMARY OF RESEARCH RESULTS

Sedimentology

In addition to various organic horizons and tephra, (Facies 1 and 2, respectively), eight clastic facies occur in the study area; Facies 3: clay-rich diamicton; Facies 4: massive and stratified silt and clay; Facies 5: massive and disorganized pebbly sand and sand; Facies 6: stratified pebbly sand and sand; Facies 7: disorganized muddy gravel; Facies 8: massive and stratified sandy gravel; Facies 9: disorganized gravel; and Facies 10: massive to crudely-stratified gravel.

Laboratory analyses show that grain sizes of less that .125 mm (very fine sand or smaller) dominate the matrix components of Facies 1 through 6, while Facies 3 and 7 are depleted in the fine to medium sand size. Facies 8, 9 and 10 are dominated by fine to medium sand in the matrix. Average mean phi values decrease from clay-rich to clay-poor facies, and average standard deviations decrease as sorting increases.

Overall grain size distribution from field estimates show that Facies 4 and 7 have significant amounts of mud, while Facies 5, 6 and 8 have significant amounts of fine to medium sand. Facies 8, 9 and 10 are dominated by gravel while Facies 3 is nearly bimodal with both mud and gravel fractions. Average mean phi values progressively decrease from muddy to sandy to gravelly facies, while average standard deviations are highest for muddy facies (Facies 3,4 and 7) and lower for sandy (Facies 5,6 and 8) and gravelly (Facies 9 and 10) facies.

Maximum particle size data is generally a function of sorting. The largest average, maximum, minimum, range and standard deviation of clast size is encountered in Facies 3 - diamicton, while Facies 6, pebbly stratified sand, has the smallest range of values.

Lithological analyses show that most clasts are composed of local bedrock (andesite, granodiorite and quartz-feldspar porphyry), however significant amounts of sedimentary clasts occur in Back Creek and Nansen Creek. This is an indication of the dominance of Facies 3, diamicton, which has a higher proportion of sedimentary clasts than all other facies.

The presence of illite/smectite mixed-layer clays is one of the diagnostic features of soils developed on pre-Reid glacial drift surfaces. Smectite or illite/smectite mixed layers were encountered in significant amounts throughout most of Facies 3, diamicton, and from samples EFN 2-1G, EFN 2-2E2, and DIS 2-9E of Facies 9 and 10. Clay mineralogy and Munsell color data indicate that measured sections EFN 2-1, EFN 2-2, and DIS 2-9 and diamicton units of Facies 3 are consistent with surfaces of pre-Reid age.

Sediments on East Fork, Weber, Nansen and Lower Back creeks contained ventifacts, and ice-cast sand wedges were encountered on Weber and Lower Back creeks. Due to the low amount of these periglacial features encountered, relative abundances (as described by Tarnocai, 1987) cannot in this instance be used to infer an age for these deposits.

Facies 3, diamicton, is genetically interpreted as glacial till. Facies 4, massive and stratified silt and clay, is interpreted as lacustrine in origin. Facies 5, massive and disorganized pebbly sand and sand, is interpreted as deposited on fluvial channels and channel margins under rapidly waning flow. Facies 6, stratified pebbly sand and sand, is interpreted as deposited on point and channel bar-tops during normal fluvial flow. Facies 7, disorganized muddy gravel, is interpreted as debris flows deposited on the proximal regions of alluvial fans. Facies 8, massive and stratified sandy gravel, is interpreted as deposited on braid bars and alluvial fans during hyperconcentrated flood flows to waning flood flows. Facies 9, disorganized gravel, is interpreted as deposited in fluvial channels and proximal alluvial fans under conditions of high fluvial flood flow. Facies 10, massive to crudely-stratified gravel, is interpreted as deposited in braided fluvial channels and proximal to medial alluvial fans under conditions of high fluvial flood flow to normal fluvial flow.

Surficial Geology

Unconsolidated sediments in the study area are interpreted to have a number of genetic origins, including 1) Holocene colluvium; 2) Holocene alluvial fans; 3) Holocene to McConnell fluvial stream deposits; 4) Reid periglacial alluvial fans; 5) Reid periglacial valley fill; 6) pre-Reid glacial deposits; 7) pre-Reid glaciofluvial terraces; and 8) pre-Reid glaciofluvial channels.

Colluvium occupies the slopes between bedrock exposures and valley-side and valley-floor alluvial deposits, and overlies older deposits of glaciofluvial gravels and till on the East Fork of Nansen Creek and on Discovery Creek.

Recent stream gravel deposits, low fluvial terraces and alluvial fans occur proximal to present stream courses in all drainages.

Reid-age remnant alluvial terraces occur along Nansen and Victoria creeks and along major tributaries such as Dome, Cabin, Weber, Dolly and Discovery creeks.

Kame terraces of pre-Reid glaciofluvial gravel occur along the southern (north-facing) valley wall of the East Fork of Nansen Creek, and an ice-marginal channel of glaciofluvial gravel cuts bedrock at the 4270 foot elevation on Discovery Creek.

Pre-Reid till occurs mixed with colluvium on the south-facing slope of Discovery Creek , in occasional pockets on the north-facing slope of Discovery Creek (where it is sometimes overlain by thin glaciofluvial gravels), and on the upper reaches of Back Creek.

Bedrock is exposed on most ridges at elevations of 4500 feet and above. Scattered tors occur at lower elevations, mainly near the 4000 feet elevation.

Paleogeographic Model and Quaternary History

During the Tertiary Period, prior to the onset of Pleistocene glaciations, a lengthy period of humid tropical weathering occurred, leaving a thick mantle of highly-weathered and eroded bedrock (Hughes et al., 1989).

At least two pre-Reid ice advances blanketed the area. The first, probably more extensive, ice advance, left only limited evidence, such as ice-marginal scours in bedrock along Mt. Nansen, and patchy occurrences of till along the valley floor of Nansen Creek.

After another lengthy period of weathering in an ice-free environment, the second pre-Reid ice event occurred. The ice advance probably originated from an ice-centre in the Dawson Range (Jackson, 1993), which presumably merged with the Cordilleran ice-sheet advancing from the south.

Following deglaciation, the climate returned at least once to warmer conditions than those of today (Foscolos et al., 1977), resulting in the extensive weathering of both bedrock and of pre-Reid glacial and glaciofluvial deposits.

During the Reid glaciation, Cordilleran glacier ice did not advance up the valleys of Nansen and Victoria creeks, however, the area was subject to extremes of temperature as the ice sheet advanced down Nisling River valley. Extensive aggradation occurred in the valleys of Nansen and Victoria Creeks, reaching its maximum extent when Reid ice was only a few kilometres to the southeast in the Nisling River valley. Periglacial conditions prevailed and gravels deposited during this time commonly contained ventifacts and ice-cast gravel and sand wedges. During deglaciation, pre-existing alluvial fans were dissected and degraded, and aggradation occurred on lower levels. This occurred at least three times, each lower fan being dissected by later degradation. Accumulations of heavy minerals were likely reworked and reconcentrated during these events.

During McConnell glaciation, ice did not advance close to Nansen and Victoria creeks, however some aggradation probably occurred in Nansen and Victoria creeks, resulting in the formation of some alluvial fans. Glacially-derived deposits of loess blanketed the area and filled hollows in tributary valleys.

In the period from the end of McConnell glaciation to the present, streams have generally degraded, leaving low relief terraces adjacent to present stream courses and further dissecting older alluvial terraces where they are proximal to present streams. Colluvial processes remained active on tributary valley slopes.

Placer Gold

Limited bulk sampling and placer mining shows that glacigenic diamicton on Klaza River, Nansen Creek and Back Creek contains significant accumulations of placer gold, primarily at the diamicton/bedrock contact. Gold is also concentrated at the gravel/diamicton and gravel/bedrock interface, primarily in Facies 9 (disorganized gravel) and Facies 10 (massive to crudely stratified gravel).

The primary mechanism of concentration in these Facies 9 and 10 is likely to be selective entrainment of lighter mineral grains during major flood events, which results in an accumulation of heavy minerals (Slingerland, 1984). Continued reworking of gravels resulted in increased concentrations of heavy minerals at bedrock and other impermeable surfaces such as the clay-rich diamicton (Cheney and Patton, 1967).

Placer gold concentration in the diamicton is likely due to glacial erosion and incorporation of a mantle of extensively eroded bedrock material. This material consisted of pre-existing alluvium and supergene-enriched residual placers.

Previous workers (Cairnes, 1915a; Bostock, 1936a; 1966) suggested that significant placer gold concentrations occur only in alluvium that lies either upon bedrock or glacial till and no gold is present either in or below the till on bedrock. New data from this study suggests that significant amounts of placer gold also occur within the diamicton, principally at the diamicton/bedrock contact.

CONCLUSIONS AND RECOMMENDATIONS FOR EXPLORATION AND FUTURE STUDY

Conclusions

Figure 72 is an idealized stratigraphic section which illustrates the following generalized stratigraphic relationships:

1) pre-Reid glacial till (diamicton) rests on bedrock, and it in turn may or may not be overlain unconformably by glaciofluvial gravels;

2) alluvial fans of Reid to McConnell age may unconformably overlie the pre-Reid glacial till, or may lie directly upon bedrock; these complexes are in turn often unconformably overlain by colluvium;

3) McConnell to Holocene-age gulch gravels may unconformably overlie both alluvial fans and pre-Reid glacial deposits, or may rest directly upon bedrock, and are themselves often overlain by colluvium; and

4) capping the entire sequence are various Holocene-age buried organic horizons, silt/clay and at least two separate tephras.

Favorable Stratigraphic Settings for Gold

Favorable stratigraphic settings as noted in Figure 72 are as follows:

1) at the glacial till (diamicton)/bedrock contact;
2) within the glacial till (diamicton) itself and in intraglacial gravels within the till;
3) at the alluvial fan gravel/glacial till unconformity;
4) scattered within alluvial fan complexes, most favorably at the apex of the fan, and
5) at the gulch gravel/alluvial fan or bedrock unconformity.

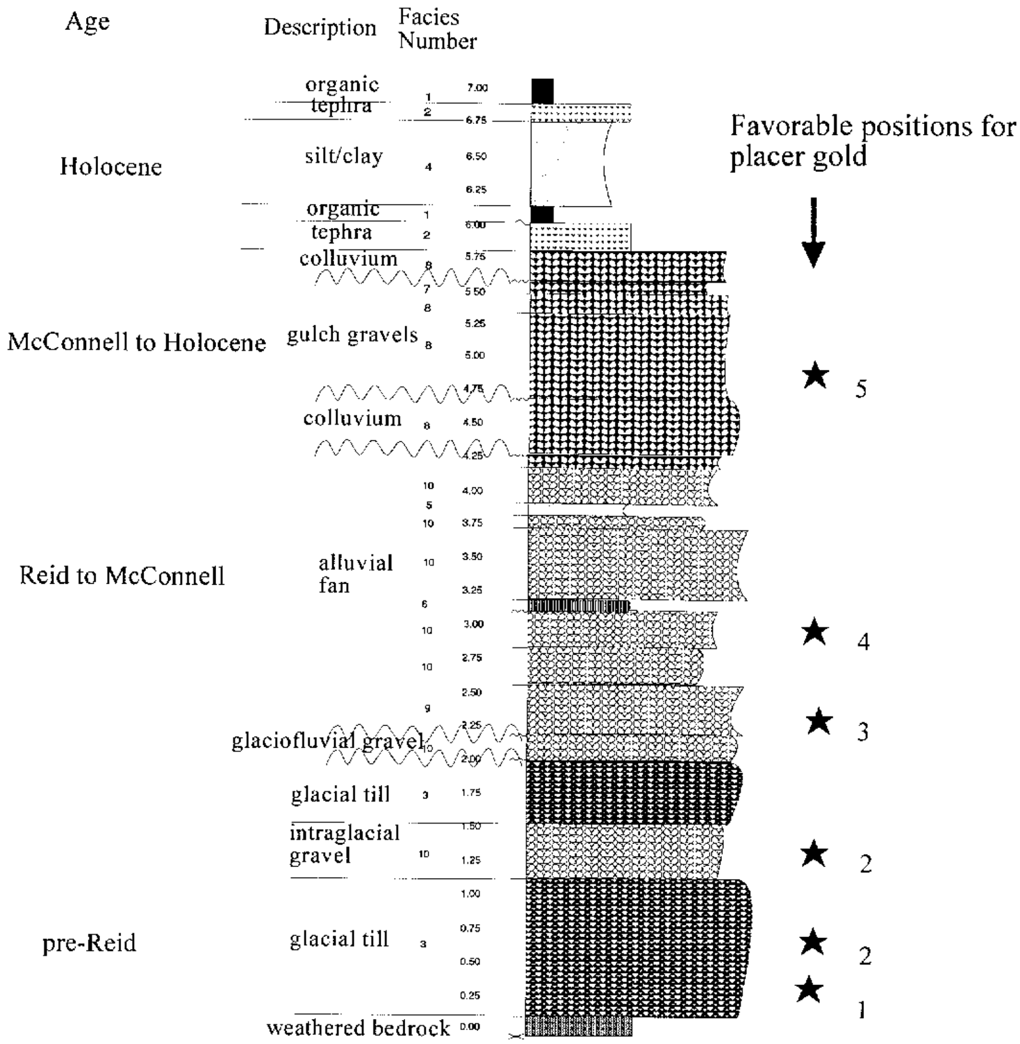

Figure 72 - Idealized Stratigraphic Section

Recommendations for Exploration and Future Study

Recommendations for Exploration

There are several possible exploration targets for placer gold in various geomorphic settings. These are shown in Figure 73 and are described as follows:

A) pre-Reid glacial till, high on valley sides, proximal to local bedrock sources of gold;

B) McConnell to Holocene gulch gravels, high in tributary valleys proximal to local bedrock sources of gold;

C) in alluvial fan complexes, most favorably near the apexes of the alluvial fans;

D) in pre-Reid till, deep in the valleys of Nansen Creek and Victoria Creek;

E) in point and channel bars of Recent gravels in the main valleys of Nansen and Victoria creeks;

F) in pre-Reid glaciofluvial deposits, generally proximal to local bedrock sources of gold; and

G) in pre-Reid till beneath Reid-age remnant alluvial terraces, and possibly within the remnant terraces themselves.

The concentration of placer gold in all of these stratigraphic and geomorphic settings can be highly variable, and depends upon a number of factors including proximity to local bedrock gold sources, amount of fluvial reworking of the gravels, and the age of the deposits. The economics of mining the placer gold in these various settings depends on a number of physical factors including the depth of overburden, the amount of frozen ground, the amount of water available for mining, and the various physical properties of the sediments themselves.

Recommendations for Future Study

A) Reid-age remnant alluvial terraces

The exact character and origin of these remnant alluvial terraces, both on tributary valleys such as Weber Creek and on the margins of the main valleys of Nansen and Victoria creeks, needs to be examined further. Exposure is typically poor as previous workers and placer miners have not generally worked these deposits.

Preliminary examinations of these deposits have shown them to have several unusual aspects including:

i) the sand matrix is unusually well-sorted, lacking in heavy minerals and sand grains are unusually well-rounded and quartz-rich;

ii) clasts within the deposits are unusually angular and are often ventifacts;

iii) the terraces comprise an unusually large volume of sediments in a relatively small basin.

B) Ages of pre-Reid sediments

It is still not possible to discern between deposits of the two pre-Reid glacial advances, except possibly in the case of the lithologically different "older till" found on Nansen Creek section NAN 1-1 and described in earlier chapters. Further work needs to be done in the Mt. Nansen area and areas adjacent to it if this distinction is to be possible.

C) Pre-Reid glacial limits - Carmacks and adjacent Aishihik and McQuesten map sheets

Due to the subdued nature of pre-Reid glacial features (Bostock, 1966), the exact limit of the pre-Reid ice advances is generally poorly-defined, in the Carmacks map area as well as in the adjacent Aishihik and McQuesten map areas. Further fieldwork must be done to identify pre-Reid deposits and map the limits of the pre-Reid glaciations.

Figure 73 - Exploration Targets - Nansen and Victoria Creeks

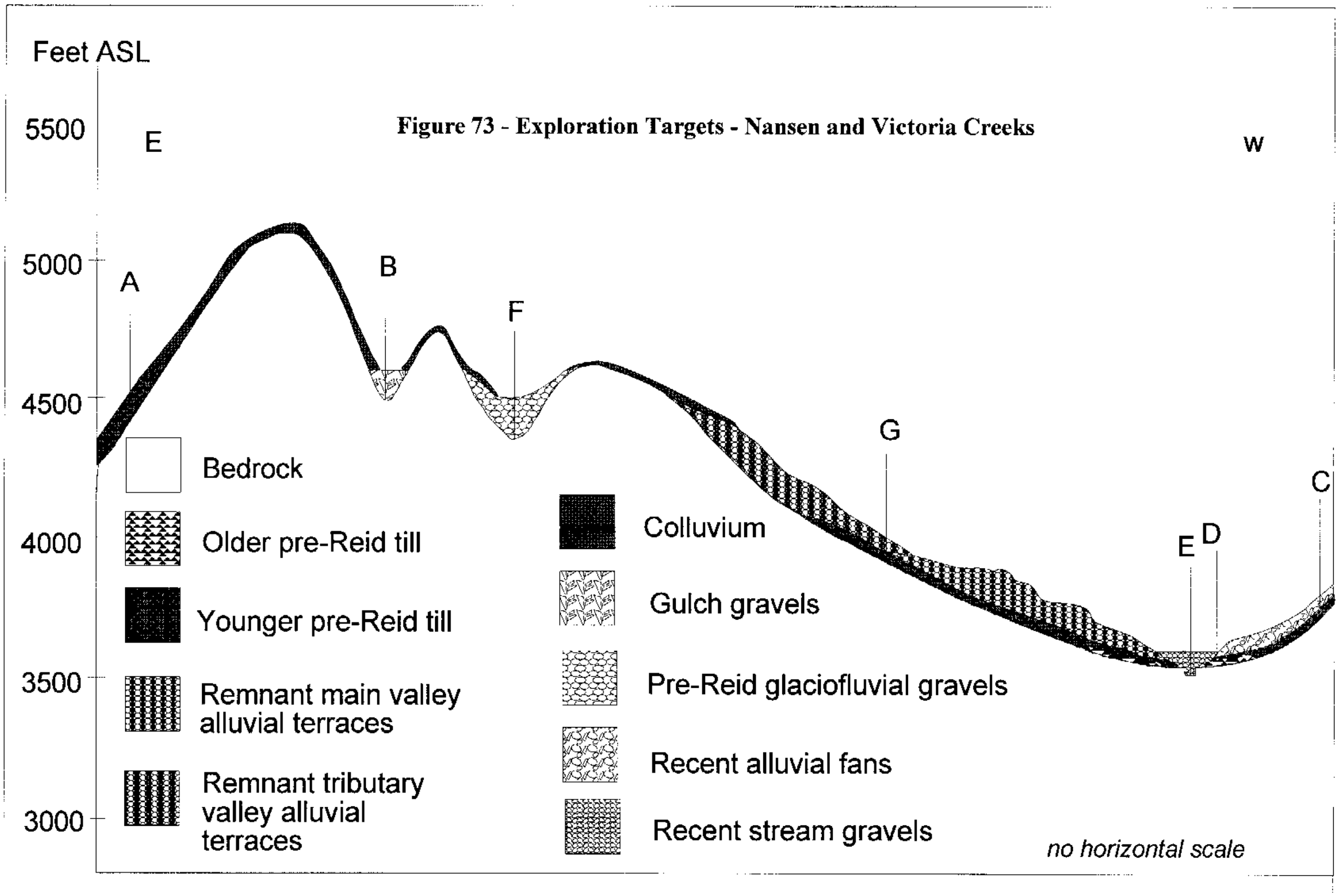

REFERENCES

Ashley, G.M, Shaw, J., and Smith, N.D., (eds.) 1985. Glacial Sedimentary Environments, SEPM Short Course No. 16, Society of Economic Paleontologists and Mineralogists, Tulsa, Oklahoma, 246 p.

Best, J.L. and Brayshaw, A.C., 1985. Flow separation - A physical process for the concentration of heavy minerals within alluvial channels. Journal of the Geological Society of London, v. 142, p. 747-755.

Blatt, H., Middleton, G., and Murray, R., 1980. Origin of Sedimentary Rocks, Second Edition, Prentiss Hall Inc., Englewood Cliffs, New Jersey, 782 p.

Bostock, H.S., 1934. Geological Survey of Canada Summary Report for 1933, Part A, p. 1-8.

Bostock, H.S., 1935. The Mining Industry of Yukon, 1934. Geological Survey of Canada Memoir 178, 10 p.

Bostock, H.S., 1936a. Carmacks District, Yukon; Geological Survey of Canada Memoir 189 (Report and Map 340 A) 67 p.

Bostock, H.S., 1936b. Mining Industry of Yukon, 1935. Geological Survey of Canada Memoir 193, 12 p.

Bostock, H.S., 1937. Mining Industry of Yukon, 1936. Geological Survey of Canada Memoir 209, 13 p.

Bostock, H.S., 1938. Mining Industry of Yukon, 1937. Geological Survey of Canada Memoir 218, 21 p.

Bostock, H.S., 1948. Physiography of the Canadian Cordillera, with Special Reference to the Area North of the Fifty-fifth Parallel; Geological Survey of Canada Memoir 247 (Report and Map 922 A). 106 p.

Bostock, H.S., 1957. Yukon Territory. Selected Field Reports of the Geological Survey of Canada, 1898 to 1933; Geological Survey of Canada Memoir 284 (Report and 5 maps). 650 p.

Bostock, H.S., 1966. Notes on Glaciation in Central Yukon Territory; Geological Survey of Canada Paper 65-36 (Report, 1 figure and 7 plates). 18 p.

Boyle, R.W., 1979. The geochemistry of gold and its deposits, Geological Survey of Canada Bulletin 280, 584 p.

Brodzikowski, K., and Van Loon, A.J., 1991. Glacigenic Sediments, Developments in Sedimentology 49, Elsevier Science Publishing Company Inc., New York, N.Y., 674 p.

Bull, W.B., 1972. Recognition of alluvial fan deposits in the stratigraphic record, in Rigby, J.K., and Hamblin, W.K., (eds.), Recognition of Ancient Sedimentary Environments, Society of Economic Paleontologists and Mineralogists, Special Publication 16, p. 63-83.

Cairnes, D.D., 1910. Preliminary Memoir on the Lewes and Nordenskiold Rivers Coal District, Yukon Territory, Geological Survey of Canada Memoir No. 5, 70 p.

Cairnes, D.D., 1915a. Exploration in Southwestern Yukon, in Summary Report of the Geological Survey, Department of Mines, 1914, GSC Sessional Paper no. 26, p. 10-28.

Cairnes, D.D., 1915b. Geological Map of Nansen and Victoria Creeks, Geological Survey of Canada Map 151A, To Accompany Memoir by D.D. Cairnes.

Carlson, G.G., 1987. Geology of Mount Nansen (115I 3) and Stoddart Creek (115I 6) Map Areas, Dawson Range, Central Yukon, INAC Yukon Division, Open File 1987-2, 181 pp. and two 1: 30 000 scale maps.

Chamley, H., 1989. Clay Sedimentology, Springer-Verlag, Berlin, Germany, 623 p.

Cheney, E.S., and Patton, T.S., 1967. Origin of the bedrock values of placer deposits, Economic Geology, v. 62, p. 852-853.

Coney, P.J., 1989. Structural aspects of suspect terranes and accretionary tectonics in western North America, in Journal of Structural Geology, Vol. 11, No. 1/2, pp. 107-125, 1989.

Coney, P.J., Jones, D.L., and Monger, J.W.H., 1980. Cordilleran suspect terranes, in Nature, Volume 288, 27 November 1980. p 329-333.

Dawson, K.M., 1990. Regional geological setting of selected mineral deposits of the Northern Cordillera, in Abbott, J.G., and Turner, R.J.W., (eds.) 1990; Mineral Deposits of the Northern Canadian Cordillera, Yukon-Northeastern British Columbia (Eighth IAGOD Symposium - Field Trip 14), Geological Survey of Canada Open File 2169, p 1-24.

Deer, W.A., Howie, R.A., and Zussman, J., 1992. An Introduction to the Rock Forming Minerals, Second Edition, John Wiley and Sons Inc., New York, N.Y., 696 p.

de Raaf, J.F.M., Reading, H.G., and Walker, R.G., 1965. Cyclic sedimentation in the Lower Westphalian of North Devon, England. Sedimentology, v.4, p. 1-52.

Detrich, R.V., Dutro, J.T., Foose, R.M., (comp.) 1982. AGI Data Sheets, for geology in the field, laboratory and office, American Geological Institute, Virginia, USA.

Eyles, N. and Kocsis, S.P., 1989. Sedimentological controls on gold in a late Pleistocene glacial placer deposit, Cariboo Mining District, British Columbia, Canada. Sedimentary Geology, v. 65, p. 45-68.

Eyles, N. and Miall, A.D., 1984. Glacial Facies, in Walker, R.G. (ed.), 1984. Facies Models, Second Edition, Geoscience Canada Reprint Series 1, p. 15-38.

Folk, R.L., 1974. Petrology of Sedimentary Rocks, Hemphill Publishing Co., Austin, 182 p.

Foscolos, A.E., Rutter, N.W., and Hughes, O.L., 1977. The use of pedological studies in interpreting the Quaternary history of central Yukon Territory, Geological Survey of Canada Bulletin 271, 48 p.

Frostick, L.E., Lucas, P.M. and Reid, I., 1984. The infiltration of fine matrices into coarse-grained alluvial sediments and its implications for stratigraphical interpretation, Journal of the Geological Society of London, v.141, p. 955-965.

Gabrielse, H., Monger, J.W.H., Wheeler, J.O., and Yorath, C.J., 1991. Chapter 2, Part A. Morphogeological belts, tectonic assemblages, and terranes; in Gabrielse, H., and Yorath, C.J. (eds.) 1991. Geology of the Cordilleran Orogen in Canada; Geological Survey of Canada, Geology of Canada, No. 4, p. 15-28.

Grond, H.C., Churchill, S.J., Armstrong, R.L., Harakai, J.E., and Nixon, G.T., 1984. Late Cretaceous age of the Hutshi, Mt. Nansen, and Carmacks groups, southwestern Yukon; Canadian Journal of Earth Sciences, v. 21, p. 554-558.

Hansen, V.L., 1989. Structural and kinematic evolution of the Teslin suture zone, Yukon; Record of an ancient transpressional margin, in Journal of Structural Geology, Vol. 11, No. 6, pp. 717-733, 1989.

Harms, J.C., Southard, J.B., and Walker, R.,G., 1982. Structures and sequences in clastic rocks, SEPM Short Course No. 9, Society of Economic Paleontologists and Mineralogists, Tulsa, Oklahoma, 249 p.

Hein, F.J., and Walker, R.G., 1977. Bar evolution and development of stratification in the gravelly, braided Kicking Horse River, British Columbia, Canadian Journal of Earth Sciences, v. 14, p. 562-570.

Herail, G., 1988. Morphological evolution of supergenetic gold particles: Geological significance and interest for mining exploration. V Congreso Geologico Chileno, Tomo 1, B 165 - B 180.

Herail, G., Fornari, M., and Rouhier, M., 1989. Geomorphological control of gold distribution and gold particle evolution in glacial and fluvioglacial placers of the Ancocala-Ananea Basin - Southeastern Andes of Peru, Geomorphology, 2, p. 369-383.

Hillhouse, J.W., and Gromme, C.S., 1980. Paleomagnetism of the Triassic Hound Island Volcanics, Alexander Terrane, southeastern Alaska, in Journal of Geophysical Research, v. 85, p 2594-2602.

Hughes, O.L., 1969. Distribution of open system pingos in central Yukon Territory with respect to glacial limits (Report and 2 figures), 8 p.

Hughes, O.L., 1987. Quaternary Geology. in Guidebook to Quaternary Research in Yukon, Morison, S.R. and Smith, C.A.S., (eds.) XII INQUA Congress, Ottawa, Canada. National Research Council of Canada, Ottawa, p. 12-16.

Hughes, O.L., Campbell, R.B., Muller, J.E., and Wheeler, J.O., 1968. Glacial Limits and Flow Patterns, Yukon Territory, South of 65 Degrees North Latitude; Geological Survey of Canada Paper 68-34 (Report and Map 6-1968). 9 p.

Hughes, O.L., Rampton, V.N. and Rutter, N.W., 1972. Quaternary Geology and Geomorphology, Southern and Central Yukon (Northern Canada); XXIV International Geological Congress, Field Excursion Guidebook A 11, 59 p.

Hughes, O. L., Rutter, N.W., and Clague, J.J., 1989. Chapter 1, Yukon Territory, Quaternary Stratigraphy and History, Cordilleran Ice Sheet, in Fulton, R.J. (ed.) 1989. Quaternary Geology of Canada and Greenland; Geological Survey of Canada, Geology of Canada, No. 1, p. 58-62.

Jackson, L.E., 1993. Origin and stratigraphy of Pleistocene gravels in Dawson Range and suggestions for future exploration of gold placers, southwestern Carmacks map area, Yukon Territory; in Current Research, Part A; Geological Survey of Canada, Paper 93-1A, p. 1-10.

Klassen, R.W., Morison, S.R. and Duk-Rodkin, A., 1987. Surficial geology, Carmacks, Yukon Territory, Geological Survey of Canada, Map 9-1985, Scale 1:250 000.

Kodama, H., Miles, N., Shimoda, S., and Brydon, J.E., 1976. Mixed-layer kaolinite-montmorillonite from soils near Dawson, Yukon Territory; Canadian Mineralogist, v. 14, p. 159-163.

LeBarge, W.P., 1990. Yukon Placer Mining 1985-1988: An Overview. in LeBarge, W.P., and Morison, S.R., (eds.) Yukon Placer Mining and Exploration 1985-1988; Exploration and Geological Services Division, Yukon, Indian and Northern Affairs Canada, 151 p.

LeBarge, W.P. and Hein, F.J., 1990. Personal field notes from a two week reconnaissance of placer mining areas in Yukon, August 1990.

Lerbekmo, J.F. and Campbell, F.A., 1969. Distribution, composition and source of the White River Ash, Yukon Territory; Canadian Journal of Earth Sciences, v. 6, p. 109-116.

Lerbekmo, J.F., Westgate, J.A., Smith, D.G.W., and Denton, G., 1975. New data on the character and history of the White River volcanic eruption, Alaska, in Suggate, R.P. and Creswall, M.M. (eds.) Quaternary Studies, The Royal Society of New Zealand Bulletin, 13, p. 203-209.

Lowden, J.A. and Blake, W. Jr., 1968. Geological Survey of Canada Radiocarbon Dates VII. Geological Survey of Canada, Paper 68-2, part B.

Mathews, W.H., 1986. Physiographic map of the Canadian Cordillera; Geological Survey of Canada, Map 1701A, Scale 1: 5 000 000.

Miall, A.D., 1977. A review of the braided river depositional environment, Earth Science Reviews, v. 13, p.1-62.

Miall, A.D., 1978. Lithofacies types and vertical profile models in braided river deposits: a summary, in Miall, A.D. (ed.)., Fluvial Sedimentology, Canadian Society of Petroleum Geologists, Memoir 5, p. 597-604.

Middleton, G.V., 1978. Facies. in Fairbridge, R.W., and Bourgeois, J., (eds.), Encyclopedia of Sedimentology. Stroudsberg, Pa., Dowden, Hutchinson and Ross, p. 323-325.

Monger, J.W.H., and Price, R.A., 1979. Geodynamic evolution of the Canadian Cordillera - Progress and problems: Canadian Journal of Earth Sciences, v. 16, p. 770-791.

Monger, J.W.H., Price, R.A. and Tempelman-Kluit, D.J., 1982. Tectonic accretion and the origin of the two major metamorphic and plutonic welts in the Canadian Cordillera; in Geology, v. 10, p 70-75, February 1982.

Moore, D.M., and Reynolds, R.C., 1989. X-Ray diffraction and the identification and analysis of clay minerals, Oxford University Press, Oxford, New York, 331 p.

Morison, S.R., 1985. Sedimentology of the White Channel placer deposits, Klondike area, west central Yukon; unpublished MSc. Thesis, University of Alberta, Edmonton, Alberta, 149 p.

Morison, S.R., 1989. Placer deposits in Canada, Chapter 11, Quaternary Resources in Canada, in Fulton, R.J. (ed.) 1989. Quaternary Geology of Canada and Greenland; Geological Survey of Canada, Geology of Canada, No. 1, p. 687-697.

Morison, S.R., and Smith, C.A.S., (eds.), 1987. Guidebook to Quaternary Research in Yukon, XII INQUA Congress, Ottawa, Canada. National Research Council of Canada, 110 pp.

Naeser, N.D., Westgate, J.A., Hughes, O.L. and Pewe, T.L., 1982. Fission-track ages of Late Cenozoic distal tephra beds in Yukon Territory and Alaska. Canadian Journal of Earth Sciences, v.19, p. 2167-2178.

Nemec, W. and Steel, R.J., 1984. Alluvial and Coastal Conglomerates: Their significant features and some comments on gravelly mass flow deposits, in Koster, E.H., and Steel, R.J., (eds.), Sedimentology of Gravels and Conglomerates, Canadian Society of Petroleum Geologists, Memoir 10, p. 1-31.

Placer Mining Section, 1991. Yukon Placer Mining Industry 1989-1990; Mineral Development Division, Yukon, Indian and Northern Affairs Canada, 125 p.

Placer Mining Section, 1993. Yukon Placer Mining Industry 1991-1992; Mineral Development Division, Yukon, Indian and Northern Affairs Canada, 145 p.

Rust, B.R., 1972. Structure and process in a braided river, Sedimentology, v. 18, p. 221-245.

Rust, B.R., 1978. A classification of alluvial channel systems, in Miall, A.D. (ed.)., Fluvial Sedimentology, Canadian Society of Petroleum Geologists, Memoir 5, p. 187-198.

Selby, M.J., 1985. Earth's Changing Surface: An Introduction to Geomorphology; Oxford University Press, New York. 607 pp.

Slingerland, R., 1984. Role of hydraulic sorting in the origin of fluvial placers, Journal of Sedimentary Petrology, v. 54, no. 1, p. 0137-0150.

Smith, C.A.S., Tarnocai, C., and Hughes, O.L., 1986. Pedological investigations of Pleistocene glacial drift surfaces in the central Yukon; Geographie physique et Quaternaire, vol. XL, no. 1, p. 29-37.

Tarnocai, C., 1987. Quaternary soils, in Guidebook to Quaternary Research in Yukon, Morison, S.R. and Smith, C.A.S., (eds). XII INQUA Congress, Ottawa, Canada. National Research Council of Canada, Ottawa, p.16-21.

Tempelman-Kluit, D.J., 1979a. Five occurrences of transported synorogenic clastic rocks in Yukon Territory; in Current Research, Geological Survey of Canada, Paper 79-1A, p 1-11.

Templeman-Kluit, D.J., 1979b. Transported cataclasite, ophiolite and granodiorite in Yukon: evidence of arc-continent collision; Geological Survey of Canada Paper 79-14.

Tempelman-Kluit, D.J., 1981. Geology and Mineral Deposits of Southern Yukon, in INAC (1981), Yukon Geology and Exploration 1979-1980; Exploration and Geological Services Division, Indian and Northern Affairs Canada, p. 7-31.

Tyrrell, J.B., and McConnell, R.G. 1898. Geological Survey of Canada Summary Report for 1898, pp. 37A-45A.

van Kalsbeek, L., 1994. Yukon Placer Mining Statistics, 1993, unpublished summary for Placer Mining Section, Yukon, Indian and Northern Affairs Canada.

Walker, R.G., 1984. General Introduction: Facies, facies sequences and facies models; in Walker, R.G., (ed), 1984. Facies Models, second edition. Geoscience Canada Reprint Series 1, 317 p.

Wells, N.A., 1984. Sheet debris flow and sheetflood conglomerates in Cretaceous cool-maritime alluvial fans, South Orkney Islands, Antarctica, in Koster, E.H., and Steel, R.J., (eds.), Sedimentology of Gravels and Conglomerates, Canadian Society of Petroleum Geologists, Memoir 10, p. 133-145.

Wentworth, C.K., 1922. A Scale of Grade and Class Terms for Clastic Sediments, Journal of Geology, v. 30, p. 377-392.

Wheeler, J.O., and McFeely, P. (comp.). 1991. Tectonic assemblage map of the Canadian Cordillera and adjacent parts of the United States of America; Geological Survey of Canada, Map 1712A, Scale 1 : 2 000 000.

Wheeler, J.O., Brookfield, A.J., Gabrielse, H., Monger, J.W.H., Tipper, H.W., and Woodsworth, G.J. (comp.), 1991. Terrane map of the Canadian Cordillera, Geological Survey of Canada, Map 1713A, Scale 1 : 2 000 000.

Wilson, A.F., 1984. Origin of quartz-free gold nuggets and supergene gold found in laterites and soils -- A review and some new observations. Australian Journal of Earth Sciences, v. 31, p. 303-316.

Yukon Minfile, 1993, Exploration and Geological Services Division, Yukon, Indian and Northern Affairs Canada.

Appendix A - Measured Stratigraphic Sections

SECTION: K-1-1 ELEVATION TOP: 4000' ELEVATION BOTTOM: 3992'
LANDFORM TYPE: alluvial fan SCALE : 1 : 35 LAT: 62°07'36" N LONG: 137°16'08" W

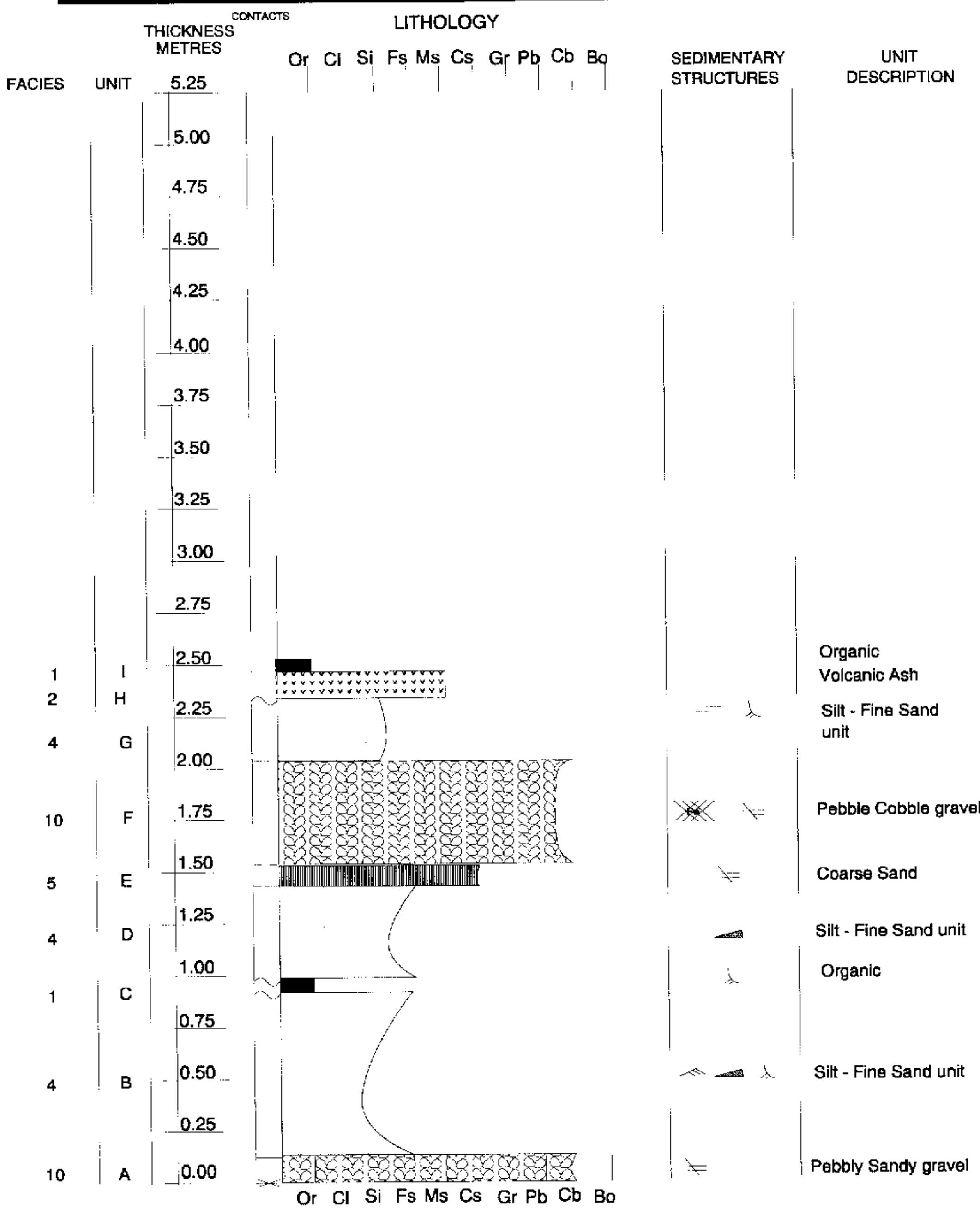

SECTION: K-1-2 ELEVATION TOP: 4000' ELEVATION BOTTOM: 3997'
LANDFORM TYPE: alluvial fan SCALE: 1 : 35 LAT: 62° 07'36" N LONG: 137° 16'08" W

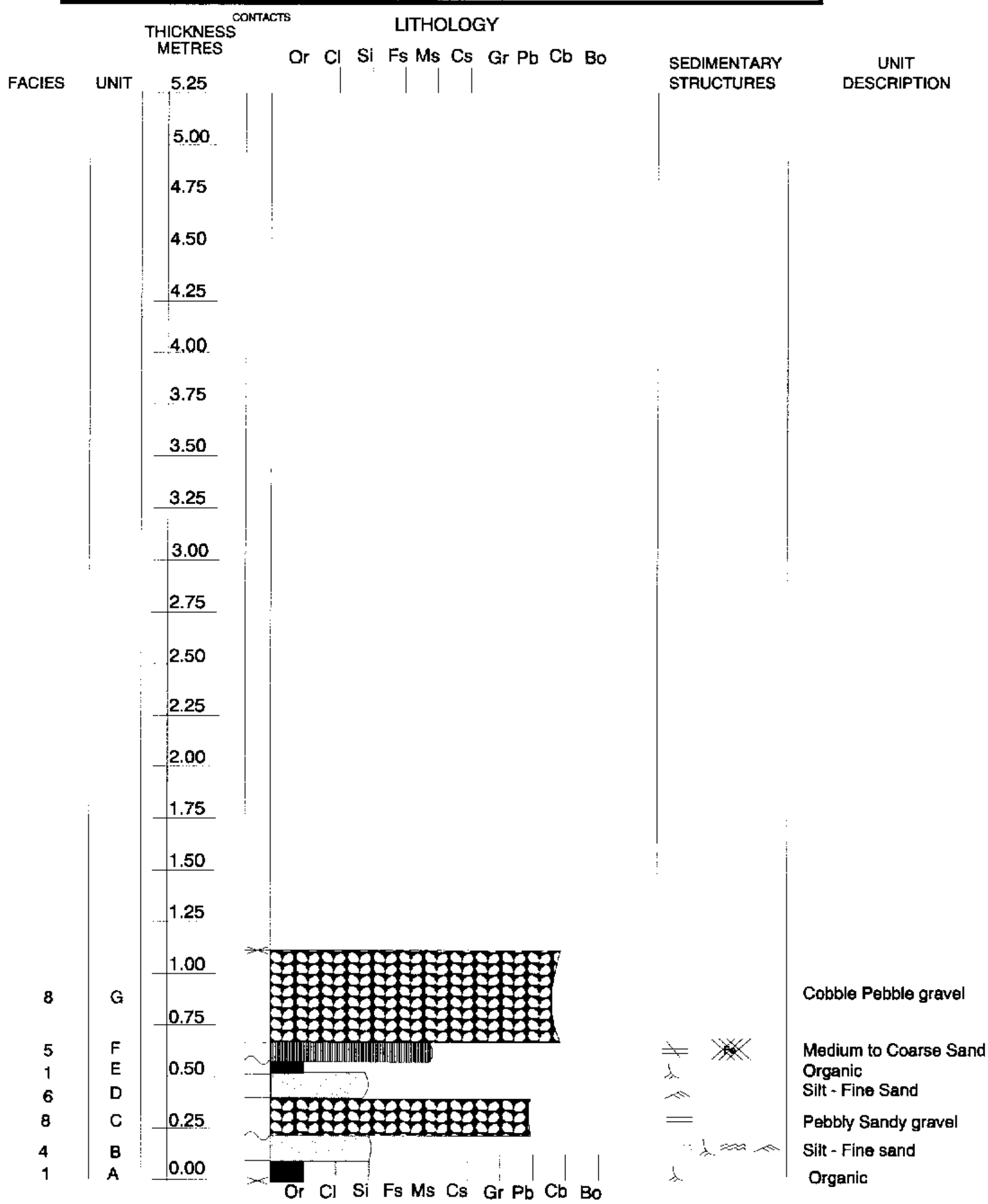

SECTION: K-1-3 *ELEVATION TOP:* 4000' *ELEVATION BOTTOM:* 3994'
LANDFORM TYPE: alluvial fan *SCALE :* 1 : 35 *LAT:* 62° 07'36" N *LONG:* 137° 16'08" W

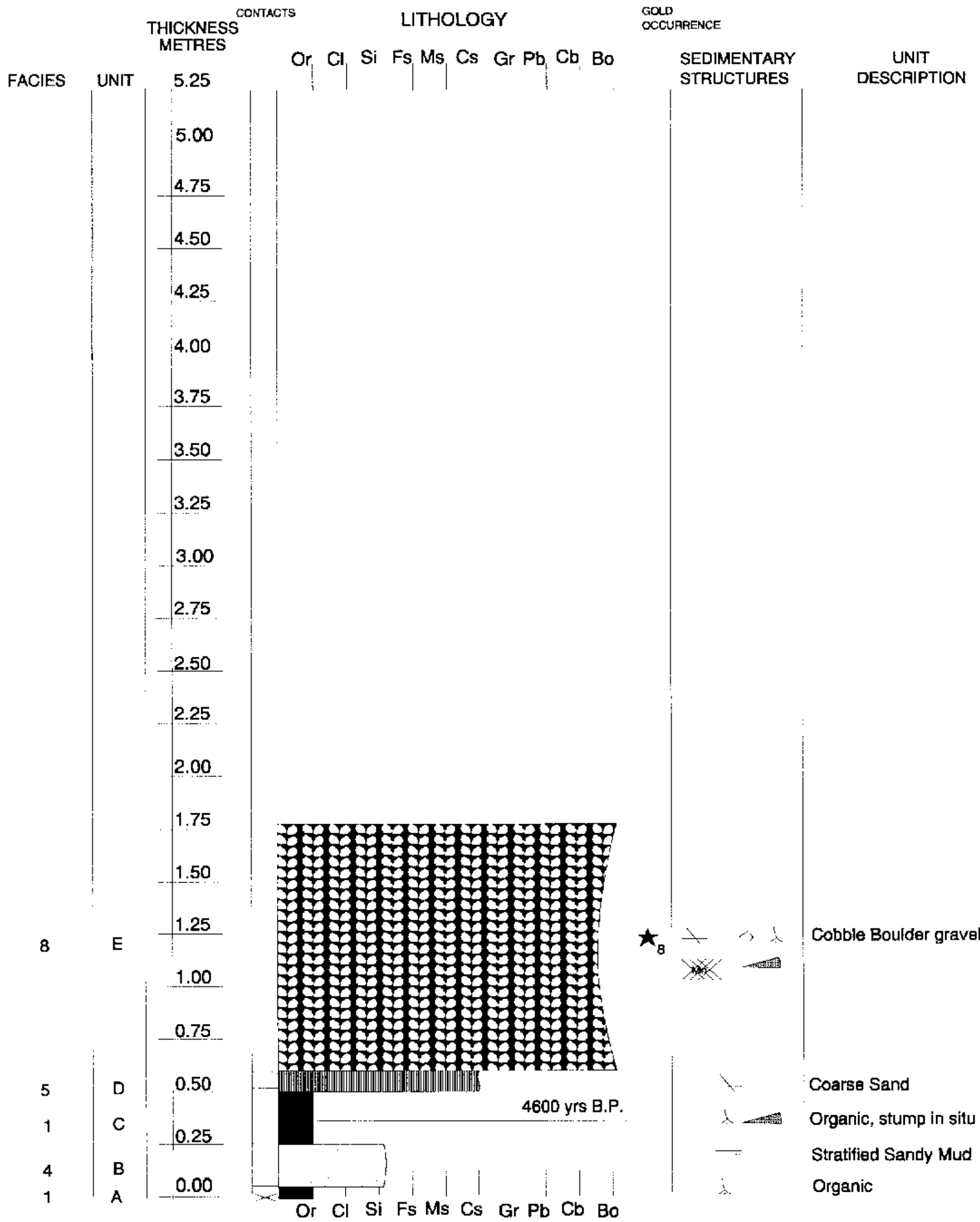

SECTION: K-2-1 ELEVATION TOP: 3981' ELEVATION BOTTOM: 3960'
LANDFORM TYPE: glacial/alluvial fan SCALE : 1 : 70 LAT: 62° 07'39" N LONG: 137° 16'08" W

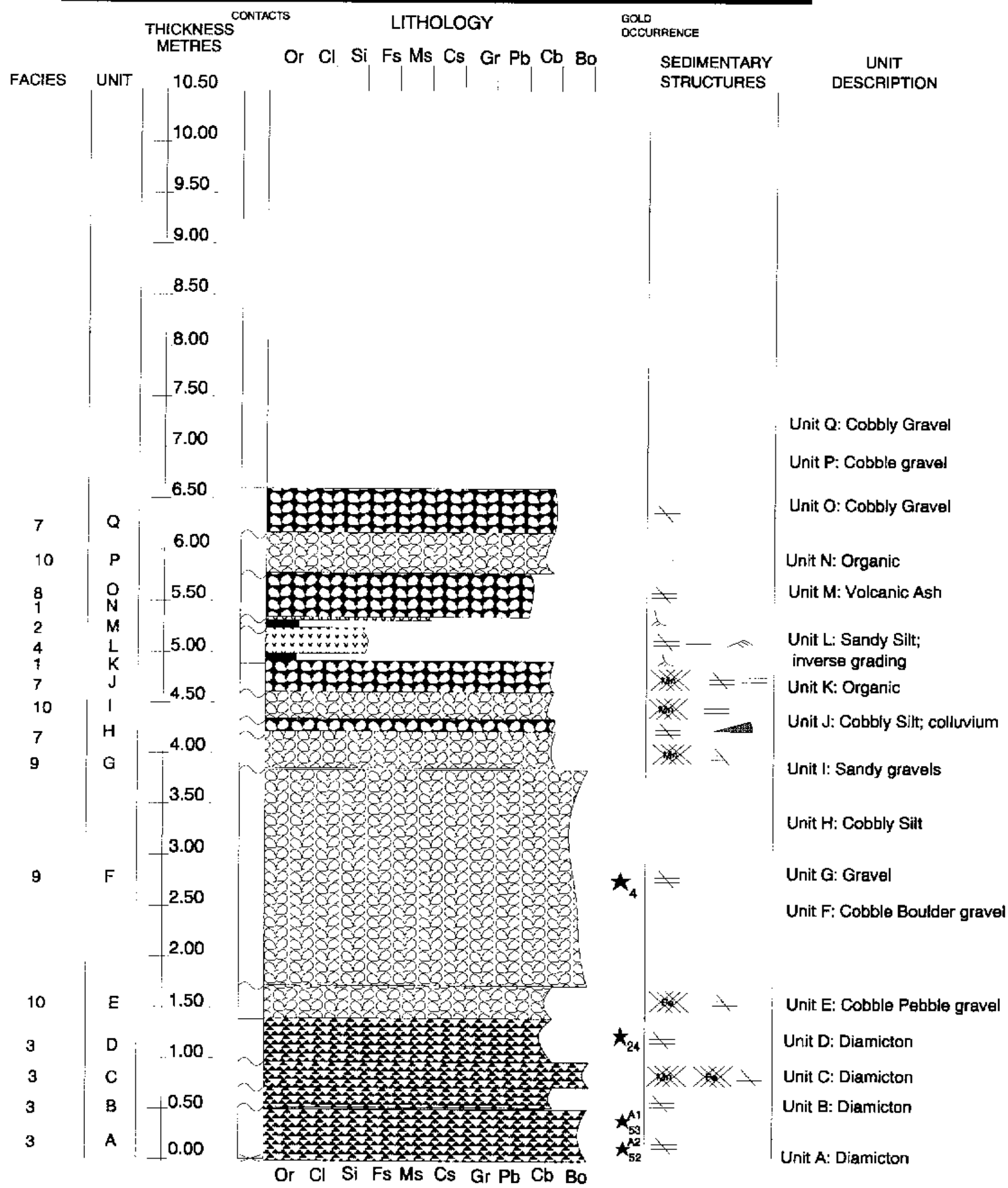

SECTION: EFN 1-1 ELEVATION TOP: 4040' ELEVATION BOTTOM: 4030'
LANDFORM TYPE: glacial/alluvial fan SCALE: 1 : 35 LAT: 62°05'48" N LONG: 137°11'26" W

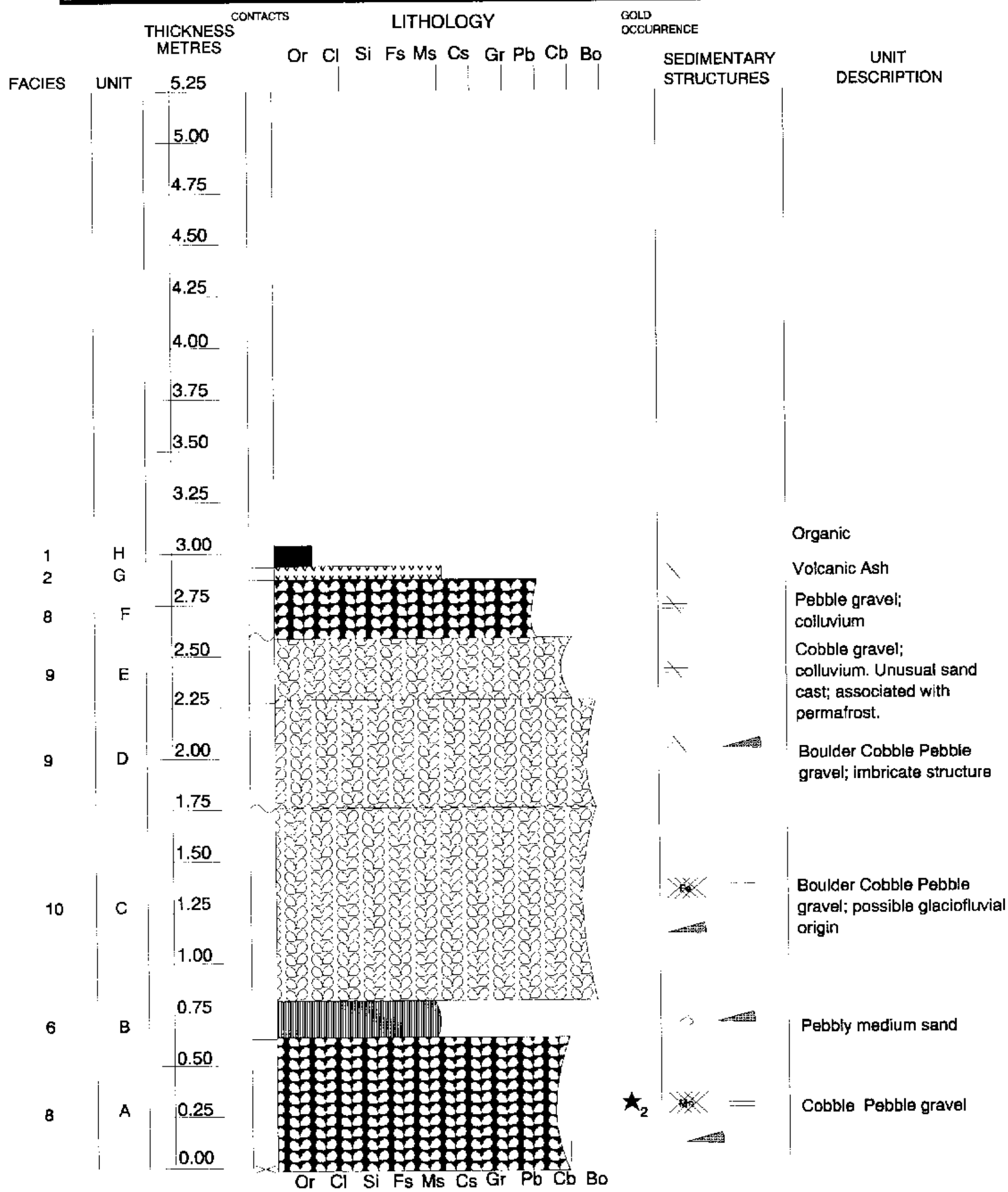

SECTION: EFN-2-1 ELEVATION TOP: 4024' ELEVATION BOTTOM: 4010'
LANDFORM TYPE: glacial/alluvial fan SCALE: 1 : 35 LAT: 62°05'48" N LONG: 137°11'26" W

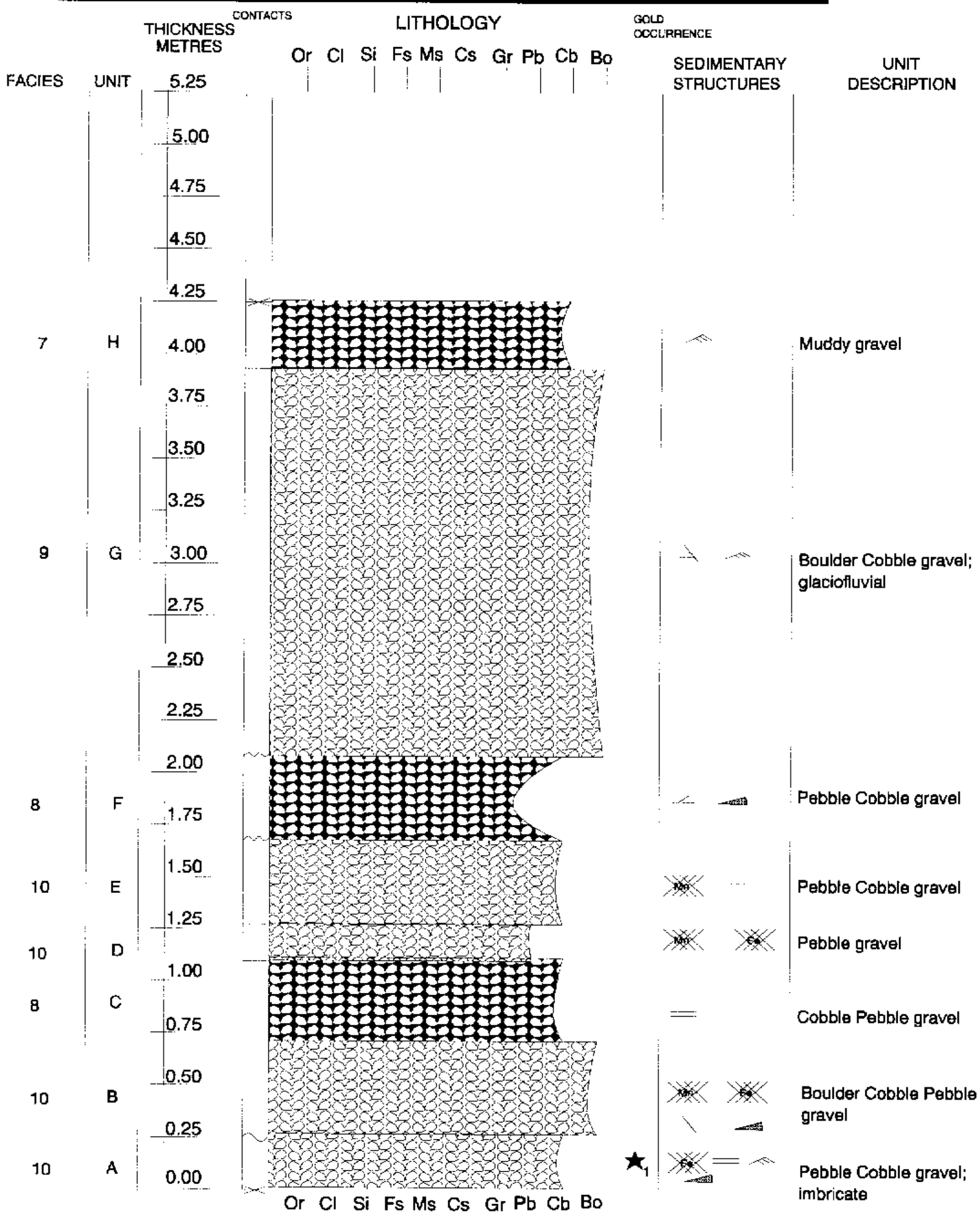

SECTION: EFN-2-2 *ELEVATION TOP:* 4030' *ELEVATION BOTTOM:* 4010'
LANDFORM TYPE: glacial/alluvial fan *SCALE :* 1 : 50 *LAT:* 62°05'48" N *LONG:* 137°11'26" W

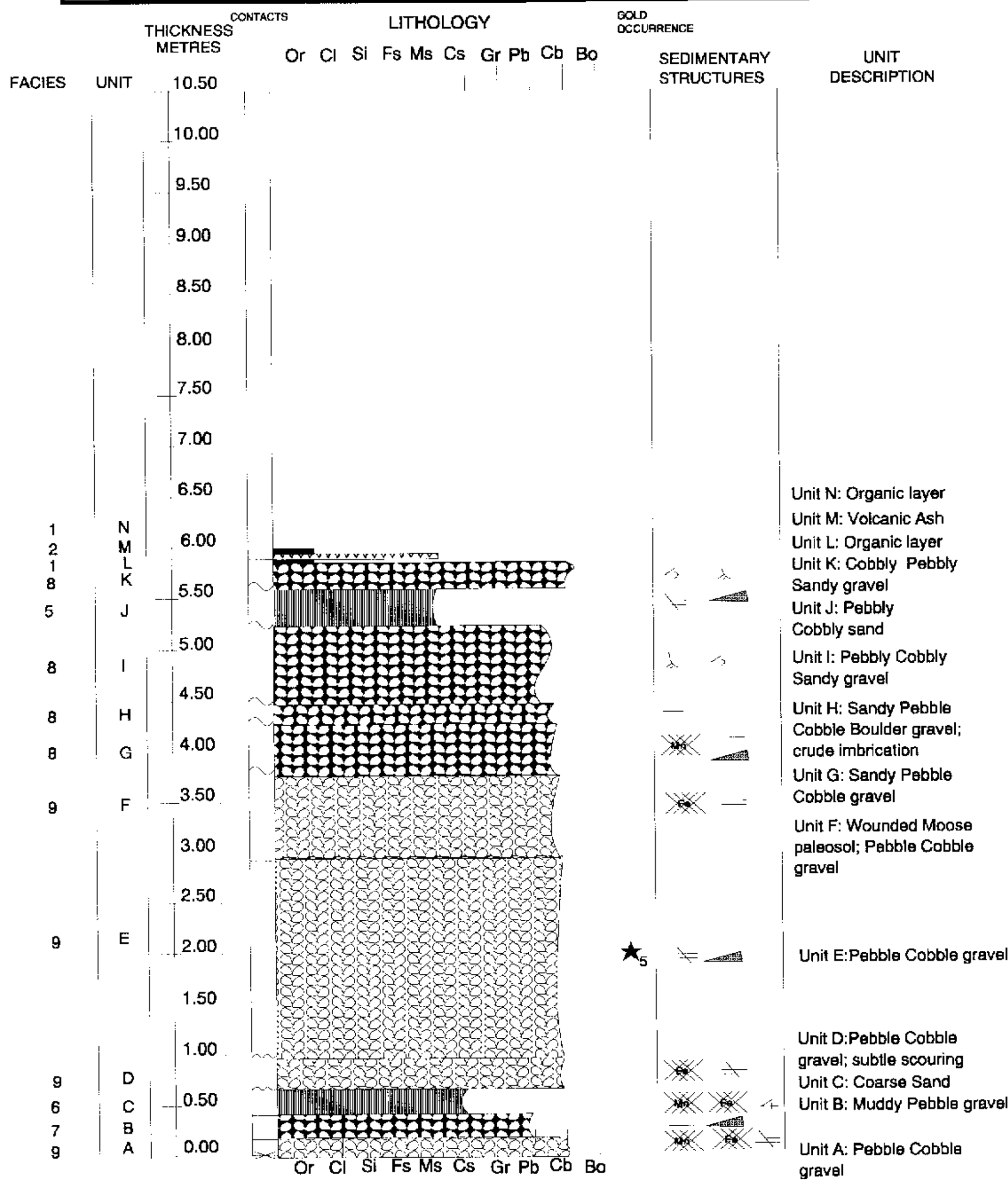

SECTION: EFN-3-1 *ELEVATION TOP:* 4004' *ELEVATION BOTTOM:* 4000'
LANDFORM TYPE: glacial/colluvium *SCALE :* 1 : 35 *LAT:* 62°05'48" N *LONG:* 137°11'26" W

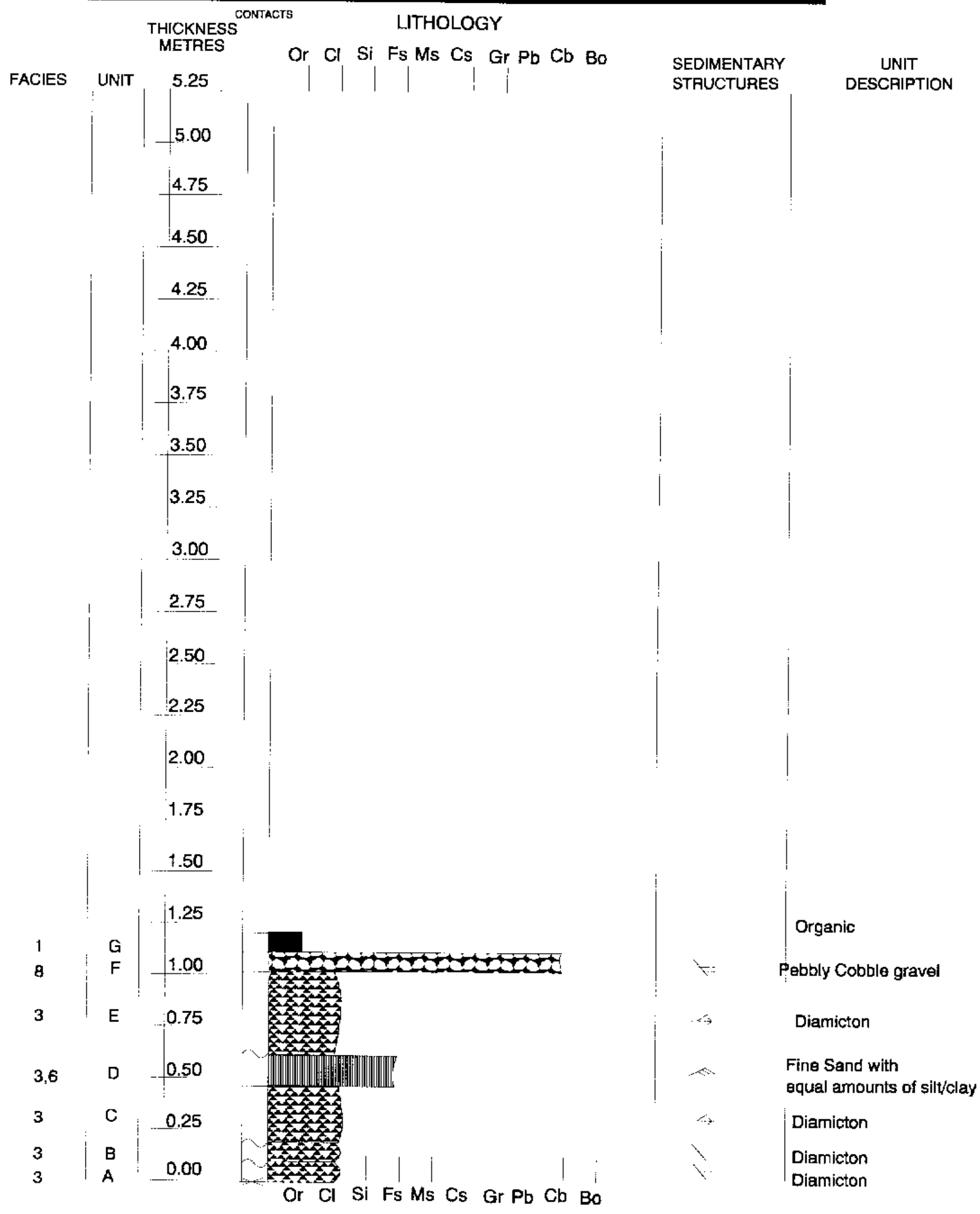

SECTION: EFN-3-2 *ELEVATION TOP:* 4003' *ELEVATION BOTTOM:* 4000'
LANDFORM TYPE: glacial/colluvium *SCALE:* 1 : 35 *LAT:* 62°05'48" N *LONG:* 137°11'26" W

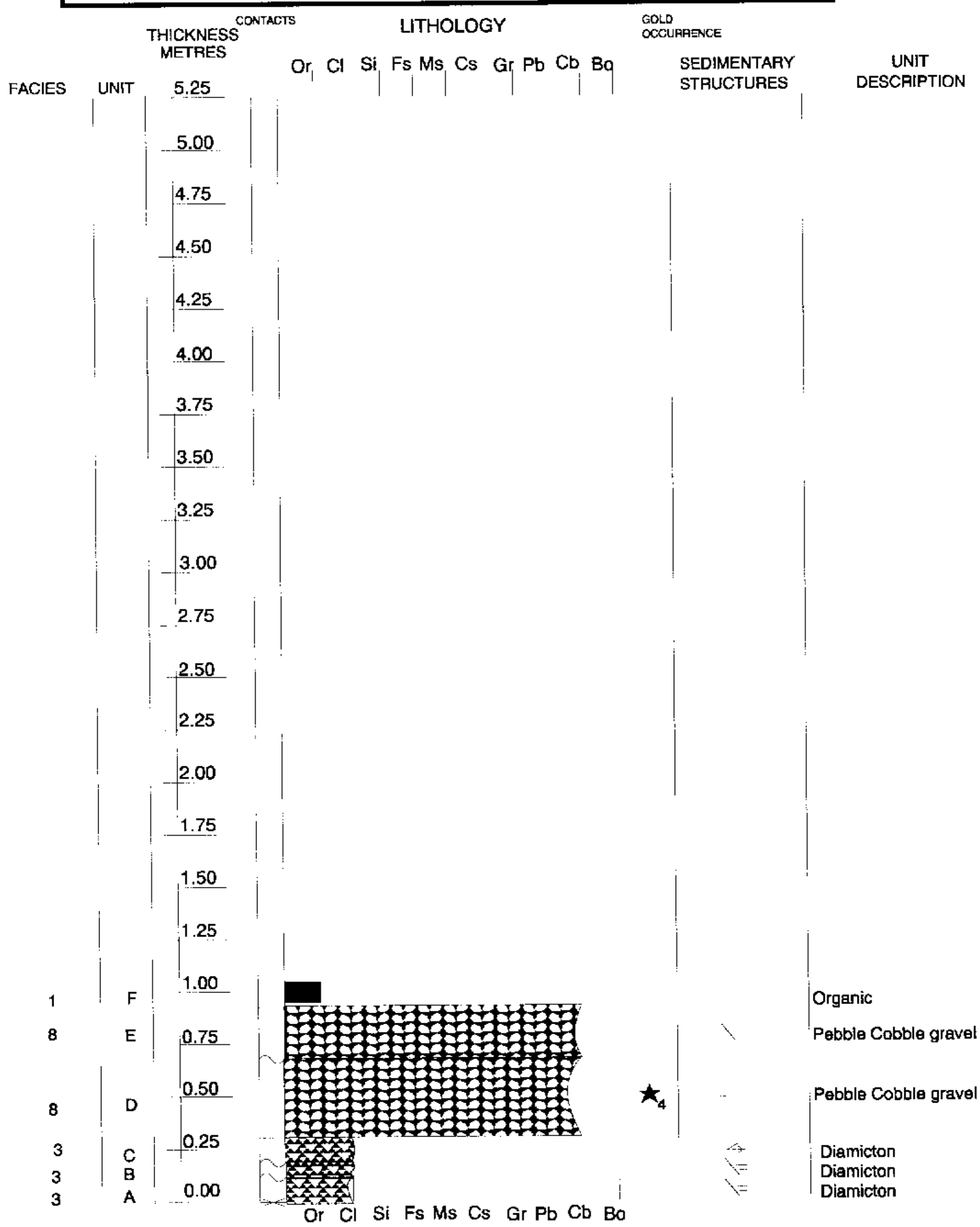

SECTION: EFN-4-1 *ELEVATION TOP:* 4203' *ELEVATION BOTTOM:* 4200'
LANDFORM TYPE: glaciofluvial *SCALE:* 1 : 35 *LAT:* 62°05'42" N *LONG:* 137°11'26" W

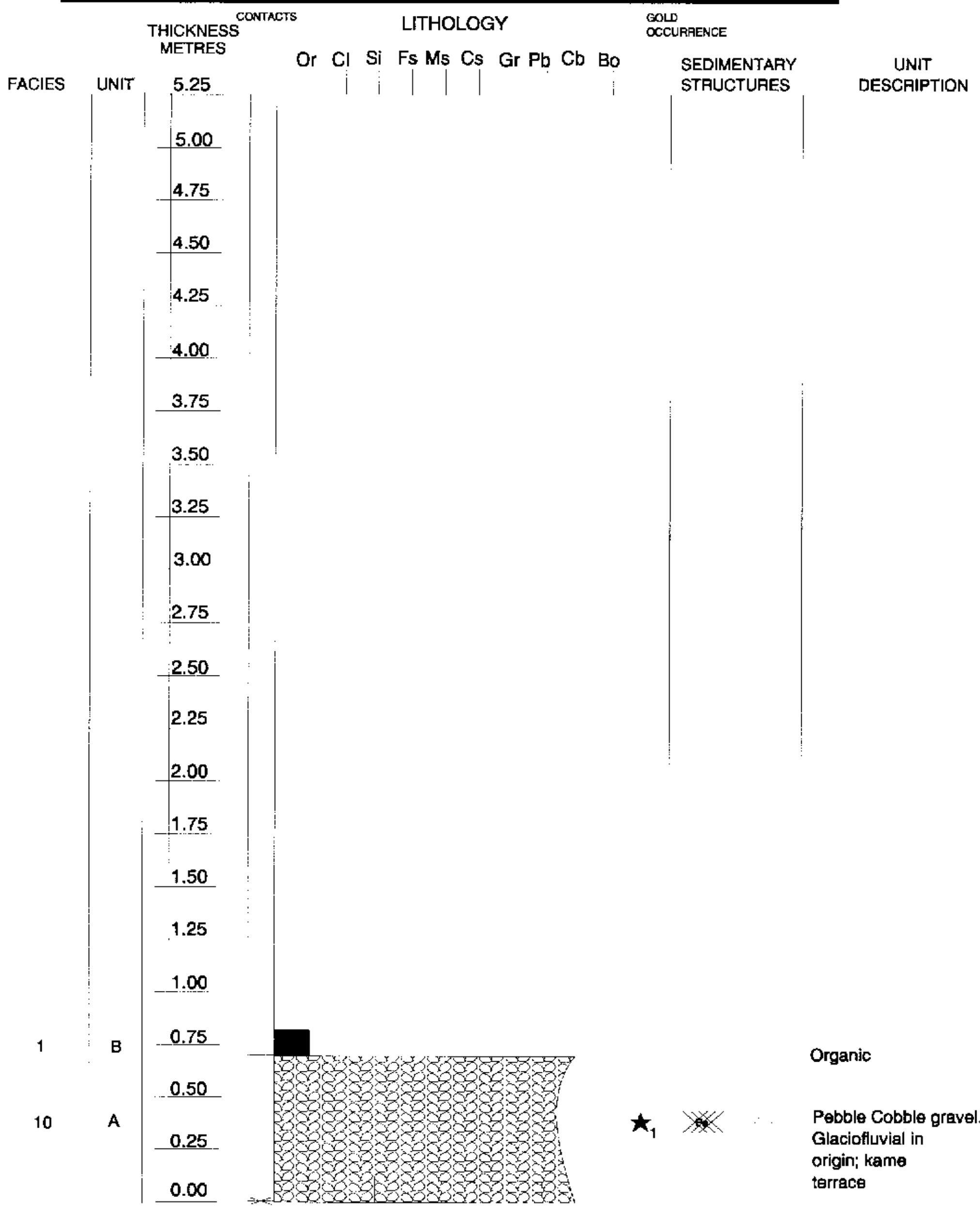

SECTION: DIS 1-1 ELEVATION TOP: 4370' ELEVATION BOTTOM: 4360'
LANDFORM TYPE: gulch SCALE: 1 : 35 LAT: 62°04'50" N LONG: 137°09'33" W

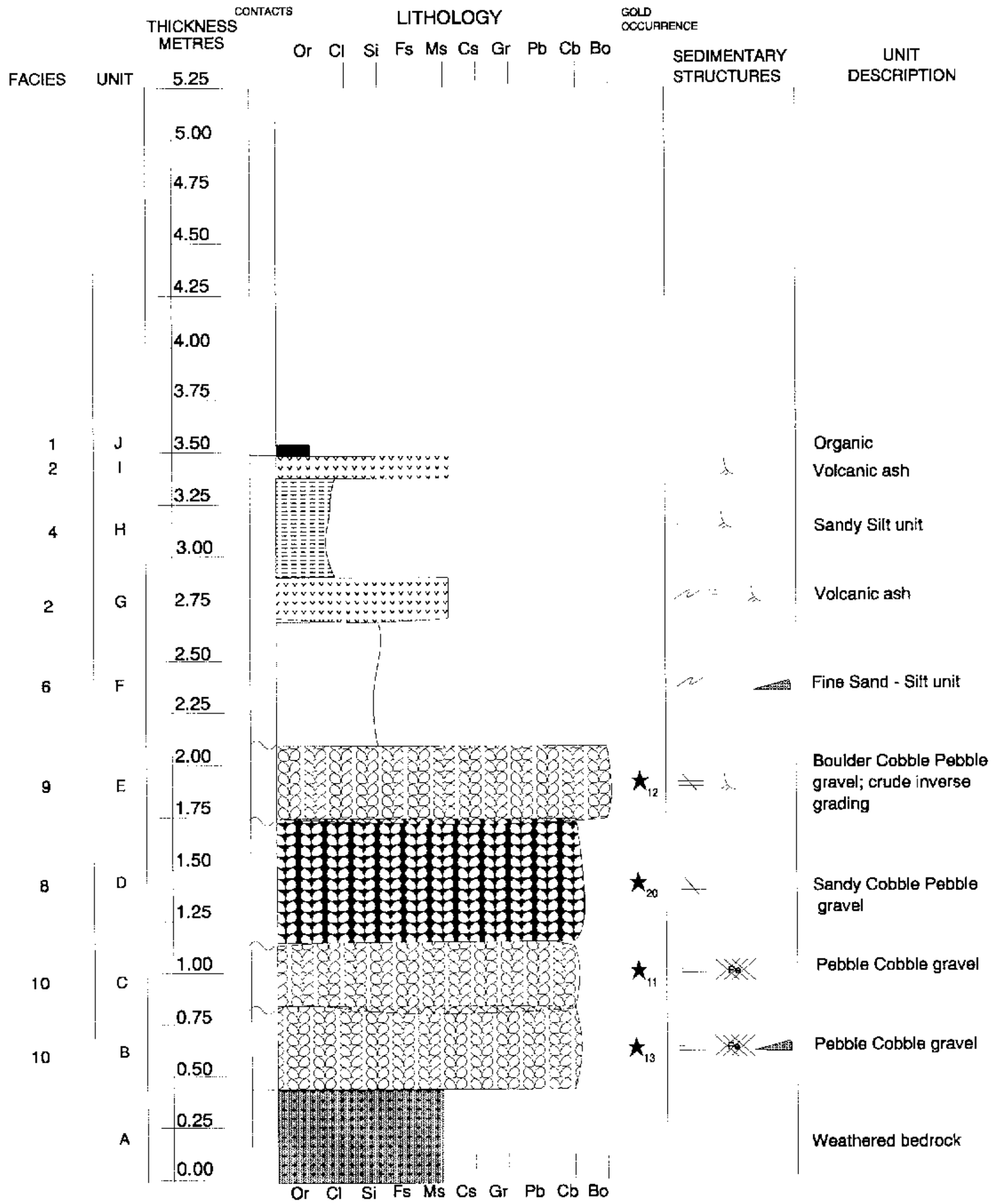

SECTION: DIS-1-2 ELEVATION TOP: 4350' ELEVATION BOTTOM: 4340'
LANDFORM TYPE: gulch SCALE: 1 : 35 LAT: 62°04'50" N LONG: 137°09'33" W

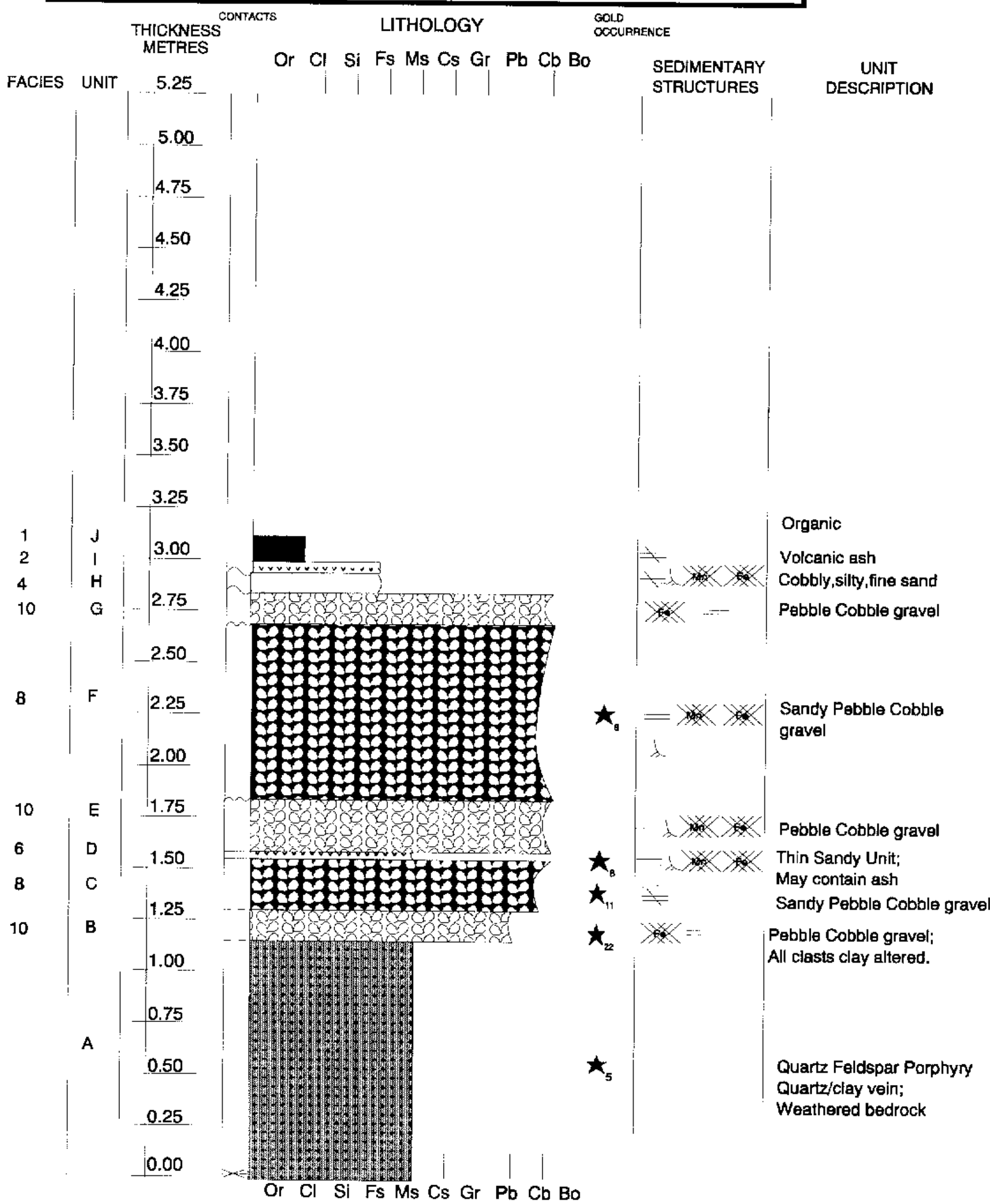

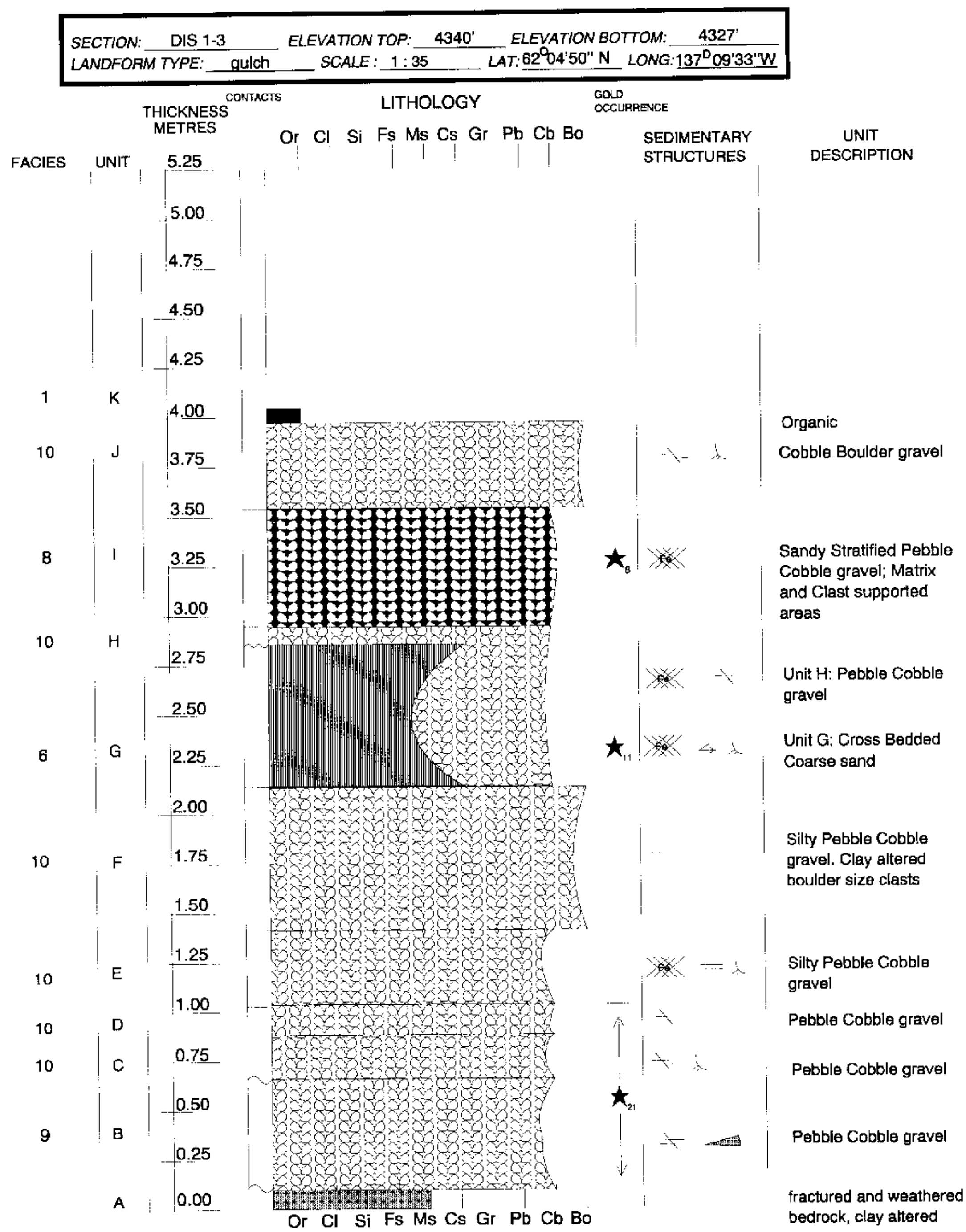
SECTION: DIS 1-3 ELEVATION TOP: 4340' ELEVATION BOTTOM: 4327'
LANDFORM TYPE: gulch SCALE: 1 : 35 LAT: 62°04'50" N LONG: 137°09'33"W
CONTACTS
THICKNESS METRES
LITHOLOGY
GOLD OCCURRENCE
Or Cl Si Fs Ms Cs Gr Pb Cb Bo
SEDIMENTARY STRUCTURES
UNIT DESCRIPTION
FACIES
UNIT
5.25
5.00
4.75
4.50
4.25
4.00
3.75
3.50
3.25
3.00
2.75
2.50
2.25
2.00
1.75
1.50
1.25
1.00
0.75
0.50
0.25
0.00
1 K Organic
10 J Cobble Boulder gravel
8 I Sandy Stratified Pebble Cobble gravel; Matrix and Clast supported areas
10 H Unit H: Pebble Cobble gravel
6 G Unit G: Cross Bedded Coarse sand
10 F Silty Pebble Cobble gravel. Clay altered boulder size clasts
10 E Silty Pebble Cobble gravel
10 D Pebble Cobble gravel
10 C Pebble Cobble gravel
9 B Pebble Cobble gravel
A fractured and weathered bedrock, clay altered
Or Cl Si Fs Ms Cs Gr Pb Cb Bo

SECTION: DIS-2-1 ELEVATION TOP: 4170' ELEVATION BOTTOM: 4160'
LANDFORM TYPE: alluvial fan SCALE: 1 : 35 LAT: 62°05'00" N LONG: 137°10'00" W

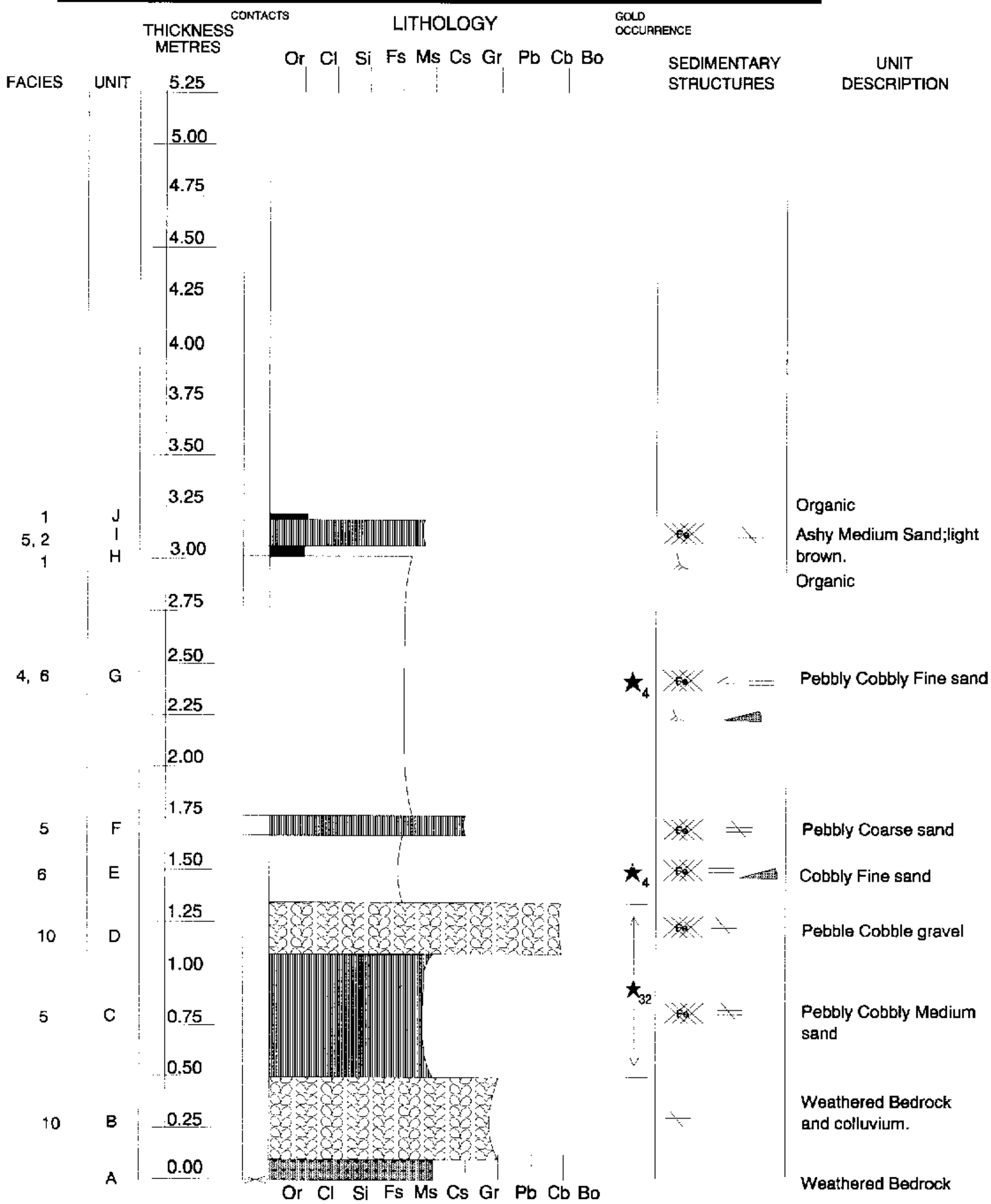

SECTION: DIS-2-9 ELEVATION TOP: 4270' ELEVATION BOTTOM: 4237'
LANDFORM TYPE: glaciofluvial SCALE: 1 : 70 LAT: 62°05'00" N LONG: 137°10'00" W

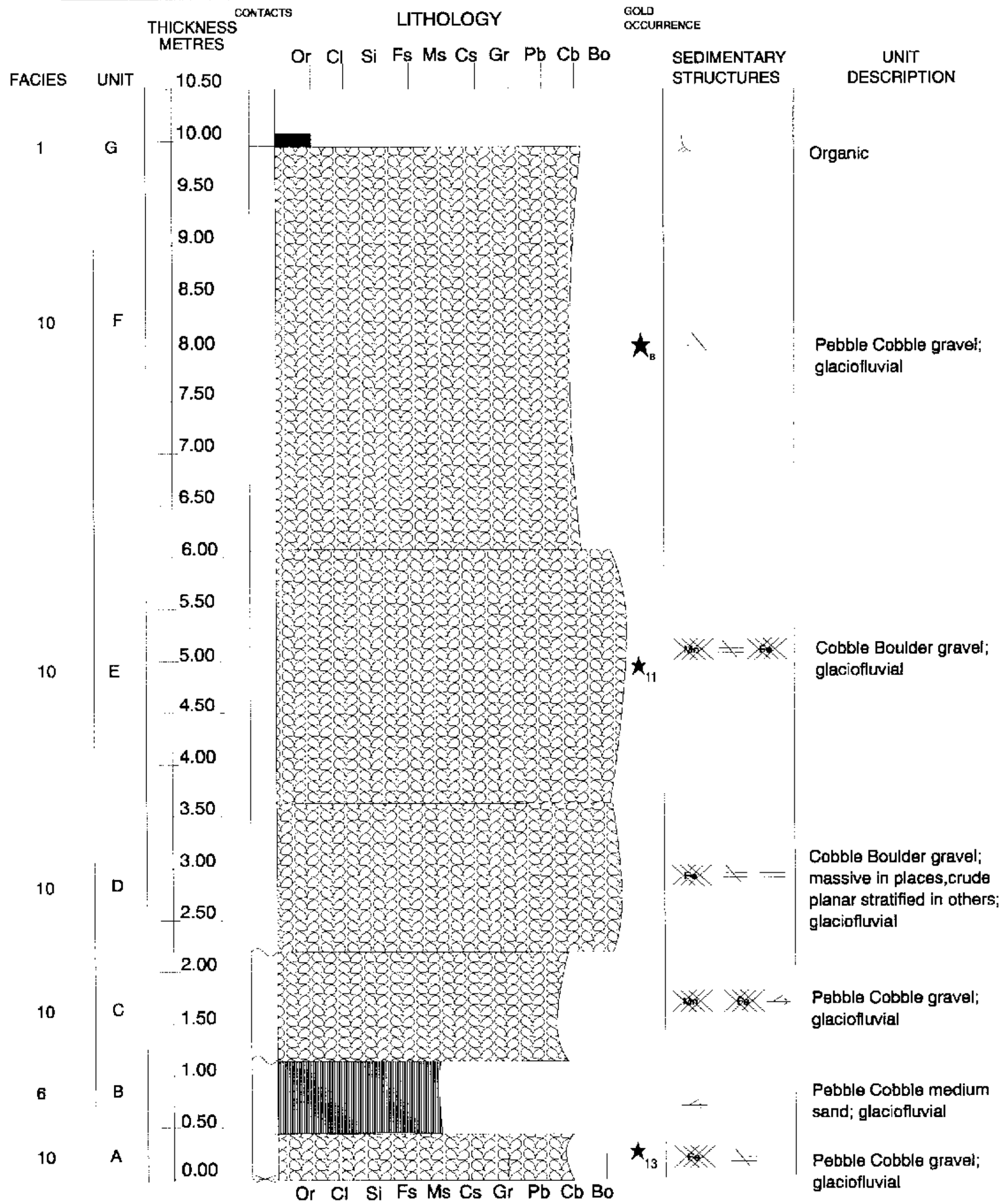

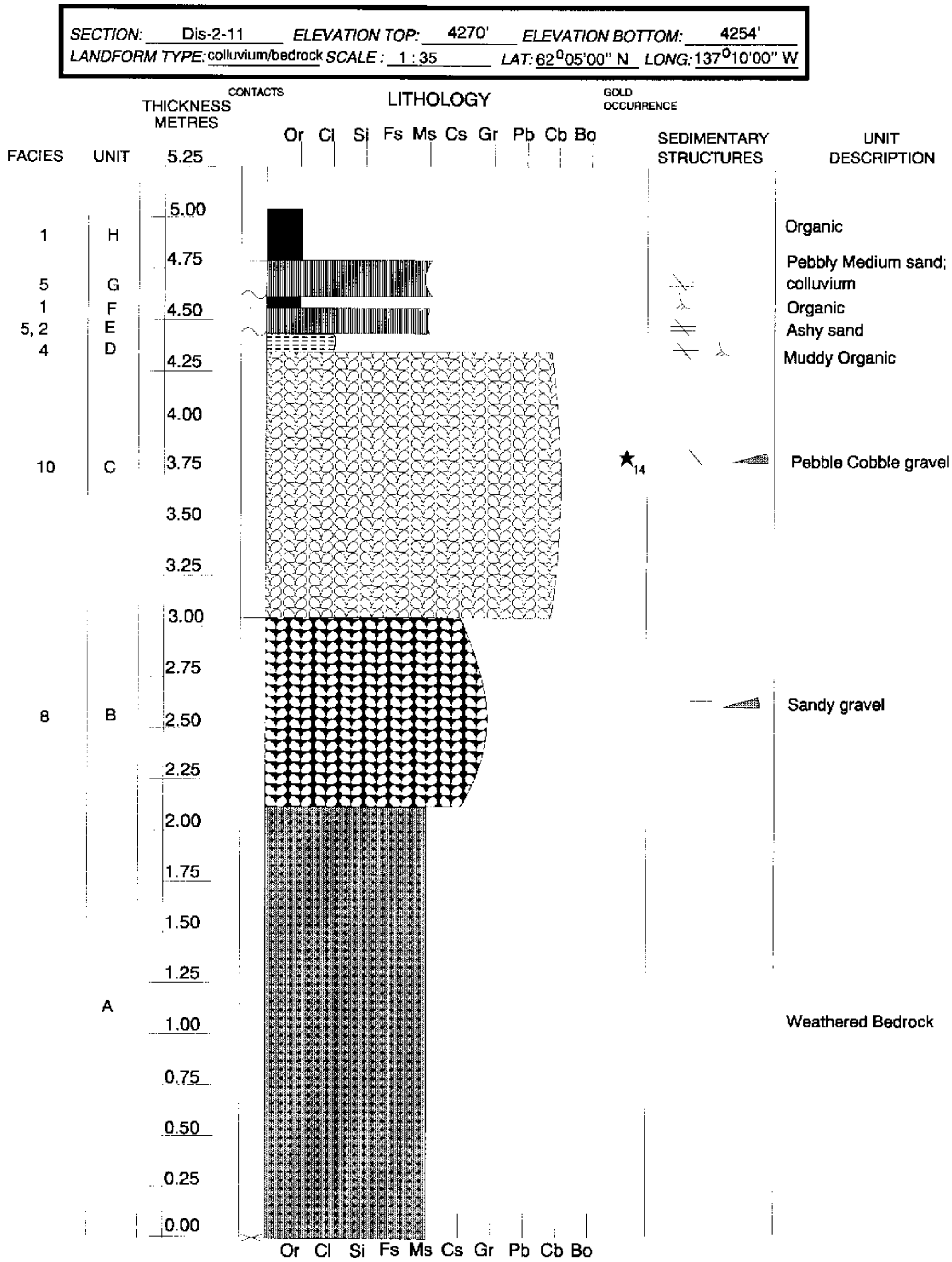

SECTION: Dis-2-11 ELEVATION TOP: 4270' ELEVATION BOTTOM: 4254'
LANDFORM TYPE: colluvium/bedrock SCALE : 1 : 35 LAT: 62°05'00" N LONG: 137°10'00" W
CONTACTS
THICKNESS METRES
LITHOLOGY
GOLD OCCURRENCE
Or Cl Si Fs Ms Cs Gr Pb Cb Bo
FACIES
UNIT
SEDIMENTARY STRUCTURES
UNIT DESCRIPTION
5.25
5.00
4.75
4.50
4.25
4.00
3.75
3.50
3.25
3.00
2.75
2.50
2.25
2.00
1.75
1.50
1.25
1.00
0.75
0.50
0.25
0.00
1 H Organic
5 G Pebbly Medium sand; colluvium
1 F Organic
5, 2 E Ashy sand
4 D Muddy Organic
10 C Pebble Cobble gravel
14
8 B Sandy gravel
A Weathered Bedrock

SECTION: Dis-2-12 ELEVATION TOP: 4270' ELEVATION BOTTOM: 4255'
LANDFORM TYPE: colluvium/bedrock SCALE : 1 : 35 LAT: 62°05'00" N LONG: 137°10'00" W

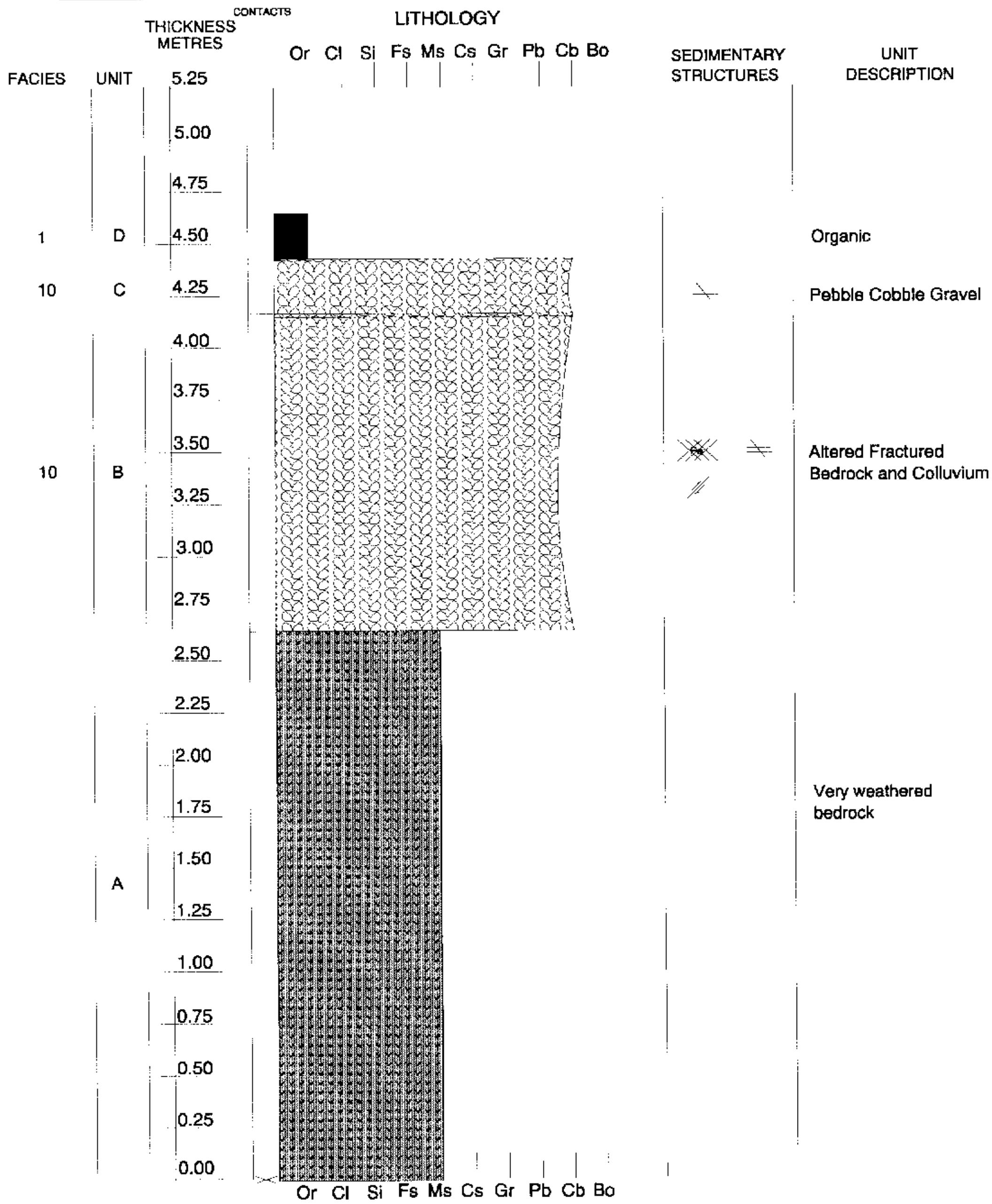

SECTION: L-DIS 1-1 *ELEVATION TOP:* 4000' *ELEVATION BOTTOM:* 3980'
LANDFORM TYPE: alluvial fan *SCALE :* 1 : 70 *LAT:* 62°04'45" N *LONG:* 137°11'08" W

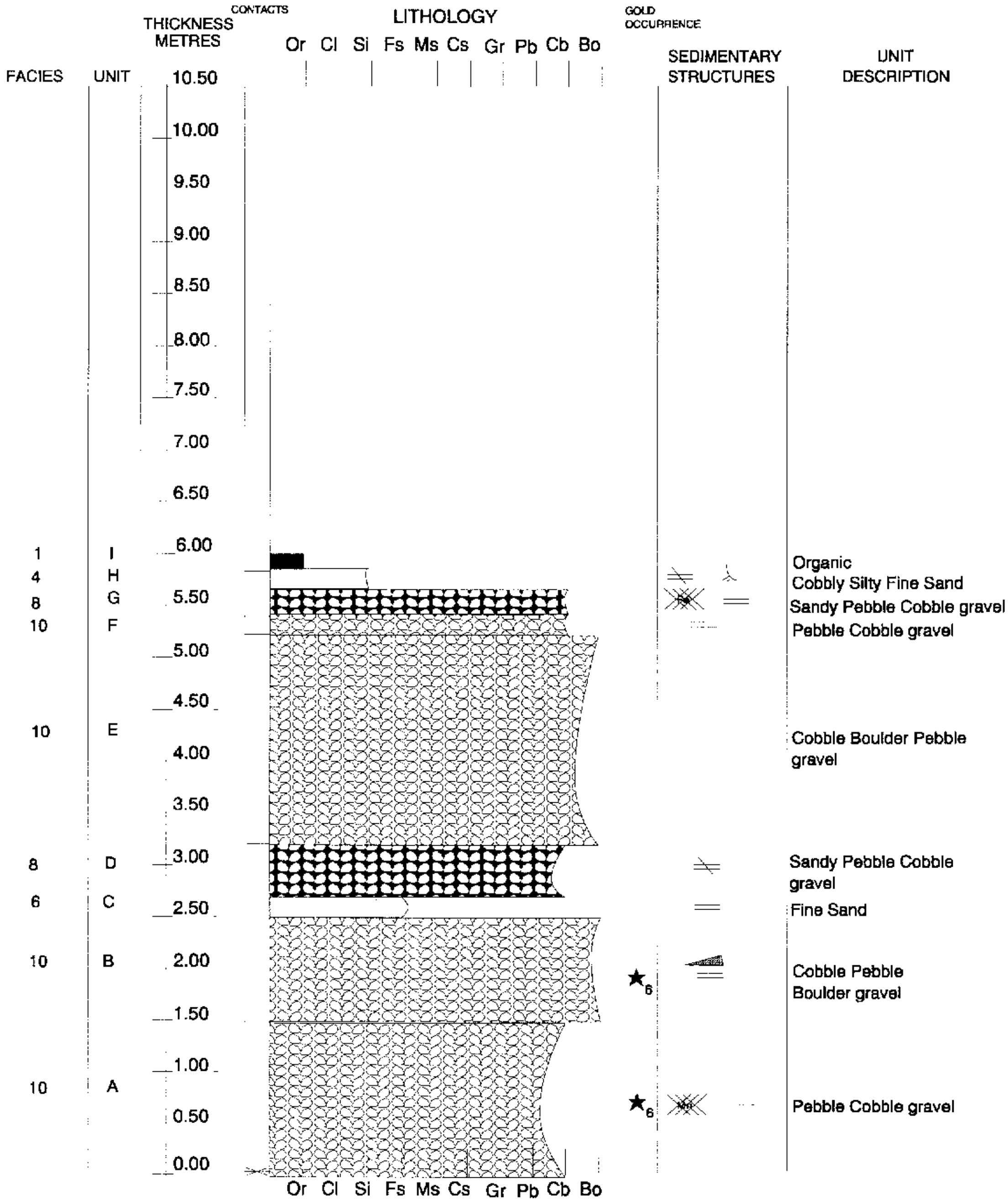

SECTION: WEB-1-1 *ELEVATION TOP:* 3950' *ELEVATION BOTTOM:* 3940'
LANDFORM TYPE: alluvial fan *SCALE:* 1 : 35 *LAT:* 62°03'31" N *LONG:* 137°10'28" W

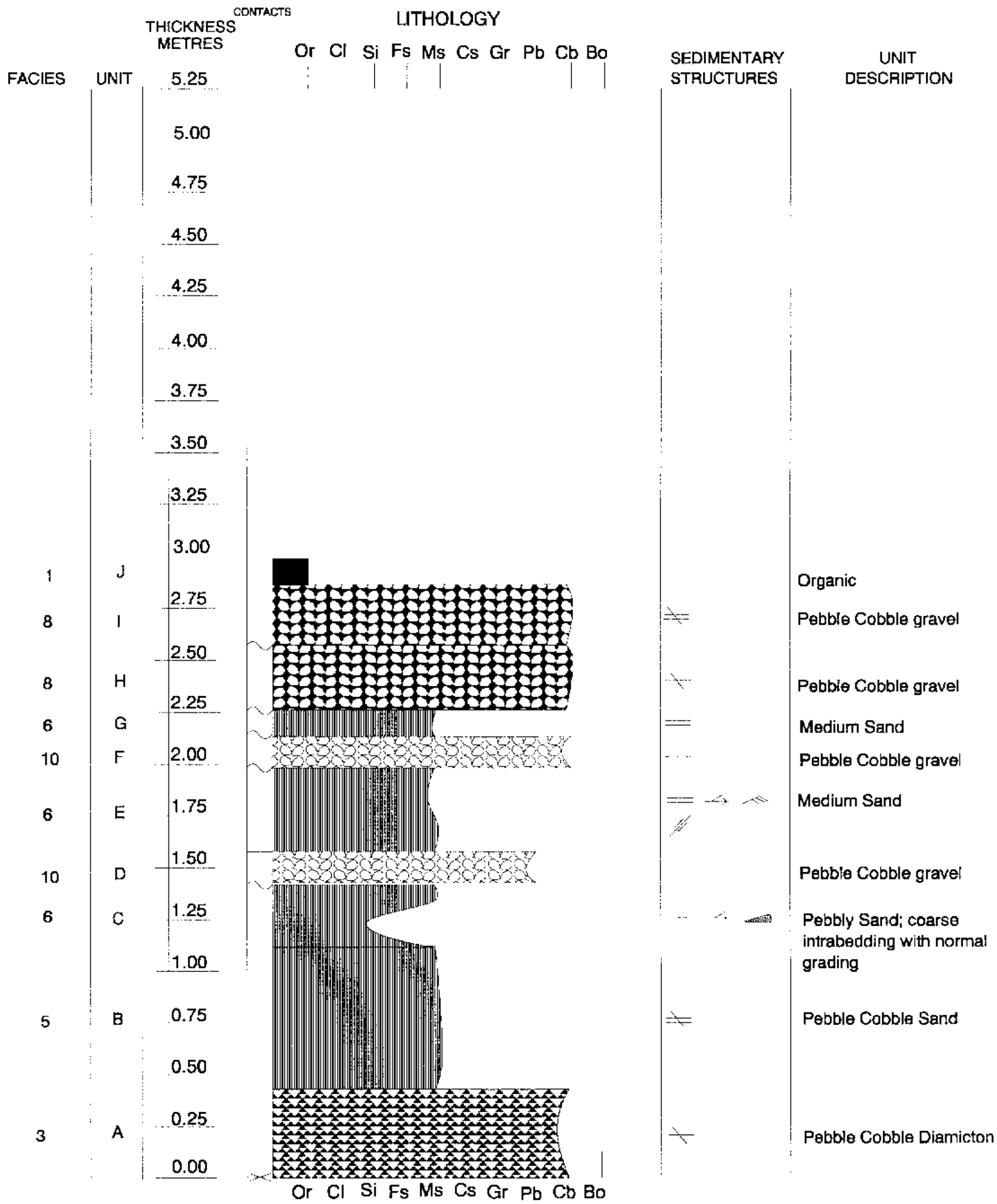

SECTION: WEB-2-1 *ELEVATION TOP:* 3960' *ELEVATION BOTTOM:* 3951'
LANDFORM TYPE: alluvial fan *SCALE :* 1 : 35 *LAT:* 62°03'27" N *LONG:* 137°10'45" W

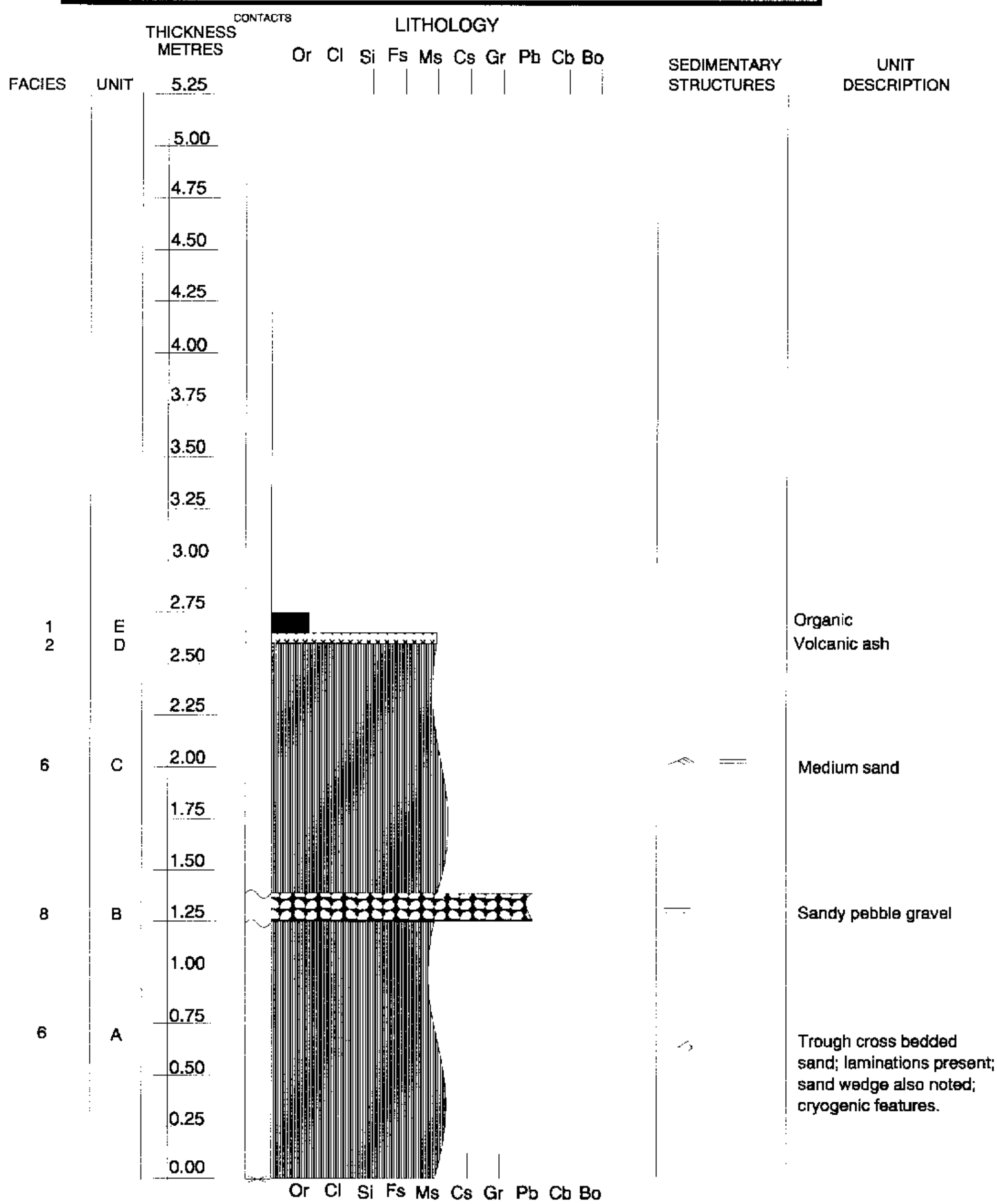

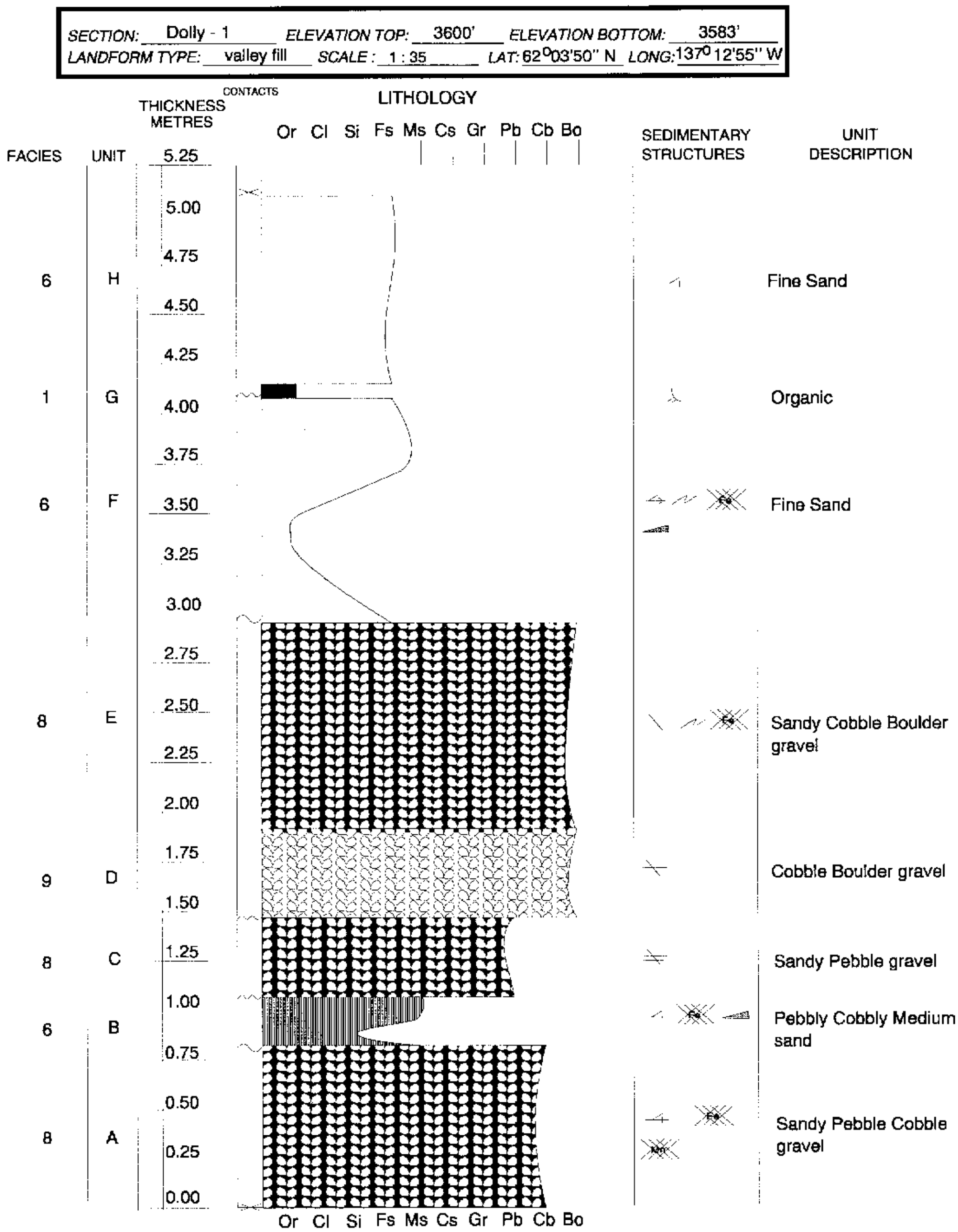
SECTION: Dolly - 1 ELEVATION TOP: 3600' ELEVATION BOTTOM: 3583'
LANDFORM TYPE: valley fill SCALE : 1 : 35 LAT: 62°03'50" N LONG: 137°12'55" W
CONTACTS
THICKNESS METRES
LITHOLOGY
Or Cl Si Fs Ms Cs Gr Pb Cb Bo
FACIES
UNIT
SEDIMENTARY STRUCTURES
UNIT DESCRIPTION
5.25
5.00
4.75
4.50
4.25
4.00
3.75
3.50
3.25
3.00
2.75
2.50
2.25
2.00
1.75
1.50
1.25
1.00
0.75
0.50
0.25
0.00
6 H Fine Sand
1 G Organic
6 F Fine Sand
8 E Sandy Cobble Boulder gravel
9 D Cobble Boulder gravel
8 C Sandy Pebble gravel
6 B Pebbly Cobbly Medium sand
8 A Sandy Pebble Cobble gravel

SECTION: Nan-1-1 *ELEVATION TOP:* 3560' *ELEVATION BOTTOM:* 3534'
LANDFORM TYPE: valley fill *SCALE :* 1 : 70 *LAT:* 62° 03'42" N *LONG:* 137° 13'00" W

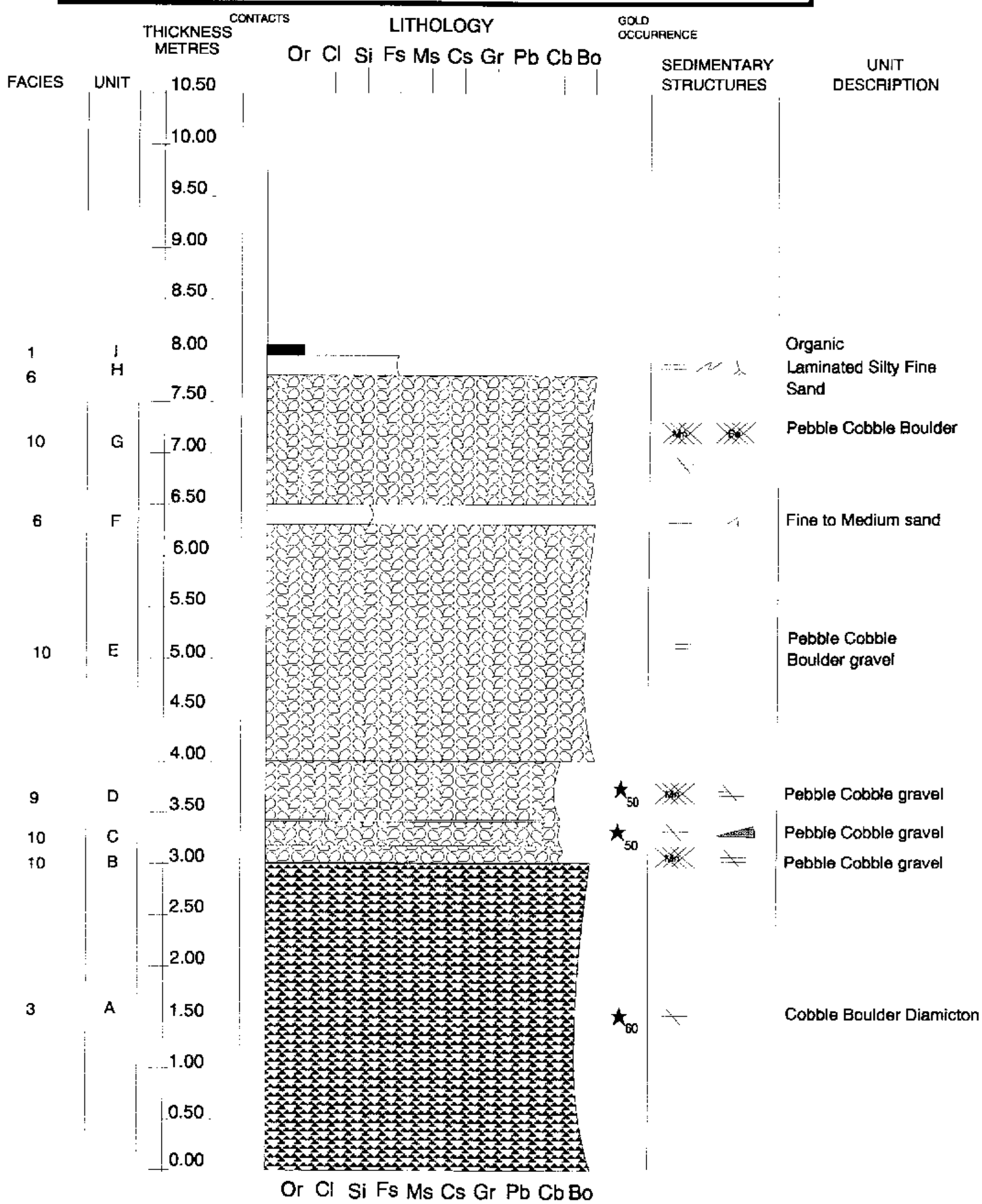

SECTION: EVA-1-1 ELEVATION TOP: 4105' ELEVATION BOTTOM: 4100'
LANDFORM TYPE: gulch SCALE: 1 : 35 LAT: 62°05'32" N LONG: 137°08'40" W

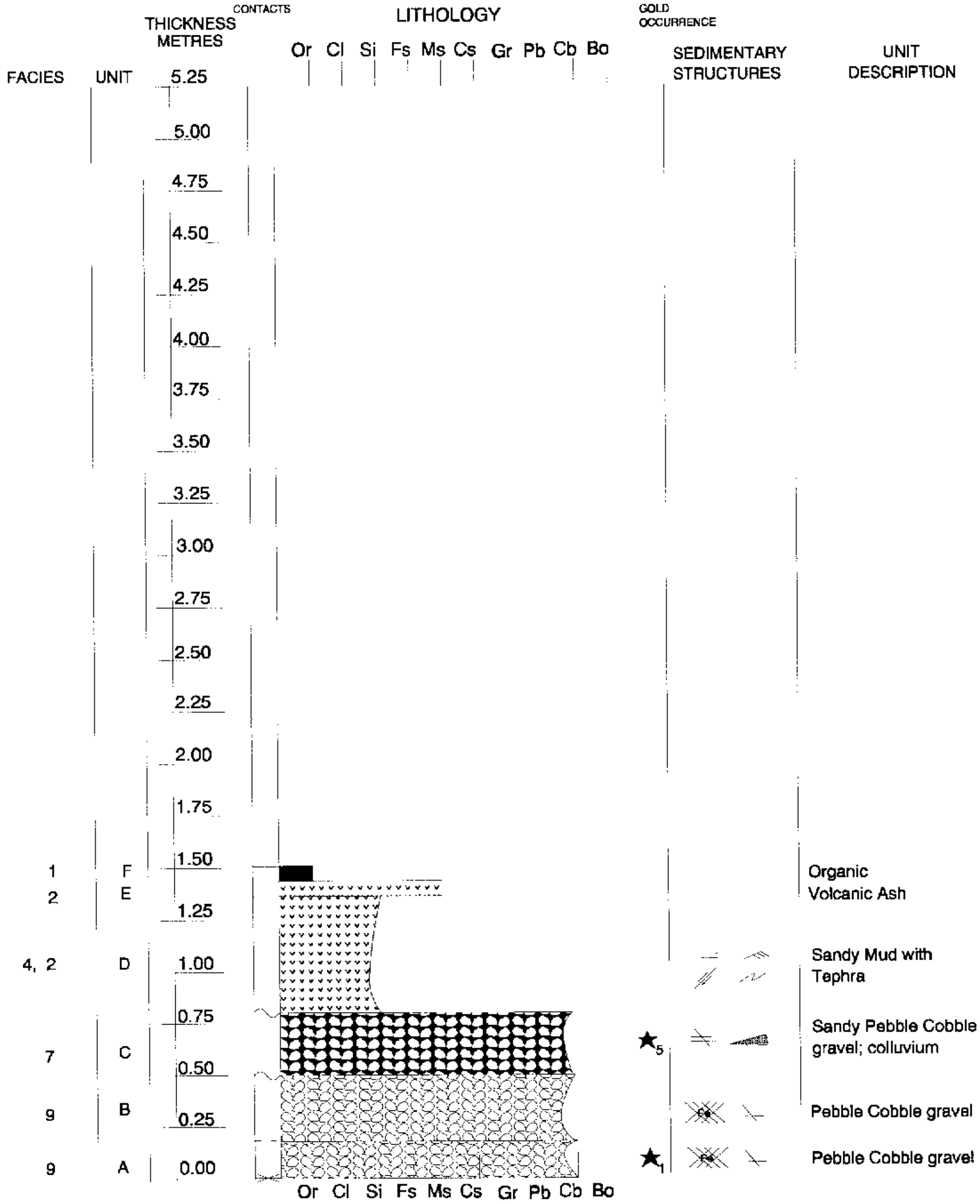

SECTION: EVA-2-1 *ELEVATION TOP:* 4015' *ELEVATION BOTTOM:* 4000'
LANDFORM TYPE: gulch *SCALE:* 1 : 35 *LAT:* 62°05'31" N *LONG:* 137°08'51" W

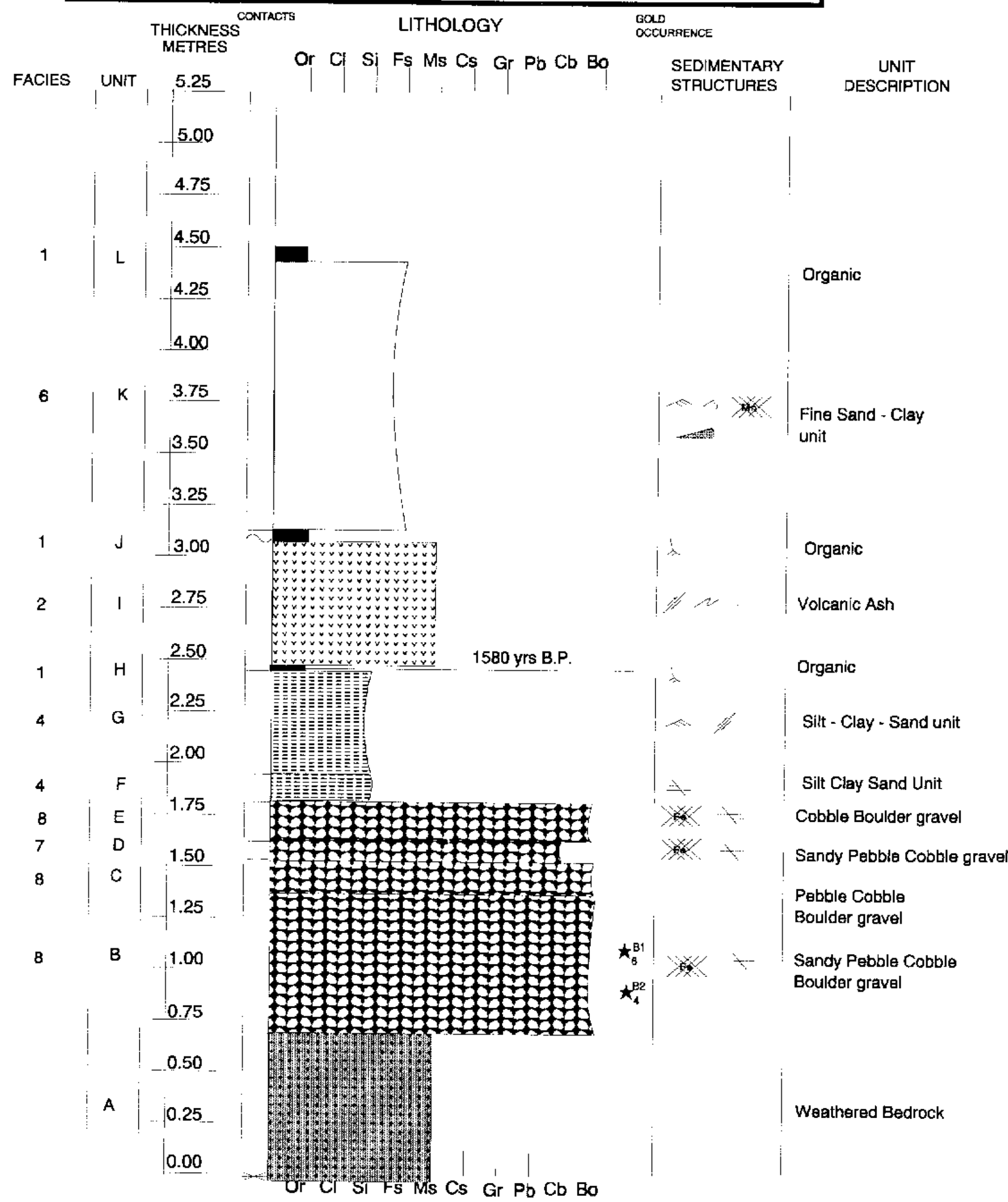

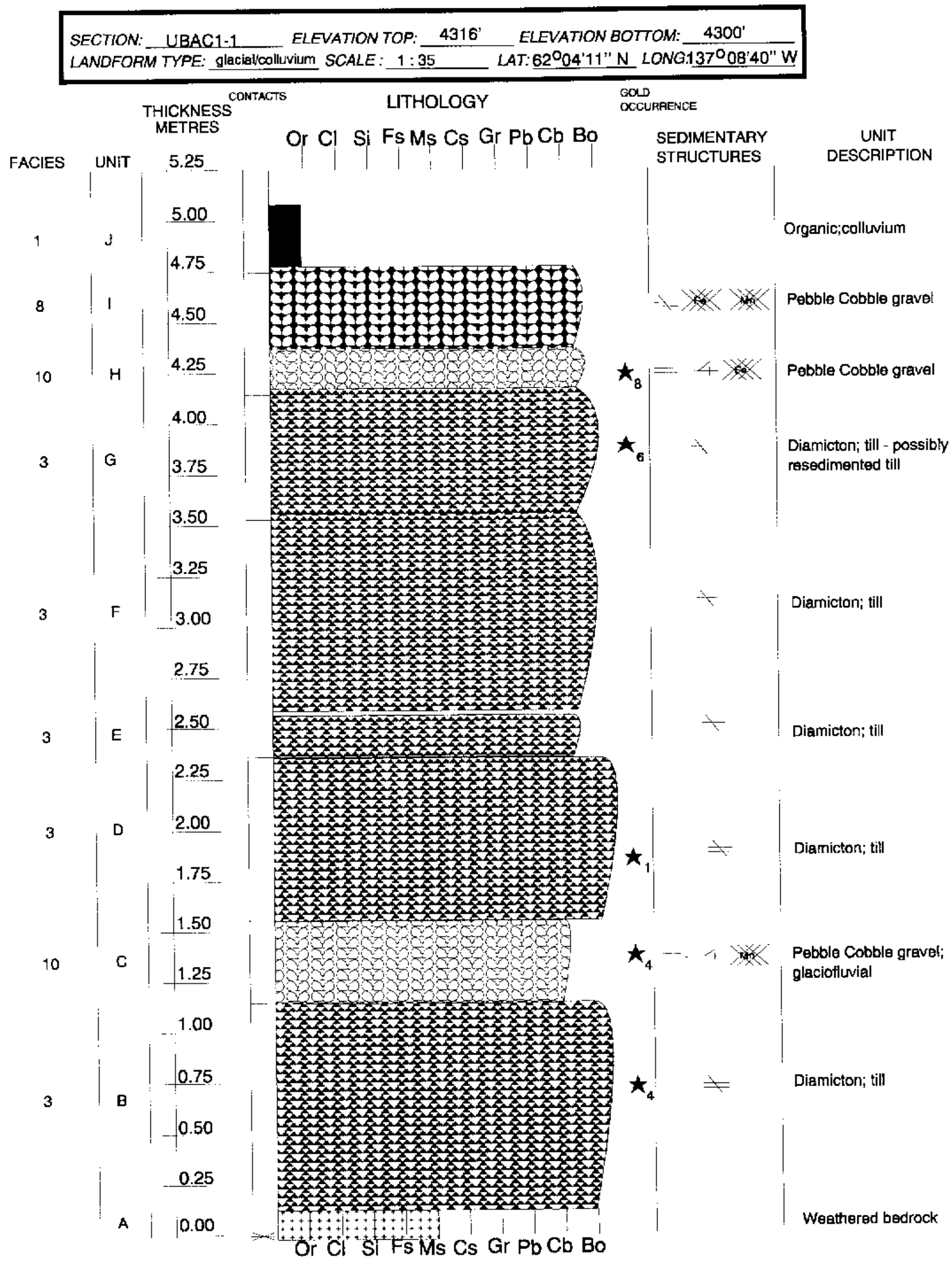
SECTION: UBAC1-1 ELEVATION TOP: 4316' ELEVATION BOTTOM: 4300'
LANDFORM TYPE: glacial/colluvium SCALE: 1 : 35 LAT: 62°04'11" N LONG: 137°08'40" W
FACIES
UNIT
THICKNESS METRES
CONTACTS
LITHOLOGY
Or Cl Si Fs Ms Cs Gr Pb Cb Bo
GOLD OCCURRENCE
SEDIMENTARY STRUCTURES
UNIT DESCRIPTION
5.25
5.00
4.75
4.50
4.25
4.00
3.75
3.50
3.25
3.00
2.75
2.50
2.25
2.00
1.75
1.50
1.25
1.00
0.75
0.50
0.25
0.00
1 J Organic;colluvium
8 I Pebble Cobble gravel
10 H Pebble Cobble gravel
3 G Diamicton; till - possibly resedimented till
3 F Diamicton; till
3 E Diamicton; till
3 D Diamicton; till
10 C Pebble Cobble gravel; glaciofluvial
3 B Diamicton; till
A Weathered bedrock

SECTION: MBAC-1-1 *ELEVATION TOP:* 4000' *ELEVATION BOTTOM:* 3985'
LANDFORM TYPE: alluvial fan *SCALE:* 1 : 35 *LAT:* 62°04'00" N *LONG:* 137°08'00" W

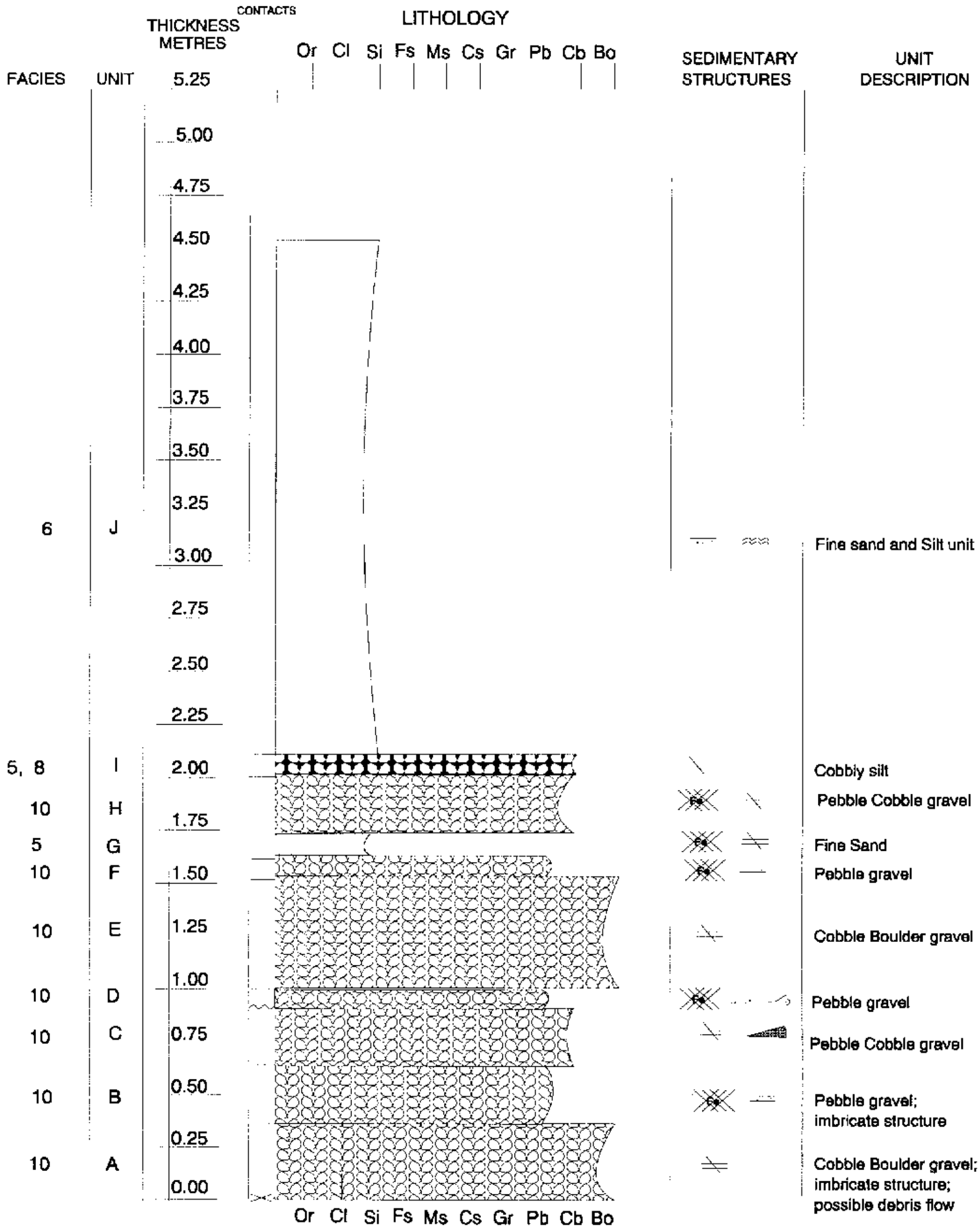

SECTION: LBAC-1-1 *ELEVATION TOP:* 3450' *ELEVATION BOTTOM:* 3442'
LANDFORM TYPE: fluvial stream *SCALE:* 1 : 35 *LAT:* 62°03'00" N *LONG:* 137°05'27" W

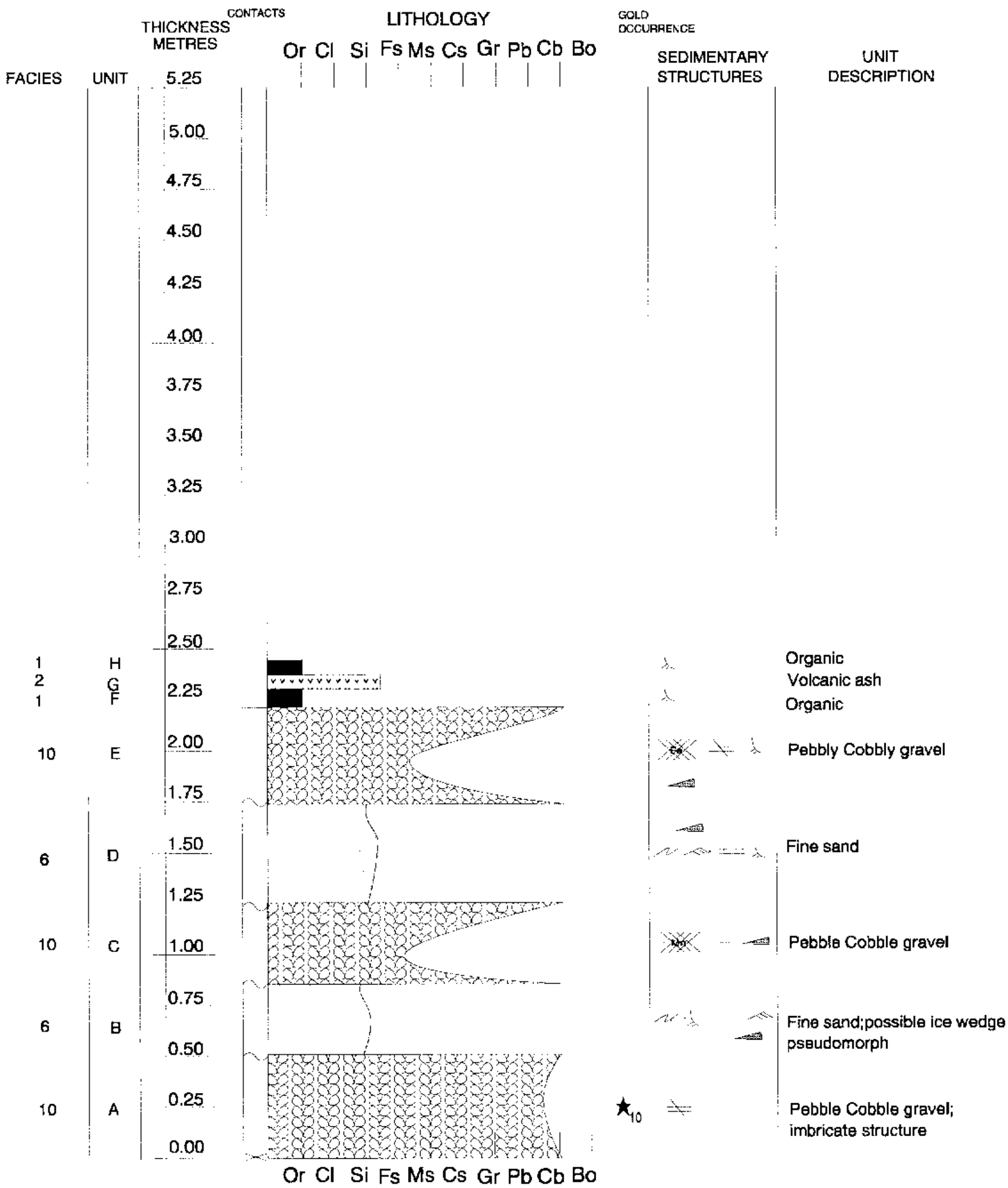

SECTION: LBAC-2-2 *ELEVATION TOP:* 3449' *ELEVATION BOTTOM:* 3440'
LANDFORM TYPE: alluvial fan *SCALE:* 1 : 35 *LAT:* 62°03'00" N *LONG:* 137°05'27" W

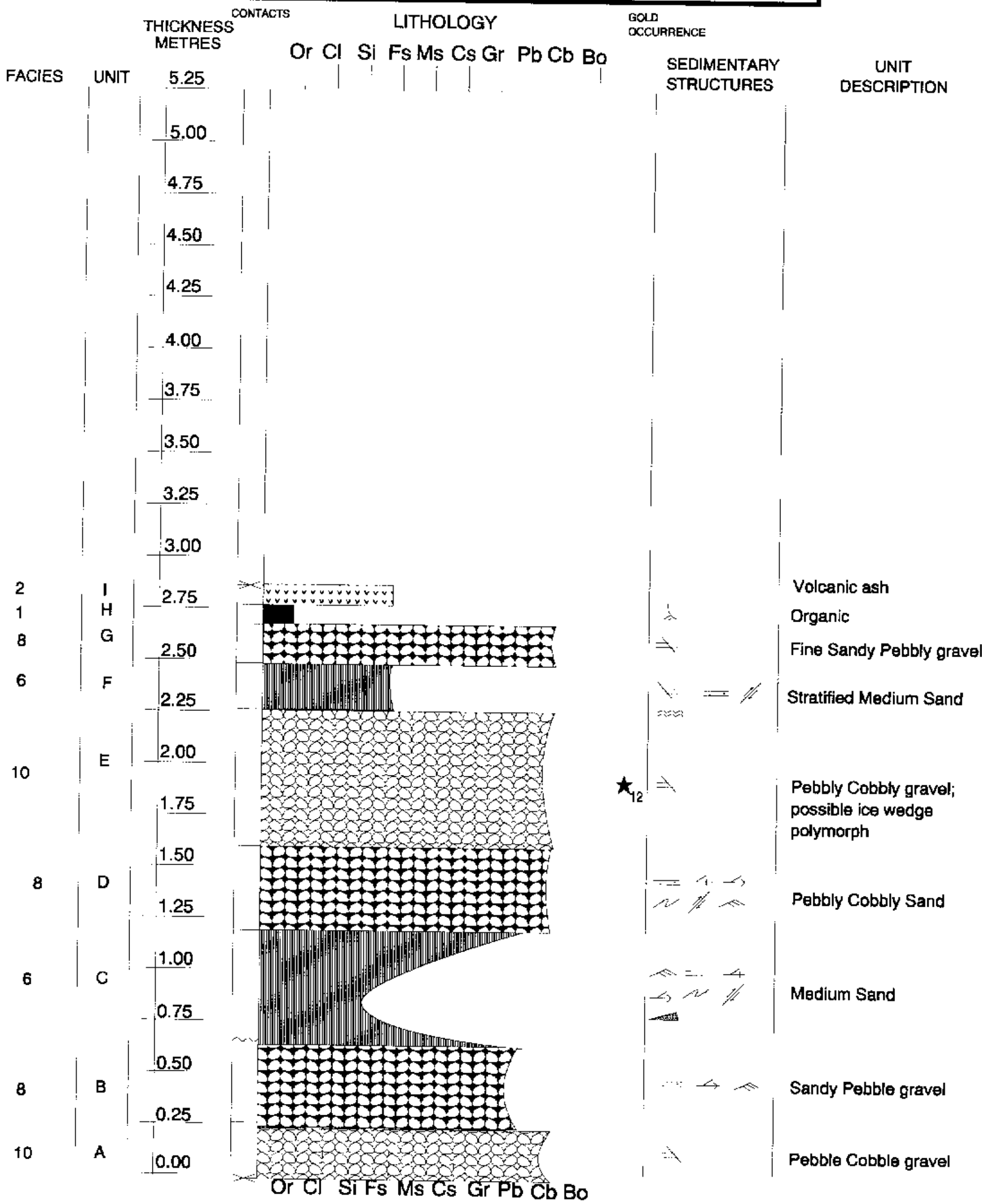

SECTION: VIC 1-1 ELEVATION TOP: 3209' ELEVATION BOTTOM: 3200'
LANDFORM TYPE: fluvial stream SCALE: 1 : 35 LAT: 62°01'30" N LONG: 137°03'02" W

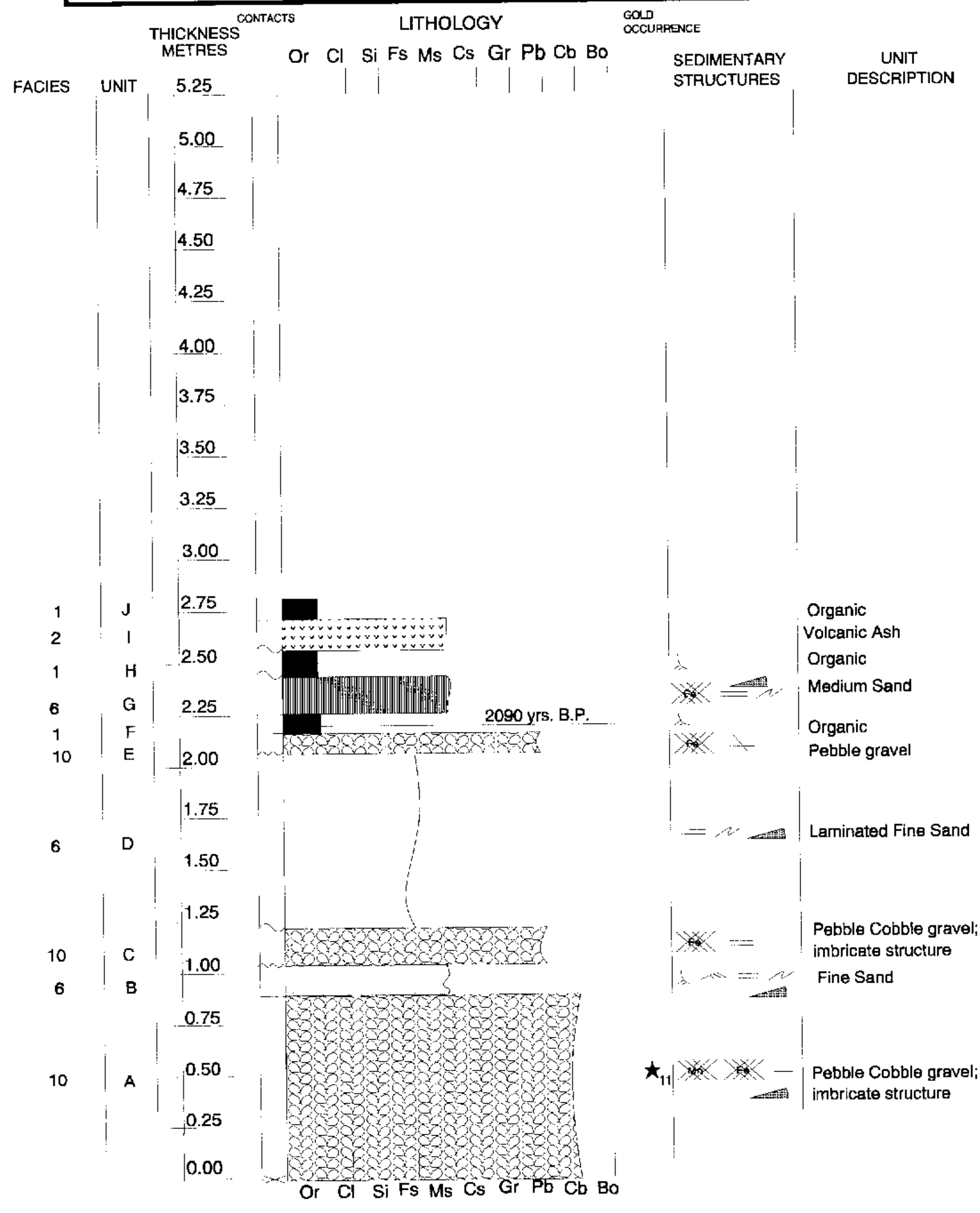

SECTION: VIC-1-2 *ELEVATION TOP:* 3218' *ELEVATION BOTTOM:* 3200'
LANDFORM TYPE: valley fill *SCALE :* 1 : 70 *LAT:* 62°01'30" N *LONG:* 137°03'02" W

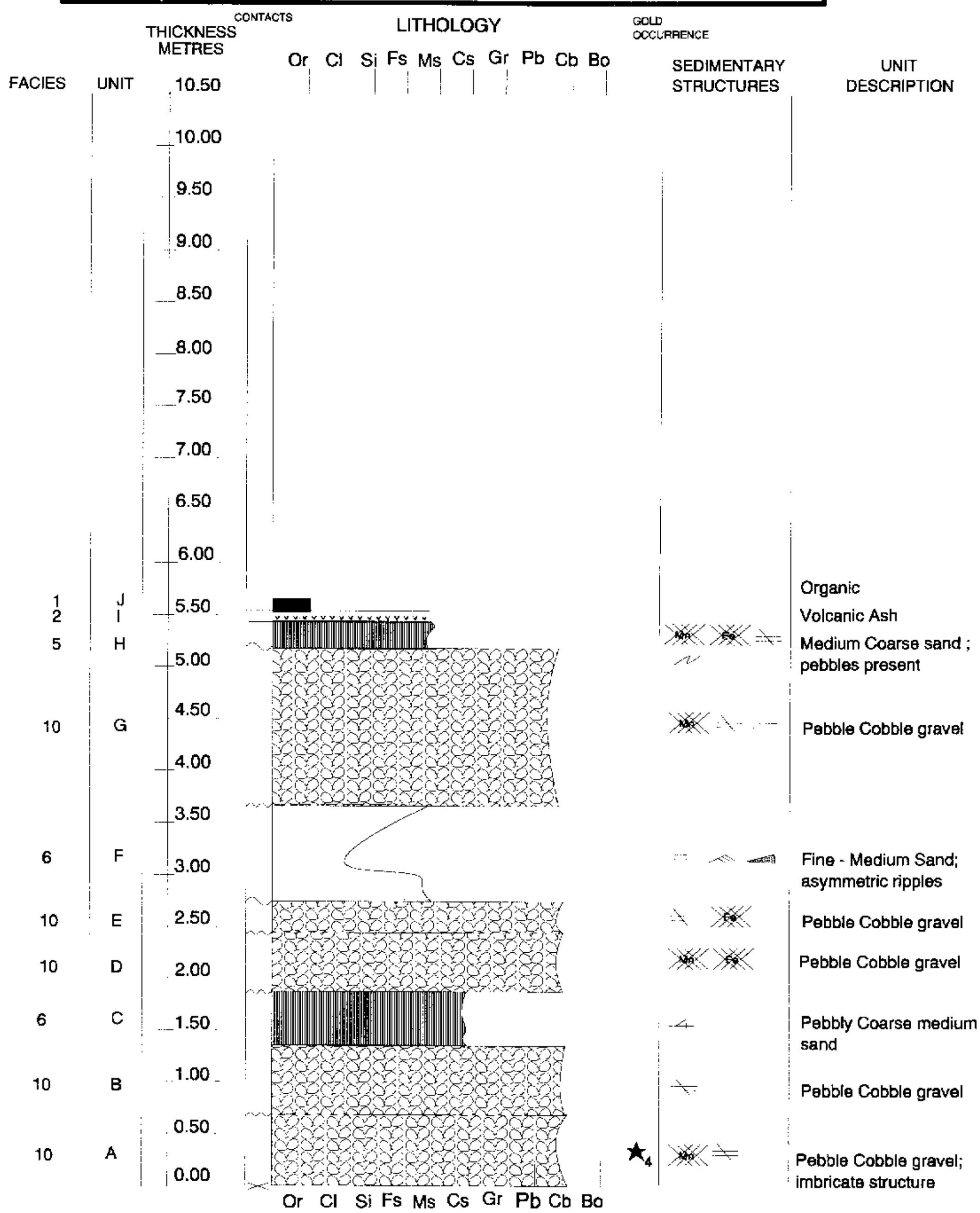

SECTION: VIC-1-3 *ELEVATION TOP:* 3223' *ELEVATION BOTTOM:* 3200'
LANDFORM TYPE: valley fill *SCALE :* 1 : 70 *LAT:* 62°01'30" N *LONG:* 137°03'02" W

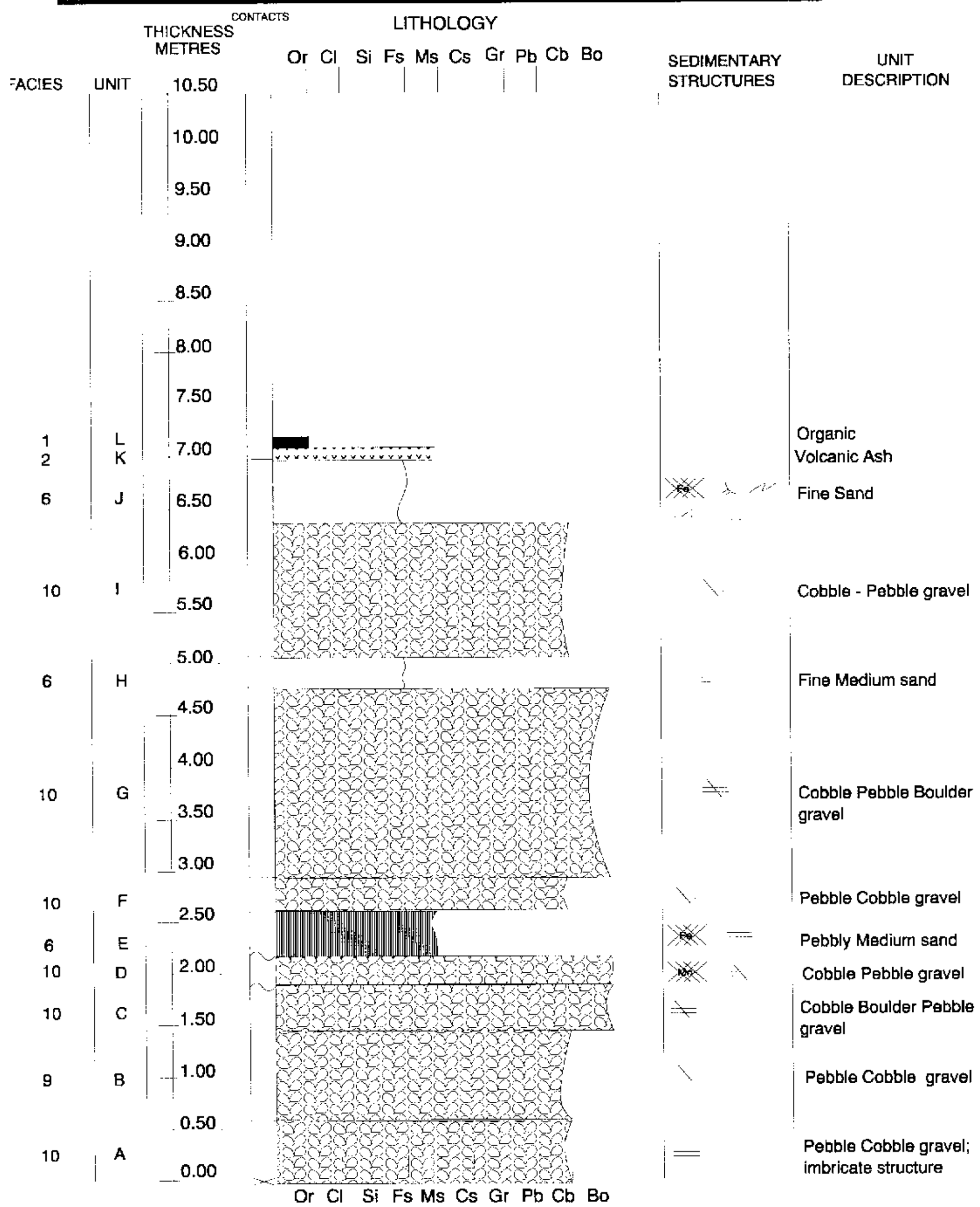

Appendix B - X-Ray Diffraction Data

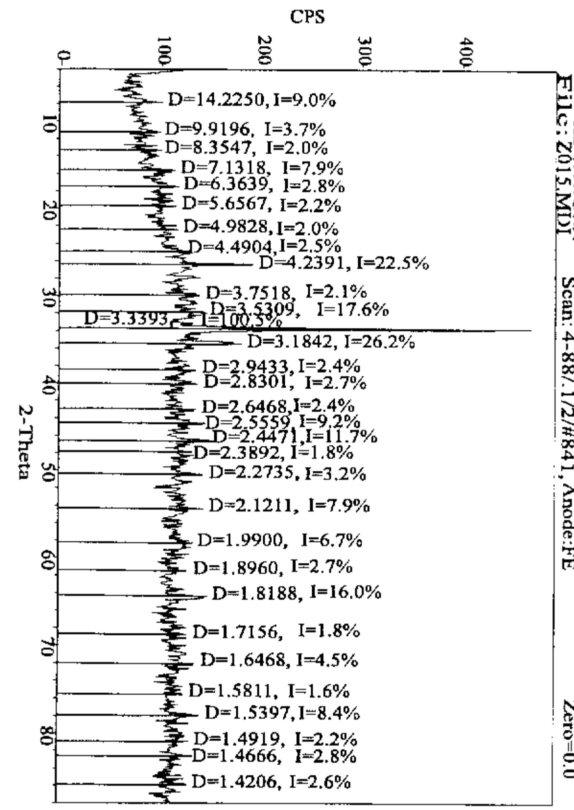
ID:K2-1A BULK
File: Z015.MDI
Scan: 4-88/.1/2/#841, Anode:FE
Zero=0.0
CPS
2-Theta
D=14.2250, I=9.0%
D=9.9196, I=3.7%
D=8.3547, I=2.0%
D=7.1318, I=7.9%
D=6.3639, I=2.8%
D=5.6567, I=2.2%
D=4.9828, I=2.0%
D=4.4904, I=2.5%
D=4.2391, I=22.5%
D=3.7518, I=2.1%
D=3.5309, I=17.6%
D=3.3393, I=100.5%
D=3.1842, I=26.2%
D=2.9433, I=2.4%
D=2.8301, I=2.7%
D=2.6468, I=2.4%
D=2.5559, I=9.2%
D=2.4471, I=11.7%
D=2.3892, I=1.8%
D=2.2735, I=3.2%
D=2.1211, I=7.9%
D=1.9900, I=6.7%
D=1.8960, I=2.7%
D=1.8188, I=16.0%
D=1.7156, I=1.8%
D=1.6468, I=4.5%
D=1.5811, I=1.6%
D=1.5397, I=8.4%
D=1.4919, I=2.2%
D=1.4666, I=2.8%
D=1.4206, I=2.6%

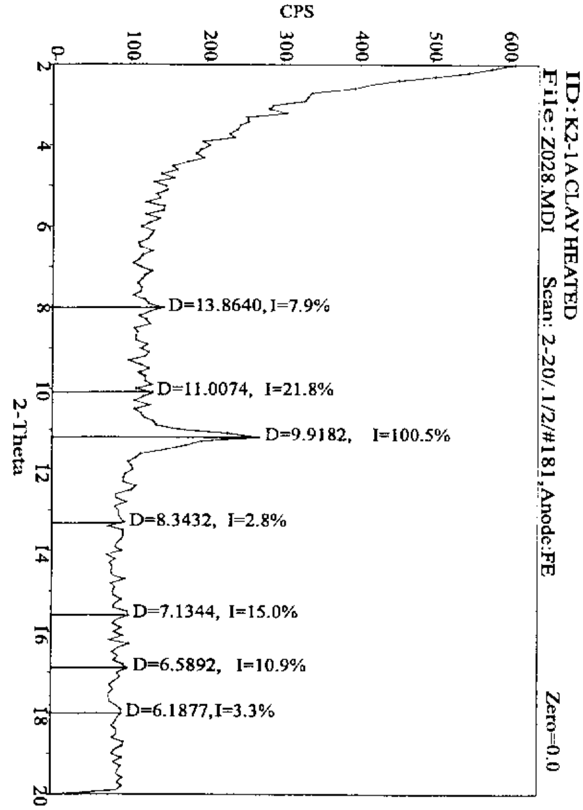
ID:K2-1A HEATED
File: Z028.MDI
Scan: 2-20/.1/2/#181, Anode:FE
Zero=0.0
CPS
2-Theta
D=13.8640, I=7.9%
D=11.0074, I=21.8%
D=9.9182, I=100.5%
D=8.3432, I=2.8%
D=7.1344, I=15.0%
D=6.5892, I=10.9%
D=6.1877, I=3.3%

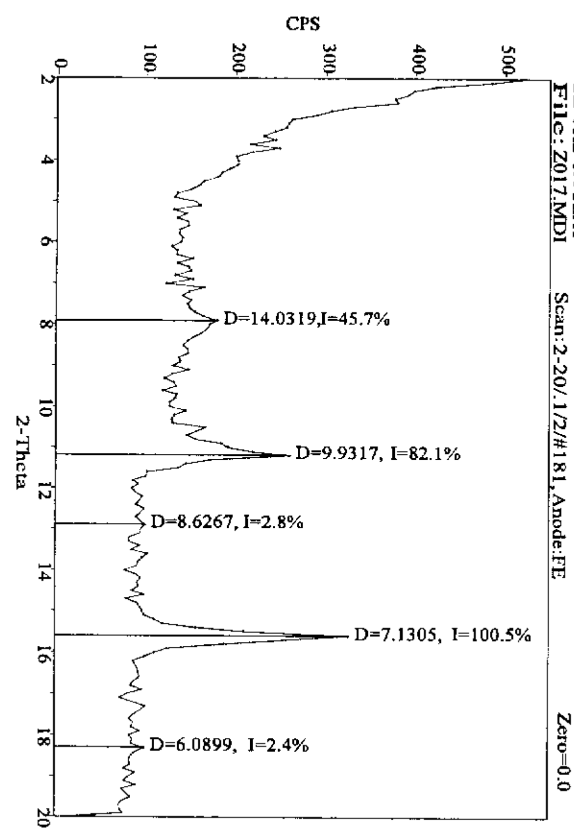
ID:K2-1A CLAY
File: Z017.MDI
Scan:2-20/.1/2/#181, Anode:FE
Zero=0.0
CPS
2-Theta
D=14.0319, I=45.7%
D=9.9317, I=82.1%
D=8.6267, I=2.8%
D=7.1305, I=100.5%
D=6.0899, I=2.4%

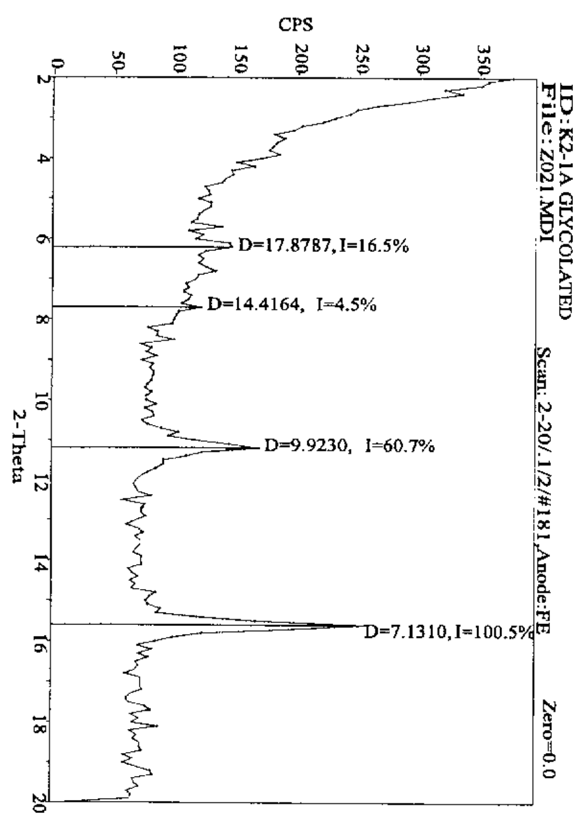
ID:K2-1A GLYCOLATED
File: Z021.MDI
Scan: 2-20/.1/2/#181, Anode:FE
Zero=0.0
CPS
2-Theta
D=17.8787, I=16.5%
D=14.4164, I=4.5%
D=9.9230, I=60.7%
D=7.1310, I=100.5%

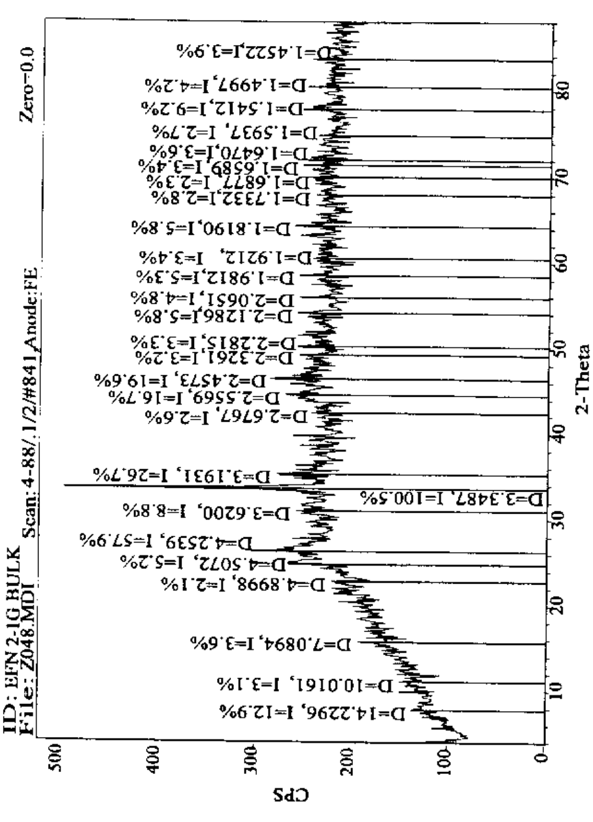
ID: EFN 2-1G BULK
File: Z048.MDI
Scan: 4-88/.1/2/#841,Anode:FE
Zero=0.0
CPS
2-Theta
D=14.2296, I=12.9%
D=10.0161, I=3.1%
D=7.0894, I=3.6%
D=4.8998, I=2.1%
D=4.5072, I=5.2%
D=4.2539, I=57.9%
D=3.6200, I=8.8%
D=3.3487, I=100.5%
D=3.1931, I=26.7%
D=2.6767, I=2.6%
D=2.5569, I=16.7%
D=2.4573, I=19.6%
D=2.3261, I=3.2%
D=2.2815, I=3.3%
D=2.1286, I=5.8%
D=2.0651, I=4.8%
D=1.9812, I=5.3%
D=1.9212, I=3.4%
D=1.8190, I=5.8%
D=1.7332, I=2.8%
D=1.6877, I=2.3%
D=1.6589, I=3.4%
D=1.6470, I=3.6%
D=1.5937, I=2.7%
D=1.5412, I=9.2%
D=1.4997, I=4.2%
D=1.4522, I=3.9%

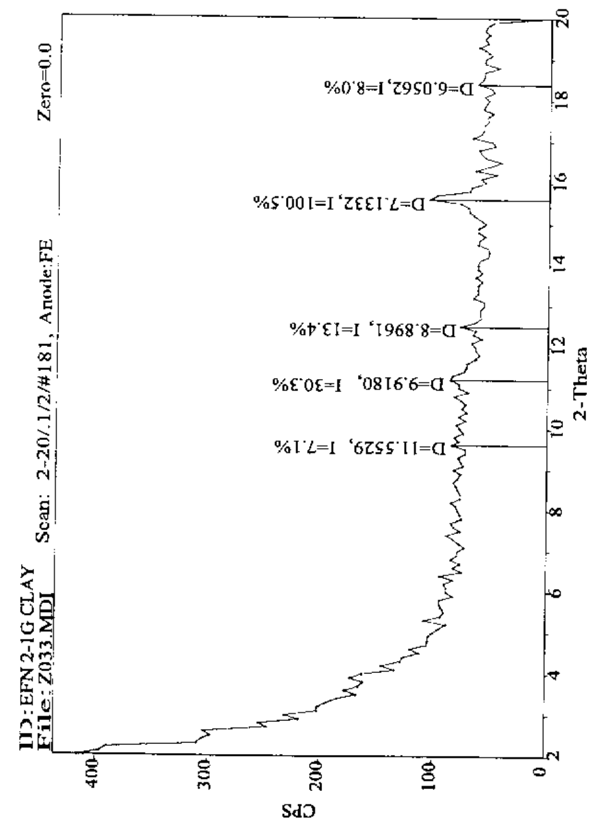
ID: EFN 2-1G CLAY
File: Z033.MDI
Scan: 2-20/.1/2/#181, Anode:FE
Zero=0.0
CPS
2-Theta
D=11.5529, I=7.1%
D=9.9180, I=30.3%
D=8.8961, I=13.4%
D=7.1332, I=100.5%
D=6.0562, I=8.0%

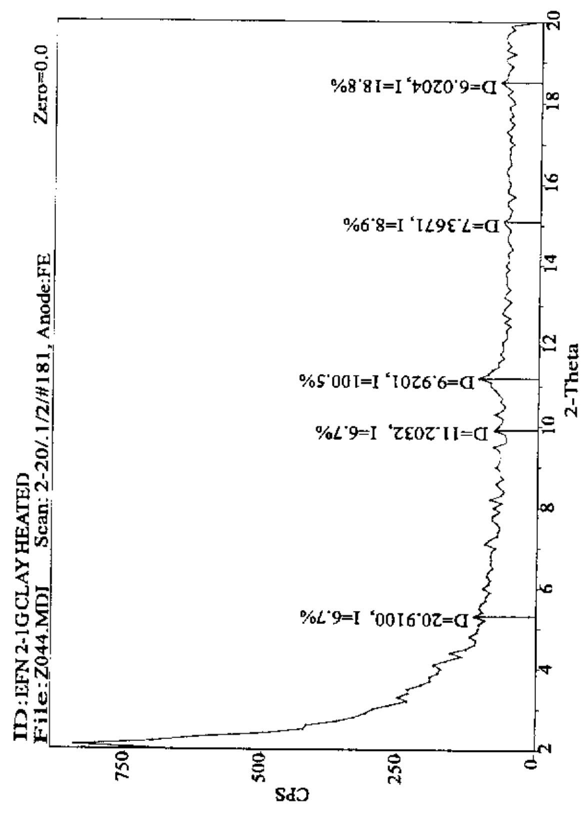
ID: EFN 2-1G CLAY HEATED
File: Z044.MDI
Scan: 2-20/.1/2/#181, Anode:FE
Zero=0.0
CPS
2-Theta
D=20.9100, I=6.7%
D=11.2032, I=6.7%
D=9.9201, I=100.5%
D=7.3671, I=8.9%
D=6.0204, I=18.8%

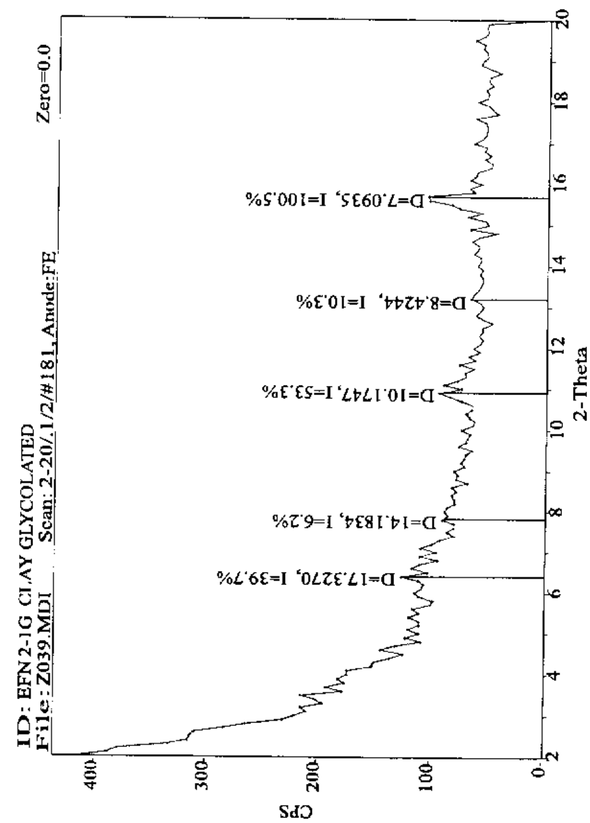
ID: EFN 2-1G CLAY GLYCOLATED
File: Z039.MDI
Scan: 2-20/.1/2/#181, Anode:FE
Zero=0.0
CPS
2-Theta
D=17.3270, I=39.7%
D=14.1834, I=6.2%
D=10.1747, I=53.3%
D=8.4244, I=10.3%
D=7.0935, I=100.5%

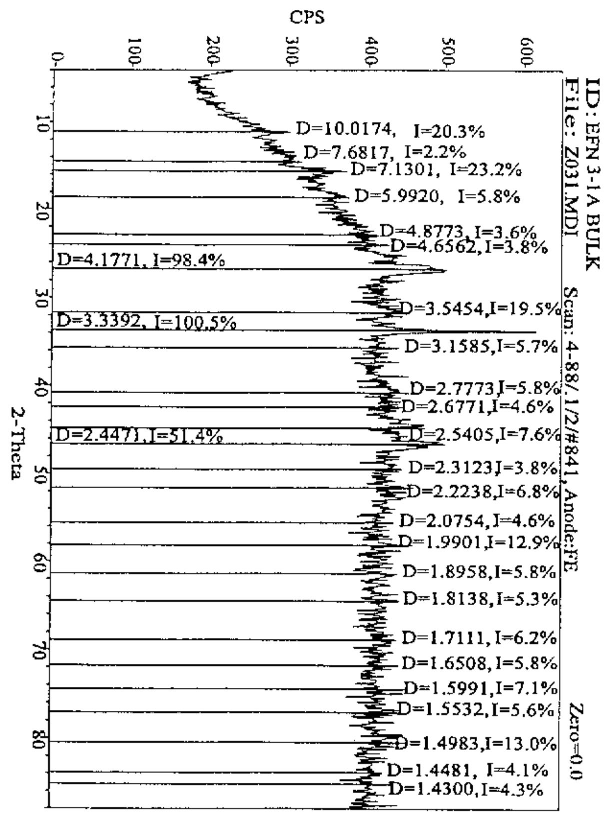
ID: EFN 3-1A BULK
File: Z031.MDI
Scan: 4-88/.1/2/#841, Anode:FE
Zero=0.0
CPS
2-Theta
D=10.0174, I=20.3%
D=7.6817, I=2.2%
D=7.1301, I=23.2%
D=5.9920, I=5.8%
D=4.8773, I=3.6%
D=4.6562, I=3.8%
D=4.1771, I=98.4%
D=3.5454, I=19.5%
D=3.3392, I=100.5%
D=3.1585, I=5.7%
D=2.7773, I=5.8%
D=2.6771, I=4.6%
D=2.4471, I=51.4%
D=2.5405, I=7.6%
D=2.3123, I=3.8%
D=2.2238, I=6.8%
D=2.0754, I=4.6%
D=1.9901, I=12.9%
D=1.8958, I=5.8%
D=1.8138, I=5.3%
D=1.7111, I=6.2%
D=1.6508, I=5.8%
D=1.5991, I=7.1%
D=1.5532, I=5.6%
D=1.4983, I=13.0%
D=1.4481, I=4.1%
D=1.4300, I=4.3%
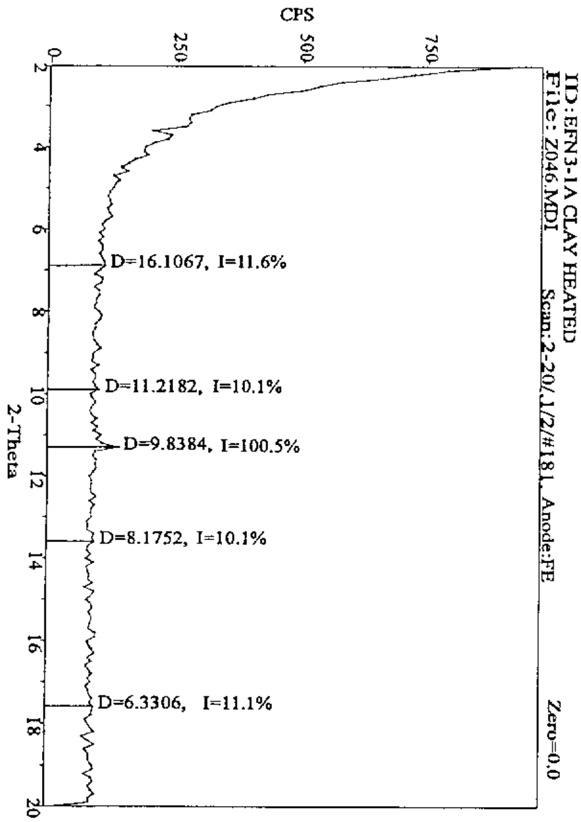
ID: EFN3-1A CLAY HEATED
File: Z046.MDI
Scan: 2-20/.1/2/#181, Anode:FE
Zero=0.0
CPS
2-Theta
D=16.1067, I=11.6%
D=11.2182, I=10.1%
D=9.8384, I=100.5%
D=8.1752, I=10.1%
D=6.3306, I=11.1%
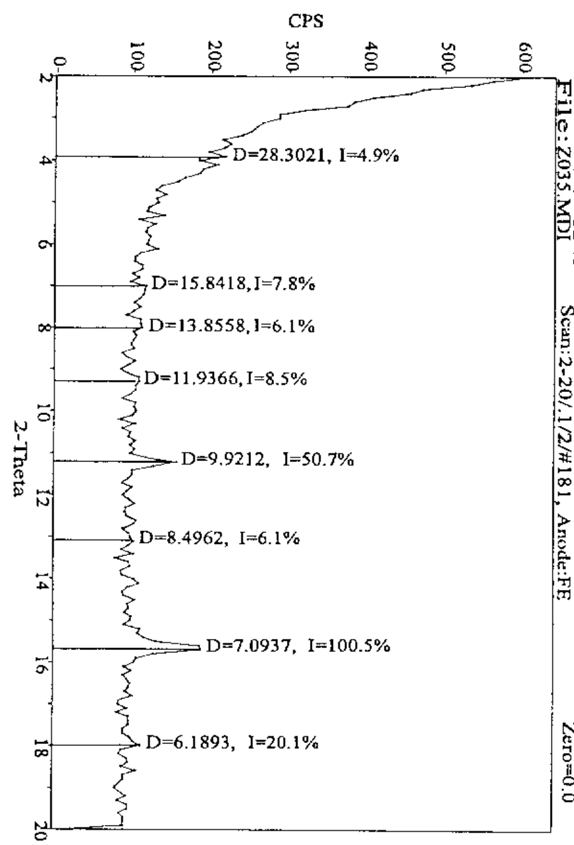
ID: EFN3-1A CLAY
File: Z035.MDI
Scan: 2-20/.1/2/#181, Anode:FE
Zero=0.0
CPS
2-Theta
D=28.3021, I=4.9%
D=15.8418, I=7.8%
D=13.8558, I=6.1%
D=11.9366, I=8.5%
D=9.9212, I=50.7%
D=8.4962, I=6.1%
D=7.0937, I=100.5%
D=6.1893, I=20.1%
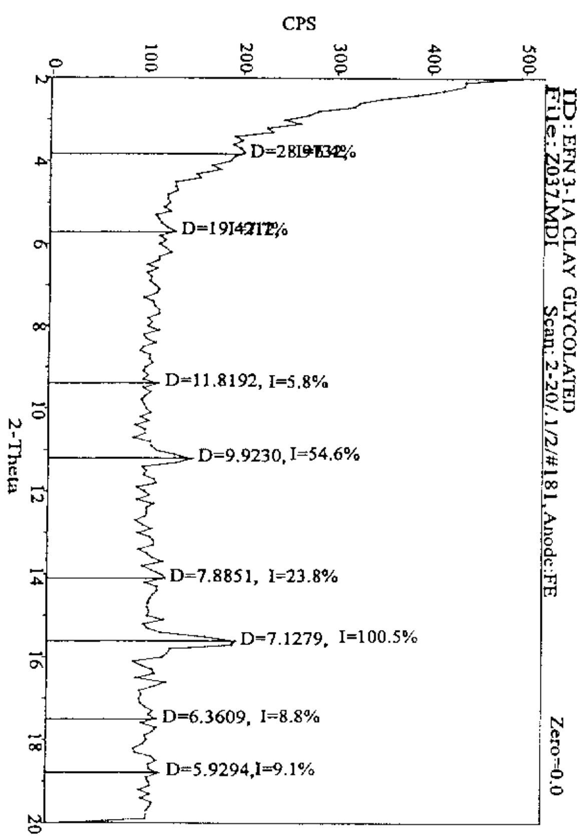
ID: EFN3-1A CLAY GLYCOLATED
File: Z037.MDI
Scan: 2-20/.1/2/#181, Anode:FE
Zero=0.0
CPS
2-Theta
D=11.8192, I=5.8%
D=9.9230, I=54.6%
D=7.8851, I=23.8%
D=7.1279, I=100.5%
D=6.3609, I=8.8%
D=5.9294, I=9.1%

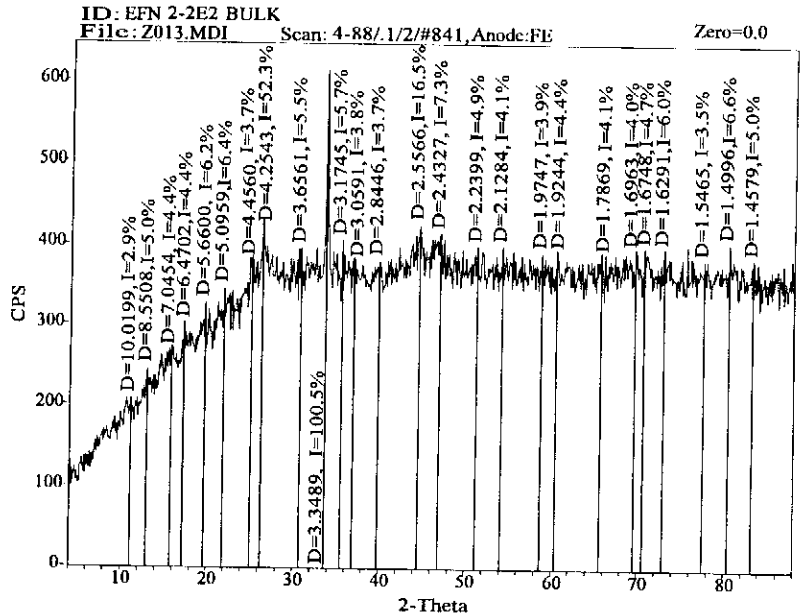
ID: EFN 2-2E2 BULK
File: Z013.MDI Scan: 4-88/.1/2/#841, Anode:FE Zero=0.0
CPS
2-Theta
D=10.0199, I=2.9%
D=8.5508, I=5.0%
D=7.0454, I=4.4%
D=6.4702, I=4.4%
D=5.6600, I=6.2%
D=5.0959, I=6.4%
D=4.4560, I=3.7%
D=4.2543, I=52.3%
D=3.6561, I=5.5%
D=3.3489, I=100.5%
D=3.1745, I=5.7%
D=3.0591, I=3.8%
D=2.8446, I=3.7%
D=2.5566, I=16.5%
D=2.4327, I=7.3%
D=2.2399, I=4.9%
D=2.1284, I=4.1%
D=1.9747, I=3.9%
D=1.9244, I=4.4%
D=1.7869, I=4.1%
D=1.6963, I=4.0%
D=1.6748, I=4.7%
D=1.6291, I=6.0%
D=1.5465, I=3.5%
D=1.4996, I=6.6%
D=1.4579, I=5.0%

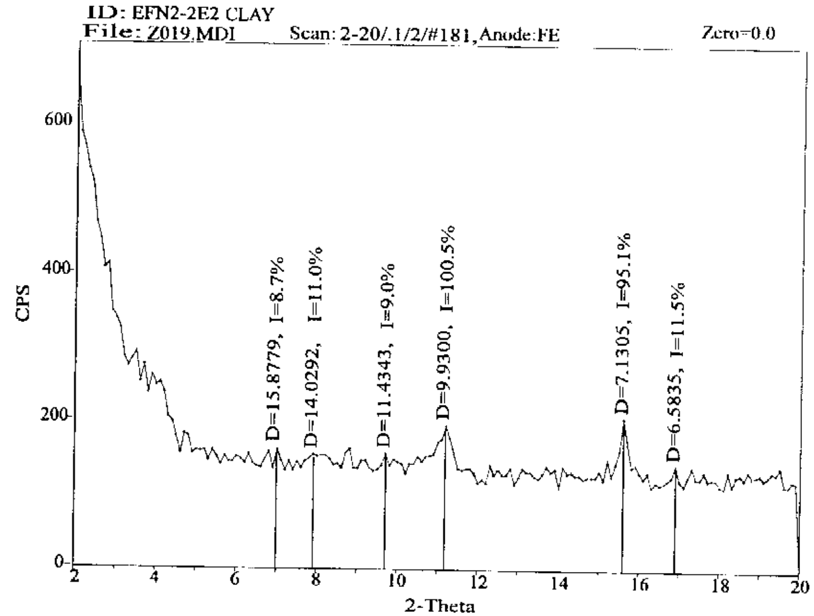
ID: EFN2-2E2 CLAY
File: Z019.MDI Scan: 2-20/.1/2/#181, Anode:FE Zero=0.0
CPS
2-Theta
D=15.8779, I=8.7%
D=14.0292, I=11.0%
D=11.4343, I=9.0%
D=9.9300, I=100.5%
D=7.1305, I=95.1%
D=6.5835, I=11.5%

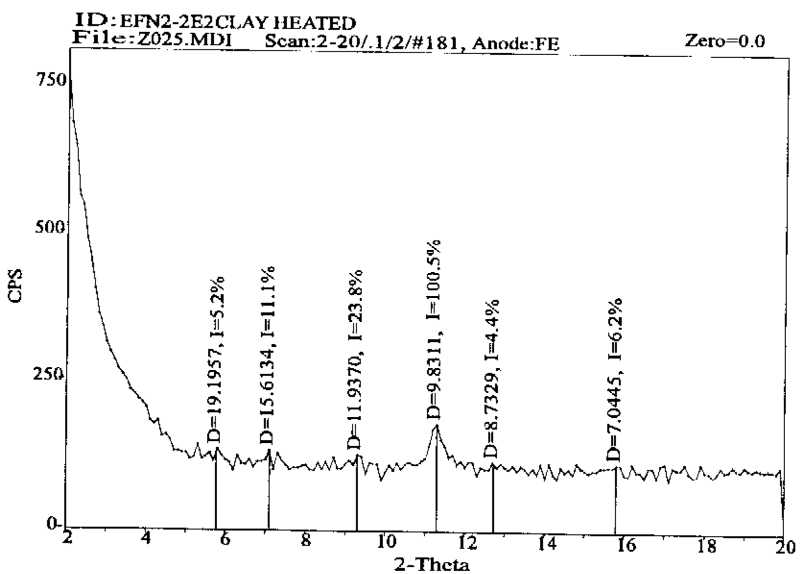
ID: EFN2-2E2CLAY HEATED
File: Z025.MDI Scan: 2-20/.1/2/#181, Anode:FE Zero=0.0
CPS
2-Theta
D=19.1957, I=5.2%
D=15.6134, I=11.1%
D=11.9370, I=23.8%
D=9.8311, I=100.5%
D=8.7329, I=4.4%
D=7.0445, I=6.2%

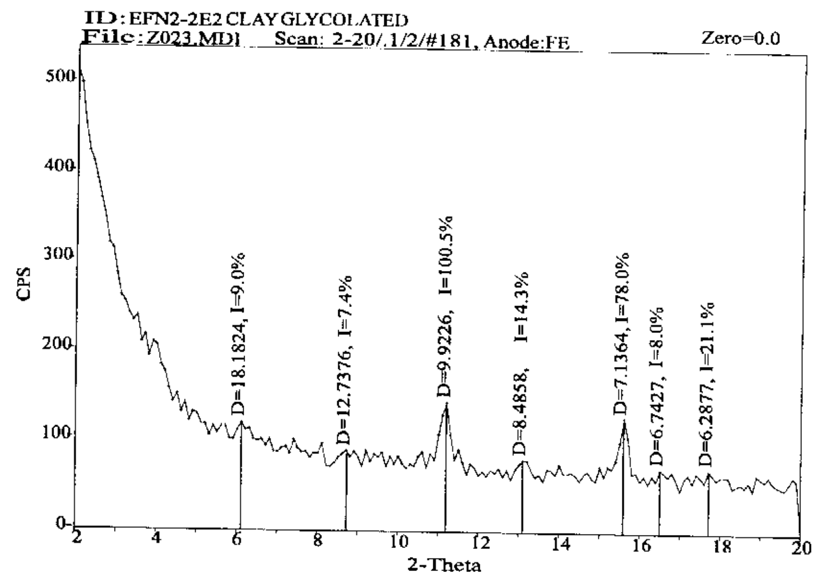
ID: EFN2-2E2 CLAY GLYCOLATED
File: Z023.MDI Scan: 2-20/.1/2/#181, Anode:FE Zero=0.0
CPS
2-Theta
D=18.1824, I=9.0%
D=12.7376, I=7.4%
D=9.9226, I=100.5%
D=8.4858, I=14.3%
D=7.1364, I=78.0%
D=6.7427, I=8.0%
D=6.2877, I=21.1%

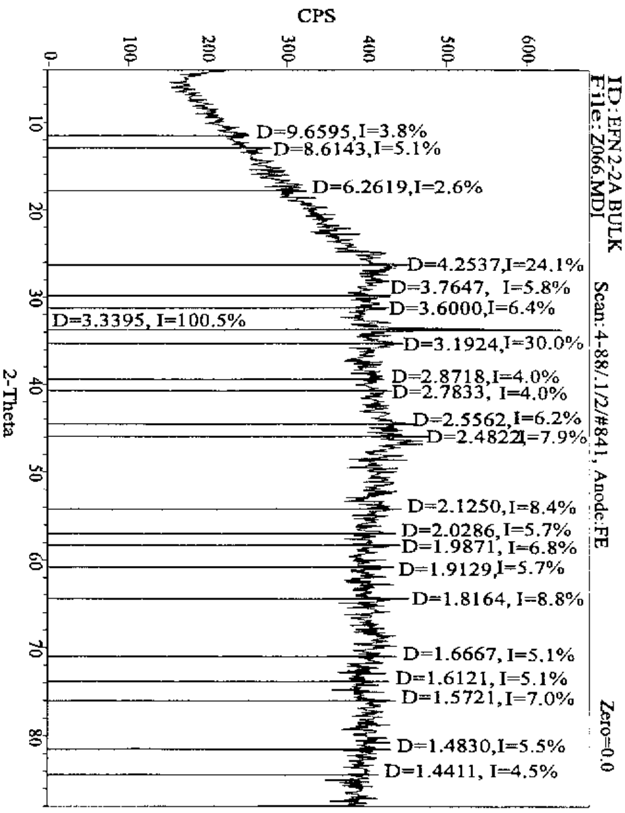
ID:EFN2-2A BULK
File:Z066.MDI
Scan: 4-88/.1/2/#841, Anode:FE
Zero=0.0
CPS
2-Theta
D=9.6595,I=3.8%
D=8.6143,I=5.1%
D=6.2619,I=2.6%
D=4.2537,I=24.1%
D=3.7647, I=5.8%
D=3.6000,I=6.4%
D=3.3395, I=100.5%
D=3.1924,I=30.0%
D=2.8718,I=4.0%
D=2.7833, I=4.0%
D=2.5562,I=6.2%
D=2.4822,I=7.9%
D=2.1250,I=8.4%
D=2.0286,I=5.7%
D=1.9871, I=6.8%
D=1.9129,I=5.7%
D=1.8164, I=8.8%
D=1.6667, I=5.1%
D=1.6121, I=5.1%
D=1.5721,I=7.0%
D=1.4830,I=5.5%
D=1.4411, I=4.5%

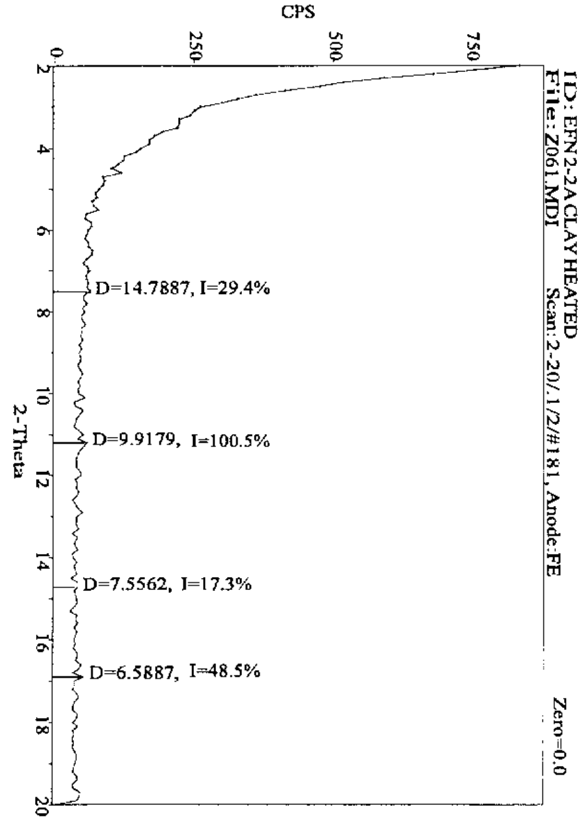
ID:EFN2-2A CLAY HEATED
File:Z061.MDI
Scan:2-20/.1/2/#181, Anode:FE
Zero=0.0
CPS
2-Theta
D=14.7887, I=29.4%
D=9.9179, I=100.5%
D=7.5562, I=17.3%
D=6.5887, I=48.5%

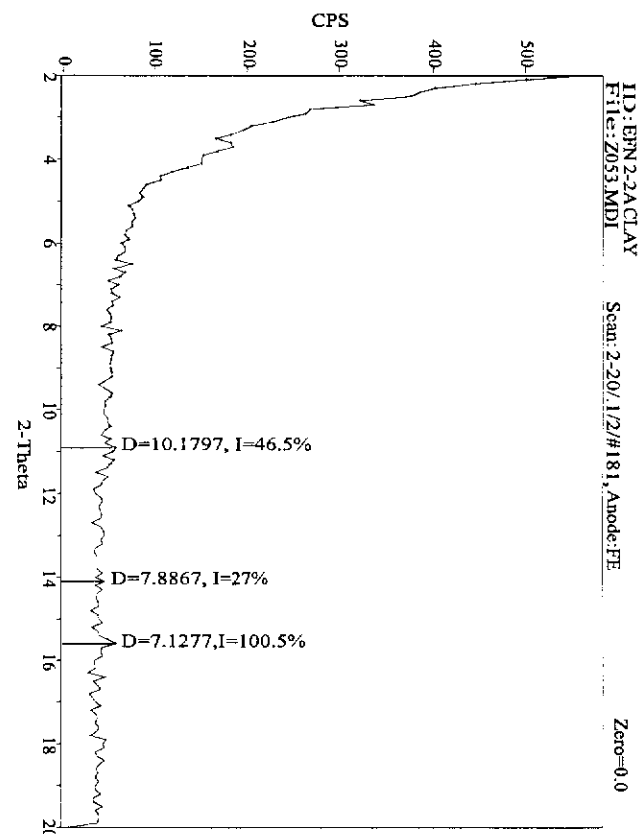
ID:EFN2-2A CLAY
File:Z053.MDI
Scan: 2-20/.1/2/#181,Anode:FE
Zero=0.0
CPS
2-Theta
D=10.1797, I=46.5%
D=7.8867, I=27%
D=7.1277,I=100.5%

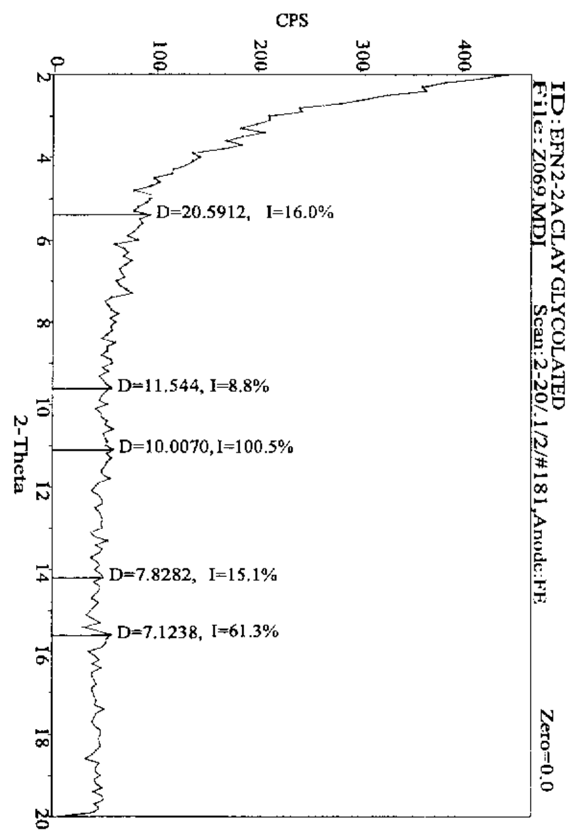
ID:EFN2-2A CLAY GLYCOLATED
File:Z069.MDI
Scan:2-20/.1/2/#181,Anode:FE
Zero=0.0
CPS
2-Theta
D=20.5912, I=16.0%
D=11.544, I=8.8%
D=10.0070,I=100.5%
D=7.8282, I=15.1%
D=7.1238, I=61.3%

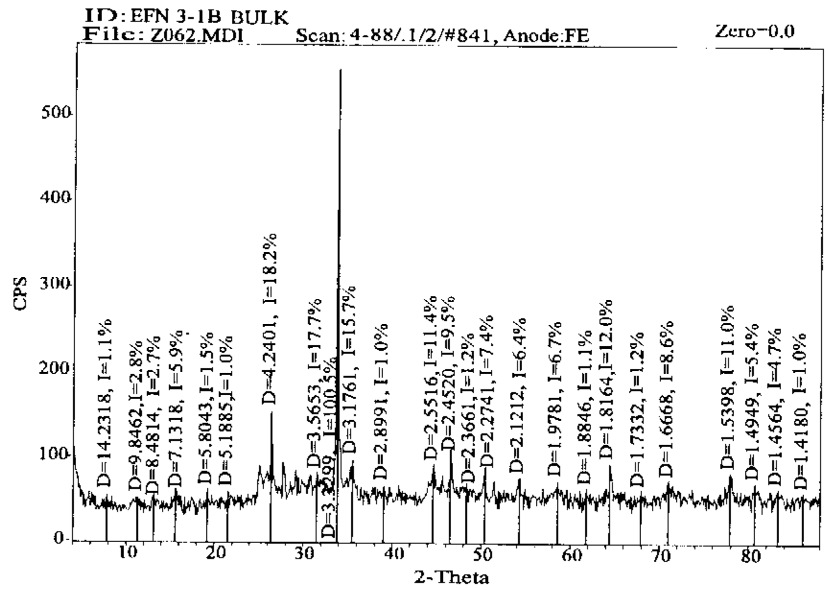
ID: EFN 3-1B BULK
File: Z062.MDI
Scan: 4-88/.1/2/#841, Anode:FE
Zero=0.0
CPS
2-Theta
D=14.2318, I=1.1%
D=9.8462,I=2.8%
D=8.4814, I=2.7%
D=7.1318, I=5.9%
D=5.8043,I=1.5%
D=5.1885,I=1.0%
D=4.2401, I=18.2%
D=3.5653, I=17.7%
D=3.3299, I=100.5%
D=3.1761, I=15.7%
D=2.8991, I=1.0%
D=2.5516,I=11.4%
D=2.4520, I=9.5%
D=2.3661,I=1.2%
D=2.2741, I=7.4%
D=2.1212, I=6.4%
D=1.9781, I=6.7%
D=1.8846, I=1.1%
D=1.8164,I=12.0%
D=1.7332, I=1.2%
D=1.6668, I=8.6%
D=1.5398, I=11.0%
D=1.4949, I=5.4%
D=1.4564, I=4.7%
D=1.4180, I=1.0%

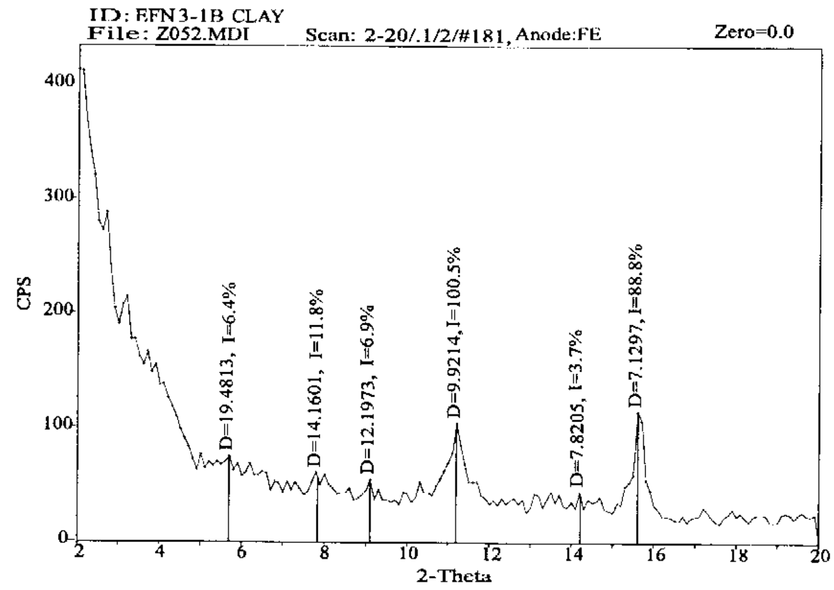
ID: EFN 3-1B CLAY
File: Z052.MDI
Scan: 2-20/.1/2/#181, Anode:FE
Zero=0.0
CPS
2-Theta
D=19.4813, I=6.4%
D=14.1601, I=11.8%
D=12.1973, I=6.9%
D=9.9214,I=100.5%
D=7.8205, I=3.7%
D=7.1297, I=88.8%

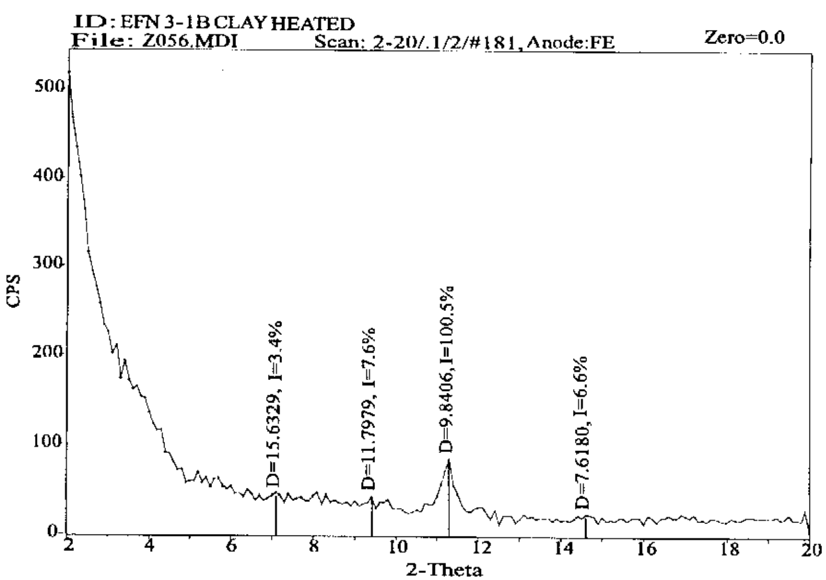
ID: EFN 3-1B CLAY HEATED
File: Z056.MDI
Scan: 2-20/.1/2/#181, Anode:FE
Zero=0.0
CPS
2-Theta
D=15.6329, I=3.4%
D=11.7979, I=7.6%
D=9.8406,I=100.5%
D=7.6180, I=6.6%

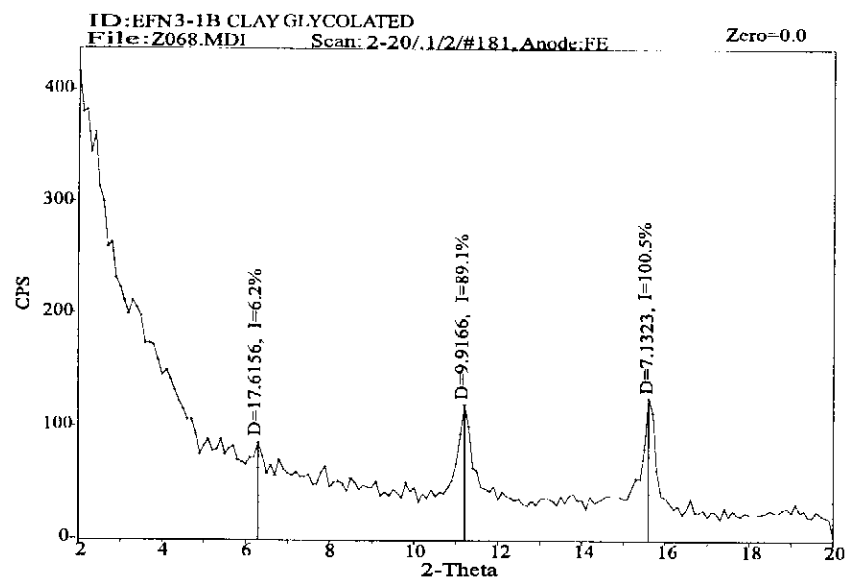
ID:EFN3-1B CLAY GLYCOLATED
File: Z068.MDI
Scan: 2-20/.1/2/#181, Anode:FE
Zero=0.0
CPS
2-Theta
D=17.6156, I=6.2%
D=9.9166, I=89.1%
D=7.1323, I=100.5%

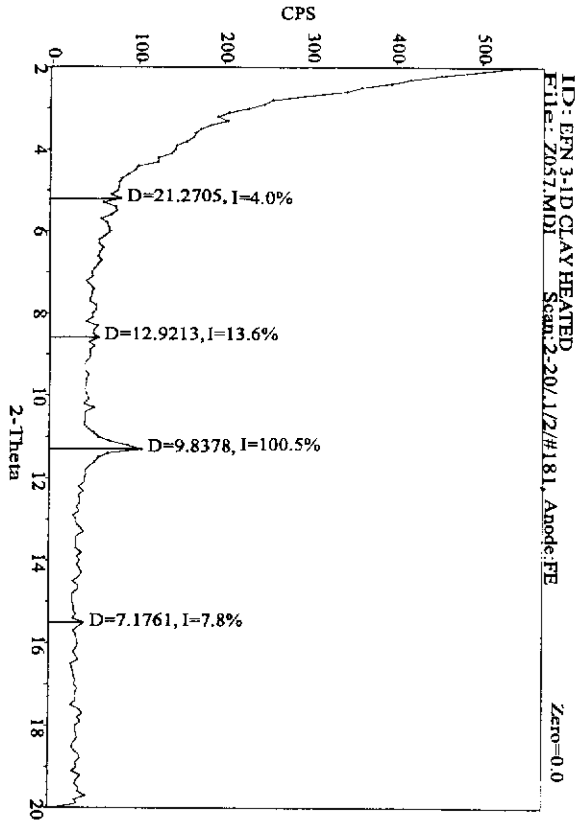
ID: EFN 3-1D CLAY HEATED
File: Z057.MDI
Scan: 2-20/.1/2/#181, Anode:FE
Zero=0.0
CPS
2-Theta
D=21.2705, I=4.0%
D=12.9213, I=13.6%
D=9.8378, I=100.5%
D=7.1761, I=7.8%

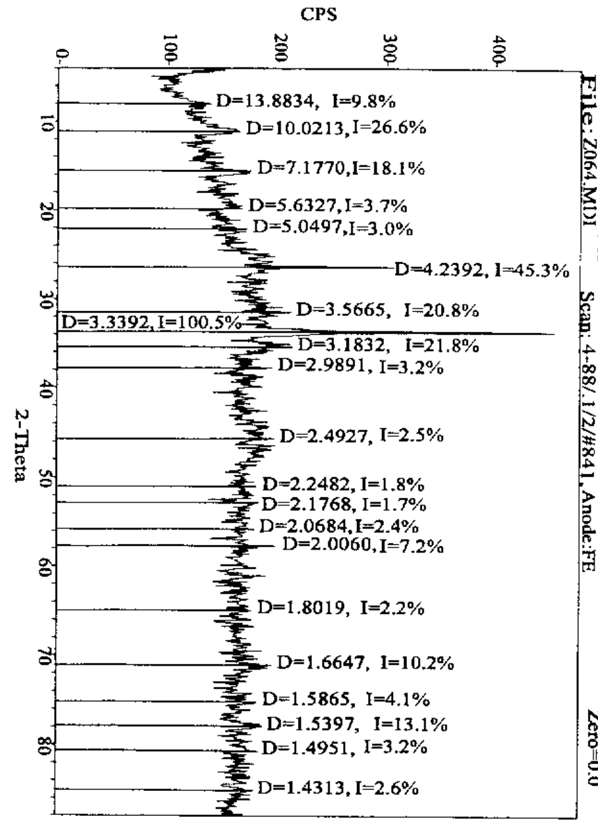
ID: EFN3-1D BULK
File: Z064.MDI
Scan: 4-88/.1/2/#841, Anode:FE
Zero=0.0
CPS
2-Theta
D=13.8834, I=9.8%
D=10.0213, I=26.6%
D=7.1770, I=18.1%
D=5.6327, I=3.7%
D=5.0497, I=3.0%
D=4.2392, I=45.3%
D=3.5665, I=20.8%
D=3.3392, I=100.5%
D=3.1832, I=21.8%
D=2.9891, I=3.2%
D=2.4927, I=2.5%
D=2.2482, I=1.8%
D=2.1768, I=1.7%
D=2.0684, I=2.4%
D=2.0060, I=7.2%
D=1.8019, I=2.2%
D=1.6647, I=10.2%
D=1.5865, I=4.1%
D=1.5397, I=13.1%
D=1.4951, I=3.2%
D=1.4313, I=2.6%

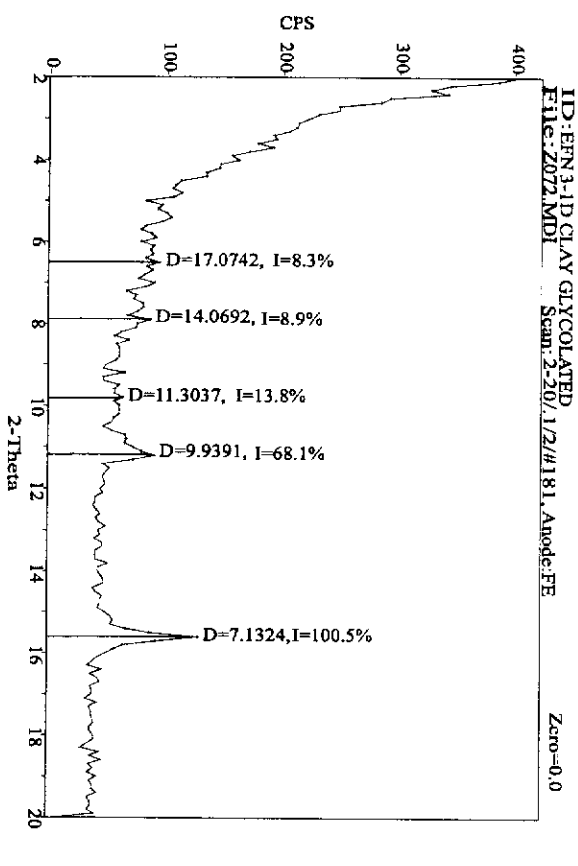
ID: EFN3-1D CLAY GLYCOLATED
File: Z072.MDI
Scan: 2-20/.1/2/#181, Anode:FE
Zero=0.0
CPS
2-Theta
D=17.0742, I=8.3%
D=14.0692, I=8.9%
D=11.3037, I=13.8%
D=9.9391, I=68.1%
D=7.1324, I=100.5%

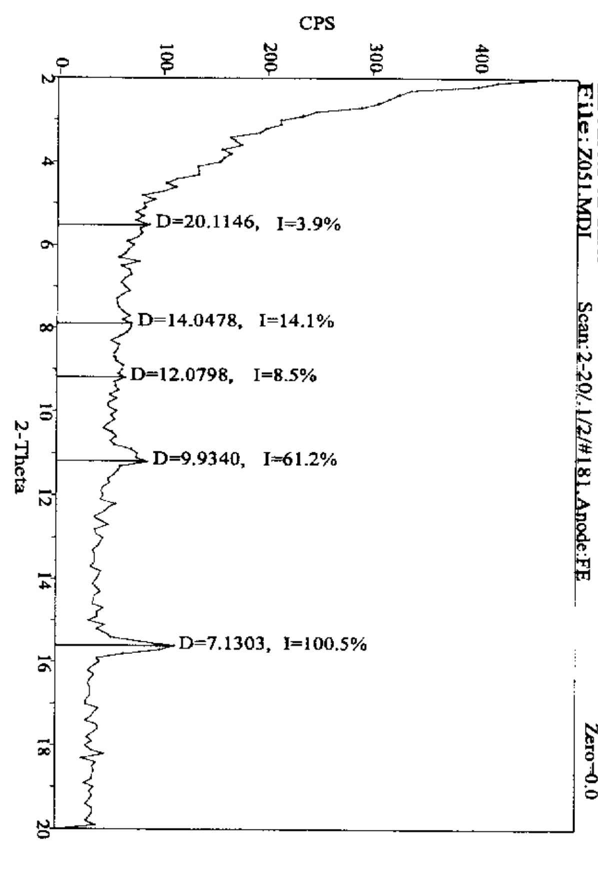
ID: EFN3-1D CLAY
File: Z051.MDI
Scan: 2-20/.1/2/#181, Anode:FE
Zero=0.0
CPS
2-Theta
D=20.1146, I=3.9%
D=14.0478, I=14.1%
D=12.0798, I=8.5%
D=9.9340, I=61.2%
D=7.1303, I=100.5%

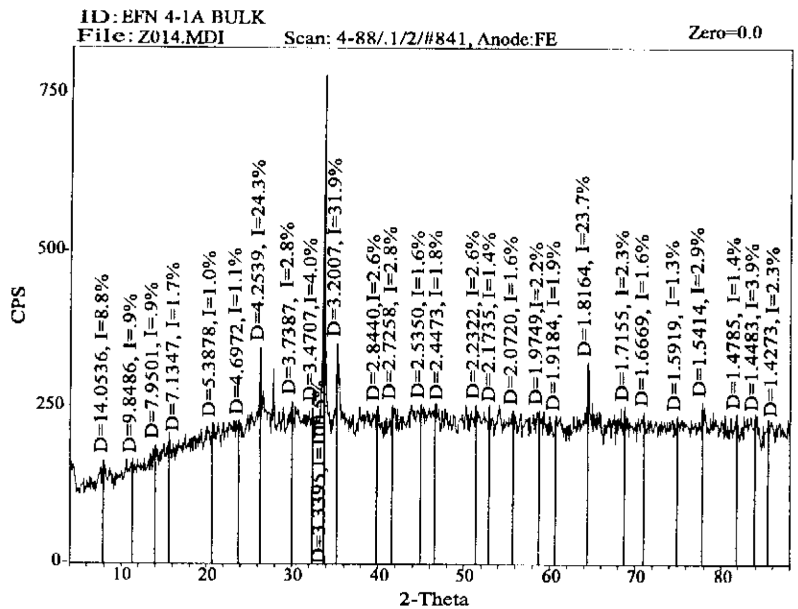
ID: EFN 4-1A BULK
File: Z014.MDI Scan: 4-88/.1/2/#841, Anode:FE
Zero=0.0
CPS
2-Theta
D=14.0536, I=8.8%
D=9.8486, I=.9%
D=7.9501, I=.9%
D=7.1347, I=1.7%
D=5.3878, I=1.0%
D=4.6972, I=1.1%
D=4.2539, I=24.3%
D=3.7387, I=2.8%
D=3.4707, I=4.0%
D=3.2007, I=31.9%
D=2.8440, I=2.6%
D=2.7258, I=2.8%
D=2.5350, I=1.6%
D=2.4473, I=1.8%
D=2.2322, I=2.6%
D=2.1735, I=1.4%
D=2.0720, I=1.6%
D=1.9749, I=2.2%
D=1.9184, I=1.9%
D=1.8164, I=23.7%
D=1.7155, I=2.3%
D=1.6669, I=1.6%
D=1.5919, I=1.3%
D=1.5414, I=2.9%
D=1.4785, I=1.4%
D=1.4483, I=3.9%
D=1.4273, I=2.3%

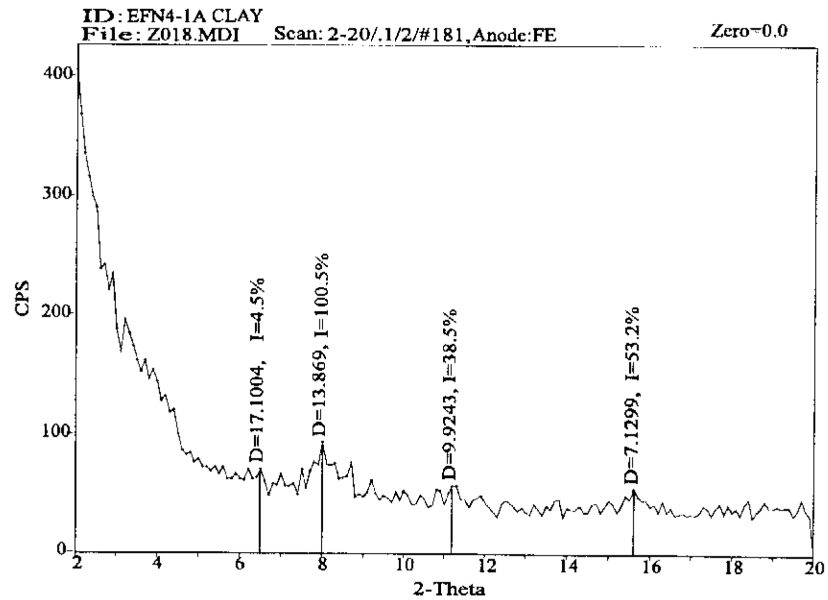
ID: EFN4-1A CLAY
File: Z018.MDI Scan: 2-20/.1/2/#181, Anode:FE
Zero=0.0
CPS
2-Theta
D=17.1004, I=4.5%
D=13.869, I=100.5%
D=9.9243, I=38.5%
D=7.1299, I=53.2%

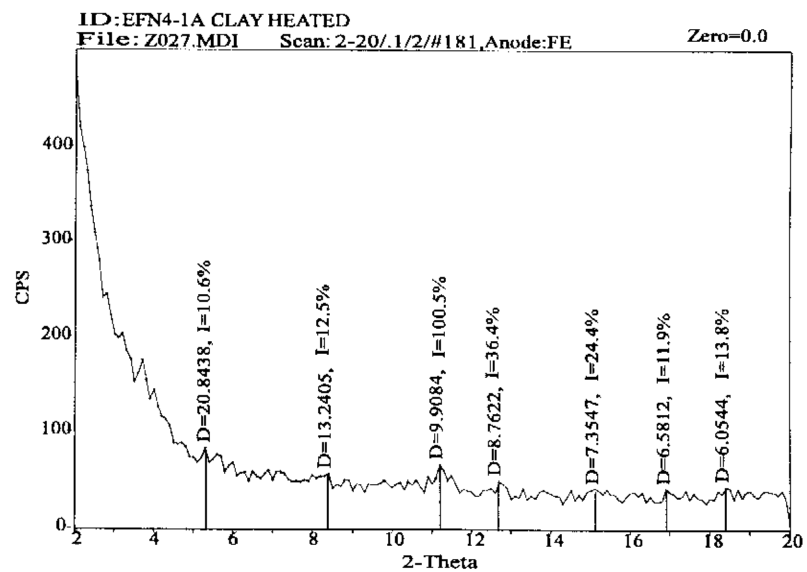
ID: EFN4-1A CLAY HEATED
File: Z027.MDI Scan: 2-20/.1/2/#181, Anode:FE
Zero=0.0
CPS
2-Theta
D=20.8438, I=10.6%
D=13.2405, I=12.5%
D=9.9084, I=100.5%
D=8.7622, I=36.4%
D=7.3547, I=24.4%
D=6.5812, I=11.9%
D=6.0544, I=13.8%

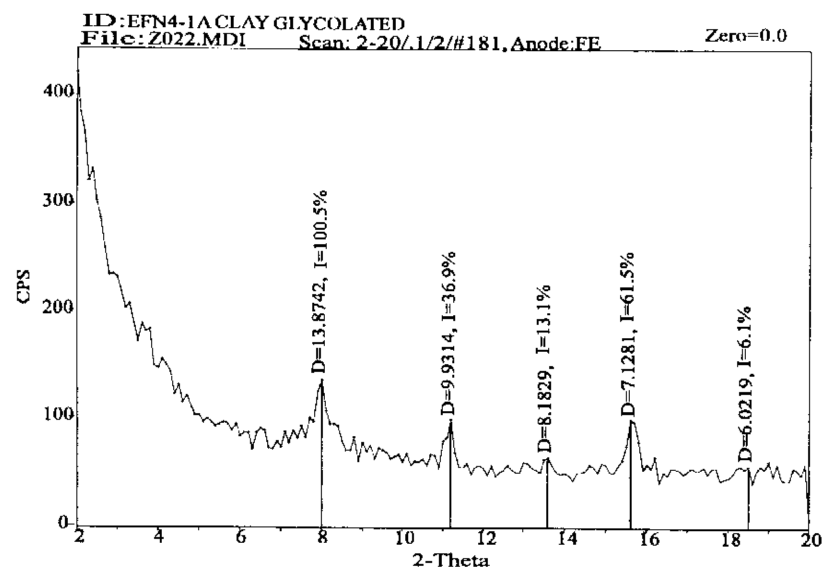
ID: EFN4-1A CLAY GLYCOLATED
File: Z022.MDI Scan: 2-20/.1/2/#181, Anode:FE
Zero=0.0
CPS
2-Theta
D=13.8742, I=100.5%
D=9.9314, I=36.9%
D=8.1829, I=13.1%
D=7.1281, I=61.5%
D=6.0219, I=6.1%

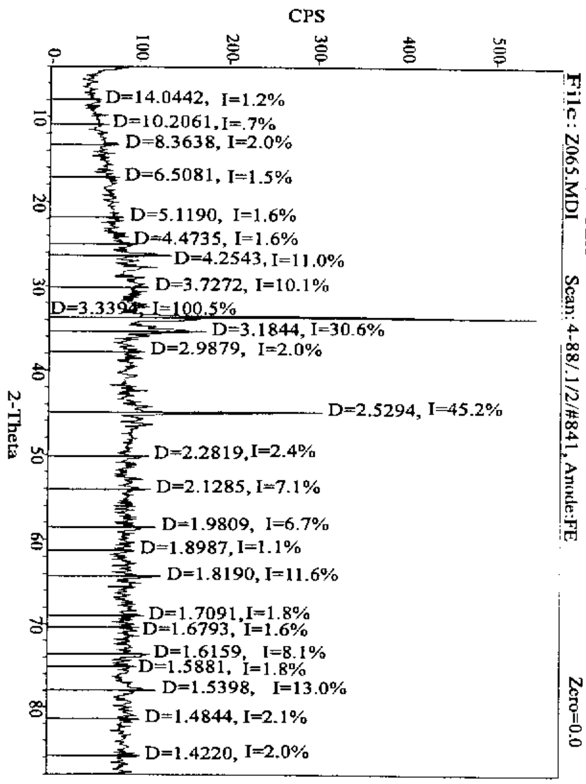
ID: DIS1-2C BULK
File: Z065.MDI
Scan: 4-88/.1/2/#841, Anode:FE
Zero=0.0
CPS
2-Theta
D=14.0442, I=1.2%
D=10.2061, I=.7%
D=8.3638, I=2.0%
D=6.5081, I=1.5%
D=5.1190, I=1.6%
D=4.4735, I=1.6%
D=4.2543, I=11.0%
D=3.7272, I=10.1%
D=3.3394, I=100.5%
D=3.1844, I=30.6%
D=2.9879, I=2.0%
D=2.5294, I=45.2%
D=2.2819, I=2.4%
D=2.1285, I=7.1%
D=1.9809, I=6.7%
D=1.8987, I=1.1%
D=1.8190, I=11.6%
D=1.7091, I=1.8%
D=1.6793, I=1.6%
D=1.6159, I=8.1%
D=1.5881, I=1.8%
D=1.5398, I=13.0%
D=1.4844, I=2.1%
D=1.4220, I=2.0%

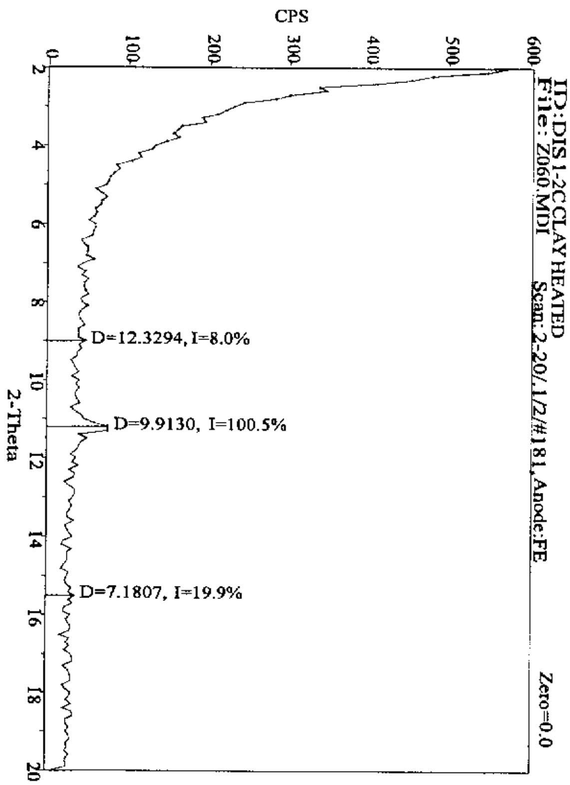
ID:DIS1-2CCLAY HEATED
File: Z060.MDI
Scan: 2-20/.1/2/#181, Anode:FE
Zero=0.0
CPS
2-Theta
D=12.3294, I=8.0%
D=9.9130, I=100.5%
D=7.1807, I=19.9%

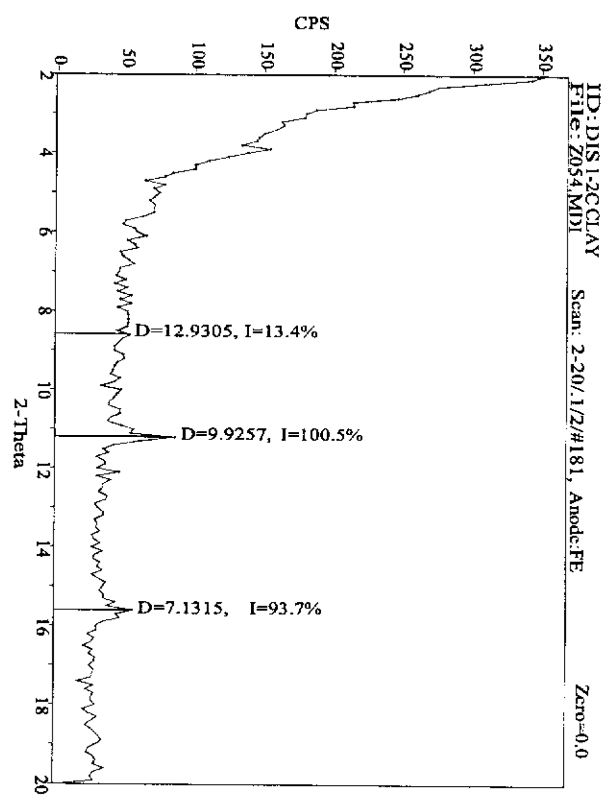
ID:DIS1-2CCLAY
File: Z054.MDI
Scan: 2-20/.1/2/#181, Anode:FE
Zero=0.0
CPS
2-Theta
D=12.9305, I=13.4%
D=9.9257, I=100.5%
D=7.1315, I=93.7%

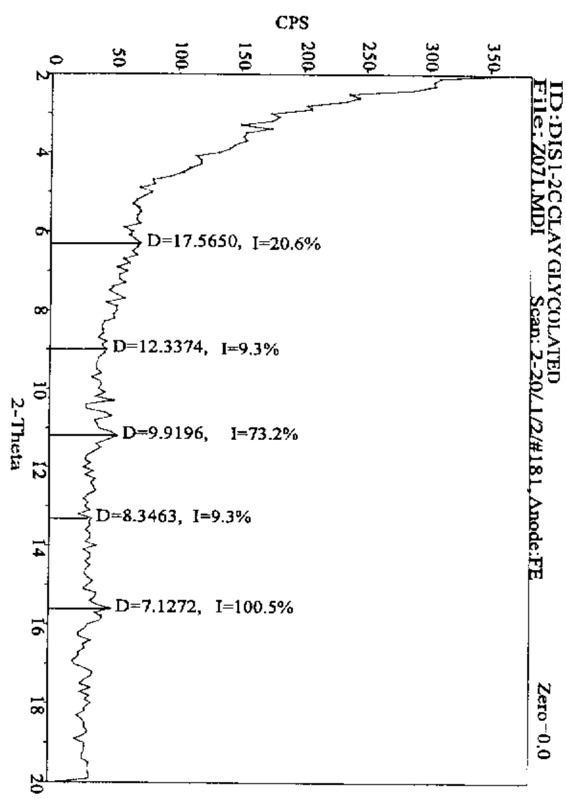
ID:DIS1-2CCLAY GLYCOLATED
File: Z071.MDI
Scan: 2-20/.1/2/#181, Anode:FE
Zero=0.0
CPS
2-Theta
D=17.5650, I=20.6%
D=12.3374, I=9.3%
D=9.9196, I=73.2%
D=8.3463, I=9.3%
D=7.1272, I=100.5%

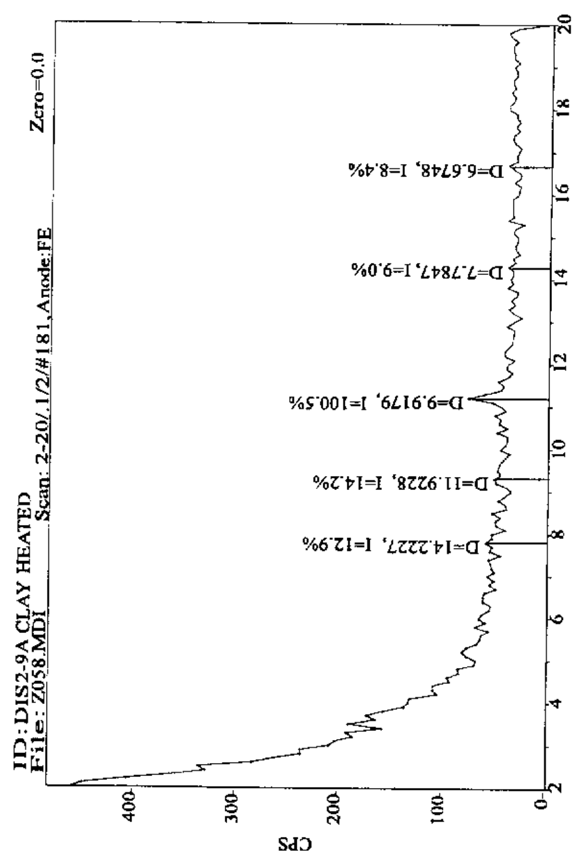
ID:DIS2-9A CLAY HEATED
File: Z058.MDI
Scan: 2-20/.1/2/#181, Anode:FE
Zero=0.0
D=14.2227, I=12.9%
D=11.9228, I=14.2%
D=9.9179, I=100.5%
D=7.7847, I=9.0%
D=6.6748, I=8.4%
CPS
2-Theta

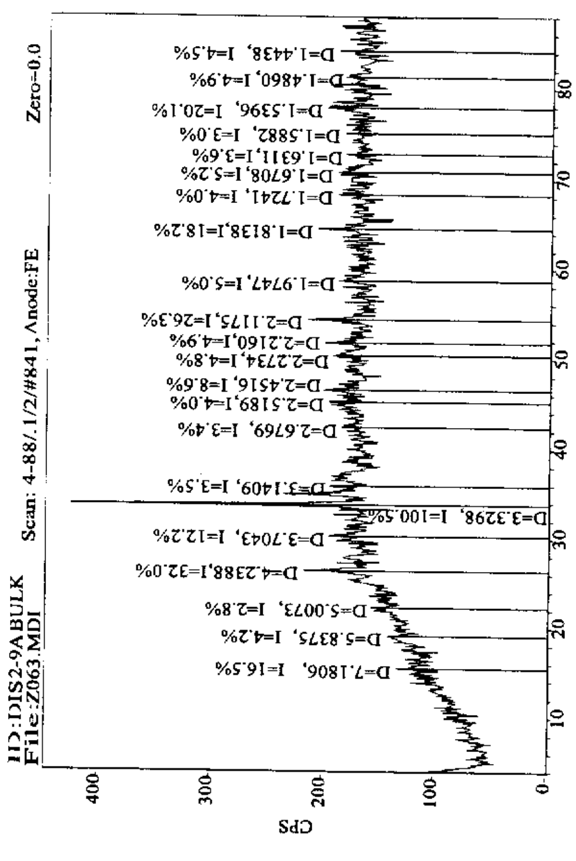
ID:DIS2-9ABULK
File:Z063.MDI
Scan: 4-88/.1/2/#841, Anode:FE
Zero=0.0
D=7.1806, I=16.5%
D=5.8375, I=4.2%
D=5.0073, I=2.8%
D=4.2388,I=32.0%
D=3.7043, I=12.2%
D=3.3298, I=100.5%
D=3.1409, I=3.5%
D=2.6769, I=3.4%
D=2.5189,I=4.0%
D=2.4516, I=8.6%
D=2.2734, I=4.8%
D=2.2160,I=4.9%
D=2.1175,I=26.3%
D=1.9747,I=5.0%
D=1.8138,I=18.2%
D=1.7241, I=4.0%
D=1.6708,I=5.2%
D=1.6311,I=3.6%
D=1.5882, I=3.0%
D=1.5396, I=20.1%
D=1.4860,I=4.9%
D=1.4438, I=4.5%
CPS
2-Theta

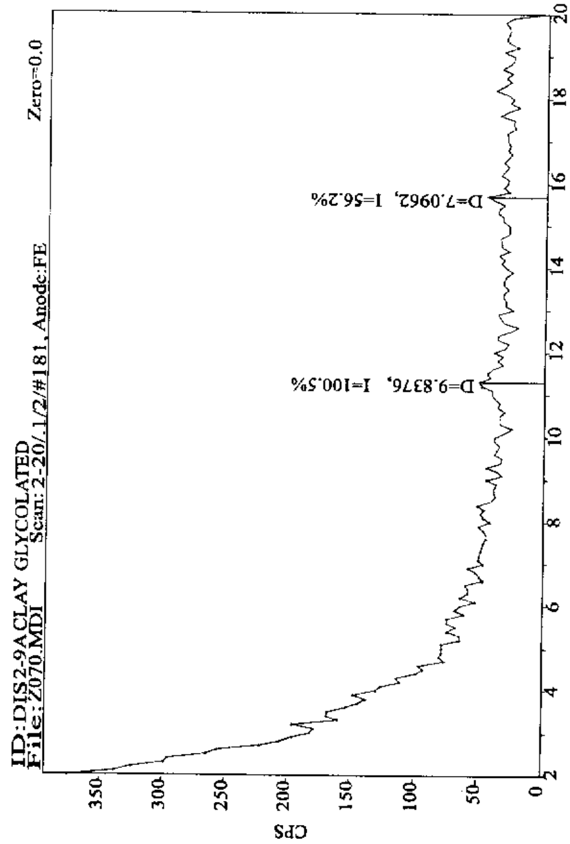
ID:DIS2-9ACLAY GLYCOLATED
File: Z070.MDI
Scan: 2-20/.1/2/#181, Anode:FE
Zero=0.0
D=9.8376, I=100.5%
D=7.0962, I=56.2%
CPS
2-Theta

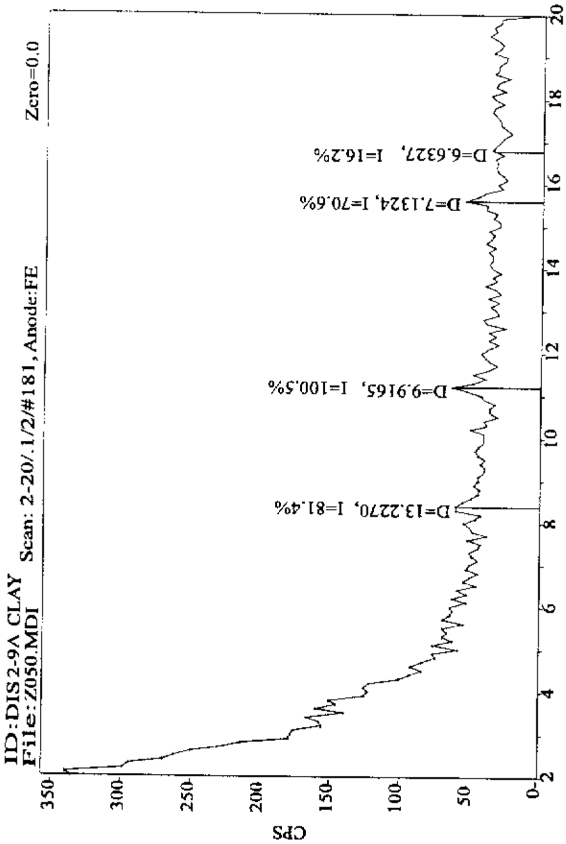
ID:DIS2-9A CLAY
File:Z050.MDI
Scan: 2-20/.1/2/#181, Anode:FE
Zero=0.0
D=13.2270, I=81.4%
D=9.9165, I=100.5%
D=7.1324, I=70.6%
D=6.6327, I=16.2%
CPS
2-Theta

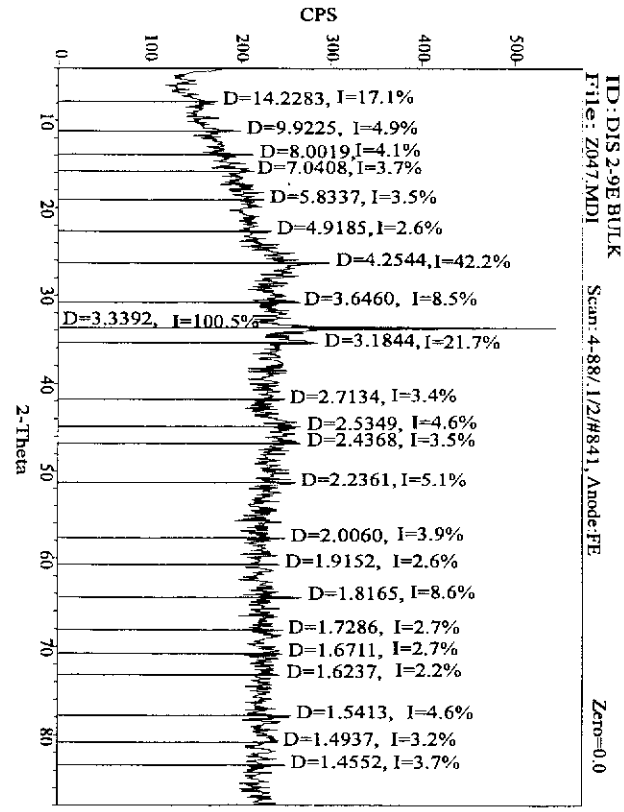
ID: DIS 2-9E BULK
File: Z047.MDI
Scan: 4-88/.1/2/#841, Anode:FE
Zero=0.0
CPS
0
100
200
300
400
500
2-Theta
10
20
30
40
50
60
70
80
D=14.2283, I=17.1%
D=9.9225, I=4.9%
D=8.0019, I=4.1%
D=7.0408, I=3.7%
D=5.8337, I=3.5%
D=4.9185, I=2.6%
D=4.2544, I=42.2%
D=3.6460, I=8.5%
D=3.3392, I=100.5%
D=3.1844, I=21.7%
D=2.7134, I=3.4%
D=2.5349, I=4.6%
D=2.4368, I=3.5%
D=2.2361, I=5.1%
D=2.0060, I=3.9%
D=1.9152, I=2.6%
D=1.8165, I=8.6%
D=1.7286, I=2.7%
D=1.6711, I=2.7%
D=1.6237, I=2.2%
D=1.5413, I=4.6%
D=1.4937, I=3.2%
D=1.4552, I=3.7%

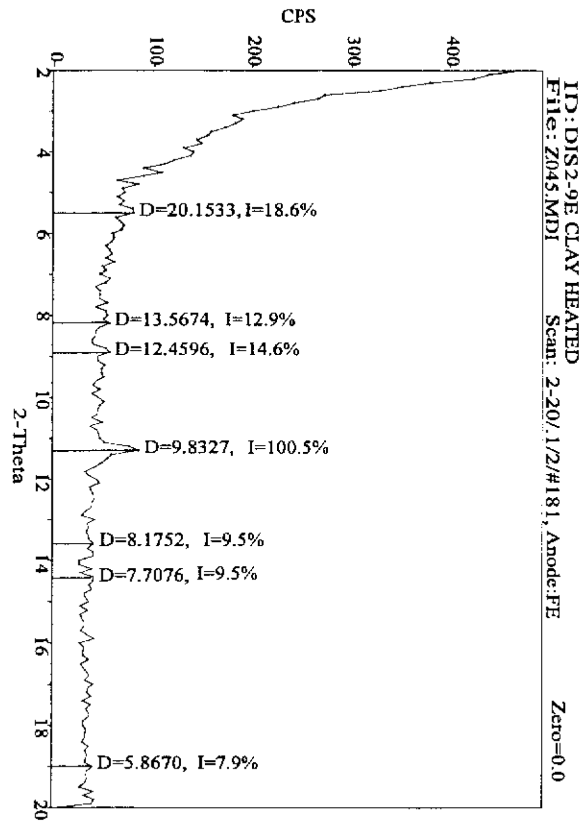
ID: DIS 2-9E CLAY HEATED
File: Z045.MDI
Scan: 2-20/.1/2/#181, Anode:FE
Zero=0.0
CPS
0
100
200
300
400
2-Theta
2
4
6
8
10
12
14
16
18
20
D=20.1533, I=18.6%
D=13.5674, I=12.9%
D=12.4596, I=14.6%
D=9.8327, I=100.5%
D=8.1752, I=9.5%
D=7.7076, I=9.5%
D=5.8670, I=7.9%

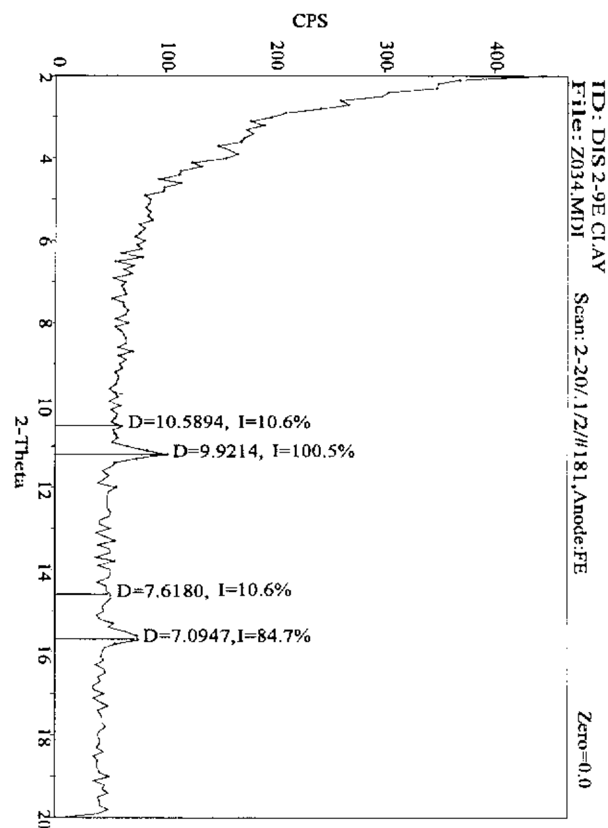
ID: DIS 2-9E CLAY
File: Z034.MDI
Scan: 2-20/.1/2/#181, Anode:FE
Zero=0.0
CPS
0
100
200
300
400
2-Theta
2
4
6
8
10
12
14
16
18
20
D=10.5894, I=10.6%
D=9.9214, I=100.5%
D=7.6180, I=10.6%
D=7.0947, I=84.7%

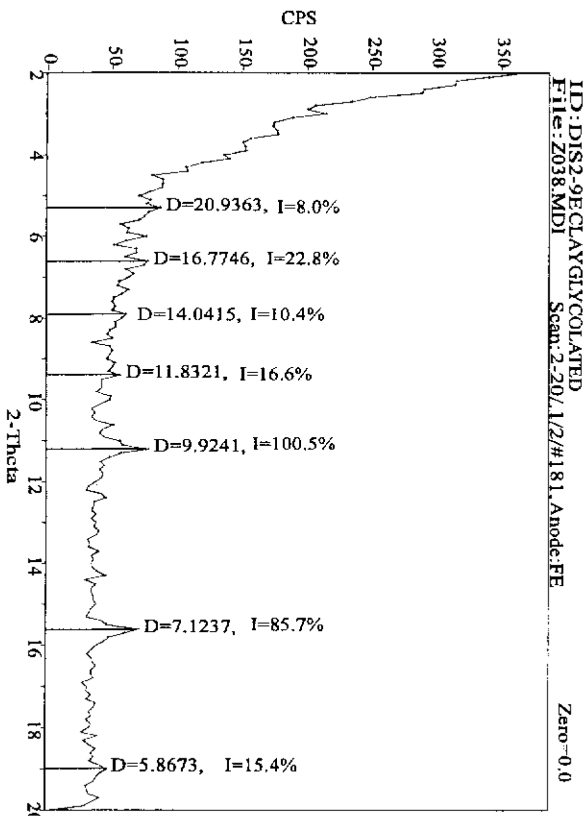
ID: DIS2-9ECLAYGLYCOLATED
File: Z038.MDI
Scan: 2-20/.1/2/#181, Anode:FE
Zero=0.0
CPS
0
50
100
150
200
250
300
350
2-Theta
2
4
6
8
10
12
14
16
18
20
D=20.9363, I=8.0%
D=16.7746, I=22.8%
D=14.0415, I=10.4%
D=11.8321, I=16.6%
D=9.9241, I=100.5%
D=7.1237, I=85.7%
D=5.8673, I=15.4%

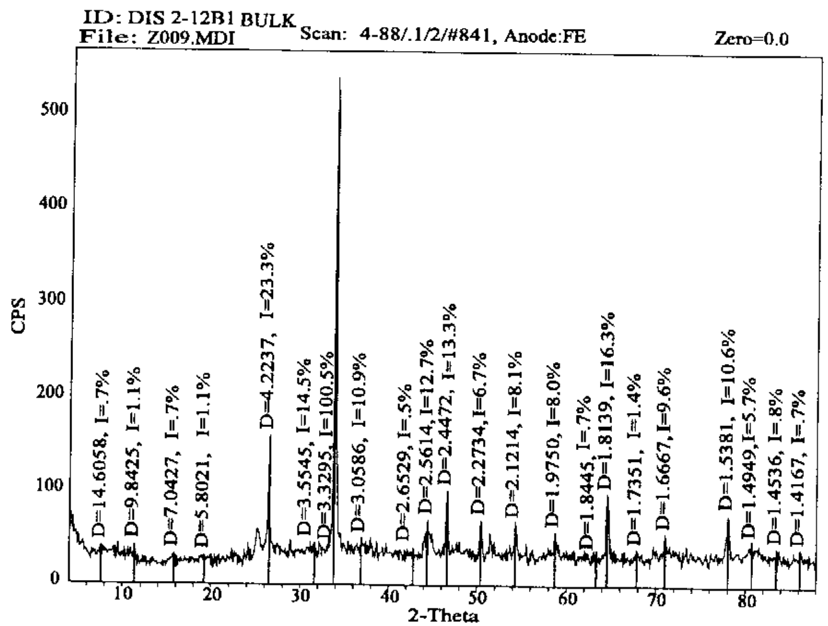
ID: DIS 2-12B1 BULK
File: Z009.MDI
Scan: 4-88/.1/2/#841, Anode:FE
Zero=0.0
CPS
2-Theta
D=14.6058, I=.7%
D=9.8425, I=1.1%
D=7.0427, I=.7%
D=5.8021, I=1.1%
D=4.2237, I=23.3%
D=3.5545, I=14.5%
D=3.3295, I=100.5%
D=3.0586, I=10.9%
D=2.6529, I=.5%
D=2.5614, I=12.7%
D=2.4472, I=13.3%
D=2.2734, I=6.7%
D=2.1214, I=8.1%
D=1.9750, I=8.0%
D=1.8445, I=.7%
D=1.8139, I=16.3%
D=1.7351, I=1.4%
D=1.6667, I=9.6%
D=1.5381, I=10.6%
D=1.4949, I=5.7%
D=1.4536, I=.8%
D=1.4167, I=.7%

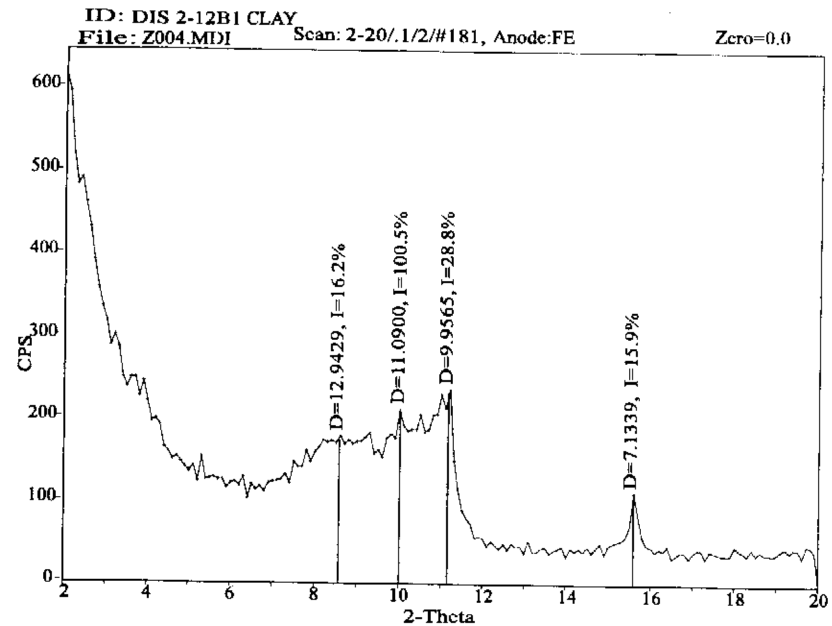
ID: DIS 2-12B1 CLAY
File: Z004.MDI
Scan: 2-20/.1/2/#181, Anode:FE
Zero=0.0
CPS
2-Theta
D=12.9429, I=16.2%
D=11.0900, I=100.5%
D=9.9565, I=28.8%
D=7.1339, I=15.9%

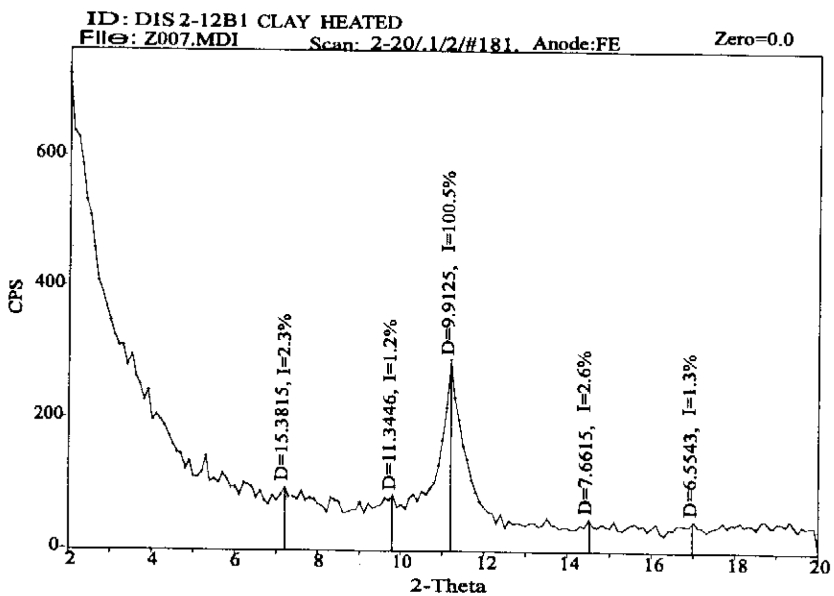
ID: DIS 2-12B1 CLAY HEATED
File: Z007.MDI
Scan: 2-20/.1/2/#181, Anode:FE
Zero=0.0
CPS
2-Theta
D=15.3815, I=2.3%
D=11.3446, I=1.2%
D=9.9125, I=100.5%
D=7.6615, I=2.6%
D=6.5543, I=1.3%

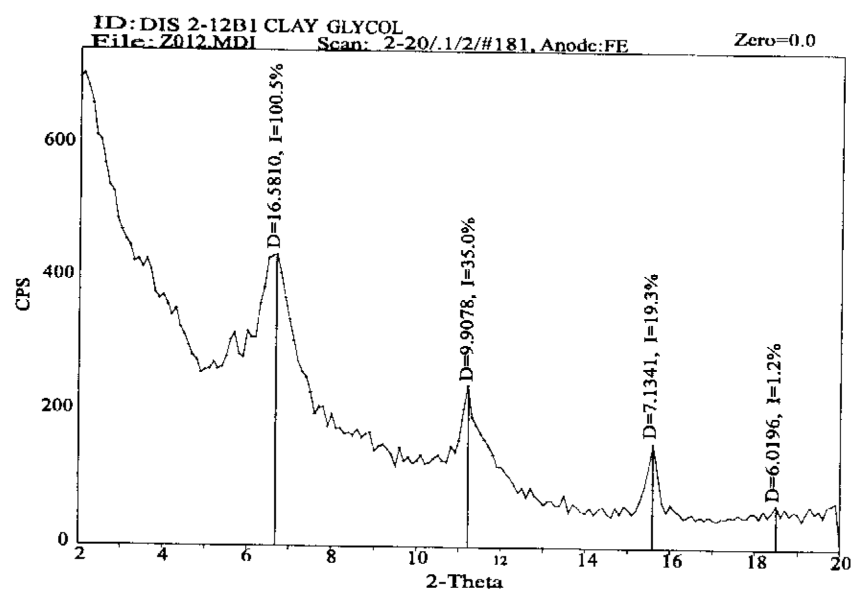
ID: DIS 2-12B1 CLAY GLYCOL
File: Z012.MDI
Scan: 2-20/.1/2/#181, Anode:FE
Zero=0.0
CPS
2-Theta
D=16.5810, I=100.5%
D=9.9078, I=35.0%
D=7.1341, I=19.3%
D=6.0196, I=1.2%

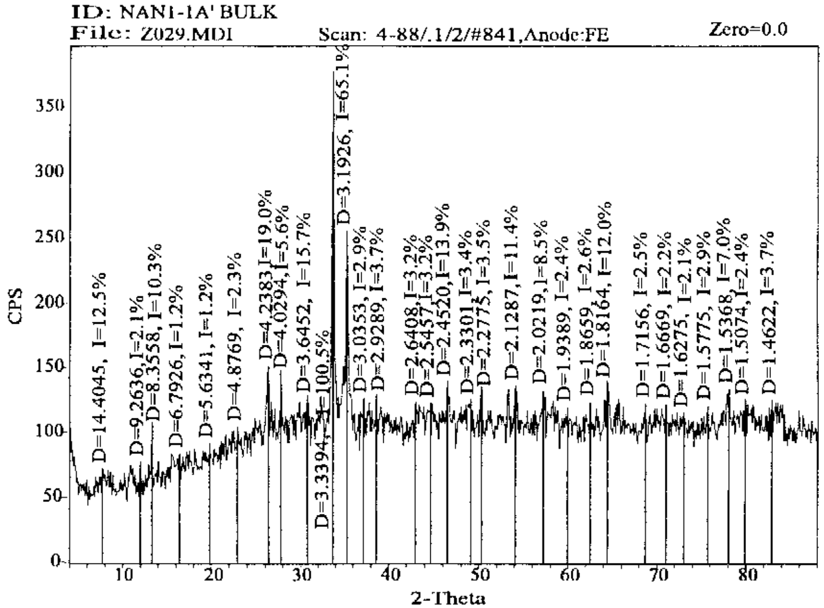
ID: NAN1-1A' BULK
File: Z029.MDI
Scan: 4-88/.1/2/#841,Anode:FE
Zero=0.0
D=14.4045, I=12.5%
D=9.2636,I=2.1%
D=8.3558, I=10.3%
D=6.7926, I=1.2%
D=5.6341, I=1.2%
D=4.8769, I=2.3%
D=4.2383,I=19.0%
D=4.0294,I=5.6%
D=3.6452, I=15.7%
D=3.3394, I=100.5%
D=3.1926, I=65.1%
D=3.0353, I=2.9%
D=2.9289, I=3.7%
D=2.6408,I=3.2%
D=2.5457,I=3.2%
D=2.4520,I=13.9%
D=2.3301,I=3.4%
D=2.2775, I=3.5%
D=2.1287,I=11.4%
D=2.0219,I=8.5%
D=1.9389, I=2.4%
D=1.8659, I=2.6%
D=1.8164, I=12.0%
D=1.7156, I=2.5%
D=1.6669, I=2.2%
D=1.6275, I=2.1%
D=1.5775, I=2.9%
D=1.5368, I=7.0%
D=1.5074, I=2.4%
D=1.4622, I=3.7%
CPS
2-Theta

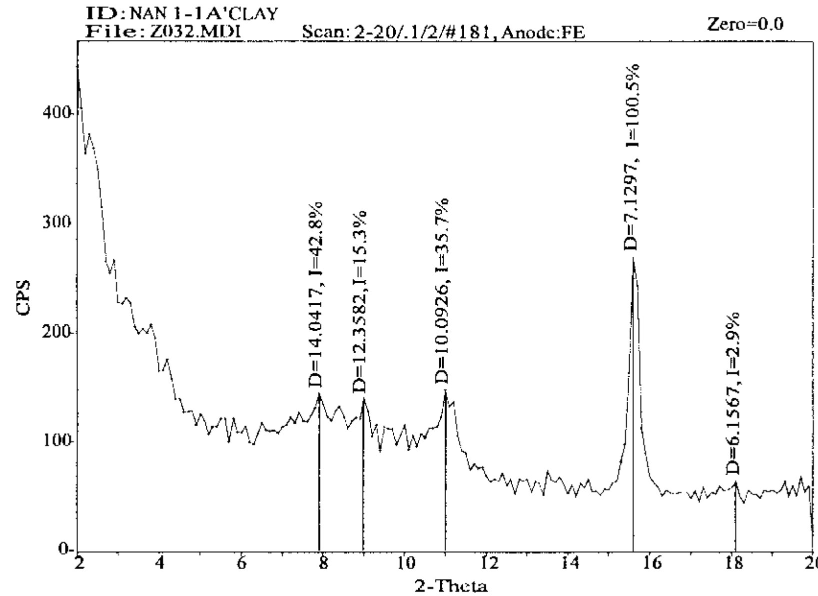
ID: NAN 1-1A'CLAY
File: Z032.MDI
Scan: 2-20/.1/2/#181, Anode:FE
Zero=0.0
D=14.0417, I=42.8%
D=12.3582, I=15.3%
D=10.0926, I=35.7%
D=7.1297, I=100.5%
D=6.1567, I=2.9%
CPS
2-Theta

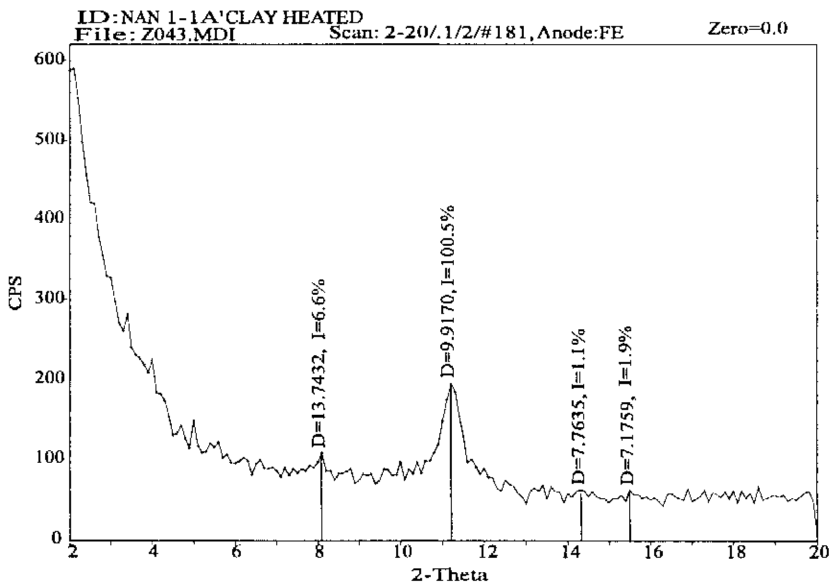
ID: NAN 1-1A'CLAY HEATED
File: Z043.MDI
Scan: 2-20/.1/2/#181, Anode:FE
Zero=0.0
D=13.7432, I=6.6%
D=9.9170, I=100.5%
D=7.7635, I=1.1%
D=7.1759, I=1.9%
CPS
2-Theta

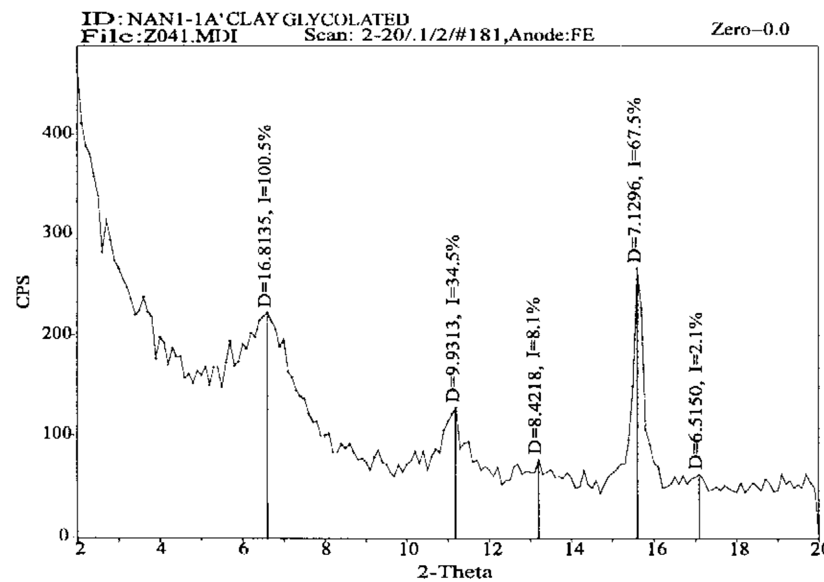
ID: NAN1-1A'CLAY GLYCOLATED
File: Z041.MDI
Scan: 2-20/.1/2/#181, Anode:FE
Zero=0.0
D=16.8135, I=100.5%
D=9.9313, I=34.5%
D=8.4218, I=8.1%
D=7.1296, I=67.5%
D=6.5150, I=2.1%
CPS
2-Theta

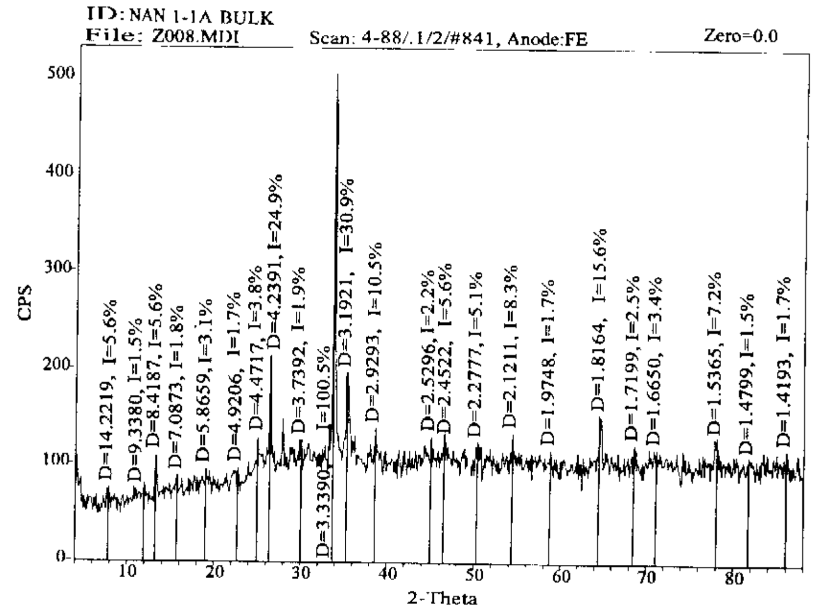
ID: NAN 1-1A BULK
File: Z008.MDI
Scan: 4-88/.1/2/#841, Anode:FE
Zero=0.0
CPS
2-Theta
D=14.2219, I=5.6%
D=9.3380, I=1.5%
D=8.4187, I=5.6%
D=7.0873, I=1.8%
D=5.8659, I=3.1%
D=4.9206, I=1.7%
D=4.4717, I=3.8%
D=4.2391, I=24.9%
D=3.7392, I=1.9%
D=3.3390, I=100.5%
D=3.1921, I=30.9%
D=2.9293, I=10.5%
D=2.5296, I=2.2%
D=2.4522, I=5.6%
D=2.2777, I=5.1%
D=2.1211, I=8.3%
D=1.9748, I=1.7%
D=1.8164, I=15.6%
D=1.7199, I=2.5%
D=1.6650, I=3.4%
D=1.5365, I=7.2%
D=1.4799, I=1.5%
D=1.4193, I=1.7%

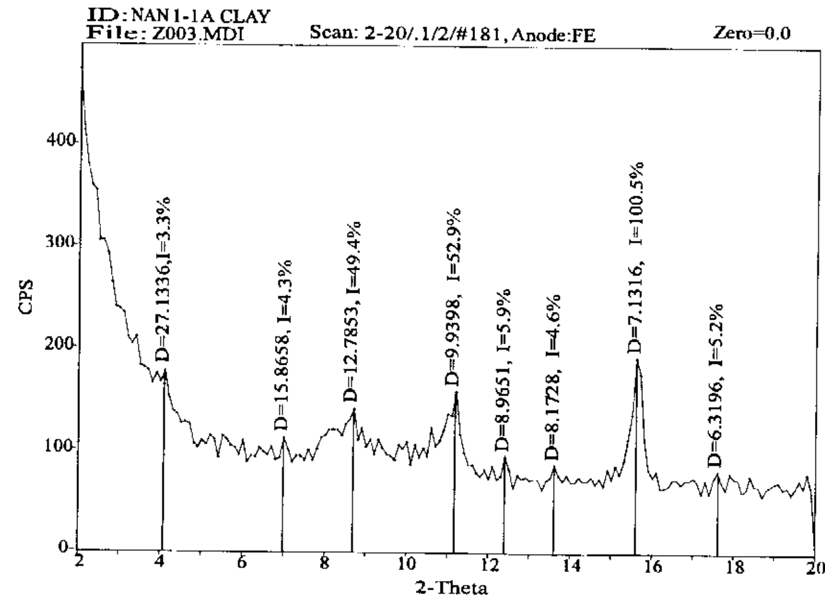
ID: NAN 1-1A CLAY
File: Z003.MDI
Scan: 2-20/.1/2/#181, Anode:FE
Zero=0.0
CPS
2-Theta
D=27.1336, I=3.3%
D=15.8658, I=4.3%
D=12.7853, I=49.4%
D=9.9398, I=52.9%
D=8.9651, I=5.9%
D=8.1728, I=4.6%
D=7.1316, I=100.5%
D=6.3196, I=5.2%

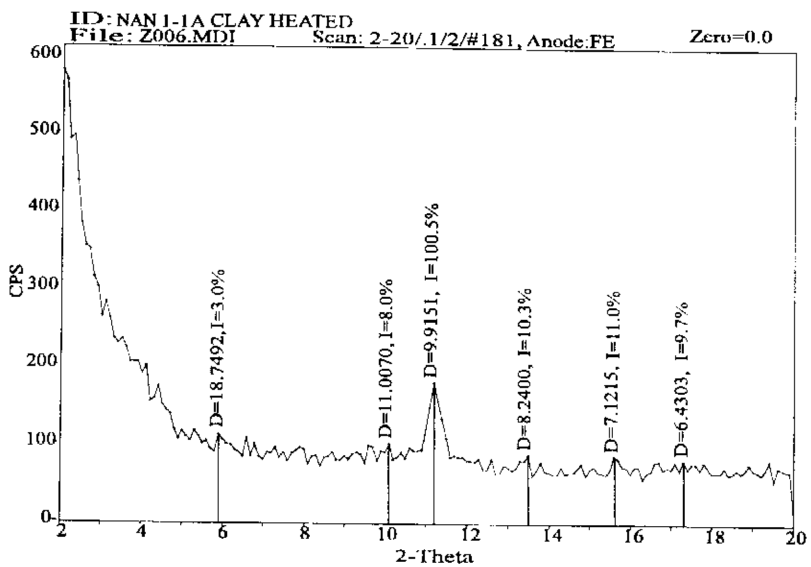
ID: NAN 1-1A CLAY HEATED
File: Z006.MDI
Scan: 2-20/.1/2/#181, Anode:FE
Zero=0.0
CPS
2-Theta
D=18.7492, I=3.0%
D=11.0070, I=8.0%
D=9.9151, I=100.5%
D=8.2400, I=10.3%
D=7.1215, I=11.0%
D=6.4303, I=9.7%

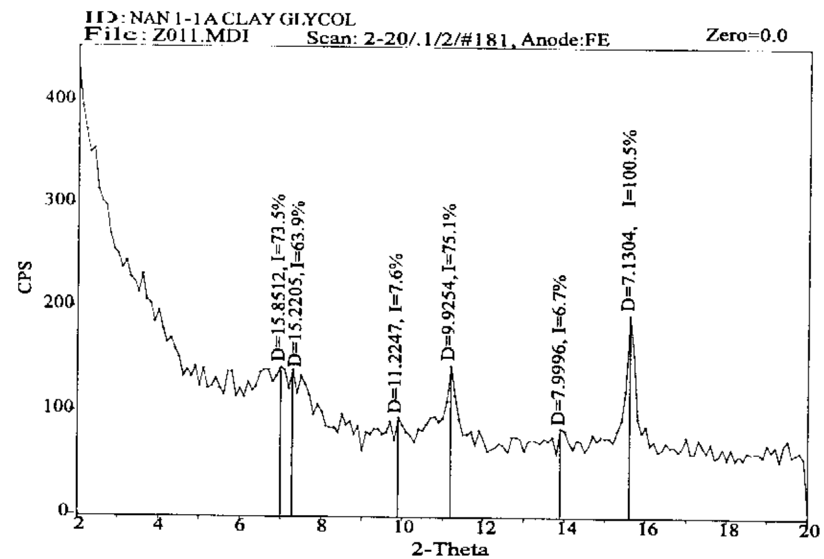
ID: NAN 1-1A CLAY GLYCOL
File: Z011.MDI
Scan: 2-20/.1/2/#181, Anode:FE
Zero=0.0
CPS
2-Theta
D=15.8512, I=73.5%
D=15.2205, I=63.9%
D=11.2247, I=7.6%
D=9.9254, I=75.1%
D=7.9996, I=6.7%
D=7.1304, I=100.5%

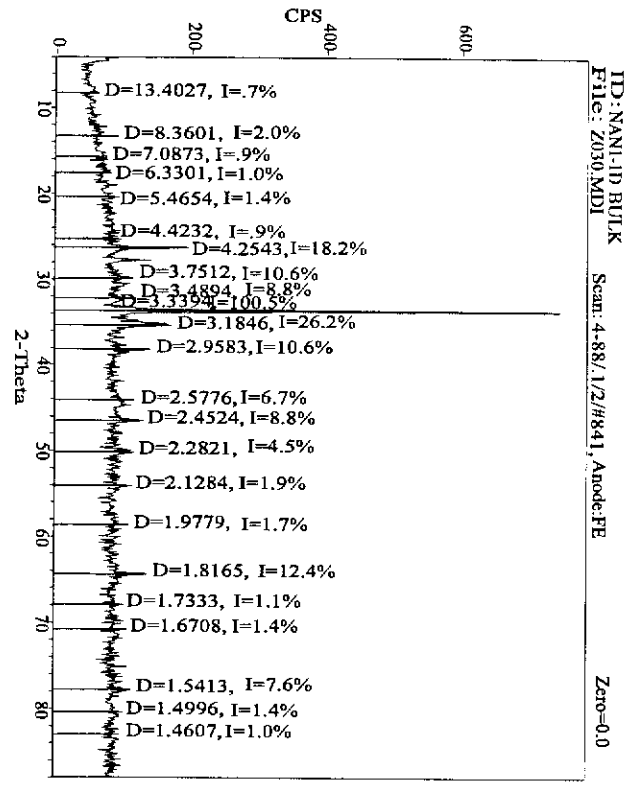
ID:NAN1-1D BULK
File: Z030.MDI
Scan: 4-88/.1/2/#841, Anode:FE
Zero=0.0
CPS
0
200
400
600
2-Theta
10
20
30
40
50
60
70
80
D=13.4027, I=.7%
D=8.3601, I=2.0%
D=7.0873, I=.9%
D=6.3301, I=1.0%
D=5.4654, I=1.4%
D=4.4232, I=.9%
D=4.2543, I=18.2%
D=3.7512, I=10.6%
D=3.4894, I=8.8%
D=3.3394, I=100.5%
D=3.1846, I=26.2%
D=2.9583, I=10.6%
D=2.5776, I=6.7%
D=2.4524, I=8.8%
D=2.2821, I=4.5%
D=2.1284, I=1.9%
D=1.9779, I=1.7%
D=1.8165, I=12.4%
D=1.7333, I=1.1%
D=1.6708, I=1.4%
D=1.5413, I=7.6%
D=1.4996, I=1.4%
D=1.4607, I=1.0%

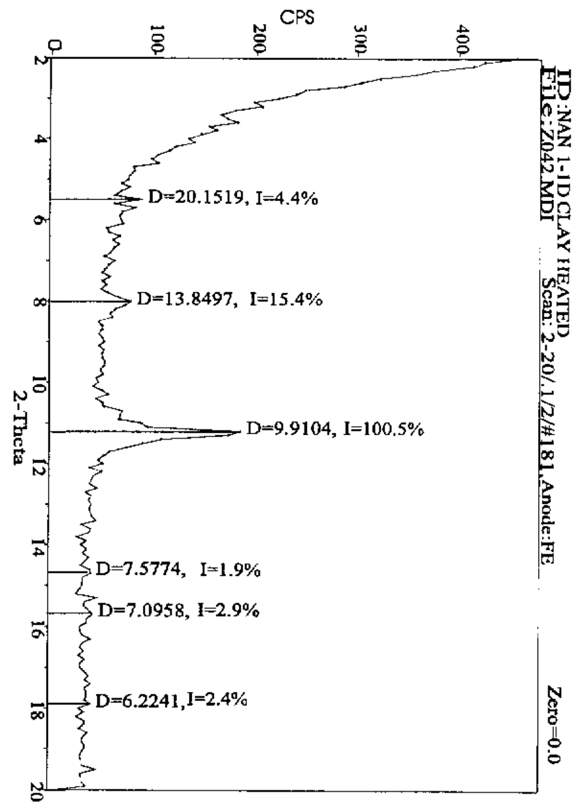
ID:NAN 1-1D CLAY HEATED
File:Z042.MDI
Scan: 2-20/.1/2/#181, Anode:FE
Zero=0.0
CPS
0
100
200
300
400
2-Theta
2
4
6
8
10
12
14
16
18
20
D=20.1519, I=4.4%
D=13.8497, I=15.4%
D=9.9104, I=100.5%
D=7.5774, I=1.9%
D=7.0958, I=2.9%
D=6.2241, I=2.4%

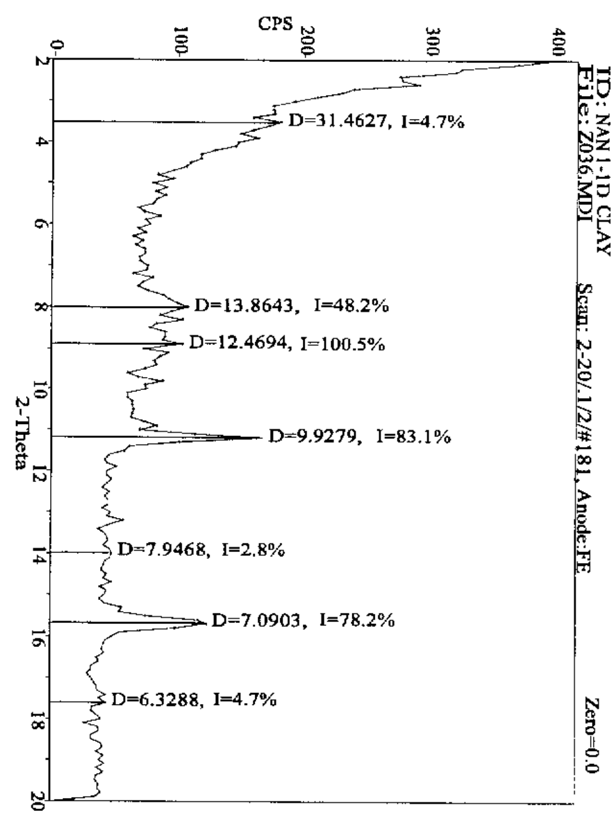
ID: NAN 1-1D CLAY
File: Z036.MDI
Scan: 2-20/.1/2/#181, Anode:FE
Zero=0.0
CPS
0
100
200
300
400
2-Theta
2
4
6
8
10
12
14
16
18
20
D=31.4627, I=4.7%
D=13.8643, I=48.2%
D=12.4694, I=100.5%
D=9.9279, I=83.1%
D=7.9468, I=2.8%
D=7.0903, I=78.2%
D=6.3288, I=4.7%

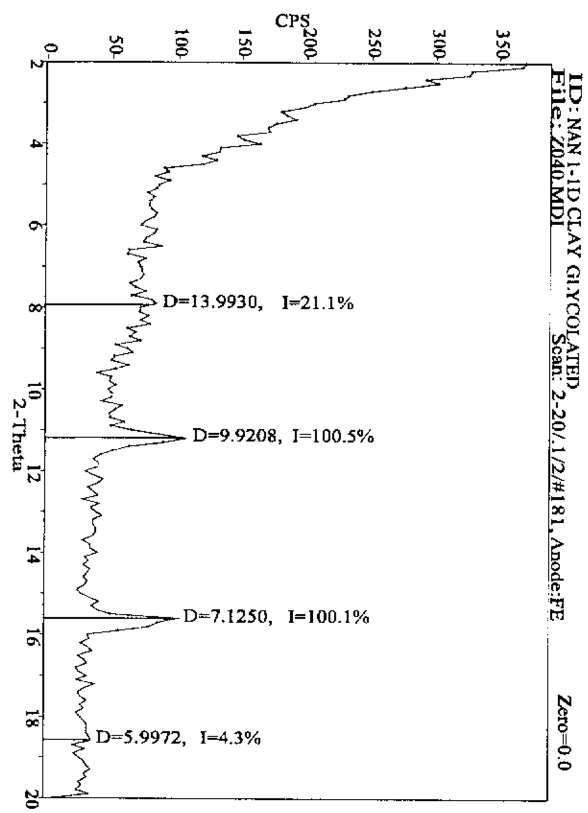
ID: NAN 1-1D CLAY GLYCOLATED
File: Z040.MDI
Scan: 2-20/.1/2/#181, Anode:FE
Zero=0.0
CPS
0
50
100
150
200
250
300
350
2-Theta
2
4
6
8
10
12
14
16
18
20
D=13.9930, I=21.1%
D=9.9208, I=100.5%
D=7.1250, I=100.1%
D=5.9972, I=4.3%

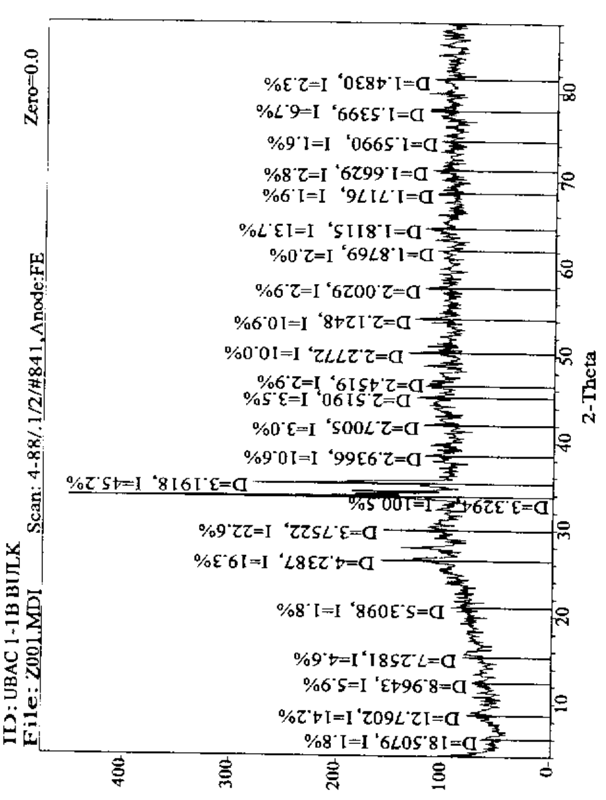
ID: UBAC 1-1B BULK
File: Z001.MDI
Scan: 4-88/.1/2/#841,Anode:FE
Zero=0.0
D=18.5079, I=1.8%
D=12.7602, I=14.2%
D=8.9643, I=5.9%
D=7.2581, I=4.6%
D=5.3098, I=1.8%
D=4.2387, I=19.3%
D=3.7522, I=22.6%
D=3.3294, I=100.5%
D=3.1918, I=45.2%
D=2.9366, I=10.6%
D=2.7005, I=3.0%
D=2.5190, I=3.5%
D=2.4519, I=2.9%
D=2.2772, I=10.0%
D=2.1248, I=10.9%
D=2.0029, I=2.6%
D=1.8769, I=2.0%
D=1.8115, I=13.7%
D=1.7176, I=1.9%
D=1.6629, I=2.8%
D=1.5990, I=1.6%
D=1.5399, I=6.7%
D=1.4830, I=2.3%
CPS
2-Theta

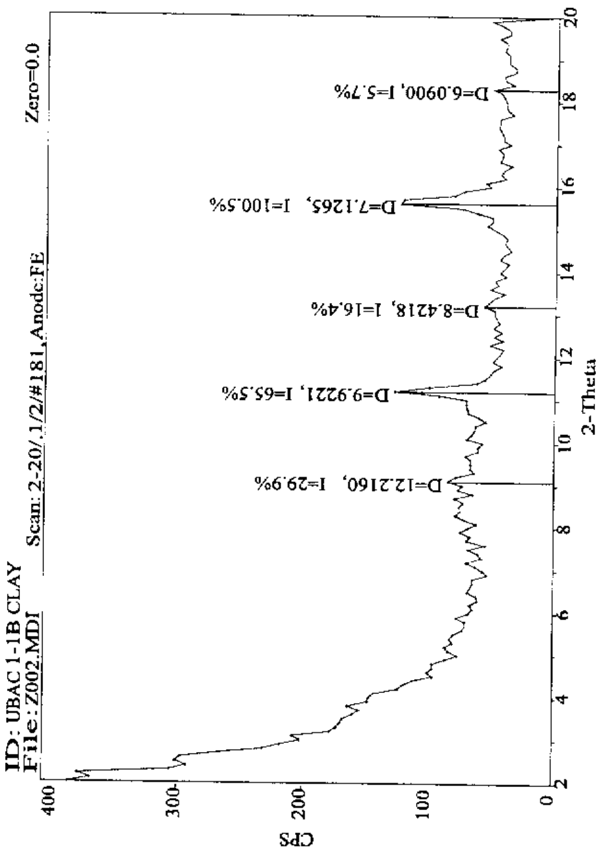
ID: UBAC 1-1B CLAY
File: Z002.MDI
Scan: 2-20/.1/2/#181,Anode:FE
Zero=0.0
D=12.2160, I=29.9%
D=9.9221, I=65.5%
D=8.4218, I=16.4%
D=7.1265, I=100.5%
D=6.0900, I=5.7%
CPS
2-Theta

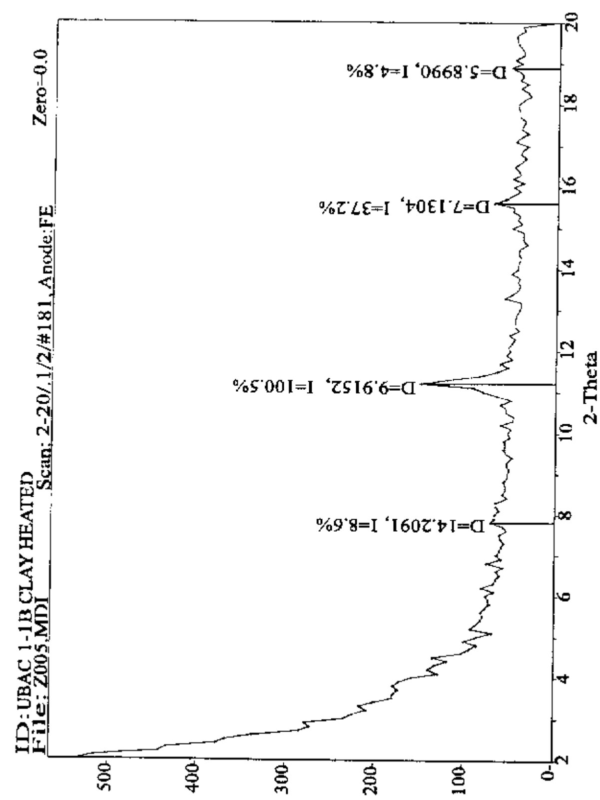
ID: UBAC 1-1B CLAY HEATED
File: Z005.MDI
Scan: 2-20/.1/2/#181,Anode:FE
Zero=0.0
D=14.2091, I=8.6%
D=9.9152, I=100.5%
D=7.1304, I=37.2%
D=5.8990, I=4.8%
CPS
2-Theta

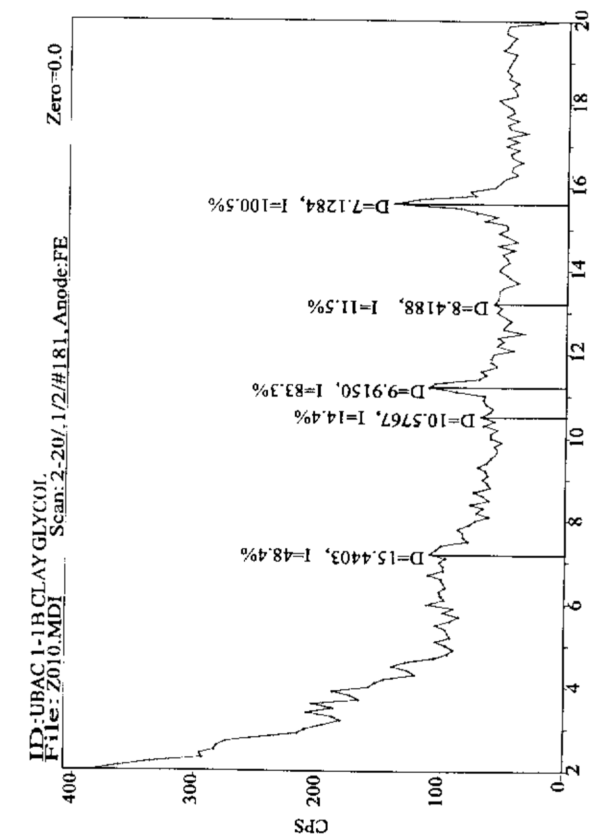
ID: UBAC 1-1B CLAY GLYCOL
File: Z010.MDI
Scan: 2-20/.1/2/#181,Anode:FE
Zero=0.0
D=15.4403, I=48.4%
D=10.5767, I=14.4%
D=9.9150, I=83.3%
D=8.4188, I=11.5%
D=7.1284, I=100.5%
CPS
2-Theta

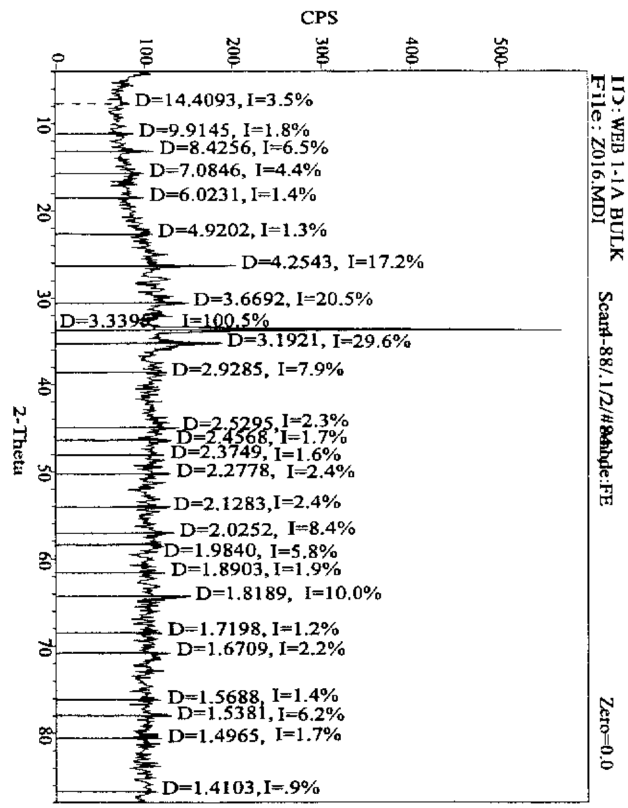
ID: WEB 1-1A BULK
File: Z016.MDI
Scan: 4-88/.1/2/#84,Anode:FE
Zero=0.0
CPS
2-Theta
D=14.4093, I=3.5%
D=9.9145, I=1.8%
D=8.4256, I=6.5%
D=7.0846, I=4.4%
D=6.0231, I=1.4%
D=4.9202, I=1.3%
D=4.2543, I=17.2%
D=3.6692, I=20.5%
D=3.3396, I=100.5%
D=3.1921, I=29.6%
D=2.9285, I=7.9%
D=2.5295, I=2.3%
D=2.4568, I=1.7%
D=2.3749, I=1.6%
D=2.2778, I=2.4%
D=2.1283, I=2.4%
D=2.0252, I=8.4%
D=1.9840, I=5.8%
D=1.8903, I=1.9%
D=1.8189, I=10.0%
D=1.7198, I=1.2%
D=1.6709, I=2.2%
D=1.5688, I=1.4%
D=1.5381, I=6.2%
D=1.4965, I=1.7%
D=1.4103, I=.9%

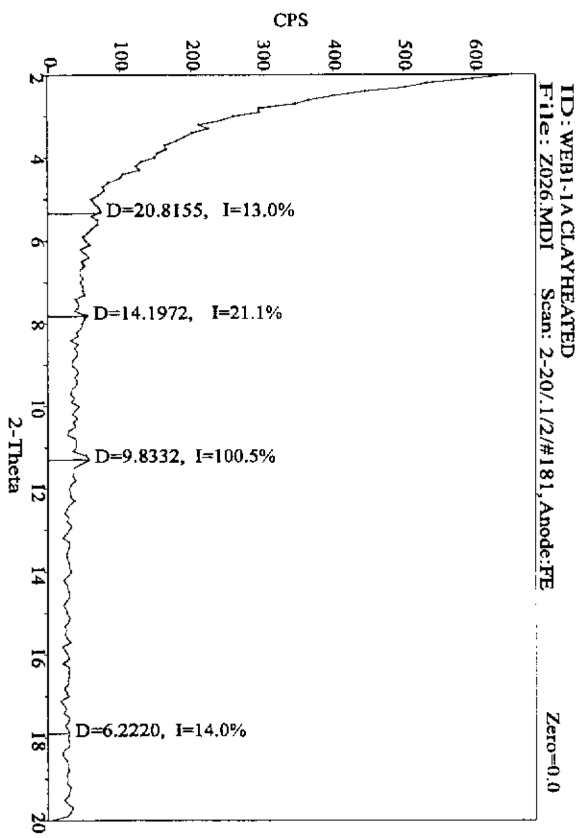
ID: WEB1-1A CLAYHEATED
File: Z026.MDI
Scan: 2-20/.1/2/#181,Anode:FE
Zero=0.0
CPS
2-Theta
D=20.8155, I=13.0%
D=14.1972, I=21.1%
D=9.8332, I=100.5%
D=6.2220, I=14.0%

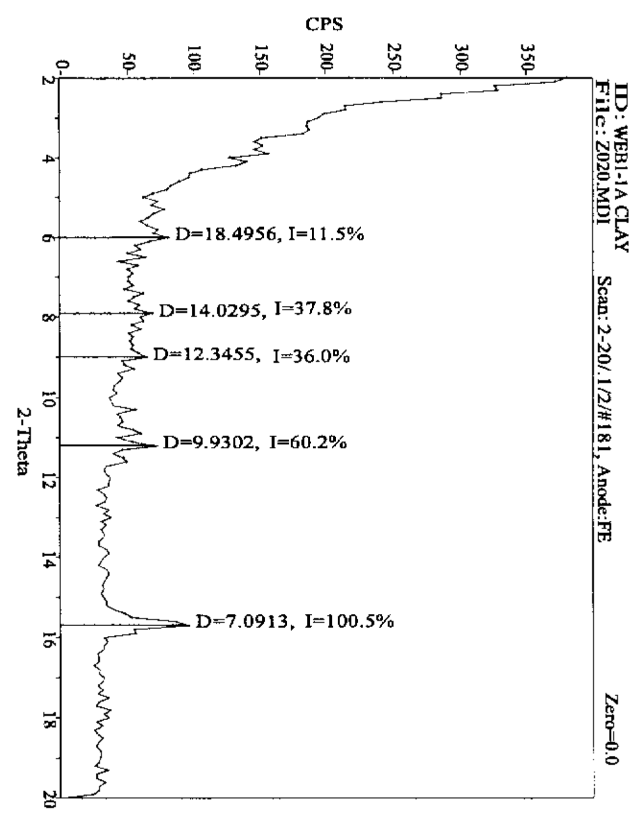
ID: WEB1-1A CLAY
File: Z020.MDI
Scan: 2-20/.1/2/#181,Anode:FE
Zero=0.0
CPS
2-Theta
D=18.4956, I=11.5%
D=14.0295, I=37.8%
D=12.3455, I=36.0%
D=9.9302, I=60.2%
D=7.0913, I=100.5%

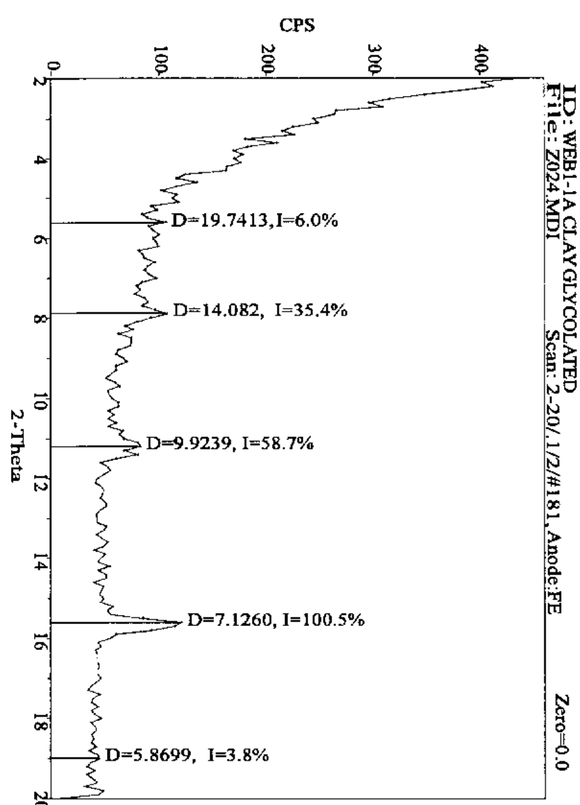
ID: WEB1-1A CLAYGLYCOLATED
File: Z024.MDI
Scan: 2-20/.1/2/#181,Anode:FE
Zero=0.0
CPS
2-Theta
D=19.7413, I=6.0%
D=14.082, I=35.4%
D=9.9239, I=58.7%
D=7.1260, I=100.5%
D=5.8699, I=3.8%

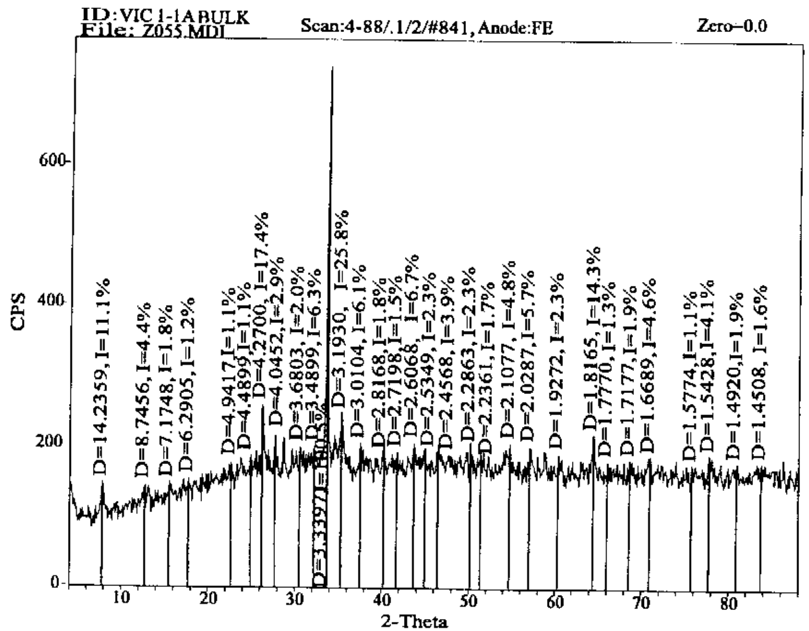
ID: VIC 1-1A BULK
File: Z055.MDI
Scan:4-88/.1/2/#841, Anode:FE
Zero=0.0
CPS
2-Theta
D=14.2359, I=11.1%
D=8.7456, I=4.4%
D=7.1748, I=1.8%
D=6.2905, I=1.2%
D=4.9417, I=1.1%
D=4.4899, I=1.1%
D=4.2700, I=17.4%
D=4.0452, I=2.9%
D=3.6803, I=2.0%
D=3.4899, I=6.3%
D=3.1930, I=25.8%
D=3.0104, I=6.1%
D=2.8168, I=1.8%
D=2.7198, I=1.5%
D=2.6068, I=6.7%
D=2.5349, I=2.3%
D=2.4568, I=3.9%
D=2.2863, I=2.3%
D=2.2361, I=1.7%
D=2.1077, I=4.8%
D=2.0287, I=5.7%
D=1.9272, I=2.3%
D=1.8165, I=14.3%
D=1.7770, I=1.3%
D=1.7177, I=1.9%
D=1.6689, I=4.6%
D=1.5774, I=1.1%
D=1.5428, I=4.1%
D=1.4920, I=1.9%
D=1.4508, I=1.6%

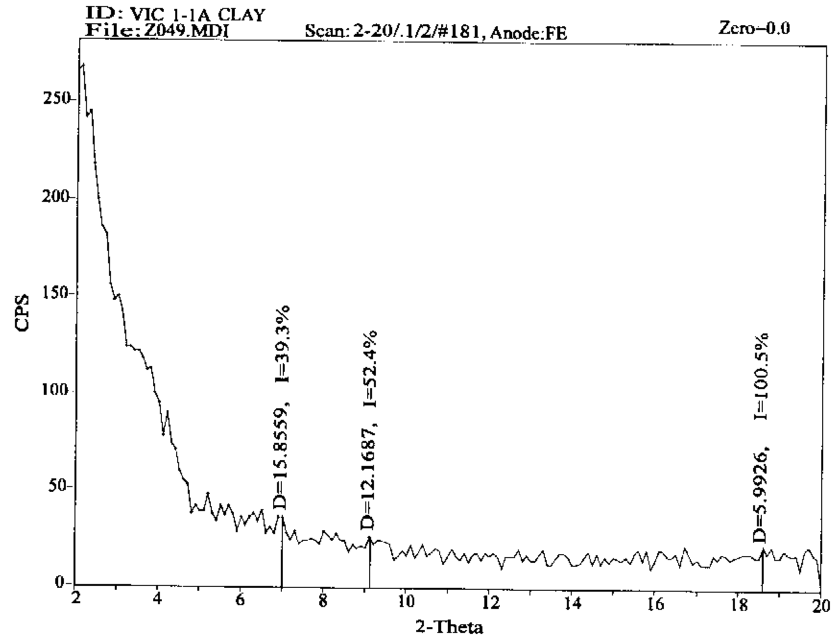
ID: VIC 1-1A CLAY
File: Z049.MDI
Scan: 2-20/.1/2/#181, Anode:FE
Zero=0.0
CPS
2-Theta
D=15.8559, I=39.3%
D=12.1687, I=52.4%
D=5.9926, I=100.5%

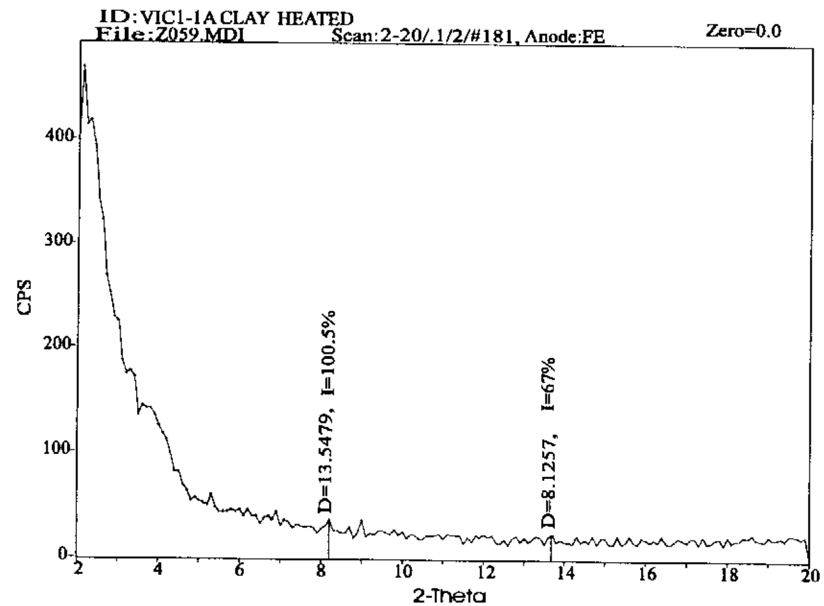
ID: VIC1-1A CLAY HEATED
File: Z059.MDI
Scan:2-20/.1/2/#181, Anode:FE
Zero=0.0
CPS
2-Theta
D=13.5479, I=100.5%
D=8.1257, I=67%

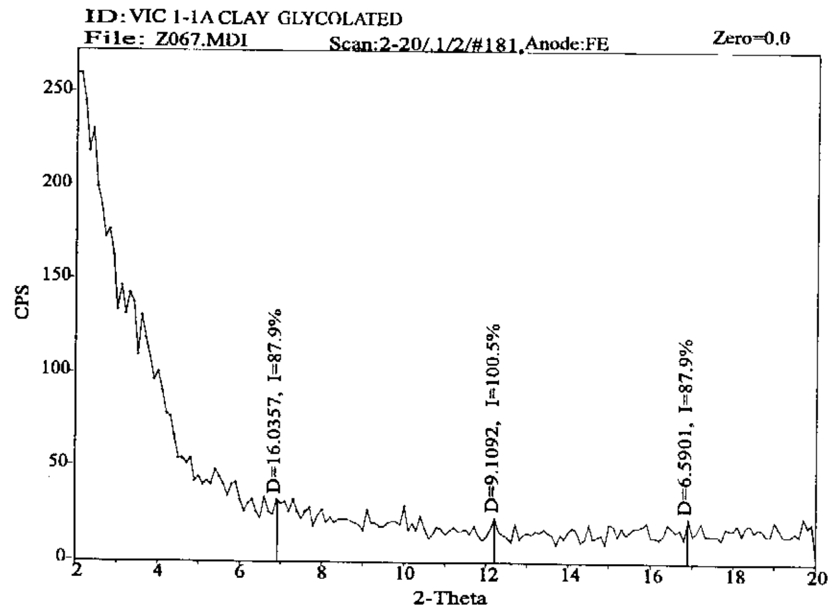
ID: VIC 1-1A CLAY GLYCOLATED
File: Z067.MDI
Scan:2-20/.1/2/#181, Anode:FE
Zero=0.0
CPS
2-Theta
D=16.0357, I=87.9%
D=9.1092, I=100.5%
D=6.5901, I=87.9%